

IAEA-TECDOC-1673

***Monitoring Isotopes in Rivers:
Creation of the Global Network of
Isotopes in Rivers (GNIR)***

Results of a Coordinated Research Project 2002–2006



IAEA

International Atomic Energy Agency

Monitoring Isotopes in Rivers:
Creation of the Global Network of
Isotopes in Rivers (GNIR)

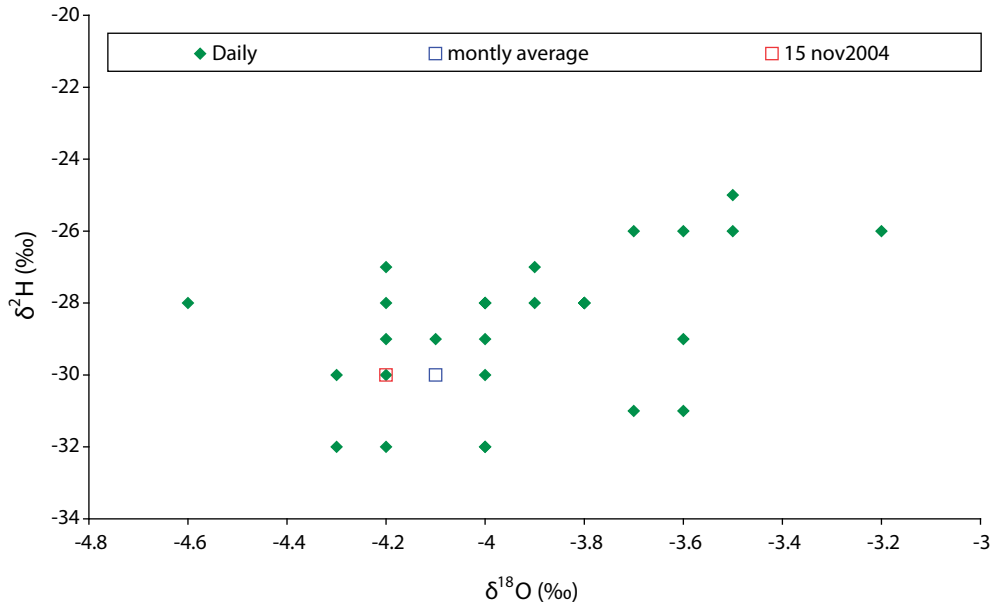


FIG. 3. Scatter plot showing the distribution of $\delta^{18}O$ vs δ^2H values of daily grab samples, the monthly average and the grab sample collected on 15 Nov. 2004.

Isotope analyses were carried out at INGEIS Laboratories. Deuterium (2H) in water samples was prepared using standard procedures [8] and for ^{18}O , the methodology described in [9] was used. Isotope ratios were measured using a multicollector McKinney type mass spectrometer, Finnigan MAT Delta S. Results are expressed in δ (‰) and defined as:

$$\delta = 1000 \frac{R_S - R_P}{R_P} \text{‰}$$

where:

- δ is isotopic deviation in ‰;
- S is sample;
- P is international standard
- R is isotope ratio ($^2H/^1H$, $^{18}O/^{16}O$).

The standard is Vienna Standard Mean Ocean Water, V-SMOW [10]. The analytical uncertainties are ± 0.1 ‰ and ± 1.0 ‰ for $\delta^{18}O$ and δ^2H respectively.

Tritium samples were measured using liquid scintillation direct counting in the the Atucha Nuclear site laboratory, Argentina. Results are expressed in TU (1 TU = $1^3H : 10^{18} H$). The detection limit is about 5 TU. Samples below this value are considered to be 1 to 3 TU.

3. RESULTS AND DISCUSSION

3.1. Paraná River discharge

Fig. 4 shows a comparative picture of discharge over several years at Corrientes station, while, Fig. 5 and Fig. 6 present the daily discharge of Paraná River at the Corrientes and Santa Fe gauge stations [11].

IAEA-TECDOC-1673

MONITORING ISOTOPES IN
RIVERS: CREATION OF
THE GLOBAL NETWORK OF
ISOTOPES IN RIVERS (GNIR)

RESULTS OF A
COORDINATED RESEARCH PROJECT 2002–2006

INTERNATIONAL ATOMIC ENERGY AGENCY
VIENNA, 2012

COPYRIGHT NOTICE

All IAEA scientific and technical publications are protected by the terms of the Universal Copyright Convention as adopted in 1952 (Berne) and as revised in 1972 (Paris). The copyright has since been extended by the World Intellectual Property Organization (Geneva) to include electronic and virtual intellectual property. Permission to use whole or parts of texts contained in IAEA publications in printed or electronic form must be obtained and is usually subject to royalty agreements. Proposals for non-commercial reproductions and translations are welcomed and considered on a case-by-case basis. Enquiries should be addressed to the IAEA Publishing Section at:

Marketing and Sales Unit, Publishing Section
International Atomic Energy Agency
Vienna International Centre
PO Box 100
1400 Vienna, Austria
fax: +43 1 2600 29302
tel.: +43 1 2600 22417
email: sales.publications@iaea.org
<http://www.iaea.org/books>

For further information on this publication, please contact:

Isotope Hydrology Section
International Atomic Energy Agency
Vienna International Centre
PO Box 100
1400 Vienna, Austria
email: Official.Mail@iaea.org

© IAEA, 2012

Printed by the IAEA in Austria
March 2012

MONITORING ISOTOPES IN RIVERS:
CREATION OF THE GLOBAL NETWORK OF
ISOTOPES IN RIVERS (GNIR)
IAEA-TECDOC-1673
ISBN 978-92-0-126810-5
ISSN 1011-4289
© IAEA, 2012
Printed by the IAEA in Austria
March 2012

FOREWORD

River runoff plays a key role in human development in all societies through the provision of water for agriculture, industry and domestic use. Although the monitoring of water availability and our understanding of the main hydrological processes at the catchment scale are relatively good, many important aspects, especially those related to the interaction of runoff and groundwater, remain poorly understood. Additionally, the impact of human activities — such as the construction of large reservoirs and diversions, and the redirection of rivers to supply drinking water or water for irrigation or hydropower — are highly relevant and, together with the predicted impact of climate change, are likely to heavily impact local water cycles. The effects of such changes include: limited availability of water; changes in flood or drought frequency; changes in water quality, sediment load and groundwater recharge; and biodiversity loss in riparian environments. Additionally, political disputes may result as water resources become affected in terms of availability and/or quality.

In most instances, stable isotopes and other water tracers provide a deeper insight into hydrological processes, especially in aspects related to water pathways, interconnections, transport of water and pollutants, and the transit time of water. To explore the contribution of these techniques in more detail, the IAEA has launched a monitoring programme, the Global Network of Isotopes in Rivers (GNIR), aimed at regular analysis of the isotope composition of runoff in large rivers. This isotope monitoring network complements an earlier precipitation network, the Global Network of Isotopes in Precipitation (GNIP). To prepare for GNIR, the IAEA launched a coordinated research project (CRP) called Design Criteria for a Network to Monitor Isotope Compositions of Runoff in Large Rivers. The main aim of the CRP was to develop a scientific rationale and a protocol for the operation of such a network, as well as to contribute to the enhancement of our understanding of hydrological processes at the catchment scale.

This publication presents several isotope datasets compiled for major rivers covering all continents as well as preliminary conclusions obtained from available isotope results. All isotope data compiled as part of the CRP have been included in IAEA isotope databases and are available on-line. The principal outcome of the CRP was to show the importance of maintaining and strengthening GNIR operation under the auspices of the IAEA. Additionally, isotope information collected as part of the CRP provided evidence of the importance of groundwater contribution to the baseflow of rivers. As a result, a follow-up CRP was launched by the IAEA dealing with the use of isotope and tracer tools to better characterize the magnitude and transit time of groundwater contribution to the baseflow of rivers.

The IAEA technical officers responsible for this publication were T. Vitvar and P.K. Aggarwal of the Division of Physical and Chemical Sciences.

EDITORIAL NOTE

The papers in these Proceedings (including the figures, tables and references) have undergone only the minimum copy editing considered necessary for the reader's assistance. The views expressed remain, however, the responsibility of the named authors or participants. In addition, the views are not necessarily those of the governments of the nominating Member States or of the nominating organizations.

Although great care has been taken to maintain the accuracy of information contained in this publication, neither the IAEA nor its Member States assume any responsibility for consequences which may arise from its use.

The use of particular designations of countries or territories does not imply any judgement by the publisher, the IAEA, as to the legal status of such countries or territories, of their authorities and institutions or of the delimitation of their boundaries.

The mention of names of specific companies or products (whether or not indicated as registered) does not imply any intention to infringe proprietary rights, nor should it be construed as an endorsement or recommendation on the part of the IAEA.

The authors are responsible for having obtained the necessary permission for the IAEA to reproduce, translate or use material from sources already protected by copyrights.

Material prepared by authors who are in contractual relation with governments is copyrighted by the IAEA, as publisher, only to the extent permitted by the appropriate national regulations.

CONTENTS

Summary	1
Introduction	5
Environmental isotope ratios of river water in the Danube Basin	13
<i>D. Rank , W. Papesch , G. Heiss , R. Tesch</i>	
Study on hydrological processes in Lena river basin using stable isotope ratios of river water.....	41
<i>A. Sugimoto , T.C. Maximov</i>	
Isotope tracing of the Paraná River, Argentina	51
<i>H.O. Panarello, C. Dapeña</i>	
South African contribution to the Rivers CRP.....	69
<i>S. Talma , S. Lorentz , S. Woodborne</i>	
Stable water isotope investigation of the Barwon–Darling River system, Australia.....	95
<i>C.E. Hughes , D.J.M. Stone , J.J. Gibson , K.T. Meredith , M.A. Sadek , D.I. Cendon , S.I. Hankin, S.E. Hollins, T.N. Morrison</i>	
Isotopic tracing of hydrological processes and water quality along the upper Rio Grande, USA.....	111
<i>J. Hogan, F. Phillips, C. Eastoe, H. Lacey, S. Mills, G. Oelsner</i>	
Chemical and isotopic compositions of the Euphrates River water, Syria	137
<i>Z. Kattan</i>	
Isotope investigations of major rivers of Indus Basin, Pakistan	167
<i>M. Ahmad, Z. Latif , J.A.Tariq, M. Rafique, W. Akram, P. Aggarwal, T. Vitvar</i>	
Isotope tracing of hydrological processes in river basins: the Rivers Danube and Sava.....	187
<i>N. Ogrinc, T. Kanduč, N. Miljević, D. Golobočanin, J. Vaupotič</i>	
Isotope composition of Mekong River flow water in the south of Vietnam.....	197
<i>K.C. Nguyen, L. Huynh, D.C. Le, V.N. Nguyen, B.L. Tran</i>	
Temporal and spatial variations of $\delta^{18}\text{O}$ along the main stem of Yangtze River, China.....	211
<i>B. Lu, T.Sun, C. Wang, S. Dai , J. Kuang , J. Wang</i>	
The role of lakes and rivers as sources of evaporated water to the atmosphere in the Amazon basin.....	221
<i>L.A. Martinelli, R.L. Victoria, J.R. Ehleringer, J.P.H.B. Ometto</i>	

SUMMARY

Following a set of preparatory activities (such as the IAEA/WMO/PAGES meeting on ‘Tracing Isotopic Composition of Past and Present Precipitation — Opportunities for Climate and Water Studies’, held in January 1995 near Bern, Switzerland), the IAEA launched a set of activities at the beginning of this millennium to establish a worldwide collection of isotope data in rivers. During the main preparatory phase in 2002–2006, the IAEA Coordinated Research Project CRP 647 ‘Design criteria for a network to monitor isotope compositions of runoff in large rivers’ was undertaken as a preparatory activity for the creation of a global monitoring programme of isotope contents in rivers. The overall objectives of this CRP were to lay the groundwork and a scientific rationale for the future design of an operational ‘Global Network of Isotopes in Rivers’ (GNIR), to enhance the understanding of the water cycle of river basins and to assess impacts of environmental and climatic changes on the continental water cycle. The principal objectives of the CRP, as stated in the project description, were the following:

- To launch and coordinate a programme for isotope sampling of river discharge and related studies via a network of research institutes worldwide, establishing linkages where appropriate to existing research and monitoring activities undertaken by national counterparts, monitoring agencies, and international research programmes;
- To contribute to the understanding of the water cycle of large river basins by developing, evaluating, and refining isotope methodologies for quantitative analysis of water balance and hydrological processes, and for tracing environmental changes;
- To develop an optimal protocol for operational river water sampling, and to design a comprehensive database to support isotope-based water balance studies and future monitoring of ongoing environmental changes.

The CRP was completed using 18 research groups, and covered research and monitoring in river basins accounting for approximately one third of mean annual runoff or about one fourth of the total land surface (Fig. 1). It included basins on all inhabited continents and a wide spectrum of geographical settings, previous experiences and possible applications. This TECDOC summarizes the achievements of the CRP, supported by 12 case studies.

The participating groups launched or continued existing isotope monitoring programmes, typically sampling ^{18}O , ^2H and sometimes ^3H (for example, for the Danube, Parana, Mississippi and Colorado rivers) on a monthly interval. Additional stations have been included or re-activated. An exchange of results and adjustment of workplans was performed at three Research Coordination Meetings in 2002, 2004 and 2005, the last providing final conclusions toward the operation of the GNIR.

Although the majority of studies focused on the multiple application of isotope records, four particular sub-topics have been addressed and elaborated in the respective studies: (a) tracing of seasonal flowpath changes between permafrost, lakes and rivers, and their impact on the runoff regime in the Northern Russia and Canadian Rivers (Lena, MacKenzie); (b) tracing of the influence of precipitation induced by regional climate phenomena (El Niño, monsoons) on the spatial and temporal runoff regime of rivers (Parana, Ganges, Mekong); (c) tracing of multiple impacts, such as recharge in mountainous headwaters, nutrient input and exchange with wetlands, downstream regulations, or transitions from dominant groundwater discharge into rivers to infiltration from rivers into aquifers, and their development along the river course (Danube, Sava, Rhine, Indus, Amazon, Yangtse, Mississippi); and (d) tracing of spatial and

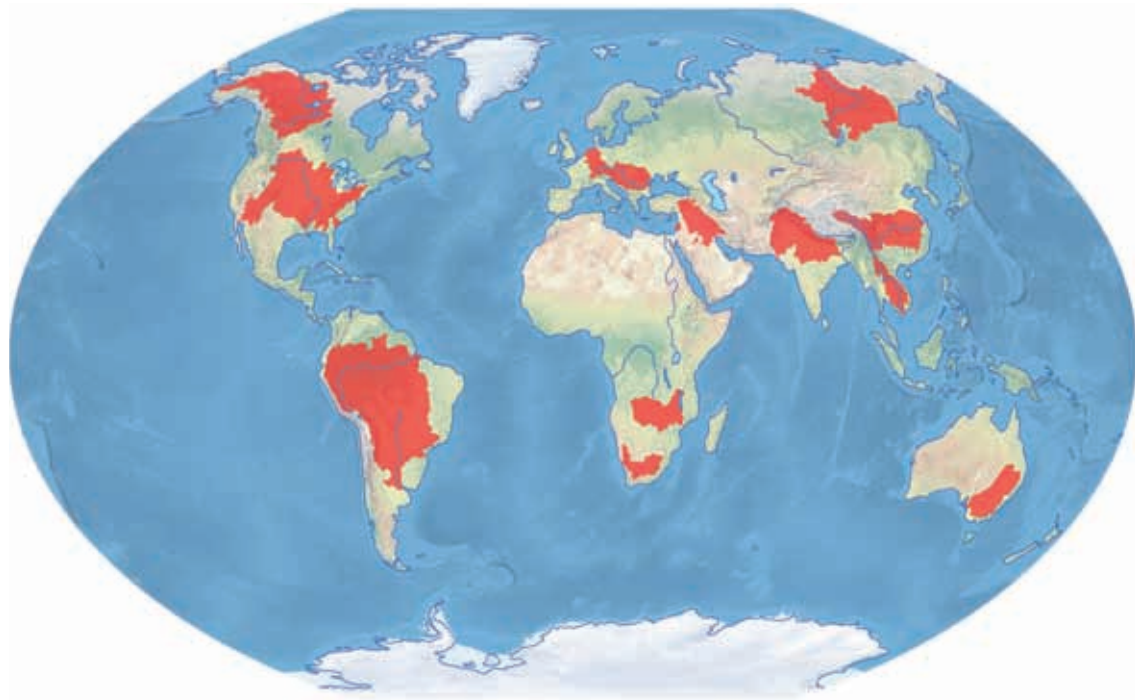


FIG. 1. Map of catchments monitored during the CRP.

temporal effects of irrigation or evaporative losses in dry and arid areas (Euphrates, Jordan, Rio Grande, Murray-Darling). Multiple impacts were typically assessed through a snapshot (synoptic) survey or monitoring at several points between headwaters and outlets.

For example in the Lena basin (Russian Federation), contributions of lakes and permafrost to runoff can be traced by using stable isotopes. Isotopically light water from the lower unfrozen layers in the Siberian Plain taiga is the dominant runoff component over the winter. The rapid decrease of $\delta^{18}\text{O}$ values in early summer indicates the discharge of melting snow, while summer increases of $\delta^{18}\text{O}$ in the Lena are attributed to summer precipitation, and do not indicate any significant impact of evaporated water from taiga lakes. These processes impact the recently identified reduction in the rate of transport of cold North Atlantic water to the deep waters of southern latitudes. This reduction is due partly to higher discharges from Siberian rivers over the past decade and can induce dramatic changes in ocean circulation. Monitoring the isotopic composition of these rivers will allow identification of the sources of increased discharge.

Monitoring the isotopic composition of the Paraná River in South America highlights the potential of stable water isotopes for tracing the influence of precipitation and other hydrological processes on runoff in tropical rivers, which contribute a large fraction of the world's surface runoff. The precipitation regime in southern Brazil is influenced strongly by seasonal changes in the Inter-Tropical Convergence Zone (ITCZ). Periodical pronounced southward inflexion of the ITCZ over the Amazon plain in the austral summer, known as El Niño Southern Oscillation (ENSO), causes intense precipitation depleted in ^2H and ^{18}O at the headwaters of the Paraná. Values of $\delta^2\text{H}$ and $\delta^{18}\text{O}$ and particularly of deuterium excess ($d\text{-excess} = \delta^2\text{H} - 8\delta^{18}\text{O}$) in the Paraná at Buenos Aires are found to be correlated with the multivariate ENSO-index with a lag of several months. The $d\text{-excess}$ value is a function of water vapour source and the degree of hydrological recycling in the basin. Increases in the $d\text{-excess}$ paralleling increases in the ENSO-index are a result of additional contributions

of recycled water vapor from evaporation of surface water and water captured through canopy interception during El Niño events.

Three longitudinal profiles along the Rio Grande in southwest USA show a large enrichment in ^{18}O reflecting typical evaporative water losses in arid catchments. The 2002/2003 winter profile from the upper two-thirds of the basin (up river from the Elephant Butte Reservoir) represents baseline conditions in the river. In the lower third of the basin, the river is dominated by irrigation return flow (enriched in $\delta^{18}\text{O}$) of water applied during the preceding dry summer of 2002. The summer trends show reservoir releases at 350 km from the headwaters (reservoirs are upstream on the Rio Chama) and at 800 km (Elephant Butte Reservoir) which reset the isotopic signal. The difference between wet and dry summers downstream of the 800 km point (a major agricultural region) reflects the release of reservoir waters that have experienced significant evaporative enrichment in $\delta^{18}\text{O}$ during a dry year (2002) versus those which have been released during a wet year (2005). This example highlights the importance of *ad hoc* synoptic studies during high and low discharge periods, yielding important information about water losses and subsurface inputs that are difficult to obtain through conventional gauging.

Attention has been paid to the spatial distribution of water isotopes in streams and their relation to basin size and topography. Previous isotope monitoring studies stated that for catchments of up to about 130 000 km², the headwater precipitation isotope signal is largely conserved in the streamflow. A revisited analysis of the Danube isotope snapshot from 1988 through this CRP revealed similar information, demonstrating that the Danube river carries the Alpine depleted stable isotope input signal up to the passage through the Hungarian Plain. From this zone downwards the river mostly recharges the adjacent aquifers, maintains a relatively stable isotope content and does not show any impact from isotopically distinct contributions. The results from snapshot isotope surveys conducted or interpreted during this CRP were used to formulate recommendations for the Joint Danube Survey conducted in 2007, in which water stable isotopes and tritium were analysed along the entire river course, including major tributaries and the zones below the confluences.

The CRP also addressed the question of type of sampling for streamflow isotope analyses (grab versus composited flow weighted samples) and stated that, based on two detailed studies in the Danube and Parana, a grab sample sufficiently represents the mean monthly composition. However, every sample should be accompanied by a discharge value and all isotope data should be interpreted with respect to flow conditions.

Although the overall objective of the CRP focused primarily on monitoring of isotopes in large river basins for continental water balance, considerable effort has been made in case studies to explore the role of systematic monitoring at smaller scales up to headwaters, with isotope values in streamflow often representing an end member of the adjacent stream-aquifer system. It has been stated that many studies, particularly in tropical countries, contain a considerable number of groundwater samples, but only a few samples from streams. The reasons are typically either logistical (regular access to rivers) or conceptual, the latter based on the premature conclusion that an often periodical streamflow is not an important part of the local groundwater system. The results of the CRP include, therefore, a consensus that the isotope monitoring of rivers should be scale flexible, allowing not only for large scale water balance, but also for assessment of patterns ('isoscapes') in smaller hydrogeological systems in watersheds.

1. INTRODUCTION

1.1. Background

The question as to what extent and why the water isotope (^{18}O , ^2H and ^3H) content in streams differs from the content in precipitation has been one of the crucial questions in the development of isotope hydrology. Isotope data from rivers and surface waters were first collected in the 1950s and addressed primarily the variability of stable water isotopes in some large rivers such as the Mississippi, Colorado [1], Thames [2] and in smaller Scandinavian watersheds [3] and New Zealand. Kaufmann and Libby [4] and Eriksson [5] reported the first tritium values in the Mississippi River and analyzed the mixing of fallout tritium from the bomb tests in the 1950s in the river and adjacent aquifers. The first thorough compilation of isotope contents in freshwaters on a global scale was provided by Craig [6]. Also this year, the International Atomic Energy Agency (IAEA), in cooperation with the World Meteorological Organization (WMO) launched a worldwide survey to measure the isotope composition of precipitation that culminated in the Global Network of Isotopes in Precipitation (GNIP), which became the main source of isotope data in atmospheric waters [7].

Whereas the GNIP rapidly became a worldwide operating network, a systematic collection of isotope data from rivers and surface waters in the 1960s remained limited to some major rivers, such as the Mississippi, Columbia, Yukon or Ottawa [8]. In Europe, the longest major river isotope records are for the Danube at Vienna and the Rhine at Mainz. These records became instrumental in tracing the hydrological response of large rivers to isotope input in precipitation, including the input of tritium due to the nuclear bomb tests in early 1960s. For example, Ref. [9] synthesized several years of ^{18}O data in rivers in the Netherlands and showed that the major fraction of water in the Rhine is snowmelt dominated, while the Meuse is rainfall dominated. In another application, Gat and Dansgaard [10] presented the use of stable water isotopes in tracing freshwater losses through evaporation in semi-arid areas.

In the late 1960s and early 1970s, streamflow isotope and related hydrochemical data were used to quantify the portion of streamflow discharged from adjacent aquifers (also referred to as groundwater runoff or baseflow) during stormflow events. The first isotopic hydrograph separation approaches using isotopes employed tritium [11] and stable isotopes of ^{18}O and ^2H [12] in two-component mixing models [13], where event water was represented by the distinct isotopic composition of rainfall/throughfall and pre-event water was represented by the distinct isotopic composition of pre-storm stream water or adjacent groundwater. These early studies opened the way for an expansion of studies on runoff generation and runoff components (event vs pre-event water) on experimental hillslopes and in catchments. The paper by Sklash et al. [14] is a benchmark study that documented the dominant role of the subsurface pre-event water in runoff generation. In general, these studies have revealed a much greater baseflow proportion in the stream discharge hydrograph [15], compared to the expected proportions derived from the early conceptual models of streamflow generation and graphical hydrograph-separation analysis [16]. In almost all cases the mobilized pre-event water accounts for over half, and usually about three-quarters of the runoff and/or peakflow associated with rainstorms [17]. These results contradicted the traditional engineering assumption of Hortonian overland flow generation [18] as the dominant component of streamflow and therefore caused

a substantial shift in the runoff generation theory. Nevertheless, these mechanisms are much less straightforward as a watershed area increases and groundwater discharge to a stream channel is replaced by river bank infiltration. The assessment of runoff generation processes through spatially more detailed isotope and hydrochemical monitoring across watershed scales thus became a motivation for a global river isotope database.

In the 1980s, the first compilation of systematic measurements of isotope contents of river waters from several continents was carried out by Mook [19], extending the study of the European rivers [9] by tracing the depleted snowmelt signal and its seasonal occurrence in the lower reaches of some tropical rivers such as the Indus or Amazon. The adaptation of lumped parameter flow models for estimation of water residence times in rivers and aquifers [20, 21] led to the application of these approaches to a variety of American basins [22], the Danube basin, and basins in Switzerland [23]. Available isotope data records in those basins were already at least one decade long and therefore also provided the possibility for seasonal or decadal trend analysis and comparison of precipitation isotope records with their response in rivers. It became a consensus of the hydrological community that isotopes are unique tracers of the rainfall-runoff response across catchment scales. On the other hand, the conceptualization of large basins using isotope data from only one station in some cases appeared to oversimplify catchment structure and bias the specific impact of particular subcatchments or particular hydrological processes. A need was therefore identified for a thorough compilation of available isotope data from both larger and smaller rivers, their coordination with hydrological and hydrochemical data and a flexible setup of monitoring points, including headwaters, mesoscale catchments and large basins. A need for synoptic surveys along the river stems was also articulated for estimating the subsequent contributions of tributaries, aquifers, irrigation or industrial waters. Addressing such needs substantially supports efforts toward a comprehensive database which allows for multiple analysis and comparison of the runoff response in catchments in different environments and at different scales [24].

There is consensus that the isotope composition of rivers is determined by the composition of rainfall and modified by processes in the vadose zone, tributaries and aquifers. These modifications are different in various climate settings and result in different pathways of water between rainfall and runoff. Recent studies (e.g. Vörösmarty and Meybeck [25]), however, suggest that the impact of storage sheds, diversions and redirection of streamflow for water supply, hydropower, and irrigation could overcome the impact of recent and anticipated future climate changes on river runoff. Consequences include changes in the frequency and extent of flooding, increased sediment load, altered groundwater recharge, and degradation of water quality and riparian ecosystems, often resulting in political disputes or upstream-downstream inequities. Reference [26] synthesizes the natural and anthropogenic origin of runoff contributions in a 'River Continuum Model', and highlights spatially distributed isotope monitoring as input for an 'Isotope River Continuum Model', which, as documented by some recent studies [27] has the potential to better partition natural and anthropogenic runoff components.

Since the 1990s, geostatistical methods and geographic information system (GIS) tools are being used to map spatial and temporal variability of isotope contents. A pioneering study on mapping of stable water isotope concentrations in rainfall and streams in the conterminous USA was performed by Kendall and Coplen [28] and several approaches have been developed, particularly for mapping and interpolation of GNIP data [29–32]. A number of atmospheric global circulation models [33–34] incorporate water isotopes in precipitation for the

validation of numerical models of atmospheric dynamics. This sophisticated understanding of global isotope patterns in precipitation has led to efforts to couple the isotopic balance of the atmosphere with runoff models and to validate gridded runoff simulation via simulation of stable water isotope partitioning during all post-precipitation hydrological processes [35–36]. This scientific frontier can be further supported by the systematic worldwide isotopic monitoring of rivers as well as by current new developments in the isotope analysis and monitoring of atmospheric moisture.

In the last years, isotope maps have been produced [37], mapping waters isotopically different from local precipitation (tapwater, irrigation return water, crops, etc.). It is of utmost importance that this research is supported through creation and maintenance of dedicated global isotope databases in more components of the water cycle than just precipitation. Reference [37] particularly highlights the role of ‘post-precipitation’ processes in the formation of the geographical patterns (isoscares) of isotope distribution in water, nutrients and materials used in forensic applications.

1.2. Objectives

This document has been created to relay the outcome of a CRP called Design Criteria for a Network to Monitor Isotope Compositions of Runoff in Large Rivers, which was launched in order to prove the value of the GNIR concept and thus establish the monitoring system. The main aim of the CRP was to develop a scientific rationale and a protocol for the operation of such a network, as well as to contribute to the enhancement of our understanding of hydrological processes at the catchment scale. The document includes case studies of large rivers, the results of which supported the creation of the GNIR programme, which will remain a regular feature of the Isotope Hydrology Section in the future.

1.3. Scope of the report

This report covers studies undertaken for major rivers worldwide, and preliminary interpretation of the data collected. These individual studies led to the creation of a database, and represent the starting point of contributions to the GNIR network. The contribution of individual studies undertaken in several countries, each highlighted here, has been invaluable in creating a framework for the establishment of the GNIR network and for supporting the theory that such a network is both possible and highly useful.

1.4. Structure

The foreword of this publication describes the importance of river runoff, and the role it plays in human development in all societies. It discusses the reason for this document: that the interaction between groundwater and runoff is poorly understood, as well as the impact of manmade activities. It goes on to outline the role of stable isotopes and other water tracers in providing information about the movement, origins and patterns of water.

The summary in Section 1 of this document outlines the undertakings which were part of the CRP and the principal objectives of the CRP, including launching and coordinating a programme for isotope sampling of river discharge and related studies; contributing to the understanding of the water cycle of large river basins by developing, evaluating and refining

TABLE 1. SAMPLING PROTOCOL OF GNIR

	Recommended data	Additional data
River basin	Name Upstream area Land use	Other relevant information on the basin
Sampling site	Name Coordinates Elevation Map and photo	Closest stations of GRDC, GEMS/Water, GNIP
Isotopic data at sampling site	$\delta^{18}\text{O}$ $\delta^2\text{H}$ Analytical uncertainties	^3H All other isotopes
Other data at sampling site	Discharge Electrical conductivity Temperature	Hydrochemistry Hydrobiology Meteorology

isotope methodologies for the quantitative analysis of water balance and hydrological processes and for tracing environmental changes; and developing an optimal protocol for operational river water sampling and design of a comprehensive database.

The background leading up to the CRP and the establishment of GNIR is outlined in the introduction, including the need for such a monitoring network and developments to date in river monitoring. Achievements and results are also discussed in Section 1, including the important conclusion that the GNIR programme is worth maintaining on a long term basis. The CRP discussed in this document led to two new CRPs, which will provide further information on groundwater recharge to rivers and the effects of snow and glaciermelt on stream flow. The work undertaken through this CRP also led to the creation of several valuable datasets, with the projection that many more will be created in the future and made available through the IAEA's online application, WISER.

The remaining sections document a series of case studies, providing detail about work undertaken with the Danube, Sava, Lena, Parana, Barwon-Darlington, Rio, Euphrates, Indus, Mekong, Yangtze, and Amazon rivers and their basins, as well as some South African rivers.

1.5. Achievements and results

The principal outcome of the CRP was the conclusion to maintain the Global Network of Isotopes in Rivers (GNIR) under the auspices of the IAEA, complementary to the GNIP and other envisaged isotope hydrology databases [38]. The main rationale for the operational phase of GNIR was summarized in Ref. [39]. Several river isotopic datasets collected and analyzed during this CRP (e.g. Danube, Indus, Mackenzie, Lena, etc.) led to follow-up activities related to two new IAEA CRPs aimed at application of isotopes for the assessment of groundwater recharge to rivers ('Isotopic Age and Composition of Streamflow as Indicators of Groundwater

Sustainability,' 2004–2010), as well as the assessment of the snow and glaciermelt component in streamflow ('Use of Environmental Isotopes in Assessing Water Resources in Snow, Glacier, and Permafrost Dominated Areas under Changing Climatic Conditions', 2010–2013).

The protocol for collection of river isotope data grants participants freedom according to their conditions, resources and research needs. However, for consistency the following approach is recommended: the default grab sampling interval should be monthly, and where possible, samples should be collected at gauge stations. Analytical responsibility remains with the countries, but the IAEA may provide analytical support and/or technical assistance on an individual basis. Special attention must be paid to simultaneous collection of runoff data at sampling sites, at least the mean daily runoff of the sampling day and the respective mean monthly runoff. Runoff values allow a proper interpretation of the isotope value in streamflow, indicating under which runoff conditions the sample was taken. Table 1 describes the information that is included in GNIR.

Based on evaluation of the results and conclusions of the CRP, the GNIR currently consists of more than 25 000 data records from more than 600 sampling points worldwide. Three types of data are included: first, regularly monitored river stations with a sampling interval of one month or less and a sampling period of at least two years; second, instantaneous spatial or profile-longitudinal surveys, and third, all remaining ad-hoc data from IAEA Technical Cooperation Projects, IAEA Coordinated Research Projects and other scientific studies worldwide. Examples of regular GNIR monitoring are a set of stations established around the year 2000, that were maintained and thoroughly interpreted in this CRP, such as the La Plata, Indus, Zambezi, Murray-Darling or Sava (Slovenia). Other examples are the stable isotope monitoring of US rivers performed in the 1990s, or isotope datasets from rivers in Switzerland, maintained for decades, but not involved in the CRP. Data from the transboundary Pan-Arctic river database (<http://www.r-arcticnet.sr.unh.edu>) have been added recently, extending knowledge of the isotope fingerprinting of streamflow in rivers such as the Lena, Yenisey, Kolyma, Yukon and MacKenzie. Examples of instantaneous longitudinal surveys include two surveys along the Danube river course, performed in 1988 and 2007.

The IAEA is carrying out a continuous compilation of available river isotope data through past IAEA projects, scientific papers, and, above all, identification of and the search for existing river isotope data from national organizations and universities. All data are being compiled and checked and made available through the online application WISER at the IAEA web page www.iaea.org/water. A two year embargo is maintained on newly received data at the submitters request, which allows the contributors to publish their data before it is publicly available. A first thorough statistical treatment of the GNIR data conducted by the IAEA is in preparation.

Finally, the GNIR is open to new scientific frontiers in the monitoring of solute isotopes (carbon, nitrogen, strontium, sulphur) in streamflow for a more routine labelling of contamination sources and pathways. Although this CRP has focused primarily on water isotopes and labelling of hydrological processes, the database also contains several datasets of isotope composition of carbonates and nitrates in streamflow (Sava, Danube).

The continuous successful development of the GNIR underlines its role as an established element of the global hydrologic databases and networks [40] and demonstrates the usefulness of the preparatory groundwork conducted in the CRP.

REFERENCES

- [1] EPSTEIN, S., MAYEDA, T., Variations of ^{18}O content of waters from natural sources, *Geochim. Cosmochim. Acta* **4** (1953) 213–224.
- [2] CLARKE, G.R., DENTON, W.H., REYNOLDS, P., Determination of the absolute concentration of deuterium in Thames River water, *Nature* **4427** (1954) 469.
- [3] DANSGAARD, W., The ^{18}O abundance in fresh water, *Geochim. Cosmochim. Acta* **6** (1954) 241–60.
- [4] KAUFMANN, S., LIBBY, W.F., The natural distribution of tritium, *Phys. Rev.* **93** 6 (1954) 1337–1344.
- [5] ERIKSSON, E., The possible use of tritium for estimating ground water storage, *Tellus* **10** (1958) 472–478.
- [6] CRAIG, H., Isotopic variations in meteoric waters, *Science* **133** (1961) 1702–1703.
- [7] IAEA/WMO, Global Network of Isotopes in Precipitation, The GNIP Database, <http://www.iaea.org/water> (2010).
- [8] BROWN, R.M., Hydrology of tritium in the Ottawa Valley, *Geochim. Cosmochim. Acta* **21** (1961) 199–216.
- [9] MOOK, W.G., Stable carbon and oxygen isotopes of natural waters in the Netherlands, *Proc. Isotope Hydrology, IAEA Vienna* (1970) 163–189.
- [10] GAT, J.R., DANSGAARD, W., Stable isotope survey of the freshwater occurrences in Israel and the northern Jordan rift valley, *J. Hydrol.* **16** (1972) 177–212.
- [11] CROUZET, E., HUBERT, P., OLIVE, P., SIWERITZ, E., Le tritium dans les mesures d'hydrologie de surface, Détermination expérimentale du coefficient de ruissellement, *J. Hydrol.* **11** (1970) 217–219.
- [12] DINÇER, T., PAYNE, R., FLORKOWSKI, T., MARTINEC, J., TONGIORGI, E., Snowmelt runoff from measurements of Tritium and Oxygen-18, *Water Resour. Res.* **5** (1970) 110–124.
- [13] PINDER, G.F., JONES, J.F., Determination of the groundwater component of peak discharge from the chemistry of total runoff water, *Water Resour. Res.* **5** (1969) 438–455.
- [14] SKLASH, M.G., FARVOLDEN, R.N., The role of groundwater in storm runoff, *J. Hydrol.* **43** (1979) 45–65.
- [15] KIRCHNER, J., A double paradox in catchment hydrology and geochemistry, *Hydrol. Proc.* **17** (2003) 871–874.
- [16] HEWLETT, J.D., HIBBERT, A.R., Factors affecting the response of small watersheds to precipitation in humid areas, *International Symposium on Forest Hydrology (SOPPER, W.E., LULL, H.W., Eds) Pergamon Press* (1967) 75–290.
- [17] GENEREUX, D.P., HOOPER, R.P., Oxygen and hydrogen isotopes in rainfall-runoff studies. *Isotope Tracers in Catchment Hydrology (MCDONNELL, J.J., KENDALL, C., Eds) Elsevier, Amsterdam* (1998) 319–346.
- [18] HORTON, R.E., The role of infiltration in the hydrologic cycle, *Trans. Amer. Geophys. Union* **14** (1933) 446–460.
- [19] MOOK, W.G., The oxygen-18 content of rivers, *Mitt. Geol-Paläont. Int. Univ. Hamburg, SCOPE/UNEP Sonderbrand* **52** (1982) 565–570.
- [20] ZUBER, A., “Mathematical models for the interpretation of environmental radioisotopes in groundwater systems”, *Handbook of Environmental Isotope Geochemistry (FRITZ, P., FONTES, J.-CH., Eds) Elsevier, Amsterdam* (1986) 1–59.

- [21] MALOSZEWSKI, P., ZUBER, A., “Lumped parameter models for the interpretation of environmental tracer data”, *Manual on Mathematical Models in Isotope Hydrology*, IAEA-TECDOC- 910, IAEA, Vienna (1996) 9–58.
- [22] MICHEL, R.L., Residence times in river basins as determined by analysis of long-term tritium record, *J. Hydrol.* **130** (1992) 367–378.
- [23] SCHOTTERER, U., FRÖHLICH, K., STICHLER, W., TRIMBORN, P., Temporal variation of ^{18}O and deuterium excess in precipitation, river and spring waters in Alpine regions of Switzerland, *Isotope Techniques in the study of Past and Current Environmental Changes in the Hydrosphere and the Atmosphere*, IAEA, Vienna (1993) 53–64.
- [24] MCDONNELL, J.J., Where does water go when it rains? Moving beyond the variable source area concept of rainfall-runoff response, *Hydrol. Proc.* **17** (2003) 1869–1875.
- [25] VÖRÖSMARTY, C.J., MEYBECK, M., Responses of continental aquatic systems at the global scale: New paradigms, new methods, *Vegetation, Water, Humans and the Climate* **3** (2004) 75–413.
- [26] GAT, J.R., “The isotopic river continuum model”, *Isotope Hydrology Water Resource Management*, IAEA, Vienna (2003) 62–63.
- [27] MARTINELLI, L.A., GAT, J.R., DE CAMARGO, P.B., LARA, L.L., OMETTO, J.H.P.B., The Piracicaba river basin: isotope hydrology of a tropical river basin under anthropogenic stress, *Isotopes in Environmental and Health Studies* **40** 1 (2004) 45–56.
- [28] KENDALL, C., COPLEN, T., Distribution of oxygen-18 and deuterium in river waters across the United States, *Hydrol. Processes* **15** (2001) 1363–1393.
- [29] BIRKS, S.J., GIBSON, J.J., GOURCY, L., AGGARWAL, P.K., EDWARDS, T.W.D., Maps and animations offer new opportunities for studying the global water cycle, *EOS Trans. AGU* **83** 37 (2002) 406.
- [30] BOWEN, G.J., WILKINSON, B.H., Spatial distribution of $\delta^{18}\text{O}$ in meteoric precipitation, *Geology* **30** 4 (2002) 315–318.
- [31] BOWEN, G.J., REVENAUGH, J., Interpolating the isotopic composition of modern meteoric precipitation, *Water Resour. Res.* **39** 10 (2003) 1299.
- [32] DUTTON, A., WILKINSON, B.H., WELKER, J.M., BOWEN G.J., LOHMANN K.C., Spatial distribution and seasonal variation in $^{18}\text{O}/^{16}\text{O}$ of modern precipitation and river water across the conterminous USA, *Hydrol. Proc.* **19** (2005) 4121–4146.
- [33] HOFFMANN, G., WERNER, M., HEIMANN, M., Water isotope module of the ECHAM atmospheric general circulation model: A study on timescales from days to several years, *J. Geophys. Res.* **103** D14 (1998) 16871–16896.
- [34] STURM, K., HOFFMANN, G., LANGMANN, B., STICHLER, W., Simulation of $\delta^{18}\text{O}$ in precipitation by the regional circulation model REMOiso, *Hydrol. Proc.* **19** 17 (2005) 3425– 3444.
- [35] HENDERSON-SELLERS, A., MCGUFFIE, K., NOONE, D., IRANNEJAD, P., Using stable water isotopes to evaluate basin-scale simulations of surface water budgets, *J. Hydrometeor.* **5** (2005) 805–822.
- [36] FEKETE, B.M., GIBSON, J.J., AGGARWAL, P., VÖRÖSMARTY, C.J., Application of isotope tracers in continental scale hydrological modelling, *J. Hydrol.* **220** (2006) 444–456.
- [37] BOWEN, G.J., EHLERINGER, J.R., CHESSON, L.A., STANGE, E., CERLING, T.E., Stable isotope ratios of tap water in the contiguous United States, *Water Resour. Res.* (2007) **43**.
- [38] AGGARWAL, P.K., ALDUCHOV, O., ARAGUÁS-ARAGUÁS, L., DOGRAMACI, S., KATZLBERGER, G., KRIZ, K., KULKARNI, K.M., KURTTAS, T., NEWMAN,

- B.D., PUCHER A., New capabilities for studies using isotopes in the water cycle, EOS Trans. AGU **88** 49 (2007) 537–538.
- [39] VITVAR, T., AGGARWAL, P.K., HERCZEG, A.L., Global Network is launched to monitor isotopes in rivers, Eos Trans. AGU **88** 33 (2007) 325–326.
- [40] AGGARWAL, P.K., ARAGUAS-ARAGUAS, L.J., GROENING. M., KULKARNI, K.M., KURTTAS, T., NEWMAN, B., VITVAR, T., “Global hydrologic isotope data and data networks”, Isoscapes — Understanding movement, pattern and process on Earth through isotope mapping, (WEST, J.B., BOWEN, G.J., DAWSON, T.E., TU, K.P., Eds) Springer 2010 (2010) 33–51.

ENVIRONMENTAL ISOTOPE RATIOS OF RIVER WATER IN THE DANUBE BASIN

D. Rank^a, W. Papesch^b, G. Heiss^b, R. Tesch^b

^a Center of Earth Sciences,
University of Vienna, Vienna, Austria

^b Austrian Institute of Technology,
Health and Environment Department, Seibersdorf, Austria

Abstract. The objectives of the Danube study were documentation of existing data and completion of long term data sets (²H, ³H, ¹⁸O), continuation of monthly sampling of river water, investigation of short term influences, and preliminary interpretation of long term isotope records of river water with respect to hydrological processes, meteorological conditions and environmental changes. Furthermore, this report includes the complete ³H and ¹⁸O data set for the Danube at Vienna (1963–2005) and a summary of the results from the Joint Danube Survey 2 (2007). $\delta^{18}\text{O}$ values of JDS2 river water samples ranged from -13.1‰ (Inn, alpine river) up to -6.4‰ (River Sio, evaporation influence). The $\delta^{18}\text{O}$ value of the Danube increased from -10.8‰ after the confluence of the Inn River with the upper Danube up to -9.6‰ at the mouth, with a major change after the inflow of Tisa and Sava. The isotopic composition of river water in the Danube Basin is mainly governed by the isotopic composition of precipitation in the catchment area, while evaporation effects play only a minor role. Short term and long term isotope signals from precipitation are thus transmitted through the whole catchment. Tritium concentrations in most parts of the Danube river system lay around 10 TU during the JDS2 period and reflected the actual ³H content of precipitation in Central Europe, but ³H values up to 40 TU in the Danube and up to 250 TU in some tributaries are clear evidence for discontinuous releases of ³H from local sources (nuclear power plants) into the rivers.

1. INTRODUCTION

Isotope ratios of hydrogen and oxygen in river water are indicators for hydrological processes in the catchment (e.g. formation of base flow), for interactions between river water and groundwater, for mixing processes in a river, for travel time and dispersion of short term pulses (e.g. pollution pulses) as well as for hydrological/climatic changes in the drainage area of a river. The investigation of such topics requires good knowledge of the ‘isotopic environment’.

The isotopic composition of hydrogen and oxygen in river water is mainly determined by the isotopic composition in precipitation water in the drainage area (altitude effect, continental effect, seasonal variations, storms; see e.g. [1, 2]). Several hydrological parameters and processes are modifying this isotopic signature and its temporal variation: delayed runoff of winter precipitation (snow cover), residence time of groundwater discharged to the river, confluence with tributaries, evaporation from lakes in the river system, climatic changes (change in environmental temperature, spatial and temporal change of precipitation distribution in the drainage area, etc.) as well as anthropogenic influences on the hydrological regime (e.g. reservoirs, irrigation).

The Danube is the second largest river in Europe, spanning a total of 2857 km between its source and its mouth in the Black Sea and covering an overall catchment area of



FIG. 1. The Danube Basin river system with indication of the sampling points of the Austrian network for isotopes in river water (based on ESRI ArcGIS 9.3).

817 000 km² with an average discharge of about 6500 m³/s at its mouth (Fig. 1). On a rough catchment scale, Lászlóffy [3] sectioned the Danube River into four general units (Upper, Middle, Lower Danube and the Danube Delta) based on geo-morphological and hydrological features. The Upper Danube covers a length of 900 km and is strongly influenced by the discharges of the alpine tributaries Isar, Inn, Traun, and Enns. The Middle Danube starts where the Danube enters the Carpatian Basin ('Porta Hungarica', river 1880 km) and stretches over 925 km. The major tributaries influencing the hydrology of the Danube within this section include Drava, Tisza, Sava, and Velika Morava. The Lower Danube section stretches over 885 km from the point where the Danube breaks through the Carpatian and Balkan Mountains (Iron Gate, around river km 1000) and passes through the Walachian Lowlands. Its major tributaries in this section include the Siret and Prut. The last section is represented by the arms of the Danube Delta.

2. SURVEY OF ISOTOPIC COMPOSITION OF RIVER WATER IN THE DANUBE BASIN

The Joint Danube Survey 2 (JDS2) in 2007, which was organized by the International Commission for the Protection of the Danube River (ICPDR), was a welcome opportunity to improve the database for environmental isotopes in the Danube Basin [4, 5]. At that time there were several regional isotope studies e.g. [6–8] and a more extensive one on the Danube between Vienna and the Black Sea [9]. There was especially a lack of isotope data from the lower part of the Danube Basin.

The core activity of the JDS2 focused on the Danube River and on the mouths of the main tributaries. Ninety-six sampling points were selected, starting near Ulm (river km 2600) on 13 August 2007 and reaching the Black Sea (river km 0) on 27 September 2007. In parallel with the core activity on the Danube River, longitudinal surveys on some major tributaries were performed at the national/regional level: Morava, Drava, Tisa, Sava, Velika Morava, Arges, Olt, Jantra, Iskar, Russenski Lom, and Prut. Also samples from the Austrian network for isotopes in rivers were included from the same time period (Fig. 1).

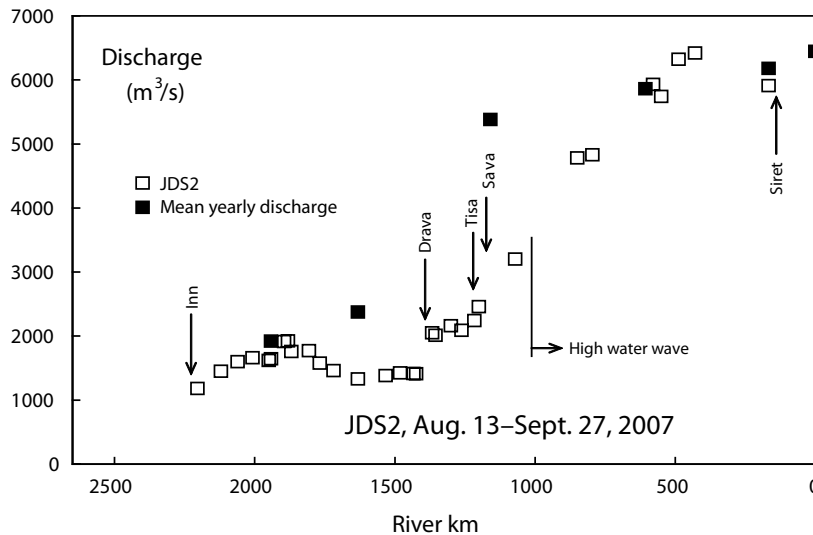


FIG. 2. Joint Danube Survey 2 (13 August–27 September 2007): discharge at the time of sampling and some mean yearly discharge values [3].

One liter PET bottles were filled with river water from the middle of the stream at the sampling points of the JDS2 and the national sampling campaigns and brought to the isotope laboratories of the Austrian Research Centers (ARC) in Seibersdorf. Stable isotope measurements were performed using isotope mass spectrometers Finnigan MAT 251 and DeltaPlusXL equipped with automatic equilibration lines. All results were reported as relative abundance ($\delta^2\text{H}$ and $\delta^{18}\text{O}$, respectively) of the isotopes ^2H and ^{18}O in permil (‰) with respect to the international standard VSMOW (Vienna Standard Mean Ocean Water). The accuracy of $\delta^2\text{H}$ and $\delta^{18}\text{O}$ measurements is better than $\pm 1.0\text{‰}$ and $\pm 0.1\text{‰}$, respectively. Samples for ^3H measurement were electrolytically enriched and analyzed using low level liquid scintillation counting (precision $\pm 5\%$, $1 \text{ TU} = 0.119 \text{ Bq/kg}$ for water). The same analytical characteristics apply to all data presented in this paper.

Low water conditions prevailed in the Danube during the first half of the JDS2 sampling period, from Ulm (river km 2600) down to the Iron Gate (about river km 1000) and also during sampling campaigns on the largest tributaries, the Inn, Drava, Tisa, and Sava (Fig. 2). Heavy storms in the upper Danube Basin on 5–7 September led to a high water situation on the upper Danube. The discharge at Vienna (rkm 1491) increased from about $1500 \text{ m}^3/\text{s}$ to more than $7000 \text{ m}^3/\text{s}$ (yearly mean about $1920 \text{ m}^3/\text{s}$) [5]. The high water wave reached the sampling ships in the region of the Iron Gate. Since the storms did not affect the lower Danube Basin, the Danube discharge downstream of the Iron Gate increased only by a factor slightly more than two and values of $6000\text{--}7000 \text{ m}^3/\text{s}$ were in the order of the yearly mean. The high water wave was probably also damped to a certain extent when it passed the Iron Gate Danube section with its two reservoirs.

2.1. Stable isotopes (^2H , ^{18}O) in river water

The spatial distribution of $\delta^{18}\text{O}$ in river water in the Danube Basin is shown in Fig. 3, with lower values in mountainous regions and higher values in lowland tributaries. The $\delta^{18}\text{O}$

value of the Danube increases from -10.8‰ after the confluence of upper Danube (generally low-lying drainage areas have higher $\delta^{18}\text{O}$ values) and the Inn River (mainly an alpine drainage area, thus with lower $\delta^{18}\text{O}$ values) up to -9.6‰ at the mouth (Figs. 3 and 4). This increase (1.2‰) is due to the decreasing influence of runoff contributions from the alpine part of the drainage area and the corresponding increase of lower elevation contributions. The Inn River with its alpine catchment has the lowest $\delta^{18}\text{O}$ value (-13.1‰) in the whole Danube Basin. The highest value (-6.4‰) was found for the River Sio with discharge from Lake Balaton. This enrichment in heavy isotopes is due to a strong evaporation influence on the lake water.

The $\delta^{18}\text{O}$ record exhibits three significant changes along the river (Fig. 4): The first is at the confluence of upper Danube and Inn; the second is caused by inflow from the tributaries Tisa and Sava with their higher ^{18}O content; the third significant change in stable isotope ratios in the region of the Iron Gate cannot be attributed to the inflow of tributaries. It is obviously caused by the extreme precipitation event in Central Europe during 5–7 September, resulting in slightly higher $\delta^{18}\text{O}$ values for the Danube between the Iron Gate and the river mouth. A comparison of the $\delta^{18}\text{O}$ values of event water (-9.8‰ , precipitation water 5–7 September) and the yearly mean values of precipitation at Vienna (2006: -9.7‰ , 2007: -9.6‰) showed that the $\delta^{18}\text{O}$ value of the event water lay close to the yearly mean values. Without a prominent differential ^{18}O signal in the rain water, there should also be only a minor influence of the high water wave on the $\delta^{18}\text{O}$ values of the lower Danube. From Fig. 3, a maximum increase of $0.2\text{--}0.3\text{‰}$ in $\delta^{18}\text{O}$ can be assessed for the JDS2 water samples downstream of the Iron Gate where the high water wave had reached the sampling ships. Approaching the Danube delta, this amount had probably become even lower because all (relatively small) tributaries of the lower Danube had significantly higher $\delta^{18}\text{O}$ values than the Danube, and their influence on the $\delta^{18}\text{O}$ values of the Danube was reduced by the high water wave.

The $\delta^2\text{H}\text{--}\delta^{18}\text{O}$ diagram (Fig. 5) shows that most of the values lie close to the Global Meteoric Water Line ($\delta^2\text{H} = 8 \times \delta^{18}\text{O} + 10$), which suggests that surface water evaporation along the Danube river course is minor and may be neglected for the Danube and the majority of tributaries. Only River Sio carries water significantly influenced by evaporation — with an



FIG. 3. $\delta^{18}\text{O}$ of river water in the Danube Basin (13 August–27 September 2007).

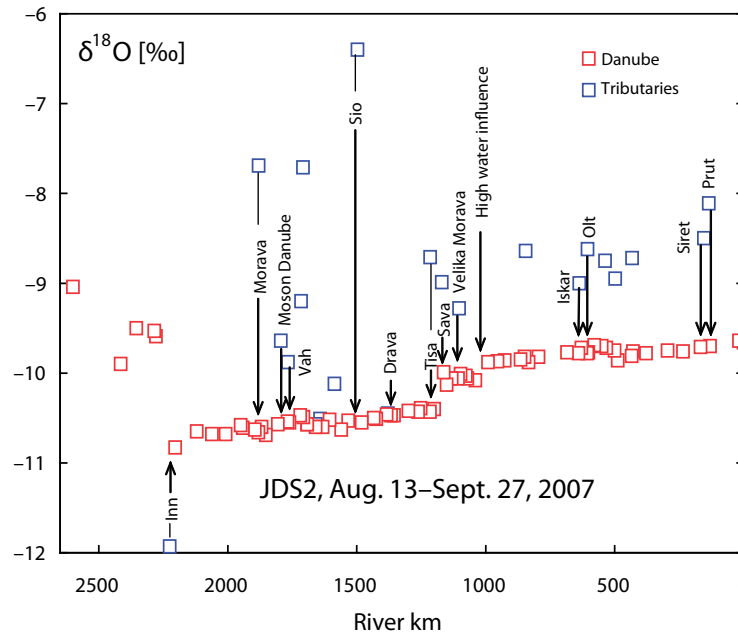


FIG. 4. Longitudinal $\delta^{18}\text{O}$ profile of the Danube (river km 2600, Ulm–river km 0, Black Sea) and $\delta^{18}\text{O}$ values of tributaries at confluence (13 August–27 September, 2007).

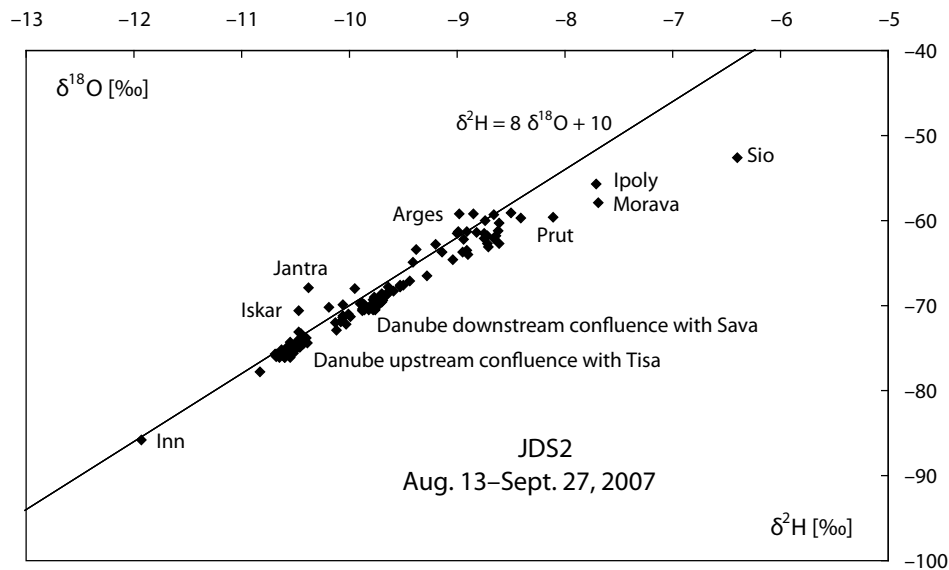


FIG. 5. $\delta^2\text{H}$ - $\delta^{18}\text{O}$ diagram for river water samples from the Danube Basin.

isotopic signal below the meteoric water line — because it contains discharge water from Lake Balaton. The tributaries Ipoly, Morava and Prut also show slightly pronounced evaporation effects, probably due to the existence of reservoirs in the river course. The higher deuterium excess values ($d = \delta^2\text{H} - 8 \times \delta^{18}\text{O}$) in the upper sections of the rivers Iskar, Jantra and Arges — with isotopic signal above the meteoric water line — are probably due to local orographic (mountainous) conditions. Such a dependence of the deuterium excess on the orographic situation was found in the Austrian Alps, where mountain and valley precipitation differed significantly in deuterium excess as a consequence of re-evaporation processes (higher d-excess values on the mountains, lower d-excess values in the valleys; [2, 10], see Section 7).

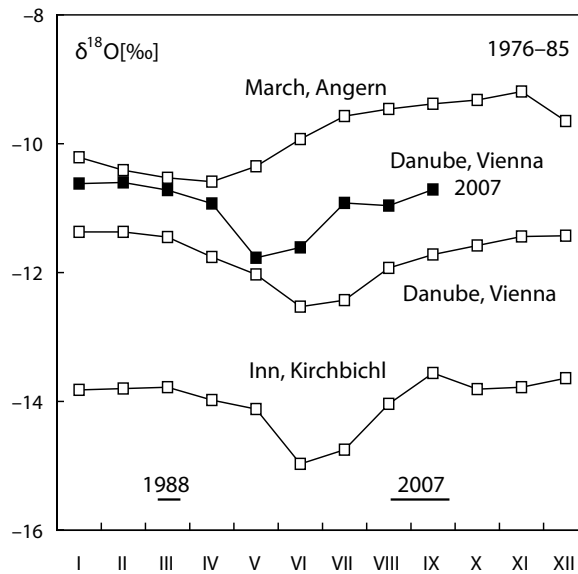


FIG. 6. Average seasonal $\delta^{18}\text{O}$ variations (1976–1985) in Austrian rivers and $\delta^{18}\text{O}$ variation in Danube water at Vienna 2007 with indication of sampling periods 1988 and 2007.

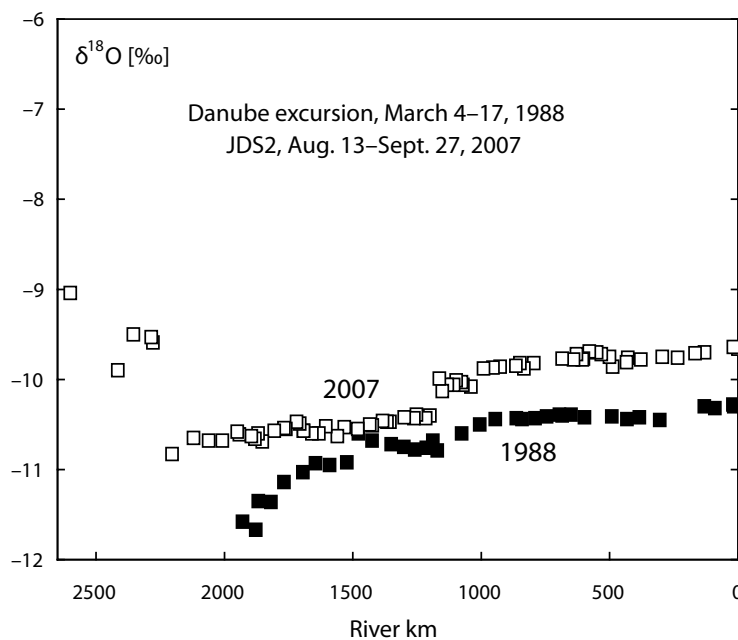


FIG. 7. Longitudinal $\delta^{18}\text{O}$ profile of the Danube: surveys 1988 and 2007 (river km 2600, Ulm–river km 0, Black Sea).

The first longitudinal isotope record for the Danube originates from a ship based scientific excursion organized by the ‘Internationale Arbeitsgemeinschaft Donauforschung’ (IAD, International Association of Danube Research) in March 1988 [9]. Although the surveys in 1988 and 2007 were performed in different seasons (March and August/September, respectively), the $\delta^{18}\text{O}$ values from both surveys seem to be comparable with each other. Regarding the seasonal $\delta^{18}\text{O}$ variation in Danube water, both sampling periods lie outside the typical summer minimum caused by snowmelt in the high alpine parts of the catchment (Fig. 6). Therefore, we could expect $\delta^{18}\text{O}$ values close to the yearly means in both cases.

A comparison of the 1988 data with the data from JDS2 highlights a significant increase in heavy isotope content during the last 20 years (Fig. 7). Even if we take into account that part of this difference is due to seasonal effects and the influence of precipitation events, the remaining part of the increase is clear evidence of hydrological/climatic changes in the drainage area of the Danube. It is probably mainly the increase in environmental temperature during the last decades which led to an increase in heavy isotope concentrations in precipitation in Central Europe as a consequence of the strong temperature dependence of isotope fractionation during evaporation and condensation processes [2, 11]. This isotopic trend in precipitation is reflected in the long term $\delta^{18}\text{O}$ record of the Danube (significant $\delta^{18}\text{O}$ increase during the 1980s; see Section 4, Fig. 11).

2.1.1. Tritium (^3H) Content of River Water

The ^3H distribution resulting from the JDS2 water samples (Figs 8 and 9) can be regarded as representative only for those parts of the river system where local ^3H releases to the rivers do not play a significant role. Since such releases — mainly from nuclear power plants — are usually in the form of short term pulses, the ^3H content measured in river water depends very much on the moment the sample is collected. The ^3H content of actual precipitation in Central Europe would lead to ^3H concentrations of about 10 TU in river water and slightly lower concentrations in tributaries, the drainage area of which is influenced by Mediterranean air masses [2]. The samples from JDS2 showed ^3H values of up to 40 TU in the Danube and up to 250 TU in the tributaries (Figs 8 and 9).

River water in most parts of the Danube Basin reflects the actual environmental ^3H level of about 10 TU with precipitation as input. Yearly mean ^3H contents of precipitation at Vienna, for instance, were 10.2 TU and 9.5 TU for 2006 and 2007, respectively. All river water values exceeding about 12 TU are believed to be the consequence of human activities. In most cases such contamination is of a short term character. This can clearly be seen, for instance, from ^3H distribution in the Sava River (Fig. 8) or from the long term ^3H record of the Danube at Vienna (see Section 4, Fig. 12). An example of such a short term contamination peak is shown in Fig. 13 (Section 6, [12]). The source of this ^3H peak was probably a nuclear power plant (NPP



FIG. 8. ^3H content of river water in the Danube Basin (13 August–27 September 2007).

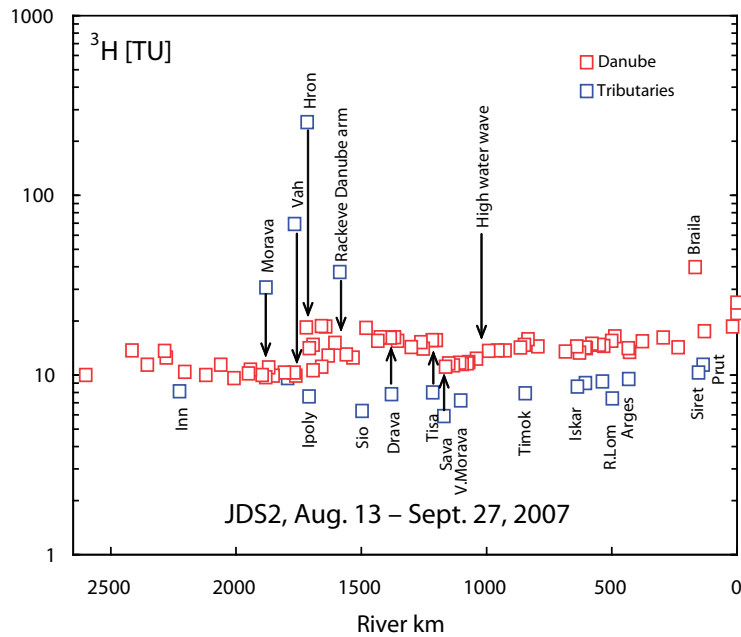


FIG. 9. Longitudinal ^3H profile of the Danube (rkm 2600, Ulm – rkm 0, Black Sea) and ^3H content of tributaries at confluence (13 August–27 September 2007).

Isar 2) some 400 km upstream of the sampling point. Although the ^3H pulse passed several dams, the half width of the ^3H peak was only about two days. On the Rhine River, such ^3H peaks originating from NPP releases were used for determining travel time and dispersion of contamination pulses [13].

In some cases it is easy to identify the source of the ^3H contamination pulses, like at the NPP Dukovany for Morava, NPP Bohunice for Vah, NPP Mohovce for Hron, NPP Krško for Sava and NPP Isar 2 for the upper Danube. For the lower sections of the Danube, it is more difficult to identify the source because all NPPs upstream of the sampling point are possible candidates. The highest ^3H content in the Danube during the JDS2 period, for instance, was found at Braila (40 TU), a single significant higher value between lower concentrations upstream and downstream. The nearest NPP is Cernavodă, some 120 km upstream, but one cannot be sure if this was the source. In such cases, the identification of the ^3H source requires sampling with good temporal and spatial resolution.

The storm event of 5–7 September 2007 with ^3H concentrations near the yearly mean values — 11.2 TU in precipitation water from 5–7 September at Vienna — led to some dilution of the ^3H concentration in the lower Danube. A ^3H content of about 60–70 TU can be assessed for the ^3H maximum at Braila (40 TU, Fig. 9) without the additional water event.

Tritium concentrations of river water in 2007 were generally lower than in 1988 (Fig. 10). This reflects a general decrease in environmental ^3H levels (see Section 4, Fig. 12). While in the 1988 record, only inflow from the Tisa and Sava, as well as higher ^3H concentrations in the NPP Kozloduj wastewater plume caused significant changes in the ^3H concentration profile of the Danube, the 2007 record exhibits much quicker changes in ^3H concentrations in the Danube stream, probably due to the operation of several NPPs along the Danube (such as Isar 2, Dukovany, Bohunice, Mohovce, Paks, Krško, Kozloduj, and Cernavodă).

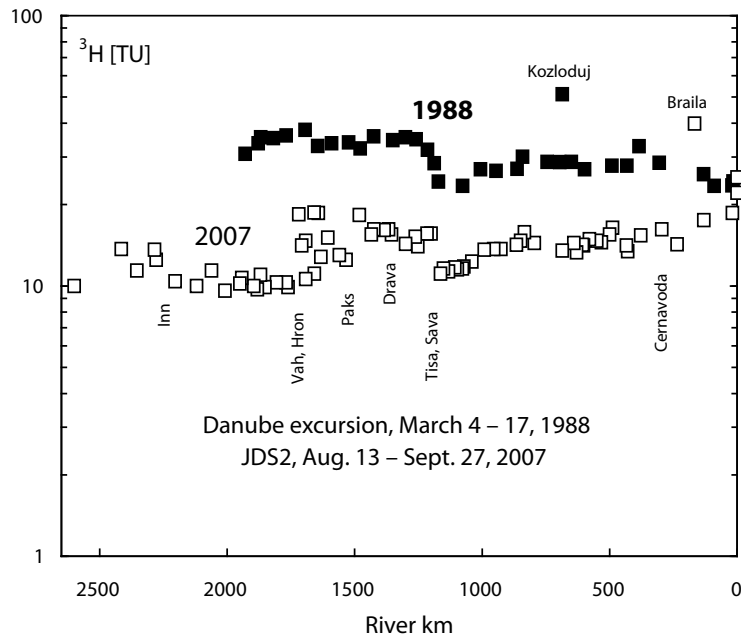


FIG. 10. Longitudinal ^3H profile of the Danube: surveys 1988 and 2007 (rkm 2600, Ulm–rkm 0, Black Sea).

3. CHARACTERISTICS OF THE UPPER DANUBE BASIN

The catchment area around Vienna (the Upper Danube Basin) is about 103 000 km². The mean annual flow rate is around 1920 m³/s, with a seasonal variation typical of alpine rivers (a minimum of about 1300 m³/s in November and a maximum of about 2700 m³/s in July).

The catchment upstream of Vienna can be divided into three sectors:

- (1) The sector upstream of Passau: This sector represents about one half of the study area. The mean annual flow rate at Passau is around 670 m³/s (35% of the flow rate at Vienna), with a maximum in March (880 m³/s) and a minimum in October (520 m³/s). The mean altitude of this sector is relatively low compared to the Alpine regions. Groundwater discharge is the main mechanism forming base flow in this part of the river. The period of high water is mainly controlled by precipitation and melting during late winter and early spring.
- (2) The catchment area of the Inn River: The Inn, which enters the Danube at Passau, has a hydrological regime typical of alpine rivers. It is the most important tributary in this sector, contributing 725 m³/s on average (38% of the flow rate at Vienna), thus doubling the flow rate when it merges with the Danube. Maximum flow rates are observed in June/July (1200 m³/s) and the minimum occurs in January (400 m³/s).
- (3) The sector between Passau and Vienna. Along this stretch other alpine rivers, with a mean annual flow rate of about 505 m³/s (27% of the flow rate at Vienna), enter the Danube. These rivers are characterized by a hydrological regime similar to that of the Inn, with maximum flow rates in May/June (800 m³/s) and a minimum in January (270 m³/s).

The amount of precipitation in the Upper Danube Basin shows a distinct gradient with altitude. It rises from 650–900 mm/a in the lowland areas up to about 3000 mm/a in the high mountain ranges exposed to the west and north. For stations located in lowland areas, summer precipitation represents more than 60% of annual precipitation. For high altitude stations, winter precipitation is more important, although it is stored on the surface as snow cover until spring and summer, when melting takes place.

4. LONG TERM ISOTOPE RECORDS OF PRECIPITATION AND RIVER WATER IN AUSTRIA

Monthly surface water samples (grab samples) were taken at about 20 locations in Austria (about 15 on rivers, Fig.1, Table 1) since 1976 (from the Danube at Vienna since the 1960s). The river samples were taken mainly at locations where the rivers cross the Austrian border. These samples are stored at the Arsenal water sample bank in Vienna. Only some of them were analyzed, but the sample material was still available for investigations within the framework of the CRP. Although the goal was to complete a long term isotope record for rivers during the CRP period, this work is not yet finished.

The updated long term isotope patterns of Austrian rivers are shown in Figs 11, 12, and 13 [8, 11]. No major changes in trends could be observed during the CRP period (2002–2005).

Isotope ratios in river water reflect the isotopic composition of precipitation in the catchment area depending on the residence time of the water in the catchment (short term and long term components), provided that evaporation influence does not significantly alter isotopic

TABLE 1. RIVER WATER SAMPLING SITES IN AUSTRIA (MONTHLY GRAB SAMPLES) WITH MEAN ANNUAL DISCHARGE (MQ), LONG TERM AVERAGE $\delta^{18}\text{O}$ VALUES (1976–1985 AND 1996–2005) AND AVERAGE ^3H CONTENT 2005 OF RIVER WATER

River	Sampling location	Latitude/longitude (degrees)	Drainage area (km ²)	MQ (m ³ /s)	$\delta^{18}\text{O}$ (‰) 1976–1985	$\delta^{18}\text{O}$ (‰) 1996–2005	^3H (TU) 2005
Danube	Engelhartszell(O-1)	48.5046/13.7361	77090	1400	-11.82	-11.24	21.9
	Wien (O-5)	78.2662/16.3695	101 731	1915	-11.75	-11.22	16.3
	Hainburg (O-9)	48.1507/16.9407	104 178	–	–	–	13.9
Drau	Lavamünd (O-10)	46.6211/14.5481	11 052	–	-11.86	-11.08	8.6
Inn	Kirchbichl (O-13)	47.5233/12.0939	9 319	289	-14.01	-13.33	9.6
	Schärding (O-12)	48.4361/13.4417	25 664	729	-12.84	-12.09	10.0
Leitha	D.-Brodersdorf (O-14)	47.9384/16.4784	1 599	10	-10.74	-10.99	10.0
March	Angern (O-15)	48.3840/16.8356	25 624	107	-9.88	-9.33	46.9
Mur	Spielfeld (O-16)	46.7106/15.6361	9 480	140	-11.49	-10.59	9.7
Salzach	Salzburg (O-18)	47.8169/13.0375	4 426	176	-13.12	–	10.0
Ill	Gisingen (O-11)	47.2609/9.5790	1 281	65	-13.46	–	10.9*
Rhine	Lustenau (O-17)	47.4482/9.6590	6 110	232	-13.58	-12.74	9.3

*) average value 2004.

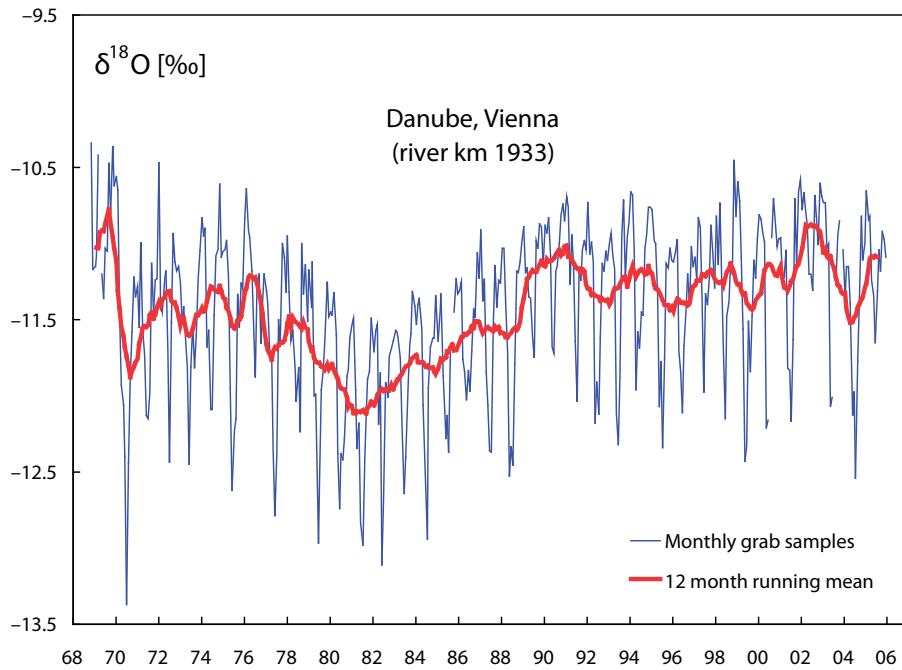


FIG. 11. $\delta^{18}\text{O}$ time series for the Danube at Vienna (monthly grab samples, 12 month running mean for $\delta^{18}\text{O}$).

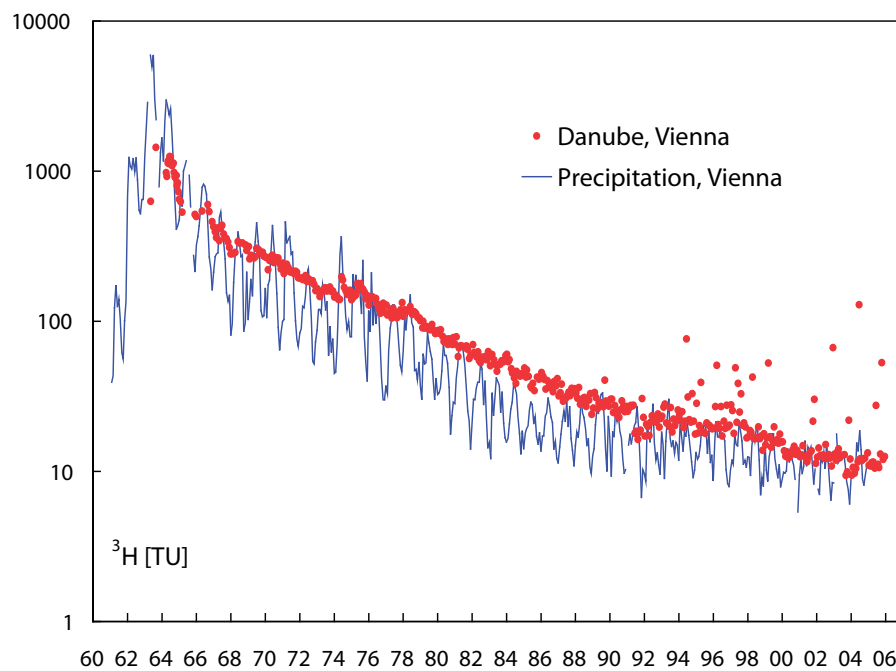


FIG. 12. Tritium time series of precipitation (monthly mean values) and Danube (monthly grab samples) at Vienna. The sometimes higher ^3H content in Danube water during the last years is due to releases from a nuclear power plant some 400 km upstream from Vienna.

composition. Isotope time series from different stations within the Austrian precipitation network show significant but not uniform long term trends. While the 10 year running means of some mountain stations exhibit a pronounced increase in $\delta^{18}\text{O}$ of about 1‰ since 1975, the change in $\delta^{18}\text{O}$ at valley stations is much lower (Fig. 14). There are also differences in temporal patterns. Differences in $\delta^{18}\text{O}$ values of sampling stations at similar altitudes can be

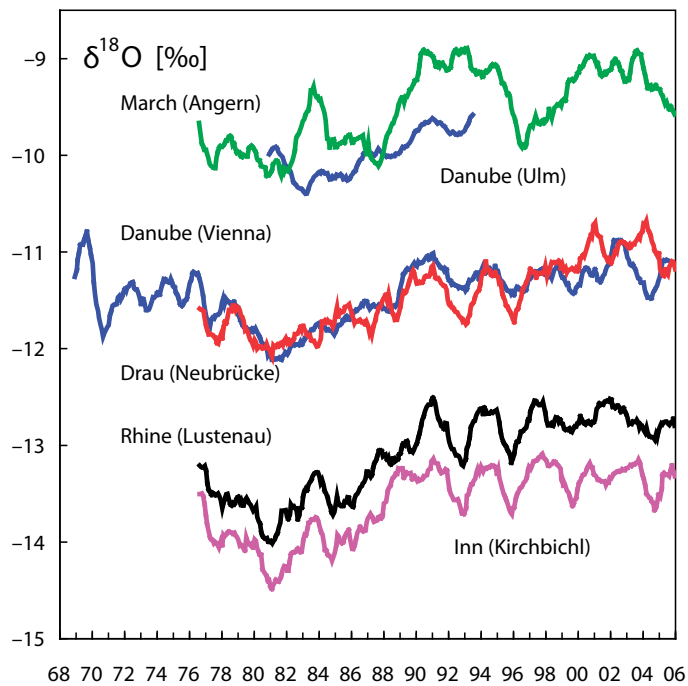


FIG. 13. $\delta^{18}\text{O}$ records of the Danube, some tributaries and the alpine part of the Rhine (12 month running mean). All the alpine rivers show a similar long term pattern (including the Inn, Drau and Rhine). This isotopic signal is also dominant in the Danube at Vienna. The upper Danube (the Ulm, data from [8]) and the March River show somewhat different isotopic behaviour.

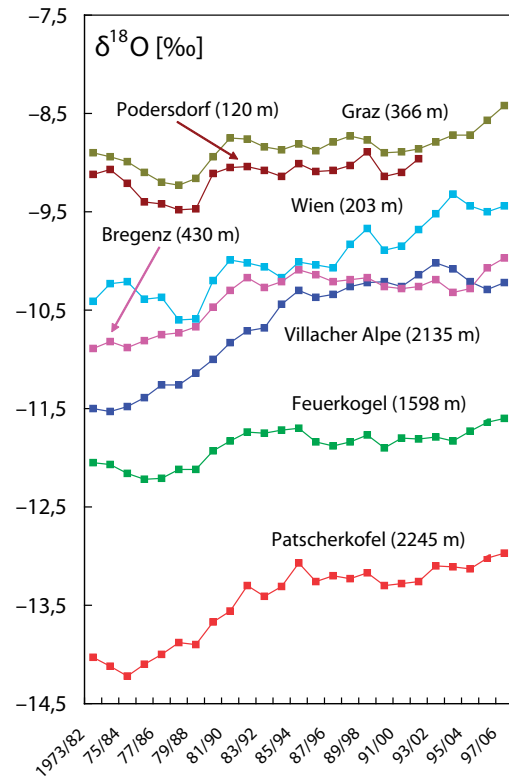


FIG. 14. Long term $\delta^{18}\text{O}$ variations (10 year running mean) at several stations of the Austrian Network for Isotopes in Precipitation [2] (updated).

explained by air moisture origins. An Atlantic influence (moisture from NW) creates lower $\delta^{18}\text{O}$ values (e.g. Patscherkofel and Bregenz) than a Mediterranean one (e.g. Villacher Alpe and Graz). The main reason for differing $\delta^{18}\text{O}$ values is that Atlantic air masses have a longer way to travel over the continent, and during the trip successive rainout (continental effect) depletes moisture stepwise of heavy isotopes.

Stable isotope variations in precipitation are a consequence of isotope effects accompanying each step of the water cycle. Temperature is the most influencing parameter, but there are also other influences, such as changes in the origin of air masses or in rain formation mechanisms [14–16]. Fluctuations in $\delta^{18}\text{O}$ values of precipitation also correlate to a large extent with those of the North Atlantic Oscillation (NAO) index, except during some years when the influence of the amount of precipitation probably dominates in rain formation mechanisms [17].

Comparisons of long term trends of stable isotope ratios in precipitation and river water (such as in Figs. 13 and 14) reveal that, in the case of the Upper Danube Basin, river water quite accurately reflects isotope trends of precipitation, such as the significant increase in $\delta^{18}\text{O}$ values during the 1980s. The different sources of air moisture (Atlantic, Mediterranean) are also clearly represented isotopically in the river system. The alpine rivers Drau (Mediterranean influence) and Inn (Atlantic influence) differ significantly in their $\delta^{18}\text{O}$ values (Fig. 13).

It became evident from long term trend curves for river water and precipitation at Vienna (Fig. 15) that the $\delta^{18}\text{O}$ signal is delayed in the Danube by approximately one year with respect

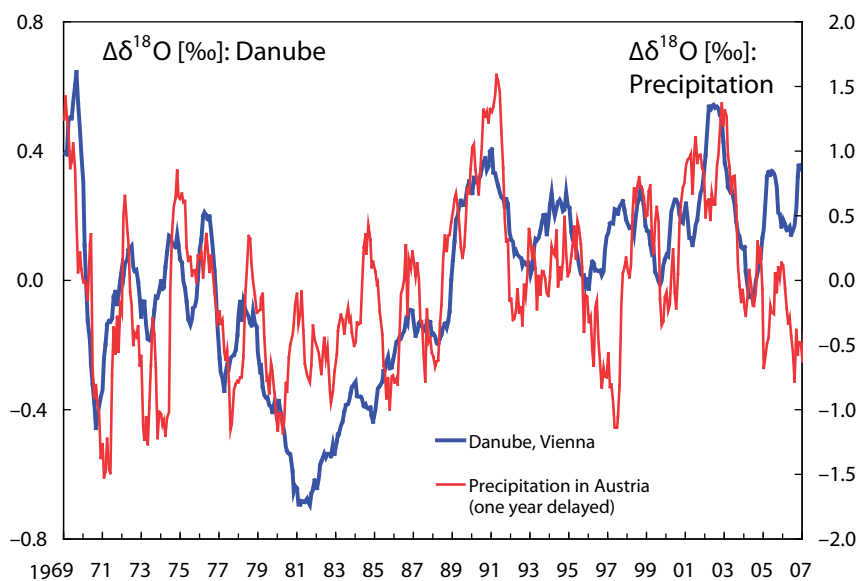


FIG. 15. Comparison of the long term trend curves of $\delta^{18}O$, expressed as departures from the long-term mean value, for the Danube and for precipitation at Vienna, shifted by 1 a.

to precipitation [8]. The agreement of trend curves is partly very good, though there are discrepancies, most probably in the specific distribution of precipitation amounts for low and high altitude portions of the catchment during this period.

Figure 6 illustrates typical seasonal isotope patterns in Austrian rivers. The Inn River represents a typical alpine river, while the March River mainly drains lowland areas. The Danube represents a mixture of these different influences, also displaying the significant alpine melting minimum in summer [8].

The 3H background concentration in Danube water at Vienna has decreased to about 10 TU in the last years (Fig. 12) and remains more or less constant at the moment. These 10 TU are very similar to the mean 3H content of precipitation in the catchment area during the last years and close to the natural 3H level. The sometimes higher 3H values in river water are due to releases from nuclear installations as discussed in Section 2.2.

The time series of 3H in the Danube were modeled using the lumped parameter approach [8]. But the comparison between measured and modeled 3H contents in the river water revealed that the best fit which could be obtained (for a mean residence time of three years) was still not satisfactory.

5. LONG TERM ISOTOPE DATA SET (2H , 3H , ^{18}O) FOR THE DANUBE AT VIENNA (1963–2005)

Table A–2 (annex) presents the actual status of the Danube isotope data set, partially published in several papers, see for example Ref. [11] and yearly reports of the BVFA Arsenal [18]. The data set is based on monthly grab samples of Danube water at Vienna. The measurements were completed as far as samples were available at the Arsenal water sample bank in Vienna

(except $\delta^2\text{H}$, measurements, which only go back to 1988). Thus the data set is now ready for evaluations and model calculations. Discharge data can be seen in Ref. [19].

6. SHORT TERM HYDROLOGICAL EVENTS AND REPRESENTATIVENESS OF MONTHLY GRAB SAMPLES

Isotope data of daily grab samples and monthly average samples were compared to assess the representativeness of monthly grab samples. A set of daily Danube water samples taken at Hainburg between March 1996 and February 1997 was used for this investigation. Samples from each third day were measured (10 samples per month) and in addition there was a monthly average sample. Results of the isotope analyses (Fig. 16, Table 2) revealed that the yearly mean $\delta^{18}\text{O}$ value calculated from monthly average samples and monthly grab samples (from the middle of the month) differed by only 0.08 ‰. Therefore, at least in the case of the Danube, monthly grab samples seem to be a reasonable instrument for tracing long term trends on the basis of 12 month running means. Daily sampling is necessary to investigate single hydrological events (e.g. high waters, snow melting processes) and short term contaminations (Fig. 17).

A detailed interpretation of the isotope data from April to June 1996 in Fig. 16 is provided in Fig. 18. During this period, quick changes were taking place in the isotopic composition of river water, either due to snow melting processes in the mountains (warm periods), causing low $\delta^{18}\text{O}$ values, or to heavy spring rains, mostly causing high $\delta^{18}\text{O}$ values.

7. DEUTERIUM EXCESS IN THE ALPINE PART OF THE DRAINAGE AREA

The deuterium excess in precipitation and river water in the Danube Basin lies at around 10 ‰ (Fig. 5). Detailed investigations were performed to gain more insight into the behaviour of deuterium excesses in precipitation over the Eastern Alps within the framework of the CRP on Isotopic Composition of Precipitation in the Mediterranean Basin in Relation to Air Circulation Patterns and Climate [2]. The evaluation of long term isotope records had shown a completely different seasonal pattern of deuterium excess at both mountain and valley stations. While valley stations exhibited the expected minimum in summer, mountain stations showed a distinct maximum between June and October. These differences occurred even if

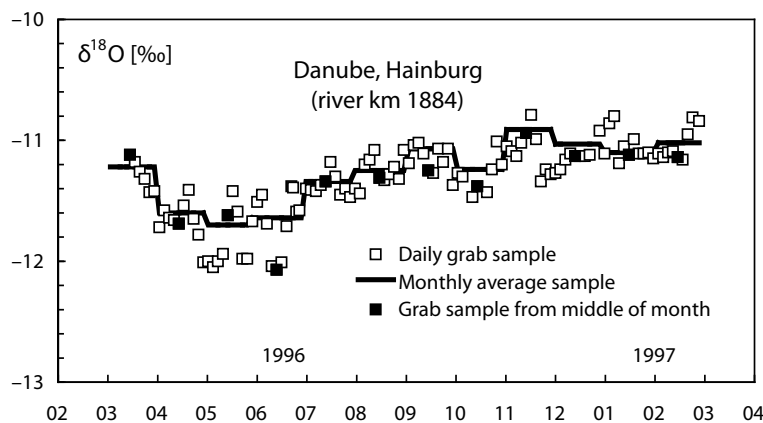


FIG. 16. $\delta^{18}\text{O}$ values of monthly averages and daily grab samples (from the Danube at Hainburg).

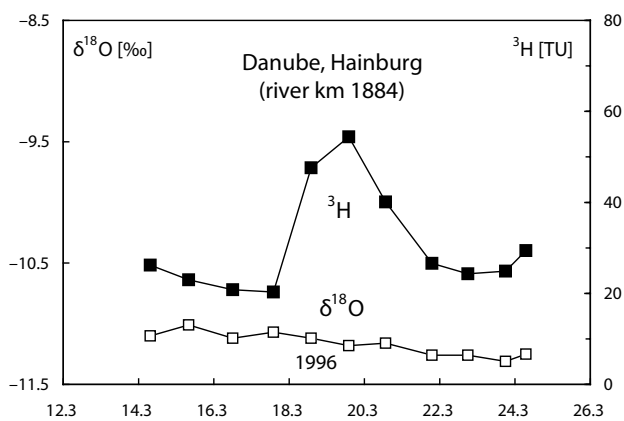


FIG. 17. Example of a ^3H contamination pulse in the Danube at Hainburg (river km 1884), probably the result of a release from a nuclear power plant some 400 km upstream [12].

TABLE 2: COMPARISON OF $\delta^{18}\text{O}$ VALUES OF MONTHLY AVERAGE AND MONTHLY GRAB SAMPLES (DANUBE AT HAINBURG)

Month	$\delta^{18}\text{O}$ [‰]		Δ
	Monthly average sample	Monthly grab sample	
Mar 1996	-11.22	-11.12	-0.10
Apr 1996	-11.60	-11.69	0.09
May 1996	-11.70	-11.62	-0.08
Jun 1996	-11.64	-12.07	0.43
Jul 1996	-11.34	-11.34	0.00
Aug 1996	-11.25	-11.31	0.06
Sep 1996	-11.07	-11.25	0.18
Oct 1996	-11.24	-11.38	0.14
Nov 1996	-10.91	-10.94	0.03
Dec 1996	-11.03	-11.13	0.10
Jan 1997	-11.10	-11.12	0.02
Feb 1997	-11.02	-11.14	0.12
12 month average	-11.26	-11.34	0.08

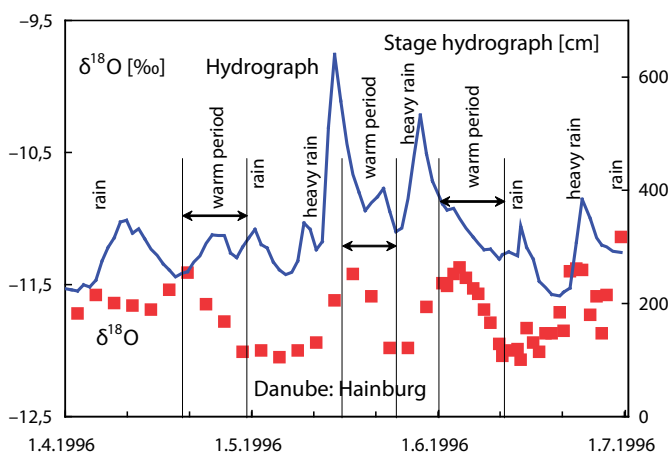


FIG. 18: Short term influences caused by snow melting processes in the mountains (warm periods) and spring rains.

the horizontal distance between mountain and valley station was only a few kilometers. From this we concluded that the reason for lower d-excess values at the valley station is obviously evaporation and/or isotopic exchange with air moisture during the falling of rain drops.

Further, an investigation was undertaken to examine whether Mediterranean influence could be the reason for higher d-excess values in the mountains. This could be excluded from trajectory studies for two mountain stations [17]. The last step was to look for the response in surface and groundwaters. For this, mountain lakes ('Salzkammergut' and the Traun River system) seemed to be good objects of investigation (Fig. 19). They are relatively deep and cold, and have a high throughflow (with a mean residence time of a few years), thus evaporation influences on the water's isotopic composition is negligible in most cases. These lakes become well mixed in late winter, so samples of outflow from the lakes taken at this time deliver more or less yearly mean isotopic values. Measured data show a clear correlation between $\delta^{18}\text{O}$ values and deuterium excess (between 7 and 13‰). From this, an altitude effect of about 0.43‰ per 100 m can be calculated regarding the deuterium excess (taking into account an altitude effect of -0.25‰ per 100 m for $\delta^{18}\text{O}$).

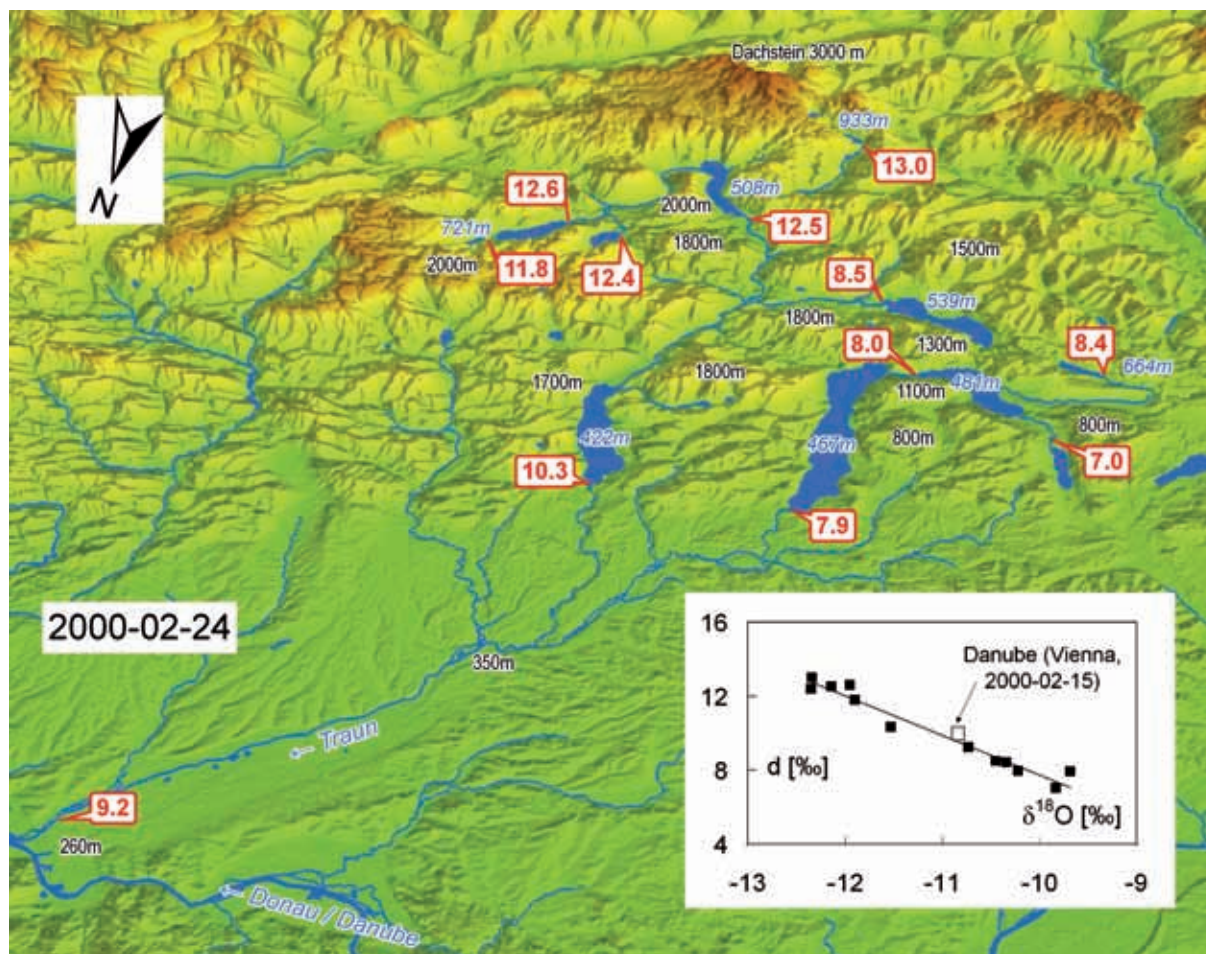


FIG. 19. Deuterium excess (red numbers) in alpine lakes of the River Traun system (Upper Austria, diagram area about 150 km × 110 km). Black numbers: elevation asl, blue: elevation of lake surface. Insert: correlation between deuterium excess and $\delta^{18}\text{O}$.

The results of these investigations lead to the conclusion that the relatively big variations of deuterium excess in Alps precipitation (with higher values in the mountains and lower values in valleys and forelands) are mainly ‘homemade’ and not the result of different origins of air masses transported into mountainous regions. Therefore, in the Alps, deuterium excess is probably no reliable tool to trace the origin of air masses and moisture coming from far away. For this purpose — to distinguish between Atlantic and Mediterranean origin — $\delta^{18}\text{O}$ (or $\delta^2\text{H}$) values and especially ^3H data are suitable instruments. River water coming from mountainous regions is a mixture of mountain and valley precipitation, so that the resulting deuterium excess is more or less ‘normal’ (around 10‰), when the river leaves the mountainous region.

Some questions still remain. The mechanism behind the higher deuterium excess in mountain precipitation is not yet clear (perhaps the influence of re-evaporation?). More detailed investigation of single precipitation events — sequential sampling — may provide more insight. The second question is, of course, can these findings in the Eastern Alps be transferred to other mountainous regions?

8. CONCLUSIONS AND OUTLOOK

Isotope ratios in Danube water reflect the isotopic composition of precipitation in the Danube Basin depending on the residence time of water in the catchment area (short term and long term components). Evaporation influences on the isotopic composition of river water play a minor role and can be neglected in most parts of the Danube Basin, including the main stream.

The ^3H and ^{18}O high resolution time series of the Danube at Vienna is one of the longest in the world for a large river (it starts from 1963). It demonstrates that not only short term signals (e. g. seasonal $\delta^{18}\text{O}$ variations or ^3H releases from nuclear facilities) but also long term changes of isotope ratios in precipitation are transmitted through the catchment and can be detected in river water. Thus also stable isotopes — such as ^2H and ^{18}O — can be used as independent tracers to simulate transport processes in river systems. Because of the relatively low amplitude of long term $\delta^{18}\text{O}$ ($\delta^2\text{H}$) changes in precipitation and in river water, this approach is useful to assess the mean transit time of the flow's fast component. For the Danube, the mean transit time derived from comparisons of $\delta^{18}\text{O}$ trend curves for precipitation and river water at Vienna is around 1 a.

The different isotopic behaviour of tributaries from different parts of the catchment area reflects differences in geographical and hydro-meteorological parameters, such as the altitude of drainage areas, spatial and temporal precipitation distribution, sources of air moisture, infiltration characteristics, residence times of ground or lake waters in drainage areas, evaporation processes and others. Long term changes in isotopic records (such as increases of $\delta^{18}\text{O}$ during the 1980s) may help to trace hydro-climatic changes in these areas which would otherwise be difficult to detect. The main reason for a $\delta^{18}\text{O}$ increase during the 1980s is probably an increase in environmental temperature. But poor snow cover in the drainage areas during some winters and changes in the spatial and in the winter/summer distribution of precipitation also play a certain role in long term isotope record changes.

The time series of tritium in the Danube were modeled using the lumped parameter approach. The comparison of measured and modelled ^3H contents in the river revealed that the best fit which could be obtained (with a mean residence time of 3 a) is still not satisfactory. The time series was completed during the CRP period and is now ready to undergo new modeling attempts.

The isotope data set generated from JDS2 river water samples is a useful basis for isotope hydrological applications. An important actual research trend is the tracing of hydrological processes in the catchment of rivers through isotope investigations of river water. The main topic thereby is the formation and age structure of the base flow (groundwater contribution to river discharge).

A classical application is the investigation of interactions between river water and groundwater, for example, in assessing the portion of bank filtration water in pumping wells supplying water. The prerequisite for such applications is a significant differential isotope signal between river and groundwater. Since the Danube stream carries a substantial portion of water from high elevations, this prerequisite is fulfilled for $\delta^2\text{H}$ and $\delta^{18}\text{O}$ values along the whole river course. The distinct difference between $\delta^{18}\text{O}$ values for the Danube and tributaries in the lower parts of the catchment area is proof of this.

Different isotope signatures — stable isotope ratios as well as ^3H concentrations — in the main stream and in tributaries enable the investigation of mixing processes of tributary and main stream water. Inn River and the upper Danube, for instance, would be ideal candidates for such an investigation, as they differ by more than 2‰ in $\delta^{18}\text{O}$ at their confluence. Smaller tributaries which bear ^3H pulses from nuclear power plant releases also offer good possibilities for mixing studies (Morava, Vah, Hron).

Tritium releases from nuclear power plants can also be used to study travel time and dispersion of contamination pulses in the Danube. This could be a basis for the development of emergency measures to deal with pollution accidents in the catchment area.

Besides its use for hydrological investigations, the JDS2 isotope data set can serve as a base line of isotope data for assessing future impacts within the Danube Basin. This includes hydrological/climatic changes (such as temperature changes and changes in precipitation distribution) as well as anthropogenic impacts on the hydrological regime (for example reservoirs and changes in land use). All these changes will more or less be reflected in the isotopic composition of river water.

The isotope data set also seems to be applicable to a certain extent in biological studies. Due to different isotopic signatures in main streams and tributaries, it should be possible to distinguish between organisms which have developed in a tributary and those which have developed in the Danube stream.

9. ACKNOWLEDGEMENTS

We would like to thank members of the JDS2 sampling team on the Danube ships and the national sampling teams on the tributaries for providing us with good quality water samples for isotope analysis as well as Joachim Heindler and Peter Kosteki for sample analyses.

REFERENCES

- [1] MOOK, W.G., *Environmental Isotopes in the Hydrological Cycle*, Technical Documents in Hydrology, 39, Vol. 1, UNESCO, Paris (2000) 280 pp.
- [2] RANK, D., PAPESCH, W., “Isotopic composition of precipitation in Austria in relation to air circulation patterns and climate”, *Isotopic composition of precipitation in the Mediterranean Basin in relation to air circulation patterns and climate*, IAEA-TECDOC-1453, IAEA, Vienna (2005) 19–36.
- [3] LÁSZLÓFFY, W., “Die Hydrographie der Donau (Der Fluss als Lebensraum)”, *Limnologie der Donau* (LIEPOLT, R., Ed). E. Schweizerbart’sche Verlagsbuchhandlung, Stuttgart (1967) 16–57.
- [4] NEWMAN, B., et al., *Isotope survey of the Danube*. In: *Joint Danube Survey 2, Final Scientific Report*, ICPDR — International Commission for the Protection of the Danube River (2008) 209–214.
- [5] RANK, D., PAPESCH, W., HEISS, G., TESCH, R., *Isotopic composition of river water in the Danube Basin — results from the Joint Danube Survey (JDS2)*, *Austrian J. Earth Sci.* **102** 2 (2009) 170–180.

- [6] MILJEVIĆ, N., GOLOBOČIĆ, A., Distribution of stable isotopes in surface water along the Danube River in Serbia, *Isotopes in Environmental and Health Studies* **44** (2008) 137–148.
- [7] PAWELLEK, F., FRAUENSTEIN, F., VEIZER, J., Hydrochemistry and isotope geochemistry of the upper Danube River, *Geochim. Cosmochim. Acta* **66** (2002) 3839–3854.
- [8] RANK, D., ADLER, A., ARAGUÁS ARAGUÁS, L., FROEHLICH, K., ROZANSKI, K., STICHLER, W., “Hydrological parameters and climatic signals derived from long-term tritium and stable isotope time series of the River Danube”, *Isotope Techniques in the Study of Environmental Change. IAEA-SM-349*, IAEA, Vienna (1998) 191–205.
- [9] RANK, D., PAPESCH, W., RAJNER, V., “Tritium (³H)- und Sauerstoff-18 (¹⁸O) — Gehalt des Donauwassers zur Zeit der Internationalen Donaubereisung 1988”, *Ergebnisse der Internationalen Donauexpedition 1988*, Internationale Arbeitsgemeinschaft Donauforschung, Wien (1990) 307–312.
- [10] FROEHLICH, K., KRALIK, M., PAPESCH, W., RANK, D., SCHEIFINGER, H., STICHLER, W., Deuterium excess in precipitation of Alpine regions — Moisture recycling, *Isotopes in Environmental and Health Studies* **44** (2008) 61–70.
- [11] RANK, D., PAPESCH, W., “Die Isotopenverhältnisse im Donauwasser als Indikatoren für Klimaschwankungen im Einzugsgebiet”, *Limnologische Berichte der 31. Arbeitstagung der Internationalen Arbeitsgemeinschaft Donauforschung*, Wissenschaftliche Referate, 1 (1996) 521–526.
- [12] RANK, D., PAPESCH, W., RAJNER, V., TESCH, R., “Kurzzeitige Anstiege der ³H-Konzentration in Donau und March”, *Limnological Reports der 33. Konferenz der Internationalen Arbeitsgemeinschaft Donauforschung*, Osijek, Croatia, 35–40 (2000).
- [13] KRAUSE, W., MUNDSCHEK, H., Zur Bestimmung von Fließgeschwindigkeiten und longitudinaler Dispersion im Mittel- und Niederrhein mit ³H¹HO als Leitstoff, *Deutsche Gewässerkundliche Mitteilungen* **38** (1994) 128–143.
- [14] RANK, D., PAPESCH, W., “Isotopenverhältnisse im natürlichen Wasserkreislauf — Indikatoren für Klimaänderungen”, *Barbara-Gespräche Payerbach 1998*, Geoschule Payerbach, Wien (2001) 241–255.
- [15] ROZANSKI, K., GONFIANTINI, R., Isotopes in climatological studies, *IAEA Bulletin* **32** 4, Vienna (1990) 9–15.
- [16] INTERNATIONAL ATOMIC ENERGY AGENCY/WORLD METEOROLOGICAL ORGANIZATION, *Global Network of Isotopes in Precipitation, The GNIP Database (2008)* <http://isohis.iaea.org>
- [17] KAISER, A., et al., Links between meteorological conditions and spatial/temporal variations in long-term isotope records from the Austrian precipitation network, *IAEA-CN-80/63*, Vienna (2001).
- [18] RANK, D., RAJNER, V., LUST, G., Der Tritiumgehalt der Niederschläge und der Oberflächenwässer in Österreich — Yearly reports, *BVFA Arsenal*, Vienna, (1984–1997).
- [19] HYDROGRAPHISCHER DIENST ÖSTERREICH, *Hydrographisches Jahrbuch von Österreich 1966–2005*, Hydrographisches Zentralbüro im Bundesministerium für Land- und Forstwirtschaft, Umwelt und Wasserwirtschaft, Wien (1970–2007).

ANNEX

TABLE A-1. DANUBE ISOTOPE DATA SET 1963–2005: (1) DISCHARGE (m³/s) (DAY OF SAMPLING IN BRACKETS), (2) ³H (TU) (UNCERTAINTY), (3) δ¹⁸O (‰) AND (4) δ²H (‰) (DEUTERIUM EXCESS (‰), STARTING 1988) OF DANUBE WATER AT VIENNA (MONTHLY GRAB SAMPLES). YEARLY MEAN VALUES ARE IN BRACKETS IF THE DATA SET IS NOT COMPLETE.

Year	Jan	Feb	Mar	Apr	May	Jun	Jul	Aug	Sep	Oct	Nov	Dec	Mean
1963	-	-	-	-	1992.(9)	-	-	1760.(27)	-	-	-	-	1546
	-	-	-	-	631.(17)	-	-	1441.(36)	-	-	-	-	-
1964	-	-	-	2029.(1)	3220.(6)	1919.(1)	1889.(2)	1384.(3)	1747.(1)	1110.(1)	1690.(3)	1859.(2)	-
	-	-	-	978.(27)	1134.(28)	1122.(22)	1233.(29)	1088.(24)	1129.(28)	910.(22)	935.(17)	836.(25)	-
	-	-	-	-	-	-	-	-	-	-	-	-	-
	-	-	-	1851.(15)	2594.(15)	1584.(15)	-	-	1251.(15)	1871.(15)	1154.(16)	1453.(15)	1579
	-	-	-	921.(26)	1173.(35)	1250.(35)	-	-	980.(22)	930.(20)	798.(21)	731.(26)	-
	-	-	-	-	-	-	-	-	-	-	-	-	-
1096.(4)	1363.(2)	964.(8)	-	-	-	-	-	-	-	-	-	1381.(2)	2554
1965	650.(17)	626.(25)	533.(32)	-	-	-	-	-	-	-	-	515.(22)	-
	-	-	-	-	-	-	-	-	-	-	-	-	-
1809.(1)	-	-	-	-	3278.(1)	-	-	-	3601.(1)	1501.(1)	-	1273.(1)	2478
1966	499.(-)	-	-	-	543.(-)	-	-	-	598.(-)	537.(-)	-	460.(-)	(527.4)
	-	-	-	-	-	-	-	-	-	-	-	-	-
1967	2761.(1)	2560.(1)	2219.(1)	2338.(1)	2344.(1)	4838.(1)	3246.(1)	2046.(1)	1419.(1)	1316.(1)	944.(1)	960.(1)	2227
	426.(-)	395.(-)	361.(-)	418.(-)	344.(-)	417.(-)	436.(-)	381.(-)	359.(-)	355.(-)	337.(-)	310.(-)	378.3
	-	-	-	-	-	-	-	-	-	-	-	-	-
1968	1463.(1)	1623.(1)	1687.(1)	2863.(1)	-	2302.(2)	2009.(6)	-	1855.(6)	-	1282.(5)	1069.(2)	1927
	281.(-)	282.(-)	282.(-)	287.(-)	-	339.(21)	332.(20)	-	332.(20)	-	323.(20)	297.(19)	(306.1)
	-	-	-	-	-	-12.21	-12.25	-	-11.49	-	-10.34	-11.17	(-11.49)

Year	Jan	Feb	Mar	Apr	May	Jun	Jul	Aug	Sep	Oct.	Nov.	Dec	Mean
	1023.(17)	1728.(3)	1362.(3)	-	2406.(7)	1517.(3)	2201.(1)	1542.(7)	2379.(1)	1018.(1)	796.(6)	875.(1)	1493
1969	314.(20)	260.(17)	275.(17)	-	264.(17)	269.(17)	306.(19)	301.(18)	294.(18)	284.(18)	288.(18)	271.(17)	(284.2)
	-11.15	-11.08	-10.42	-	-11.20	-11.36	-11.03	-11.05	-10.47	-10.80	-10.36	-10.62	(-10.87)
	797.(8)	1005.(2)	2631.(2)	2359.(1)	3966.(12)	3490.(1)	3470.(1)	2689.(3)	2518.(1)	1458.(2)	1805.(2)	1724.(1)	2530
1970	268.(17)	265.(17)	220.(12)	254.(14)	271.(14)	275.(15)	246.(13)	254.(14)	265.(14)	264.(14)	241.(13)	223.(12)	253.8
	-10.56	-10.65	-11.45	-11.93	-12.06	-12.40	-13.37	-12.44	-11.88	-11.58	-11.22	-11.35	-11.74
	1002.(4)	1283.(1)	1098.(1)	1603.(1)	1650.(4)	1882.(2)	2786.(2)	1321.(2)	2236.(1)	1188.(4)	796.(2)	953.(2)	1430
1971	244.(13)	208.(11)	218.(11)	240.(13)	228.(12)	214.(11)	213.(11)	216.(11)	208.(11)	215.(11)	212.(11)	195.(10)	217.6
	-11.28	-11.55	-10.99	-11.57	-11.73	-12.13	-12.15	-11.98	-11.13	-11.45	-11.24	-11.23	-11.54
	963.(3)	715.(1)	951.(1)	1310.(14)	1461.(2)	1813.(6)	1698.(3)	2330.(2)	1276.(1)	884.(2)	1156.(2)	1426.(4)	1402
1972	194.(10)	194.(10)	190.(10)	189.(10)	201.(11)	184.(10)	192.(10)	188.(10)	183.(10)	186.(10)	176.(9)	160.(8)	186.4
	-10.47	-11.38	-11.45	-11.22	-11.18	-11.71	-12.44	-11.52	-10.93	-11.12	-11.18	-11.15	-11.31
	947.(2)	1018.(5)	997.(1)	2449.(4)	3086.(2)	2195.(1)	2273.(2)	1763.(2)	1383.(3)	1247.(2)	1238.(2)	1266.(3)	1656
1973	165.(9)	158.(8)	146.(8)	158.(8)	157.(8)	165.(9)	167.(9)	159.(8)	161.(9)	169.(9)	158.(8)	159.(8)	160.2
	-11.25	-11.53	-11.41	-11.65	-11.81	-12.45	-11.81	-11.53	-11.82	-11.60	-11.23	-11.05	-11.60
	1189.(7)	1581.(4)	1632.(1)	2110.(1)	1994.(2)	2460.(5)	3780.(1)	2366.(2)	1660.(2)	1509.(7)	1719.(7)	2666.(2)	2151
1974	145.(8)	149.(8)	146.(8)	140.(8)	140.(8)	198.(11)	188.(10)	168.(9)	160.(9)	151.(8)	158.(8)	161.(9)	158.7
	-10.83	-10.95	-10.90	-11.68	-11.57	-12.09	-12.09	-11.47	-11.08	-11.04	-10.61	-11.09	-11.28
	3788.(2)	2914.(3)	1286.(3)	1497.(3)	2451.(5)	2895.(2)	4244.(14)	1796.(12)	2236.(5)	1175.(6)	974.(4)	1195.(2)	2139
1975	139.(7)	143.(8)	154.(8)	149.(8)	178.(10)	163.(9)	178.(10)	166.(9)	163.(9)	156.(9)	141.(8)	148.(8)	156.5
	-11.05	-11.04	-10.98	-11.22	-11.95	-12.62	-12.23	-12.15	-11.33	-11.55	-11.26	-11.30	-11.56
	2127.(8)	1410.(4)	1144.(9)	1283.(1)	1678.(7)	4027.(3)	1189.(5)	1876.(3)	1791.(9)	1366.(8)	1041.(4)	1341.(1)	1530
1976	128.(7)	141.(8)	146.(8)	144.(7)	141.(7)	142.(7)	130.(6)	122.(6)	113.(5)	124.(6)	132.(8)	115.(6)	131.5
	-10.83	-10.64	-10.91	-10.96	-11.18	-11.52	-11.88	-11.27	-11.20	-11.66	-11.40	-11.20	-11.22
	984.(12)	1822.(1)	2930.(7)	1793.(12)	3387.(4)	1970.(3)	1926.(8)	3707.(5)	2226.(1)	1154.(11)	1096.(11)	1118.(13)	1969
1977	128.(6)	110.(5)	111.(5)	120.(6)	105.(5)	122.(6)	115.(5)	106.(5)	106.(5)	109.(5)	119.(6)	133.(6)	115.3
	-11.31	-11.39	-11.70	-11.76	-12.36	-12.79	-12.38	-11.50	-11.68	-11.00	-11.09	-11.32	-11.69

Year	Jan	Feb	Mar	Apr	May	Jun	Jul	Aug	Sep	Oct.	Nov.	Dec	Mean
	1467.(3)	1154.(2)	2346.(3)	2459.(5)	2305.(17)	2689.(1)	3131.(14)	2776.(10)	1467.(5)	2151.(3)	1411.(6)	1535.(14)	1889
1978	108.(5)	119.(6)	116.(6)	117.(7)	121.(6)	125.(6)	111.(5)	116.(5)	115.(6)	112.(5)	106.(5)	105.(5)	114.3
	-10.95	-11.32	-11.64	-11.57	-11.83	-12.04	-11.81	-12.24	-11.00	-11.33	-11.14	-11.51	-11.53
	1611.(2)	2004.(20)	1293.(1)	2746.(4)	2459.(2)	4350.(18)	2518.(5)	2404.(4)	1693.(6)	1691.(2)	1926.(15)	1870.(10)	2198
1979	101.(4.7)	90.2.(4.2)	100.(4.7)	90.1.(4.2)	92.5.(4.3)	89.3.(4.1)	91.0.(4.2)	87.8.(4.1)	95.3.(4.4)	87.6.(4.1)	82.7.(3.9)	86.1.(4.0)	91.1
	-11.17	-11.42	-11.12	-12.00	-11.99	-12.97	-12.55	-11.96	-11.83	-11.64	-11.25	-11.48	-11.78
	1184.(14)	1384.(1)	1360.(7)	2453.(18)	3027.(12)	3413.(12)	3140.(3)	2569.(5)	2082.(1)	2042.(15)	1437.(6)	1191.(4)	2148
1980	86.7(4.0)	83.3.(3.9)	87.8.(4.2)	79.1.(3.8)	73.3.(3.5)	73.0.(3.6)	76.1.(3.7)	70.1.(3.4)	76.2.(3.7)	71.7.(3.5)	70.1.(3.4)	77.8.(3.7)	77.1
	-11.45	-11.47	-11.32	-11.60	-12.38	-12.74	-12.38	-12.42	-12.28	-11.87	-11.83	-11.62	-11.95
	2448.(6)	1107.(3)	5699.(13)	3762.(1)	1971.(6)	2199.(3)	1728.(16)	1945.(14)	1425.(7)	2448.(2)	3103.(4)	2608.(3)	2239
1981	70.5(3.4)	78.8.(3.7)	58.2.(2.8)	66.4.(3.2)	68.7.(3.3)	68.2.(3.3)	67.7.(3.3)	66.5.(3.2)	68.4.(3.3)	64.9.(3.2)	56.5.(2.8)	59.3.(2.9)	66.2
	-11.54	-11.49	-11.96	-12.35	-12.18	-12.83	-12.98	-12.43	-12.14	-11.89	-11.84	-11.49	-12.09
	1985.(19)	1925.(18)	1789.(18)	2957.(8)	2371.(7)	3285.(3)	3027.(2)	2325.(3)	1313.(15)	1245.(6)	952.(12)	1323.(13)	2025
1982	69.9.(3.3)	62.0.(2.9)	60.8.(2.8)	58.0.(2.7)	62.5.(2.9)	54.5.(2.6)	53.0.(2.5)	57.7.(2.8)	56.2.(2.7)	58.1.(2.7)	55.3.(2.7)	62.7.(2.9)	59.2
	-11.71	-11.57	-11.53	-12.19	-11.85	-13.11	-12.65	-11.91	-12.01	-11.74	-11.69	-11.64	-11.97
	1689.(24)	1515.(15)	2095.(1)	2787.(11)	2859.(11)	3514.(16)	2024.(15)	1353.(24)	1417.(22)	1698.(13)	921.(4)	911.(16)	1828
1983	50.5.(2.5)	58.5.(2.7)	60.1.(2.7)	55.4.(2.6)	51.6.(2.5)	46.5.(2.4)	51.0.(2.5)	51.7.(2.5)	54.5.(2.5)	54.5.(2.5)	53.8.(2.5)	59.0.(2.5)	53.9
	-11.57	-11.58	-11.61	-11.75	-12.20	-12.64	-12.40	-11.93	-11.67	-11.59	-11.31	-11.41	-11.81
	1106.(12)	2527.(8)	1161.(1)	1823.(13)	1765.(4)	2008.(15)	1783.(19)	1896.(2)	1813.(7)	1336.(19)	955.(8)	917.(7)	1622
1984	60.3.(2.1)	53.7.(2.6)	55.5.(2.2)	48.2.(1.8)	45.3.(2.2)	42.0.(2.1)	38.6.(2.4)	46.3.(2.4)	44.5.(1.9)	43.1.(1.7)	44.6.(2.6)	43.7.(2.7)	47.2
	-11.53	-11.40	-11.36	-11.56	-12.06	-12.56	-12.94	-11.95	-11.68	-11.62	-11.62	-11.34	-11.80
	854.(17)	1110.(20)	1497.(6)	1895.(12)	2778.(30)	2128.(19)	1690.(15)	2416.(15)	-	1013.(15)	976.(21)	1472.(16)	1729
1985	48.8.(1.8)	42.5.(1.7)	47.4.(1.7)	42.9.(1.7)	36.8.(1.5)	35.9.(1.5)	38.6.(1.7)	34.5.(1.5)	-	42.4.(2.0)	41.1.(1.9)	41.9.(2.0)	(41.2)
	-11.64	-11.44	-11.33	-11.87	-12.28	-12.13	-12.37	-11.72	-	-11.45	-11.23	-11.33	(-11.71)
	3835.(15)	1055.(17)	1581.(14)	2032.(14)	2484.(15)	2723.(16)	1716.(15)	1841.(14)	1170.(15)	897.(10)	871.(17)	797.(15)	1694
1986	45.5.(2.1)	42.9.(2.0)	41.0.(1.9)	35.3.(1.6)	40.3.(1.9)	36.5.(1.8)	36.2.(1.8)	38.5.(1.9)	33.9.(1.6)	39.7.(1.8)	37.1.(1.8)	41.5.(2.0)	39.0
	-11.31	-11.25	-11.76	-11.84	-12.03	-11.83	-11.97	-11.71	-11.43	-11.49	-11.06	-11.23	-11.58

Year	Jan	Feb	Mar	Apr	May	Jun	Jul	Aug	Sep	Oct	Nov.	Dec	Mean
1987	1192.(15)	2003.(16)	1474.(17)	2264.(17)	3188.(15)	3220.(15)	2601.(15)	2142.(15)	1556.(14)	1083.(15)	1119.(16)	1083.(15)	2229
	31.8.(1.5)	33.4.(1.6)	38.1.(1.9)	29.3.(1.4)	30.7.(1.5)	30.7.(1.5)	32.1.(1.5)	33.7.(1.5)	31.9.(1.6)	35.7.(1.7)	33.3.(1.6)	35.5.(1.7)	33.0
	-10.91	-11.38	-11.23	-11.85	-12.06	-12.36	-12.37	-11.54	-11.14	-11.42	-11.24	-11.26	-11.56
1988	1358.(15)	1424.(15)	3251.(15)	4030.(15)	2809.(16)	2779.(15)	3123.(15)	1483.(16)	2004.(19)	1227.(17)	1507.(15)	3500.(15)	2220
	33.3.(1.6)	30.7.(1.5)	36.2.(1.7)	28.0.(1.3)	29.1.(1.4)	30.7.(1.4)	31.1.(1.5)	27.1.(1.3)	29.7.(1.4)	29.8.(1.4)	32.9.(1.6)	24.0.(1.2)	30.2
	-11.03	-11.03	-11.40	-11.72	-12.53	-12.33	-12.46	-11.79	-11.18	-11.19	-11.12	-10.99	-11.56
1989	1830.(16)	1323.(15)	2042.(15)	1925.(14)	2074.(12)	1768.(15)	3179.(14)	1863.(16)	1730.(15)	1922.(13)	1349.(15)	1130.(15)	1848
	26.4.(1.3)	33.5.(1.6)	31.0.(1.5)	26.1.(1.2)	28.4.(1.3)	28.8.(1.4)	28.3.(1.4)	26.9.(1.3)	40.5.(1.9)	29.4.(1.4)	28.2.(1.4)	27.2.(1.3)	29.6
	-10.89	-11.19	-11.16	-11.35	-11.36	-11.61	-11.75	-10.98	-11.03	-10.87	-10.89	-11.14	-11.19
1990	-77.9.(9.2)	-80.4.(9.1)	-79.1.(10.2)	-80.4.(10.4)	-80.9.(10.0)	-82.3.(10.6)	-83.1.(10.9)	-77.2.(10.6)	-77.4.(10.8)	-77.3.(9.7)	-77.7.(9.4)	-79.3.(9.8)	-79.4.(10.1)
	928.(15)	2011.(15)	1980.(15)	1497.(17)	1788.(15)	2682.(13)	2275.(16)	1350.(10)	1509.(14)	1145.(15)	1270.(15)	1167.(14)	1639
	30.2.(1.5)	30.3.(1.5)	24.7.(1.2)	27.4.(1.4)	25.1.(1.3)	23.6.(1.2)	22.9.(1.1)	25.6.(1.2)	29.5.(1.4)	27.1.(1.4)	25.0.(1.2)	27.1.(1.3)	26.5
1991	-10.88	-10.93	-10.83	-11.08	-11.68	-11.72	-11.18	-11.15	-11.00	-10.81	-10.74	-10.85	-11.07
	-77.3.(9.7)	-77.9.(9.5)	-76.6.(10.0)	-79.0.(9.6)	-83.3.(10.1)	-83.6.(10.2)	-79.2.(10.2)	-80.1.(9.1)	-78.4.(9.6)	-76.8.(9.7)	-76.9.(9.0)	-77.3.(9.5)	-78.9.(9.7)
	1438.(18)	891.(15)	1151.(19)	1011.(15)	2460.(15)	2361.(14)	2620.(15)	1824.(19)	990.(17)	916.(15)	984.(15)	778.(16)	1674
1992	25.1.(1.3)	26.5.(1.2)	27.5.(1.3)	27.2.(1.3)	27.6.(1.3)	17.9.(1.9)	18.5.(2.0)	16.3.(2.0)	18.2.(2.0)	18.8.(2.0)	30.5.(2.1)	22.9.(2.0)	23.1
	-10.69	-10.76	-11.27	-10.94	-11.13	-11.64	-12.04	-11.17	-11.24	-11.04	-10.98	-11.04	-11.16
	-76.3.(9.2)	-78.5.(7.6)	-80.4.(9.8)	-78.3.(9.2)	-79.8.(9.2)	-82.7.(10.4)	-85.6.(10.7)	-79.8.(9.6)	-80.5.(9.4)	-78.6.(9.7)	-79.0.(8.8)	-79.6.(8.7)	-79.9.(9.4)
1993	1235.(15)	1769.(17)	2122.(16)	1903.(15)	2935.(15)	2533.(15)	1467.(20)	1206.(14)	1109.(15)	874.(15)	1451.(16)	2376.(15)	1767
	17.2.(2.0)	20.6.(2.1)	19.9.(2.1)	17.3.(2.0)	21.2.(2.1)	23.4.(2.1)	22.2.(2.2)	22.9.(1.2)	21.3.(1.1)	24.1.(1.5)	19.7.(1.0)	22.5.(1.0)	21.0
	-10.73	-11.07	-10.99	-11.12	-12.18	-11.91	-12.12	-11.62	-11.13	-11.18	-11.05	-11.11	-11.35
1994	-76.2.(9.6)	-79.1.(9.5)	-76.9.(11.0)	-79.2.(9.8)	-85.9.(11.5)	-85.6.(9.7)	-87.1.(9.9)	-83.9.(9.1)	-78.6.(10.4)	-79.6.(9.8)	-79.3.(9.1)	-80.1.(8.8)	-81.0.(9.8)
	1749.(15)	1182.(15)	1313.(15)	1862.(15)	1857.(14)	1570.(16)	2240.(15)	1694.(16)	2221.(15)	1629.(15)	1190.(15)	1719.(16)	1861
	23.3.(1.0)	26.8.(1.4)	28.1.(1.3)	21.0.(1.1)	20.7.(1.1)	19.9.(1.0)	26.6.(1.7)	18.3.(1.8)	22.3.(1.6)	20.2.(1.8)	21.8.(1.2)	25.6.(1.8)	22.9
1995	-11.00	-10.93	-11.07	-11.17	-12.12	-12.32	-11.89	-10.94	-10.71	-11.23	-10.96	-10.86	-11.27
	-78.8.(9.2)	-78.5.(8.9)	-79.6.(9.0)	-80.5.(8.9)	-86.6.(10.4)	-88.7.(9.9)	-85.2.(9.9)	-78.1.(9.4)	-75.7.(10.0)	-80.3.(9.5)	-77.7.(10.0)	-77.9.(9.0)	-80.6.(9.5)

Year	Jan	Feb	Mar	Apr	May	Jun	Jul	Aug	Sep	Oct	Nov	Dec	Mean
1994	1630.(14)	1456.(15)	2478.(15)	4748.(15)	2163.(16)	2327.(14)	1601.(15)	1315.(12)	1379.(14)	1026.(14)	1324.(14)	1569.(15)	1855
	23.8.(1.7)	21.8.(1.6)	25.0.(1.7)	19.6.(1.1)	21.6.(1.2)	76.2.(3.5)	31.3.(1.6)	22.1.(1.1)	21.3.(1.2)	32.9.(1.6)	21.6.(1.2)	17.7.(1.0)	27.9
	-10.66	-10.68	-11.05	-11.96	-11.58	-11.69	-11.45	-11.47	-11.03	-10.94	-10.76	-10.76	-11.17
	-76.0.(9.3)	-75.9.(9.5)	-78.6.(9.8)	-86.4.(9.3)	-82.9.(9.7)	-83.9.(9.6)	-81.6.(10.0)	-82.1.(9.7)	-78.6.(9.6)	-78.2.(9.3)	-78.2.(7.9)	-77.0.(9.1)	-80.0.(9.4)
1995	1171.(16)	2338.(20)	1415.(15)	2559.(18)	2791.(17)	3530.(13)	2518.(13)	1989.(16)	2441.(11)	1108.(16)	1441.(15)	1113.(14)	2232
	28.4.(1.5)	18.0.(1.0)	20.2.(1.0)	39.1.(1.8)	18.3.(1.0)	18.3.(1.0)	17.9.(0.9)	21.0.(1.0)	20.5.(1.1)	20.2.(1.1)	19.5.(1.1)	19.2.(0.9)	21.7
	-10.78	-10.98	-11.00	-11.32	-12.07	-11.77	-12.34	-11.76	-11.13	-11.16	-11.03	-11.11	-11.37
	-77.5.(8.7)	-78.7.(9.1)	-78.7.(9.3)	-81.1.(9.5)	-86.3.(10.3)	-85.3.(8.9)	-88.6.(10.1)	-84.2.(9.9)	-79.5.(9.5)	-79.6.(9.7)	-79.1.(9.1)	-79.3.(9.6)	-81.5.(9.5)
1996	1254.(15)	1131.(19)	1078.(19)	1815.(15)	4756.(14)	2264.(14)	4204.(12)	1807.(16)	1799.(12)	1466.(16)	1635.(14)	1402.(13)	1815
	19.4.(1.0)	27.0.(1.3)	50.8.(2.3)	20.5.(1.0)	19.3.(1.0)	27.0.(1.2)	17.2.(0.9)	21.6.(1.1)	19.3.(1.0)	27.6.(1.3)	19.8.(1.0)	20.3.(1.0)	24.2
	-11.12	-11.05	-10.97	-11.71	-11.84	-12.11	-11.67	-11.43	-11.20	-11.41	-11.02	-11.15	-11.39
	-79.7.(9.3)	-80.2.(8.2)	-80.0.(7.8)	-83.0.(10.7)	-83.7.(11.0)	-86.2.(10.7)	-82.6.(10.8)	-80.9.(10.5)	-76.7.(12.9)	-80.9.(10.4)	-78.2.(10.0)	-77.9.(11.3)	-80.8.(10.3)
1997	1046.(14)	1795.(14)	1450.(14)	2067.(16)	2628.(15)	2147.(13)	2578.(15)	1701.(14)	1122.(16)	1878.(15)	1012.(14)	2372.(15)	1840
	27.7.(1.2)	25.4.(1.1)	17.9.(1.1)	48.9.(1.4)	21.2.(1.6)	38.5.(1.9)	24.8.(3.0)	32.8.(1.3)	20.3.(1.2)	21.0.(1.2)	19.8.(1.1)	16.7.(1.0)	26.3
	-11.09	-11.24	-10.83	-10.89	-11.35	-11.98	-11.33	-11.40	-11.22	-10.88	-11.05	-11.29	-11.21
	-79.6.(9.1)	-80.2.(9.7)	-77.0.(9.6)	-77.2.(9.9)	-80.2.(10.6)	-85.1.(10.7)	-79.9.(10.7)	-81.0.(10.2)	-79.7.(10.1)	-76.7.(10.3)	-78.3.(10.1)	-80.2.(10.1)	-79.6.(10.1)
1998	1213.(14)	1022.(16)	1581.(16)	1651.(15)	1982.(15)	2630.(15)	3128.(10)	1235.(17)	2458.(15)	1971.(15)	3908.(13)	4040.(15)	1785
	17.0.(1.1)	18.7.(1.0)	18.2.(0.9)	42.4.(1.9)	16.5.(0.8)	16.5.(0.9)	16.7.(0.9)	19.8.(1.0)	16.5.(0.9)	17.2.(0.8)	13.8.(0.7)	17.8.(1.0)	19.3
	-10.82	-11.14	-10.73	-11.22	-11.70	-12.15	-11.48	-11.38	-11.13	-11.20	-10.45	-10.82	-11.19
	-76.7.(9.9)	-79.4.(9.7)	-76.4.(9.4)	-79.8.(10.0)	-83.4.(10.2)	-86.9.(10.3)	-81.6.(10.2)	-81.0.(10.0)	-78.2.(10.8)	-79.6.(10.0)	-74.4.(9.2)	-77.8.(8.8)	-79.6.(9.9)
1999	1617.(15)	1274.(15)	3051.(15)	2797.(14)	4301.(17)	2565.(15)	2983.(15)	1445.(16)	1269.(15)	1275.(15)	1180.(15)	1527.(15)	2162
	15.0.(0.8)	16.7.(0.7)	52.7.(2.4)	17.0.(0.8)	14.5.(0.7)	15.9.(0.8)	19.8.(1.0)	15.6.(0.7)	16.2.(0.7)	15.4.(0.7)	17.7.(1.0)	15.7.(0.8)	19.4
	-10.59	-10.72	-11.09	-11.56	-12.43	-12.33	-11.51	-11.84	-11.47	-11.11	-11.23	-10.97	-11.40
	-75.1.(9.6)	-76.3.(9.5)	-78.6.(10.1)	-82.1.(10.4)	-89.2.(10.2)	-88.2.(10.4)	-81.9.(10.2)	-85.1.(9.6)	-81.7.(10.1)	-79.1.(9.8)	-80.6.(9.2)	-78.1.(9.7)	-81.3.(9.9)

Year	Jan	Feb	Mar	Apr	May	Jun	Jul	Aug	Sep	Oct.	Nov.	Dec	Mean
2000	1366.(13)	2218.(15)	3147.(15)	2391.(14)	3070.(15)	2304.(15)	2705.(14)	2024.(15)	1481.(14)	2090.(16)	1221.(15)	1335.(14)	2156
	15.7(0.9)	13.7(0.7)	12.6(0.8)	13.4(0.7)	12.3(0.7)	12.6(0.7)	13.3(0.7)	13.9(0.7)	14.7(0.7)	13.0(0.7)	13.8(0.7)	13.1(0.7)	13.5
	-10.81	-10.84	-10.93	-10.99	-12.21	-12.16	-	-10.96	-10.70	-10.87	-11.02	-10.97	(-11.13)
	-77.9(8.6)	-76.5(10.2)	-77.8(9.6)	-78.3(9.6)	-87.6(10.1)	-87.4(9.9)	-	-77.6(10.1)	-75.8(9.8)	-77.7(9.3)	-75.6(12.6)	-78.1(9.7)	-79.1(9.9)
2001	1352.(15)	1677.(15)	2979.(15)	2505.(17)	2335.(15)	3163.(18)	1821.(13)	1724.(14)	3469.(13)	1189.(15)	1314.(15)	1420.(18)	2057
	12.5(0.6)	12.9(0.7)	14.8(0.7)	12.6(0.6)	12.6(0.7)	11.6(0.6)	12.4(0.7)	13.3(0.7)	13.7(0.7)	21.6(1.0)	30.2(1.4)	11.3(0.6)	15.0
	-10.96	-11.22	-11.22	-11.04	-11.82	-11.83	-12.17	-11.63	-10.70	-11.13	-10.66	-10.58	-11.25
	-78.4(9.3)	-79.6(10.2)	-80.5(9.3)	-79.4(8.9)	-84.7(9.9)	-84.6(10.0)	-87.8(9.6)	-83.0(10.0)	-75.9(9.7)	-78.7(10.3)	-76.2(9.1)	-75.9(8.7)	-80.4(9.6)
2002	1184.(16)	2360.(15)	1557.(18)	1758.(15)	2211.(15)	1986.(17)	1543.(15)	3295.(19)	1475.(16)	2398.(15)	3553.(17)	1635.(17)	2451
	12.4(0.6)	14.3(0.7)	12.7(1.4)	12.6(0.7)	12.9(0.7)	12.2(0.7)	15.1(0.8)	12.2(0.5)	12.9(0.7)	12.3(0.5)	10.9(0.6)	66.7(2.9)	17.3
	-10.78	-10.66	-10.79	-10.88	-11.20	-11.20	-11.31	-10.68	-10.82	-11.01	-10.60	-10.69	-10.89
	-77.6(8.6)	-75.3(10.0)	-76.6(9.7)	-78.1(8.9)	-82.8(6.8)	-78.2(11.4)	-80.6(9.9)	-75.2(10.2)	-76.9(9.7)	-77.1(11.0)	-73.7(11.1)	-76.8(8.7)	-77.4(9.7)
2003	2190.(15)	1355.(17)	2453.(14)	1317.(14)	2156.(14)	1780.(13)	-	904.(18)	1503.(16)	1549.(16)	864.(18)	930.(15)	1492
	13.0(0.7)	11.9(0.7)	13.4(0.7)	14.1(0.7)	12.3(0.6)	12.8(0.7)	-	12.9(0.6)	9.4(0.5)	9.9(0.5)	21.9(1.1)	12.1(0.6)	(13.1)
	-10.73	-10.73	-11.03	-11.00	-12.07	-12.01	-	-11.24	-10.95	-10.85	-	-11.04	(-11.17)
	-76.4(9.4)	-77.6(8.2)	-78.1(10.1)	-77.7(10.3)	-85.9(10.7)	-86.4(9.7)	-	-79.8(10.1)	-76.7(10.9)	-76.5(10.3)	-	-78.8(9.5)	-79.4(9.9)
2004	2380.(19)	1640.(12)	1761.(17)	1602.(15)	1809.(28)	2618.(22)	2028.(13)	1236.(20)	986.(21)	1201.(22)	1249.(12)	887.(21)	1703
	9.4(0.5)	10.6(0.5)	9.7(0.5)	10.5(0.6)	11.6(0.6)	129(4.8)	12.1(0.7)	11.8(0.7)	12.1(0.7)	12.2(0.7)	-	13.3(0.6)	(22.0)
	-11.35	-11.15	-11.15	-11.39	-12.13	-11.97	-12.54	-11.77	-11.35	-10.82	-11.11	-11.00	-11.48
	-82.3(8.5)	-79.7(9.5)	-80.4(8.8)	-82.3(8.8)	-87.2(9.8)	-86.5(9.3)	-90.6(9.7)	-85.0(9.2)	-81.4(9.4)	-77.2(9.4)	-79.6(9.3)	-77.6(10.4)	-82.5(9.3)
2005	1220.(14)	1461.(23)	1058.(15)	1934.(15)	3082.(20)	1736.(15)	1646.(25)	5404.(17)	1561.(15)	1283.(14)	889.(14)	914.(15)	1909
	11.0(0.7)	10.9(0.5)	11.4(0.7)	11.5(0.7)	10.5(0.6)	27.5(1.2)	11.2(0.7)	10.6(0.6)	13.0(0.6)	52.9(2.3)	12.0(0.7)	12.6(0.6)	16.3
	-10.65	-10.84	-10.82	-11.24	-11.34	-11.65	-11.31	-11.04	-11.18	-10.92	-10.97	-11.09	-11.09
	-77.3(7.9)	-77.7(9.0)	-77.5(9.1)	-80.4(9.5)	-81.1(9.6)	-83.1(10.1)	-79.9(10.6)	-78.4(9.9)	-79.8(9.6)	-77.0(10.4)	-79.0(8.8)	-79.2(9.5)	-79.2(9.5)

STUDY ON HYDROLOGICAL PROCESSES IN LENA RIVER BASIN USING STABLE ISOTOPE RATIOS OF RIVER WATER

A. Sugimoto^a, T.C. Maximov^b

^a Faculty of Environmental Earth Science, Hokkaido University, Hokkaido, Japan

^b Institute for Biological Problems of Cryolithozone, Siberian Branch of the Russian Academy of Sciences, Yakutsk, Russian Federation

Abstract. Lena river water was sampled at Yakutsk and its isotope ratios were observed. The isotopic composition of river water showed a clear seasonality, with a pulse of low δ values due to runoff of snow meltwater, and following an increase in δ values during summer, which may be caused by a recession of snow meltwater and runoff originating from summer precipitation with more positive δ values. The isotope ratios of river water slightly decreased again during the freezing period, when there was low discharge. As the freezing process of the ground progresses from the surface down, the soil layers producing runoff may become deeper. This may cause the gradual decrease in δ values observed in winter. It has been pointed out that winter discharge showed an increasing trend in eastern Siberia. An increasing trend is most obvious in the area covered by permafrost. Monitoring of isotope ratios of river water may improve our understanding of the source and process of increasing winter discharge.

1. INTRODUCTION

The Lena river is one of the largest rivers in the world, bringing freshwater to the Arctic Sea throughout the year. Recently, Yang et al. [1] pointed out that Lena discharge, especially during winter, has been on the rise since the 1960s. The Northern part of the Eurasian continent is one of the regions where the largest increase in air temperature has been observed [2]. The degradation of permafrost is one of the possible reasons for an increase in winter discharge, though the reason for it has not yet been clarified. An increase in river discharge to the Arctic Ocean may affect sea ice dynamics, thus creating a global climate impact through changes in ocean circulation and atmospheric patterns such as the NAO [3, 4]. The influx of freshwater from the Lena to the Laptev Sea thus may affect water dynamics of the Arctic Ocean.

The Lena river runs through the permafrost area in eastern Siberia, thus it is likely that its water isotope signal is considerably different from other rivers without permafrost in the watershed. The Lena river basin consists of three parts from a hydrological point of view; the mountain taiga area in the south, the central plain taiga area, and the tundra area near the river mouth. It is expected that each area contributes differently to runoff. The mountain taiga in the southern part of the river basin is expected to make the largest contribution to discharge, because the amount of precipitation in this area (~500 mm) is much larger than that in the plain taiga area (~200 mm) [5]. We also expect each area to have a characteristic isotope signature, thus reflecting the unique and characteristic water regime in each area.

The isotopic composition of river water may be a potentially powerful tool for investigation of the source region of discharge and detection of a water cycle change, through monitoring of the isotopic signature of river water and observation of the isotopic composition of ground ice which may thaw, resulting in additional runoff. River water isotopes are expected to give us

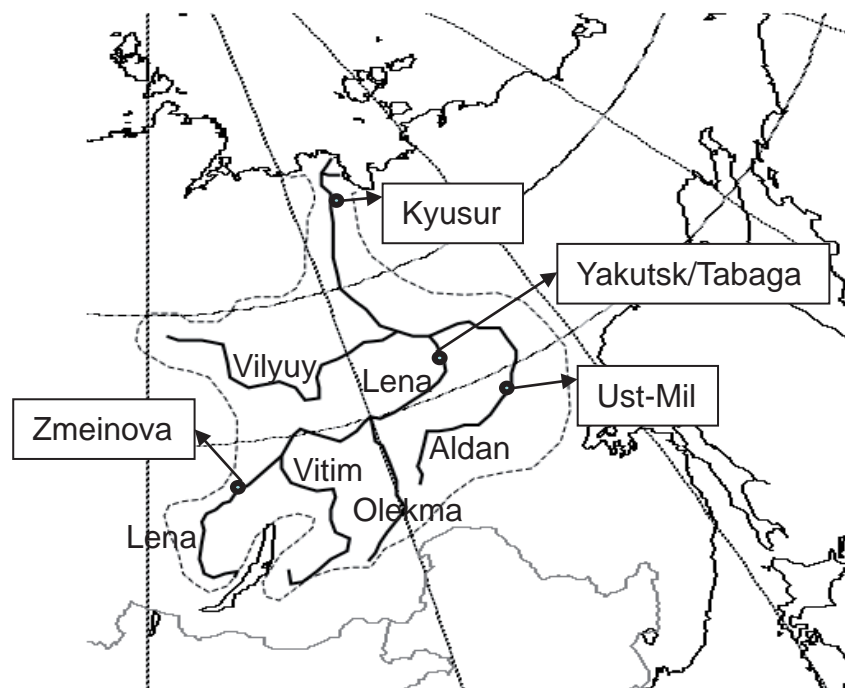


FIG. 1. Lena river basin. River water was sampled at Yakutsk.

useful information on the cause of increasing river discharge. For this purpose, Lena river water was sampled and its water isotopic composition was analyzed under an IAEA Coordinated Research Programme entitled, “Isotope Tracing of Hydrological Processes in Large River Basins” [6].

2. OBSERVATION AND ISOTOPE ANALYSIS

Lena river water was sampled monthly or weekly at Yakutsk, which is located in the plain Taiga area (Fig. 1). During the summer (non-freezing season) river water was taken from land (river bank) at a Ferry terminal (62°0’N, 129°50’E), and during the freezing season, water was taken by making a hole in the ice. There is no way to take reliable river samples during ice breaking (usually May) and ice formation periods, because it is impossible to step on the ice, and river water near land may be isolated from the stream due to freezing.

Nine gauging stations are in operation along the main stream of Lena. The nearest station is Tabaga, 25 km south of Yakutsk. Since there is no large tributary between the two sites, discharge at Yakutsk seems to be identical to that observed at Tabaga. Discharge data observed at Tabaga, Zmeinova (near Kirensk) Tommot and Ust-Mil along the Aldan river were obtained from the State Hydrology Institute. Locations for these stations are shown in Fig. 1.

Water samples were brought to Japan for isotope measurement. Oxygen and hydrogen isotope ratios were analyzed using a MAT 252 mass spectrometer with CO₂/H₂/H₂O equilibration device at the Center for Ecological Research, Kyoto University, and using Delta V with Gas Bench at Faculty of Environmental Earth Science, Hokkaido University. Analytical errors were less than ±0.2 and 2 ‰ for δ¹⁸O and δD respectively.

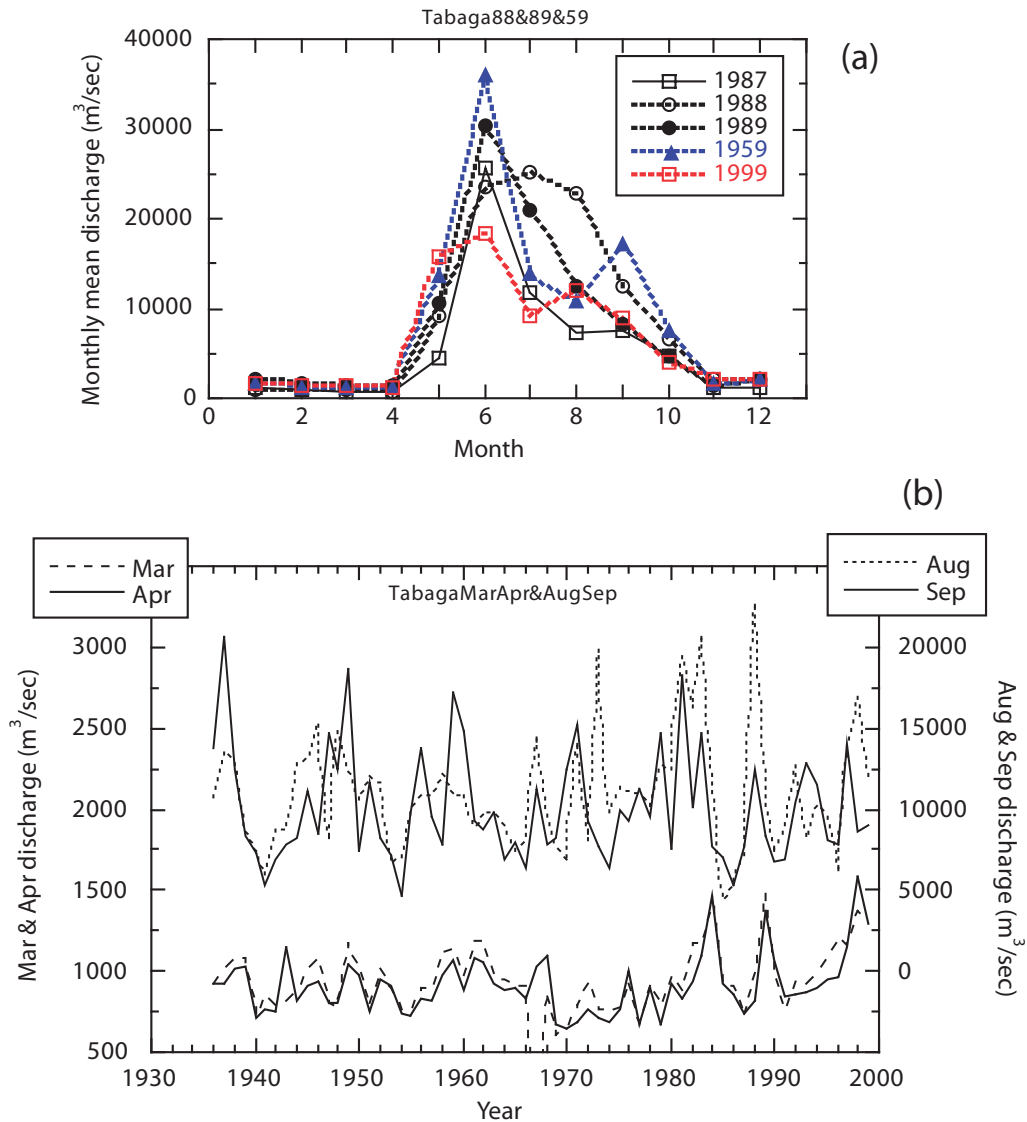


FIG. 2. Monthly mean discharge in 1959, 1987, 1988, 1989, and 1999 observed at Tagaba (a), and inter-annual variations in winter (March and April) and summer (August and September); discharges from 1936 to 1999 at Tabaga (b).

3. RESULTS AND DISCUSSION

3.1. River discharge

Figure 2 shows river discharge (monthly mean) observed at Tabaga, located 25 km south of Yakutsk. River discharge usually reached a maximum value in June due to the runoff of snow meltwater from the watershed, and decreased rapidly during summer (Figure 2a). Discharge typically decreased during summer, however, patterns differ from year to year. For example, discharge decreased from June to November with only one peak in June in 1989, whereas two peaks were seen in June and September of 1959 and in June and August of 1999. These were probably stemming from summer precipitation and consequent runoff from the watershed. During the river's freezing period (from November to April), river discharge decreased gradually, but never froze completely up.

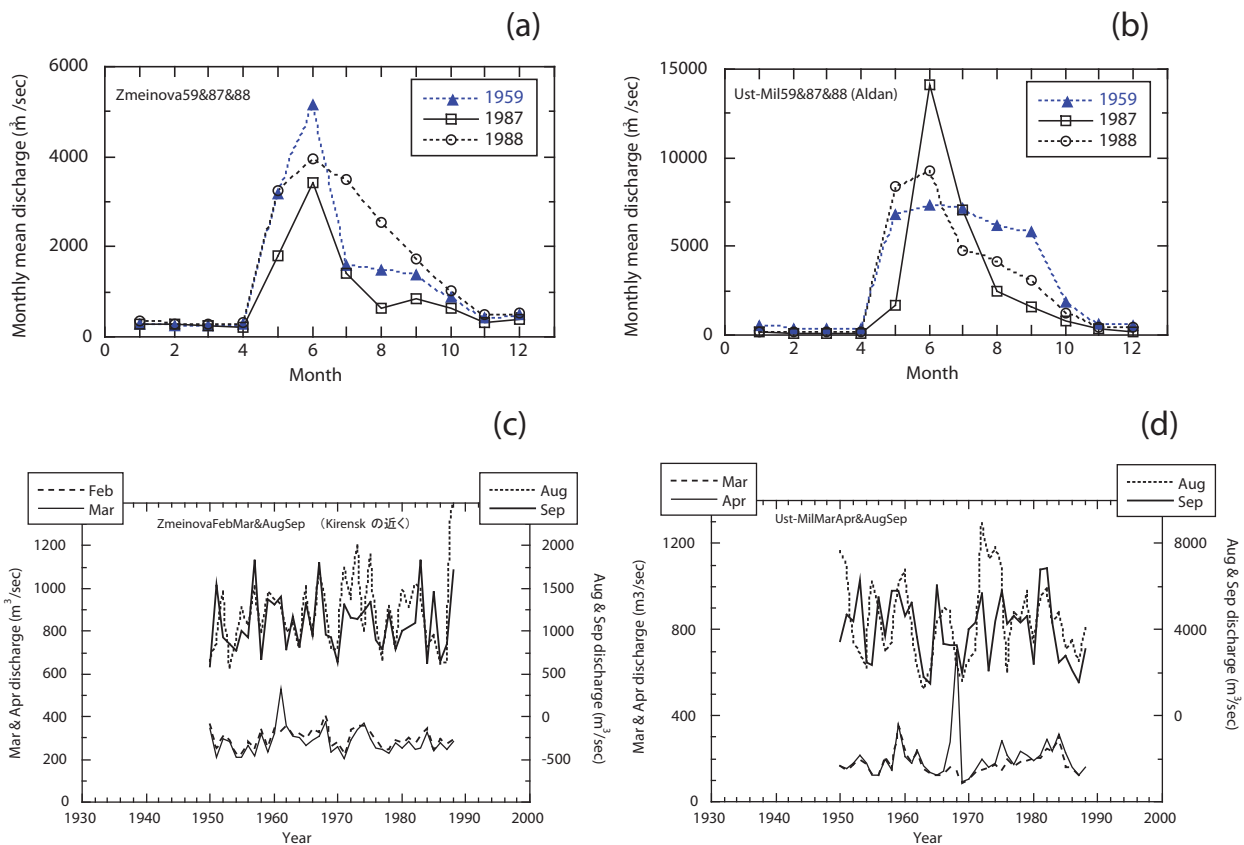


FIG. 3. Monthly mean discharges in 1959, 1987, 1988 observed at Zmeinova (a) and Ust-Mil (b), and interannual variations in winter and summer discharges from 1950 to 1988 at Zmeinova (c) and Ust-Mil (d). February and March, and March and April are shown for Zmeinova and Ust-Mil, respectively.

The upper Lena showed a similar pattern to that observed at Tabaga. Figures 3a and 3b present discharge observed at Zmeinova (near Kirensk, Fig. 1). The maximum value was observed in June, decreasing rapidly over summer rapidly and gradually during the river's freezing period (Fig. 3a). Similar seasonal variations were also observed at Ust-Mil in Aldan (Figs 3c and 3d).

Rapid decrease in discharge during the summer can be explained by receding snowmelt water, while the gradual decrease during the river's freezing period should be elucidated with the source area of the water discharge. Since most of the area around middle and lower Lena is affected by permafrost, no groundwater exists generally. As a rule, winter discharge can only be produced in the upper Lena, where no or discontinuous permafrost exists. As described later, the isotope ratio of river water during winter is an indicator of water source.

There are large interannual variations in winter and summer discharge (Figs. 2 and 3). As pointed out by Yang et al. [1], different trends in long term variation can be seen in winter discharge between the upper Lena and Aldan rivers. Figures 2b, 3b and 3d show a long year to year variation in winter discharge (March and April, or February and March) and late summer (August and September) at Tabaga (middle Lena), Zmeinova (upper Lena), and Ust-Mil (upper Aldan). Winter discharge increased after 1970 in the upper Aldan and middle Lena, where both receive runoff from the eastern part of the southern mountain taiga. The upper Lena is located

in the western part of the southern mountain taiga in the Lena river basin, where little area is covered by permafrost, and no significant increase in winter discharge was observed (Fig. 3b). On the other hand, Zmeinova in the upper Aldan and Tabaga in the middle Lena, where large parts of the watershed is covered by permafrost, showed increase in winter discharge. One of the possible reasons for the difference is degradation of permafrost in the eastern part of southern mountain taiga, however, this has not yet been confirmed.

3.2. River water $\delta^{18}\text{O}$ and d-excess observed at Yakutsk

River water $\delta^{18}\text{O}$ and d-excess obtained at Yakutsk are shown in Fig. 4. Clear seasonal variation was found in the $\delta^{18}\text{O}$ value, with a minimum peak (-23 to -24‰) in May or June and a maximum peak (-18 to -17‰) in August or September. The $\delta^{18}\text{O}$ of river water decreased in fall, and during the river’s freezing period it remained almost constant or slightly decreased. Observed d-excess values are rather scattered, however, slightly higher d-excess values were accompanied by a spike of low $\delta^{18}\text{O}$ values due to the runoff of snowmelt water greater than that of summer discharge, with slightly low d-excess values. Unlike observational results in tributaries of the Mackenzie river basin, where river water isotopes are affected by the evaporation of surface water [7], there was no significant indication of the evaporative

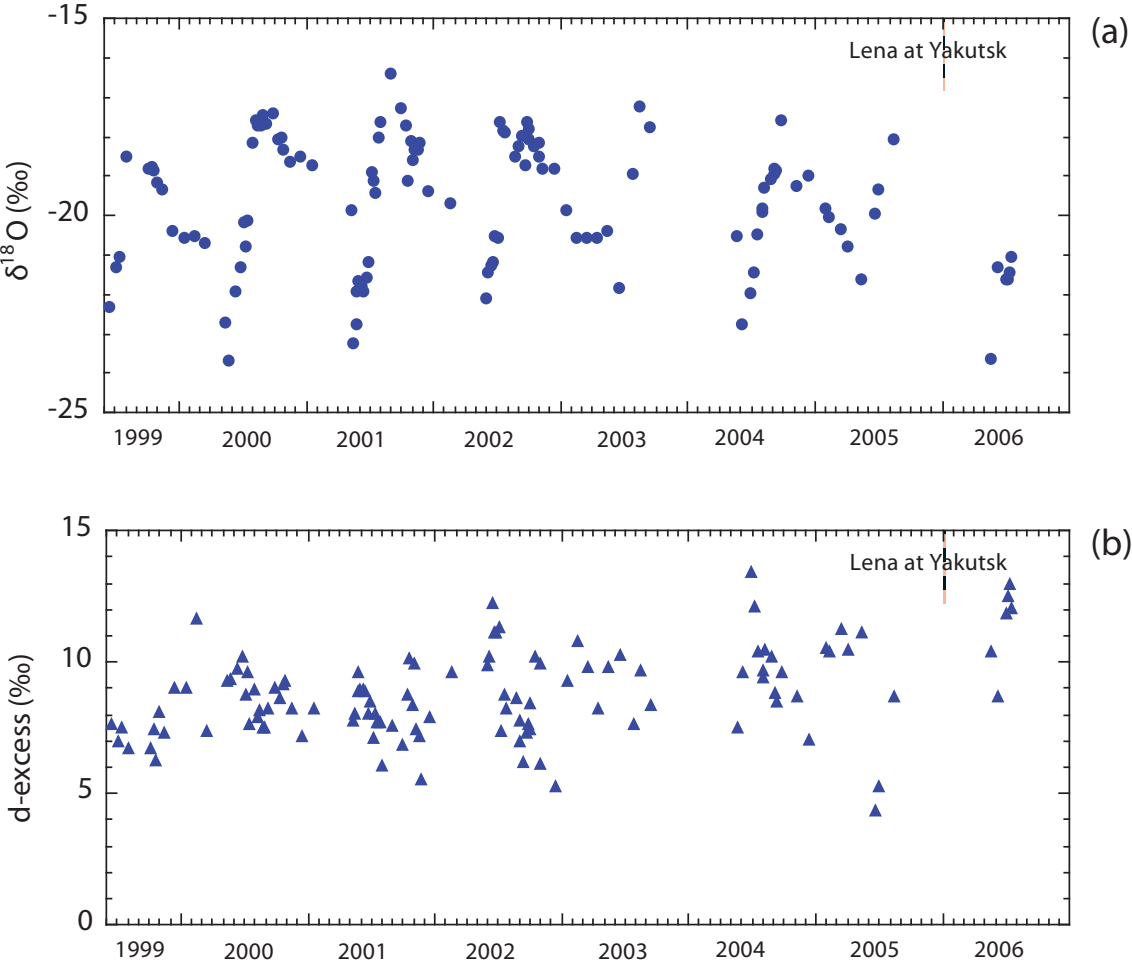


FIG. 4. The $\delta^{18}\text{O}$ (a) and d-excess (b) of Lena river water, obtained at Yakutsk.

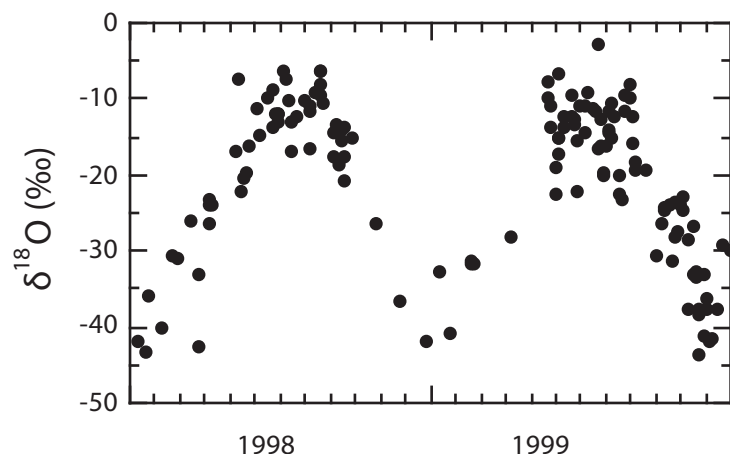


FIG. 5. Seasonal variation in the daily $\delta^{18}\text{O}$ of precipitation observed at Yakutsk or Spasskaya Pad, an experimental forest located 30 km northeast of Yakutsk.

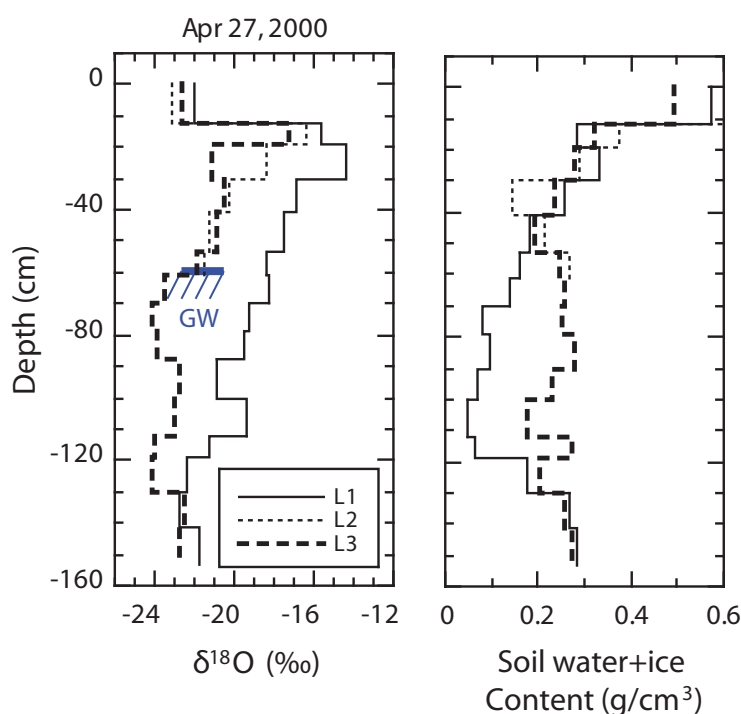


FIG. 6. Vertical profiles of the $\delta^{18}\text{O}$ of soil moisture (water and ice) (a) and soil moisture (water and ice) content (b) observed in April in 2000 at Spasskaya Pad experimental forest, located 30 km northeast of Yakutsk.

signal observed in Lena river water. This difference may be attributed to dry surface conditions in the plain taiga in midstream Lena.

A decrease in the $\delta^{18}\text{O}$ of river water in May and June corresponds to an increase in discharge due to the runoff of snowmelt water. Snow cover $\delta^{18}\text{O}$ at Yakutsk showed very low values (-30‰), since winter snowfall at Yakutsk has extremely low $\delta^{18}\text{O}$ values (-45 to -25‰), as seen in Fig. 5. Snowfall $\delta^{18}\text{O}$ in the upstream area is also expected to be low because of the high altitude. Actually, the observed $\delta^{18}\text{O}$ of snow at Tynda in the southern mountain taiga was

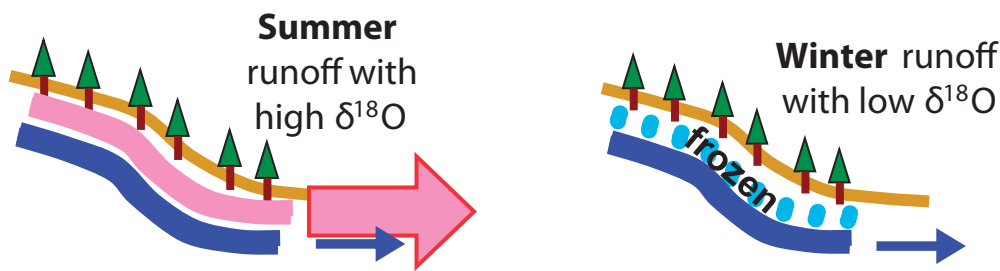


FIG. 7. Schematic figure to explain the difference in the $\delta^{18}\text{O}$ of runoff water during summer and winter in the area without permafrost. As the shallow soil layer freezes down during fall, contribution of runoff from shallow soil layer decreases. As a result, contribution of runoff from deeper soil layer with more negative $\delta^{18}\text{O}$ increases.

as low as that at Yakutsk. Therefore, runoff with snowmelt water having a low $\delta^{18}\text{O}$ causes clear seasonality with a strong spike of low $\delta^{18}\text{O}$ in river water isotope data.

An increase in $\delta^{18}\text{O}$ during summer is primarily explained by the recession of snowmelt water. In addition, the runoff of summer precipitation with high $\delta^{18}\text{O}$ can be a main factor for the increase. However, the contribution of summer precipitation runoff from the plain taiga area near Yakutsk is not significant. This is expected, not only because of the amount of precipitation but also from the results of water isotope data. As explained below, the maximum value observed in August or September (-18 to -17‰) suggests that runoff from the southern mountain taiga area is the main component of discharge at Yakutsk.

Soil moisture observed at Yakutsk at a depth of 45–90 cm showed a $\delta^{18}\text{O}$ of around -24 to -22‰ [8], indicating mixing between summer precipitation and snowmelt water in the soil. It is also expected that runoff from this area (the plain taiga area) has a similar value (-24 to -22‰) if it exists, except for surface runoff during snow thaw. Fig. 6 shows the vertical profile of $\delta^{18}\text{O}$ and soil moisture content (water and ice) observed in April 2000. Due to heavy rainfall in the summer of 1999, soil moisture content was extremely high during the winter of 1999–2000, then some parts of soil moisture carried over without freezing. As seen in Fig. 6, tentative groundwater with a $\delta^{18}\text{O}$ of -22‰ was observed during the winter of 1999–2000 [9]. It is expected that excess soil water with a $\delta^{18}\text{O}$ of -24 to -22‰ runs off from the area, although runoff from the plain taiga area is usually insignificant, except for surface runoff during snowmelt. Actually, Ichiyanagi et al. [10] estimated that excess soil water with a $\delta^{18}\text{O}$ value of -23‰ flowed into a small water reservoir called alas during the summer of 2000, through the use of the isotope mass balance calculation for alas water. It is thus expected that runoff water from this area has a $\delta^{18}\text{O}$ as low as that of excess soil water. If runoff from the plain taiga area contributes significantly to the discharge observed at the Yakutsk, river water $\delta^{18}\text{O}$ would not be as high as the value observed here (-18 to -17‰). Observed results therefore indicate that the source area of discharged water is in the upper stream, where soil water $\delta^{18}\text{O}$ is higher than that in the plain taiga because of the larger contribution of summer precipitation.

The decrease in $\delta^{18}\text{O}$ in fall and winter is quite an interesting phenomenon. A relatively rapid decrease during the period of September – November suggests a change in the source of runoff water. One of the possible causes of this decrease is a change in the depth of soil layer producing runoff water, schematically shown in Fig. 7. As temperature decreases, the shallow soil layer freezes down, and the generation depth of runoff water moves down. Water

in the deeper soil layer is expected to have more negative $\delta^{18}\text{O}$ values, because of a smaller contribution of summer rainfall than in the shallow soil layer. An increase in the contribution of runoff from deeper soil layers may cause a decrease in $\delta^{18}\text{O}$ values during the fall.

During the mid-winter to spring period, observed river water $\delta^{18}\text{O}$ values were constant or slightly more negative. Winter discharge means runoff water generation from a non-freezing area (or site), and it generally occurs in the area of the site without permafrost in the southern mountain taiga. Runoff water, however, may also be generated at plain taiga during winter, as described later, causing a different $\delta^{18}\text{O}$ signal for river water. If permafrost degrades, runoff water generation may be enhanced. Since the observed $\delta^{18}\text{O}$ value reflects that of groundwater in the source area, it can be a potential indicator of permafrost degradation.

3.3. Interannual variation in river water $\delta^{18}\text{O}$

Large interannual variation was also found in the $\delta^{18}\text{O}$ values of river water. Maximum values are found in August or September and the $\delta^{18}\text{O}$ value in mid winter differs from year to year. Variation in the amount of precipitation in the upstream and plain taiga areas may also be a large factor controlling these interannual variations.

As seen in the hydrograph at Tabaga (Fig. 2a), after a maximum peak in June, a second peak of discharge in August or September was also observed in some years. These peaks are attributed to runoff after summer rainfall. Runoff generated after summer rainfall is a factor controlling year to year variations in summer discharge as shown in Fig. 2b, therefore, it can also be a factor controlling interannual variations in river water $\delta^{18}\text{O}$ during summer.

As described before, the summer of 1999 was extremely wet because of heavy rainfall in the taiga plain area. Extremely wet soil, the water of which had $\delta^{18}\text{O}$ values ranging from -24 to -22‰ could generate runoff water with the same $\delta^{18}\text{O}$ value, which was much lower than that of runoff water in the upstream area (the mountainous taiga area). A maximum value of $\delta^{18}\text{O}$ in September 1999 was lower than that in dry years (2001 – 2003). One of the possible causes for lower maximum values of $\delta^{18}\text{O}$ in September of 1999 and lower minimum values of $\delta^{18}\text{O}$ in the winter of 1999–2000 is runoff after heavy rainfall in the summer of 1999 in the Plain taiga area.

4. CONCLUDING REMARKS

Lena river water stable isotope ratios obtained at Yakutsk in the plain taiga area showed a clear and characteristic seasonal variation with strong spike of low $\delta^{18}\text{O}$ values related to the runoff of snowmelt water and an increase in the $\delta^{18}\text{O}$ during summer caused by the following recession and runoff of summer rainfall from the southern mountain taiga in upstream area. During winter, a gradual decrease was followed by a rapid decrease in $\delta^{18}\text{O}$ values during fall.

Observed constant $\delta^{18}\text{O}$ values in river water during mid-winter may elucidate the source area and depth of runoff water generation, because soil water and groundwater are expected to show characteristic isotope ratios depending on geographical region. For example, runoff water originating from the mountain taiga area is expected to have more positive $\delta^{18}\text{O}$ values higher than those from the plain taiga area.

Isotope ratios of river water can be a potential tool for detecting change in a water cycle such as permafrost degradation in a river basin, through further investigation on the isotope ratios of water and ice in permafrost as well as those in river water and precipitation.

5. ACKNOWLEDGEMENTS

River discharge data were obtained from the State Hydrology Institute through Valery Vuglinsky (State Hydrology Institute) and Tetsuo Ohata (Institute of Observational Research for Global Change, Japan Agency for Marine-Earth Science and Technology).

REFERENCES

- [1] YANG, D.Q., et al., Siberian Lena River hydrologic regime and recent change, *J. Geophys. Res.* **107** No. D23, D234694 (2002).
- [2] LEMKE, P., et al., “Observations: Changes in Snow, Ice and Frozen Ground”, *Climate Change 2007: The Physical Science Basis, Contribution of Working Group I to the Fourth Assessment Report of the Intergovernmental Panel on Climate Change* (SOLOMON, S. et al., Eds), Cambridge University Press, Cambridge and New York (2007).
- [3] PETERSON, B.J., et al., Increasing river discharge to the Arctic Ocean, *Science* **298** 5601 (2002) 2171–2173.
- [4] PETERSON, B.J., et al., Trajectory shifts in the Arctic and subarctic freshwater cycle, *Science* **313** 5790 (2006) 1061–1066.
- [5] MA, X.Y., et al., A macro-scale hydrological analysis of the Lena River basin, *Hydrol. Process.* **14** 3 (2000) 639–651.
- [6] GIBSON, J., et al., Isotope studies in large river basins: a new global research focus, *EOS* **83** 52 (2002) 613.
- [7] GIBSON, J.J., et al., Progress in isotope tracer hydrology in Canada, *Hydrol. Process.* **19** (2005) 303–327.
- [8] SUGIMOTO, A., et al., Characteristics of soil moisture in permafrost observed in East Siberian taiga with stable isotopes of water, *Hydrol. Process.* **17** 6 (2003) 1073–1092.
- [9] SUGIMOTO, A., et al., Spatial and seasonal variations in surface soil moisture around Yakutsk observed in 2000, *Proceedings of GAME/Siberia Workshop; GAME Publication No. 30* (2001) 63–73.
- [10] ICHIYANAGI, K., SUGIMOTO, A., NUMAGUTI, A., KURITA, N., ISHII, Y., OHATA, T., Seasonal variation in stable isotopes in alpine lakes near Yakutsk, Eastern Siberia, *Geochem. J.* **37** (2003) 519–530.

ISOTOPE TRACING OF THE PARANÁ RIVER, ARGENTINA

H.O. Panarello, C. Dapeña

Instituto de Geocronología y Geología Isotópica (INGEIS-CONICET-UBA),
Buenos Aires, Argentina

Abstract. The Río de la Plata estuary is the collector of a vast drainage basin of about 3.1×10^6 km². There are many tributaries to the estuary but the Paraná and Uruguay rivers directly discharge more than 99% of the average discharge (24 000 m³/s). The stable isotope composition of water in this estuary has been monitored since 1997. From 120 isotopic pairs, it could be established that ¹⁸O and ²H exhibit a cyclical pattern with a maximum in November and a minimum in May. Values correspond to the ITCZ position. When it is located near 8°N, the amount of precipitation over the basin decreases and hence the isotopic composition of both elements is more positive. Conversely, when the ITCZ moves southward, the pluviosity increases, leading to more negative $\delta^{18}\text{O}$ and $\delta^2\text{H}$ values. This isotopic signal is recorded with a delay of ca 4 month in the estuary. The derivate magnitude, deuterium excess, showed important variations, from 1 to $\delta 18\%$, with the higher values being related to positive ENSO (El Niño) phases and lower values to negative ENSO (La Niña). Despite the interactions with groundwater and physical processes along ca. 2800 km, the Paraná River still reflects at its mouth all these climatic phenomena that control the $\delta^2\text{H}$ and $\delta^{18}\text{O}$ contents at its catchment areas.

1. INTRODUCTION

The Río de la Plata estuary is the collecting area of a vast drainage basin of about 3.1×10^6 km² known as the ‘Cuenca del Plata’ (Fig. 1, Table 1). Its major tributaries are the Paraná and Uruguay rivers. The main course of the Paraná River starts at the ‘Planalto do Brasil’, located in central-eastern Brazil. The Pilcomayo and Bermejo rivers contribute to the Paraná with water from the high Andes range. Paraguay River releases into the Paraná water coming from the Mato Grosso, forming the largest wetland in the world named ‘El Pantanal’ [1] which behaves as a buffer. The Uruguay River, and the Iguazú River through the Paraná River, also contribute to the estuary. Less significant are other rivers such as the Salado del Norte, Negro, etc., although between April and May, 2003 the Salado del Norte River produced

TABLE 1. AREAS COVERED IN
SOUTH AMERICA BY THE CUENCA DEL PLATA

Country	Covered area $\times 10^3$ km ²	% of total area
Argentina	890	32
Bolivia	200	19
Brasil	1.410	17
Paraguay	410	95
Uruguay	150	80
Total area	3.209	100

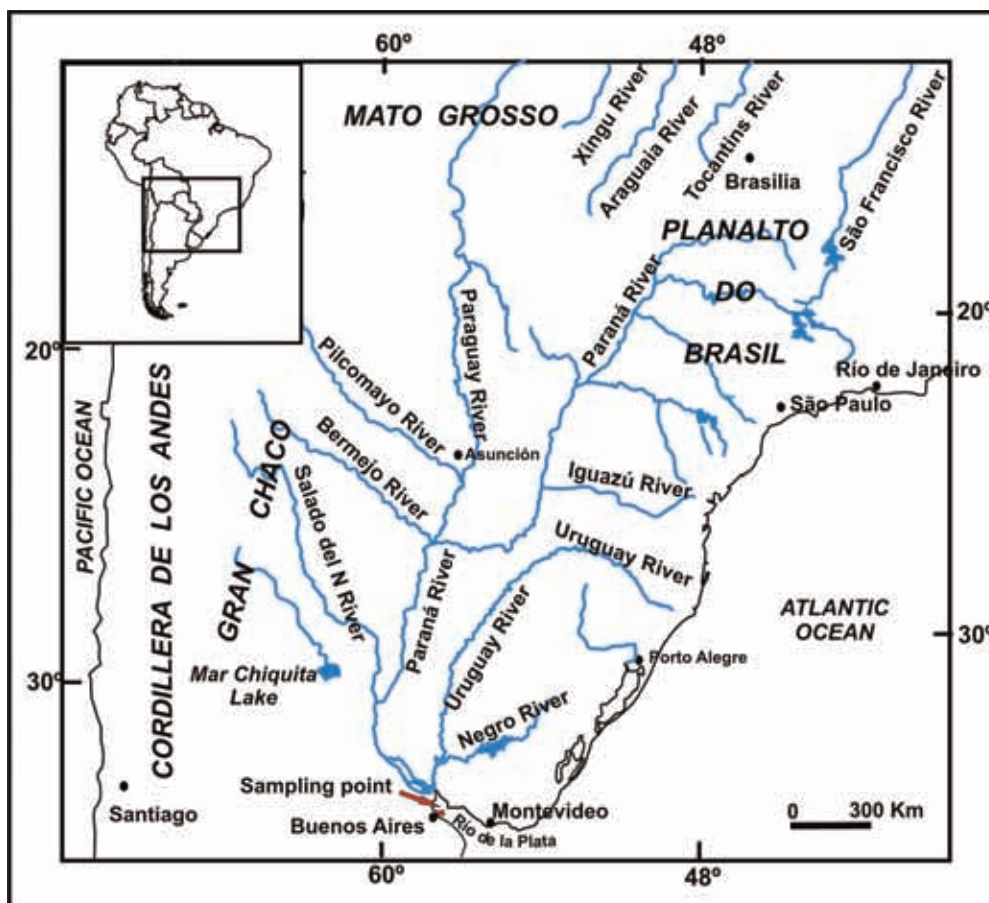


FIG. 1. Map of the del Plata basin showing the main contributors.

catastrophic flooding in Santa Fe City, Argentina, with water levels reaching more than 7 m over the normal level [2].

The Paraná River discharges an average of 17 300 m³/s with peak values of up to 54 000 m³/s (1958), causing major floods in nearby cities. High river discharges and subsequent floods in its last 1000 km towards the Río de la Plata estuary were related to the El Niño South Oscillation Phenomena (ENSO) [3, 4]. Isotopic studies carried out with data from the Global Network for Isotopes in Precipitation (GNIP-IAEA-WMO) and our National Network account for an increase in rainfall and yearly enlargement of the zone of South America affected by the Intertropical Convergence Zone (ITCZ) [5, 6]. As was preliminarily demonstrated in [7], it is possible to relate stable isotope compositions of hydrogen and oxygen to the ITCZ winter–summer movement and to the ENSO. The deuterium excess is associated to variations in kinetic fractionation factors during evaporation produced by ENSO related phenomena, and to the capture of recycled moisture from the Amazon rainforest during enhanced ITCZ shifts. In addition, ENSO signals and the ITCZ movements reach the estuary in ca. 4 months, due to the mean transit time from catchment areas to the sampling point.

The Instituto de Geocronología y Geología Isotópica (INGEIS) started to measure the isotopic composition of the Río de la Plata Estuary at the coast near Buenos Aires city in 1997 (Fig. 1). Studies carried out on the zone and satellite images demonstrated that the Uruguay River has no influence on the Buenos Aires coast, thus isotopic values obtained up to today only reflect

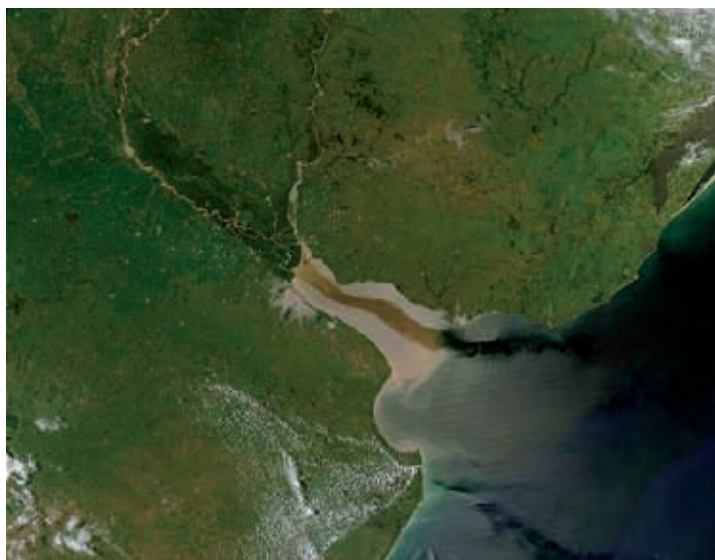


FIG. 2. Landsat image of the Rio de la Plata showing that the Uruguay river has no influence on the Buenos Aires coast.

the composition of the Paraná River (Fig. 2), allowing us to compare river composition at different localities, i.e. Corrientes and Santa Fe.

2. MATERIALS AND METHODS

A two liter sample has been collected every 15 days at a sampling point near the water works of Buenos Aires city in front of the Ciudad Universitaria. Since November, 2004 samples were taken daily. Composite 30 days grab samples and day by day samples were analyzed for November 2004 – May 2005, in most cases representing the lowest and highest values respectively. Another aliquot was used for tritium analysis. In addition, monthly cumulative humidity samples were collected during the year in the tank of the main engine of the central air compressed service of the INGEIS. Humidity in the air of the INGEIS building is considered to be in isotopic equilibrium with river water given its proximity (ca. 300 m) to the river.

In order to check the reliability of grab samples, daily samples from May and November were analyzed for deuterium and oxygen-18. Figure 3 shows the distribution of daily samples and the value of the grab sample taken on 15 November (which had been taken as representative for the 30 days). In this case, $\delta^2\text{H}$ values are the same for monthly averaged daily samples and the grab sample of 15 November but the composite $\delta^{18}\text{O}$ value is slightly different (Fig. 3). As a data quality check, a sample obtained for the mixture of 30 subsamples of 1 mL was also analyzed, and its isotopic values were identical to the arithmetic mean of the 30 individual analyses.

At the time of completion of this report not all May samples were measured (only deuterium is available), but it is probable that daily samples averaged on a monthly basis more accurately represent the mean isotopic composition of the river for the period of a month. In addition individual samples are available for further studies to be carried out when it is possible for the laboratory to measure such a set of samples.

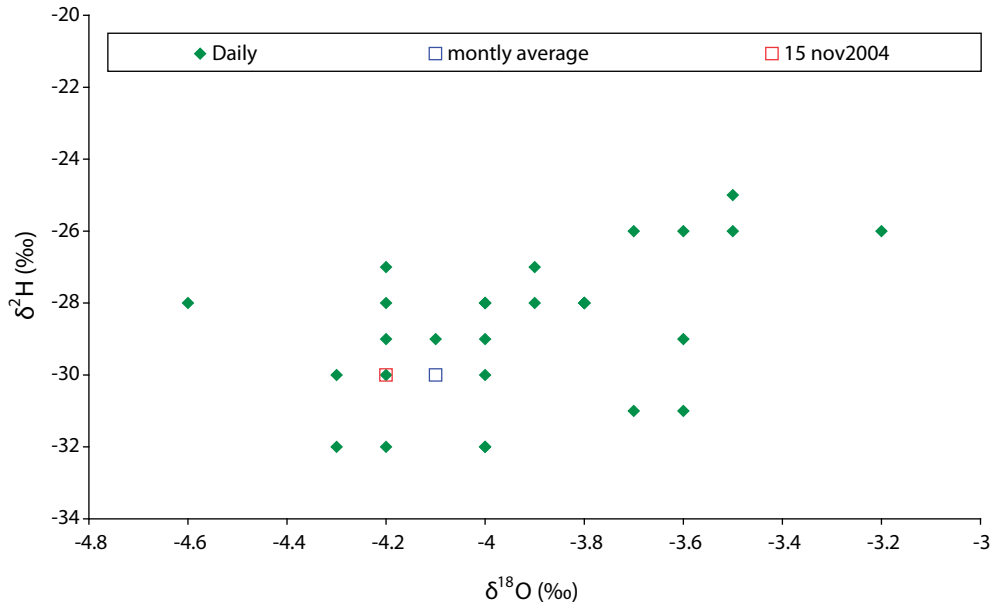


FIG. 3. Scatter plot showing the distribution of $\delta^{18}O$ vs δ^2H values of daily grab samples, the monthly average and the grab sample collected on 15 Nov. 2004.

Isotope analyses were carried out at INGEIS Laboratories. Deuterium (2H) in water samples was prepared using standard procedures [8] and for ^{18}O , the methodology described in [9] was used. Isotope ratios were measured using a multicollector McKinney type mass spectrometer, Finnigan MAT Delta S. Results are expressed in δ (‰) and defined as:

$$\delta = 1000 \frac{R_S - R_P}{R_P} \text{‰}$$

where:

- δ is isotopic deviation in ‰;
- S is sample;
- P is international standard
- R is isotope ratio ($^2H/^1H$, $^{18}O/^{16}O$).

The standard is Vienna Standard Mean Ocean Water, V-SMOW [10]. The analytical uncertainties are ± 0.1 ‰ and ± 1.0 ‰ for $\delta^{18}O$ and δ^2H respectively.

Tritium samples were measured using liquid scintillation direct counting in the the Atucha Nuclear site laboratory, Argentina. Results are expressed in TU ($1 \text{ TU} = 1^3\text{H} : 10^{18} \text{ H}$). The detection limit is about 5 TU. Samples below this value are considered to be 1 to 3 TU.

3. RESULTS AND DISCUSSION

3.1. Paraná River discharge

Fig. 4 shows a comparative picture of discharge over several years at Corrientes station, while, Fig. 5 and Fig. 6 present the daily discharge of Paraná River at the Corrientes and Santa Fe gauge stations [11].

As previously mentioned, a delay of about 4–5 months was observed between the time of the meteorological event and its signal in the estuary. It was assumed that this is related to the mean transit time from the catchments to the sampling point. An estimation of the feasibility of this number was made during a seven year study of the time required by the Paraná river to cover the trajectory between the Corrientes and Santa Fé stations (about 600 km) (Fig. 7). Calculations were made characterizing maximum and minimum peaks in Corrientes and their homologues in Santa Fe (Fig. 8).

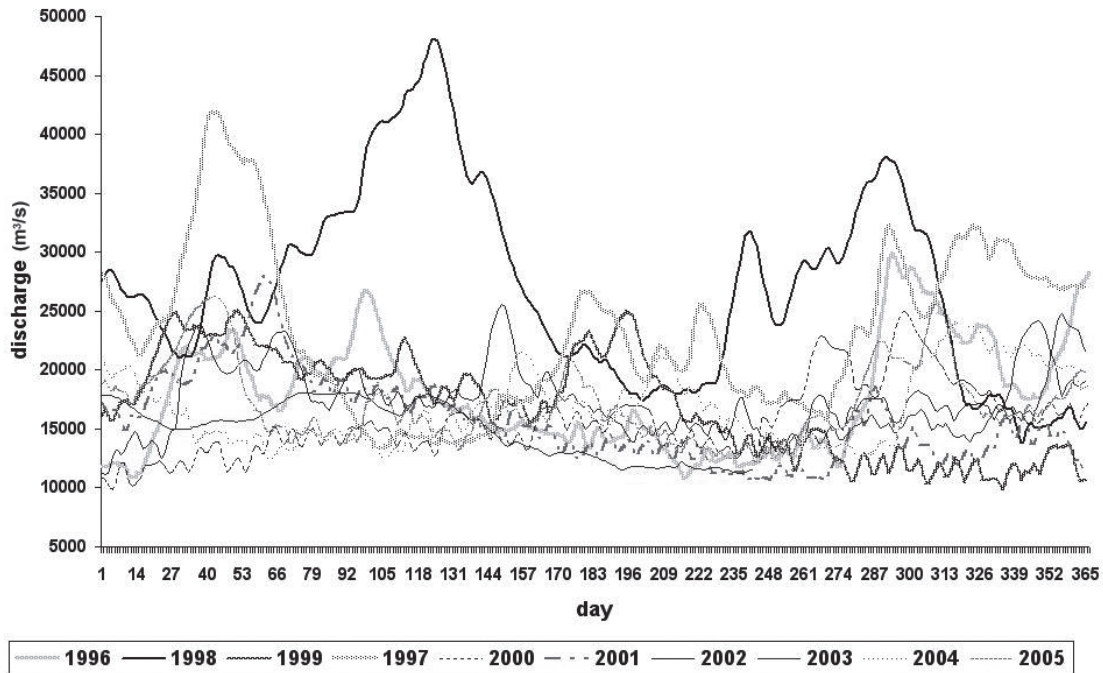


FIG. 4. Discharge of the Paraná River at the Corrientes station. Note the increased volumes during 'El Niño' years (See Fig. 18).

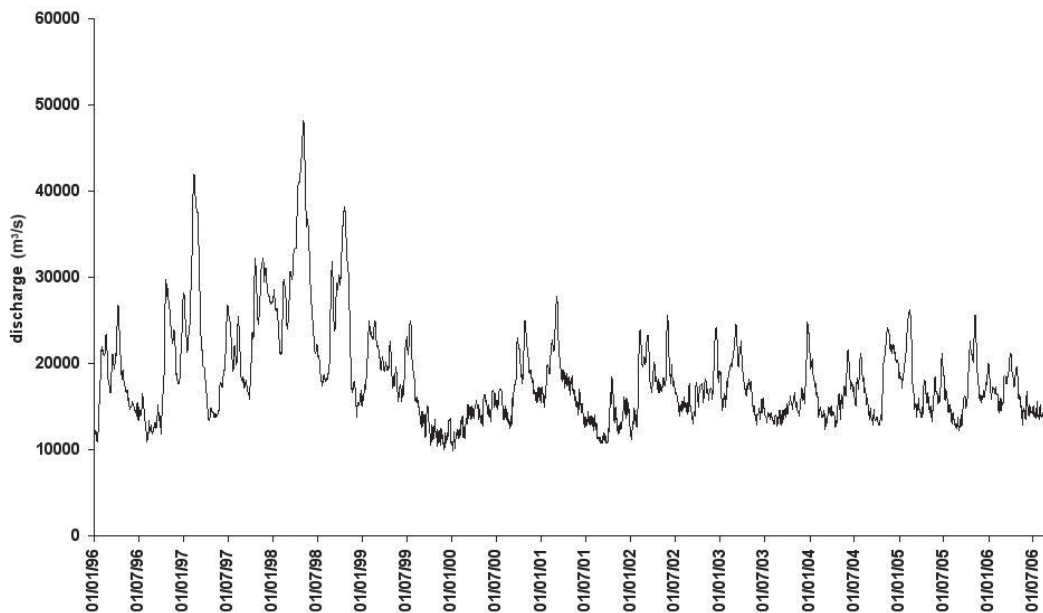


FIG. 5. Daily discharge of the Paraná River at the Corrientes station period 01/1996–08/2006 [11].

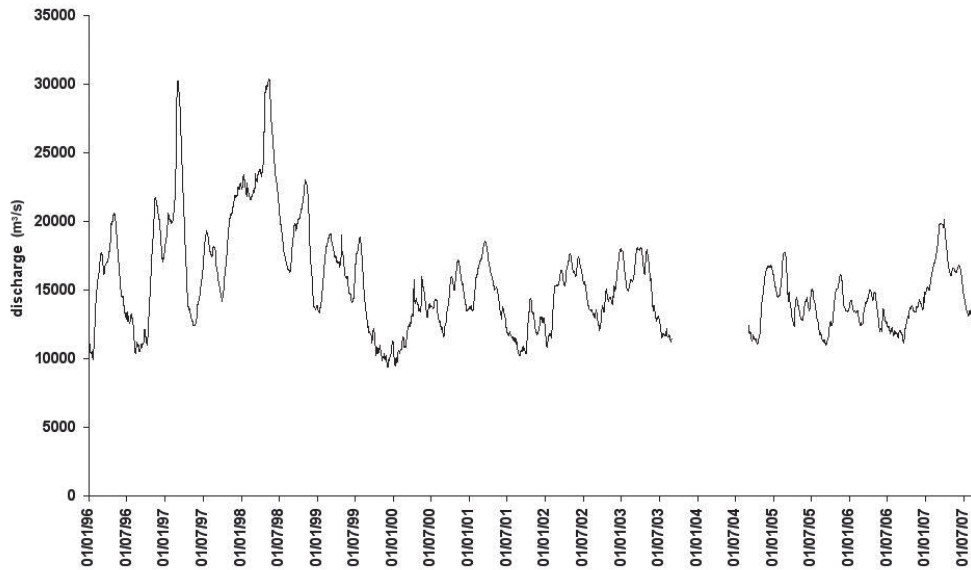


FIG. 6. Daily discharge of the Paraná River at Santa Fe station period 01/1996–08/2007 [11].



FIG. 7. Location of Santa Fe and Corrientes stations. The distance between the cities is marked in red.

If we consider the time span between the occurrence of a peak (valley) in Corrientes and the same peak (valley) in Santa Fe and plot them *versus* discharge in the Corrientes, we obtain the graph in Fig. 8. A weak correlation is shown, suggesting that transit time increases with discharge, ranging from 3 to 24 days, and averaging a medium speed of 38 km/day. Taking into account basin dimensions, catchment signals would be reflected in the sampling point delayed by about three months, and an observed time of four months is considered reasonable taking into account the dams and natural flooding that hold back the flow in zones occurring along the river course. Figure 9 shows a transit time simulation between the Corrientes and Santa Fe stations (Fig. 7). It consists of a shift in the discharge corresponding to the Santa Fe

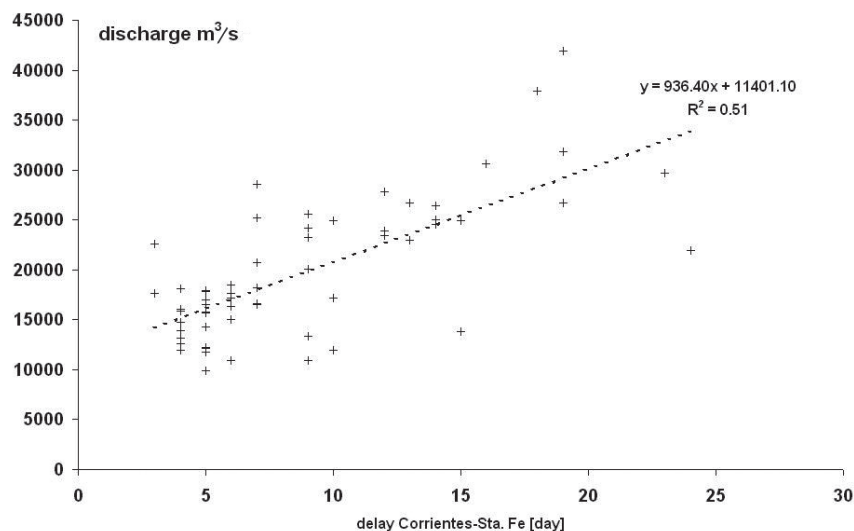


FIG. 8. Correlation between discharge at Corrientes and the transit time Corrientes–Santa Fe (570 km).

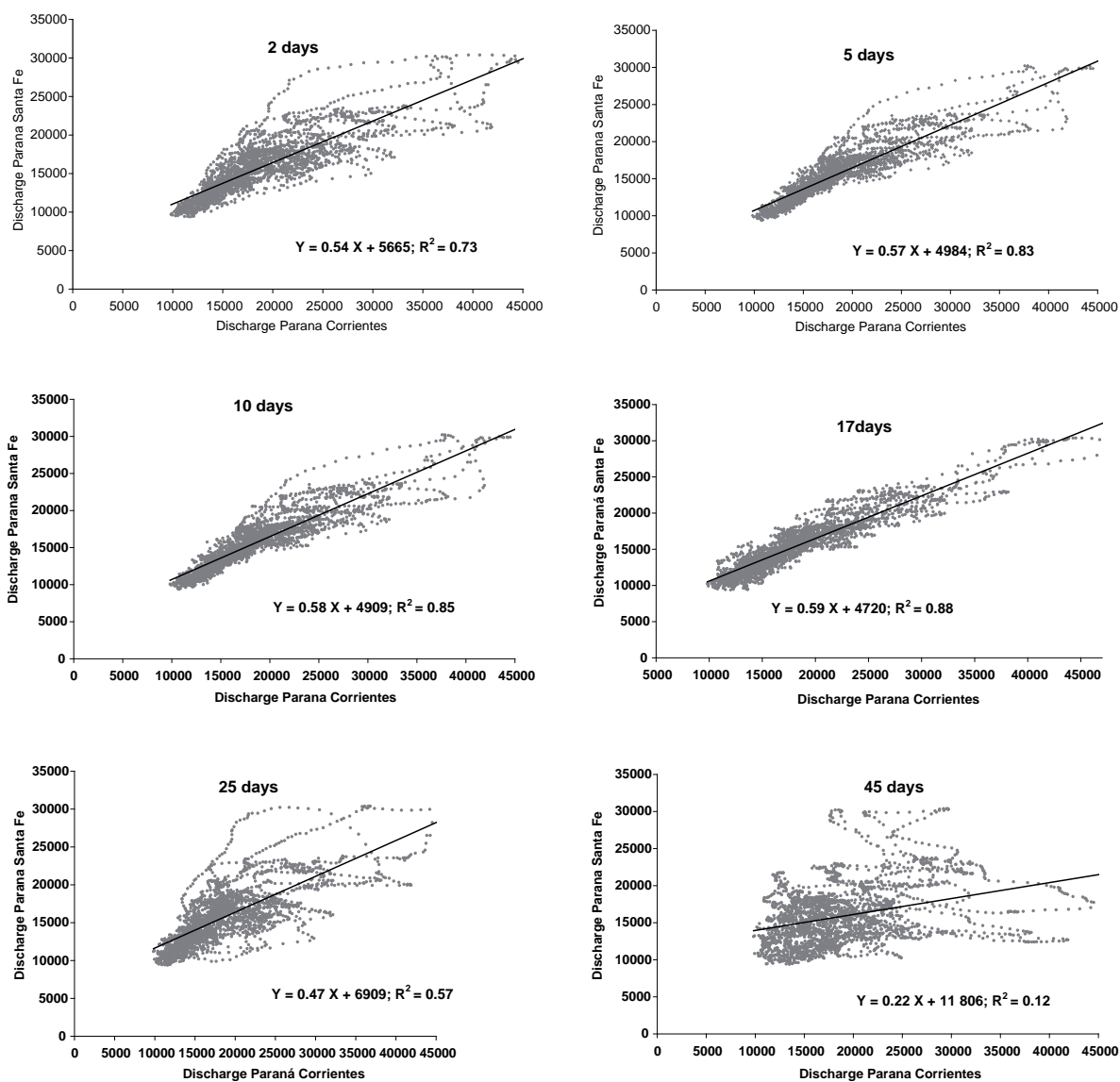


FIG. 9. Transit time simulation between the Corrientes and Santa Fe stations. Note that the best fit corresponds to $\tau = 17$ days

station keeping that of the Corrientes constant. The best fit corresponds to $\tau = 17$ days, which is the average span time that best explains the correspondence between peaks and valleys.

3.2. Stable Isotopes

Figures 10, 11 and 12 show the time series for $\delta^{18}\text{O}$, $\delta^2\text{H}$ and deuterium excess at the Ciudad University Station in Buenos Aires. In Fig. 10, the isotope concentration of ^{18}O is presented. It follows a well defined cyclic pattern with time. The $\delta^2\text{H}$ values exhibit a similar scheme for the first two periods, but the third and fourth periods present more negative isotope values in comparison to the others (Fig. 11). This fact can also be observed in the time series for the d-excess parameter, produced by the depletion of deuterium, which is not associated to a parallel ^{18}O decrease (Fig. 12).

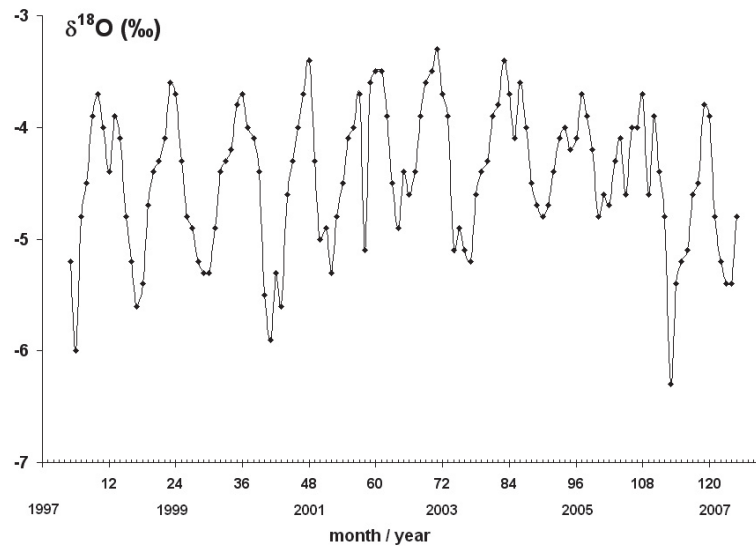


FIG. 10. $\delta^{18}\text{O}$ time series for the period 1997–2007 at Ciudad University Station.

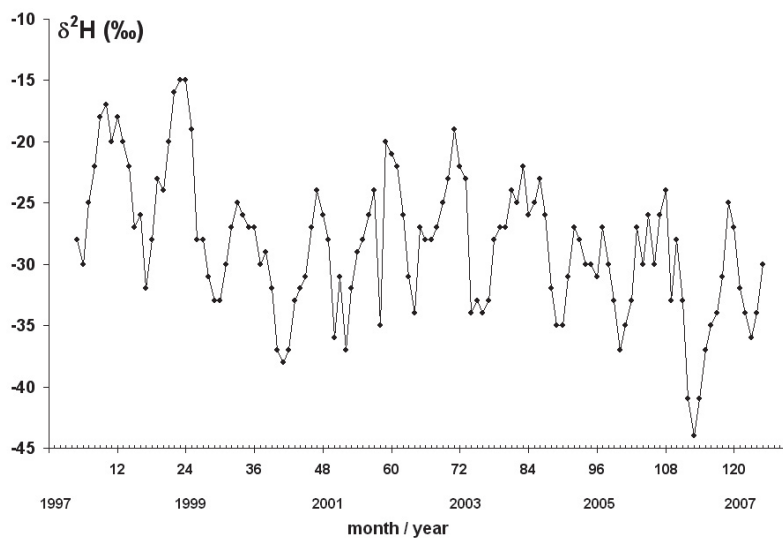


FIG. 11. $\delta^2\text{H}$ time series for the period 1997–2007 at Ciudad University Station.

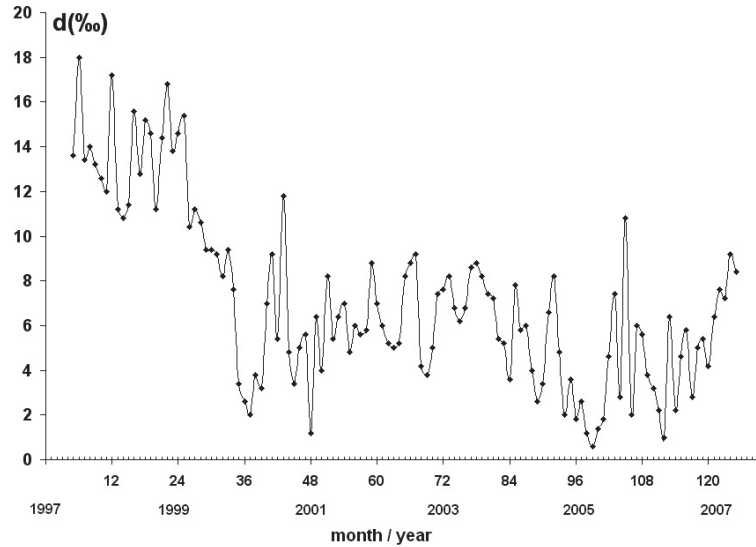


FIG. 12. Deuterium excess time series for the period 1997–2007 at Ciudad University Station.

4. BACKGROUND

4.1. The amount effect

As was first noted by [12] and proven in later works, the so-called ‘amount effect’ governs stable isotopic composition in tropical zones, where temperature dependence is less significant than in middle and high latitudes. Albero and Panarello [13] observed the existence of this effect in Belem, Brazil, where temperature variations are negligible throughout the year. Figure 13 shows clustered samples in months with heavy rain of around -5‰ in $\delta^{18}\text{O}$. Conversely the ‘dry’ season exhibits enriched values similar of those of ocean. Also in Río de Janeiro, Brazil (Fig. 14), a correlation between amount and isotope depletion was found, indicating corresponding regression lines for both to more than one source of water vapour [14].

The amount effect is considered to be the consequence of a Rayleigh condensation of vapour and rainout. As condensation proceeds, the isotopic composition of raindrops decreases as a function of the remaining vapour fraction of the cloud, thus as precipitation progresses, the isotopic composition of rain becomes lighter. This effect can be expressed as follows:

$$\delta = \delta_i - \varepsilon \ln f$$

Where f is the remaining fraction of vapour in the cloud W/W_0 , and δ_i is the starting isotope composition of the cloud.

4.2. Hadley cells and the ITCZ

At low latitudes, air columns rise and move poleward on either side of the Equator. At higher latitudes, cooling air causes the columns to descend. This results in the development of large convective wind cells, called Hadley cells, with low pressure centres along the equator and high pressure belts at around 30° latitude (Fig. 15).

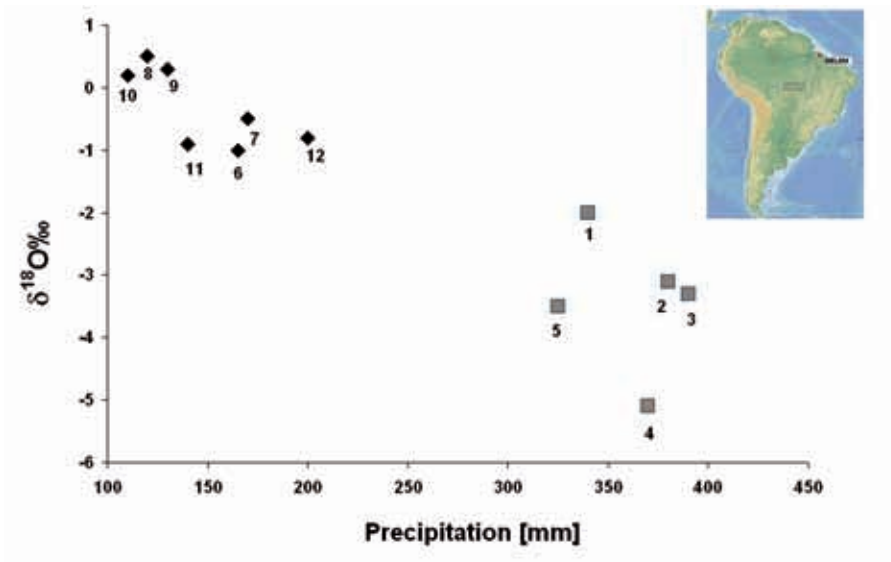


FIG. 13. Amount effect in Belem, after [13].

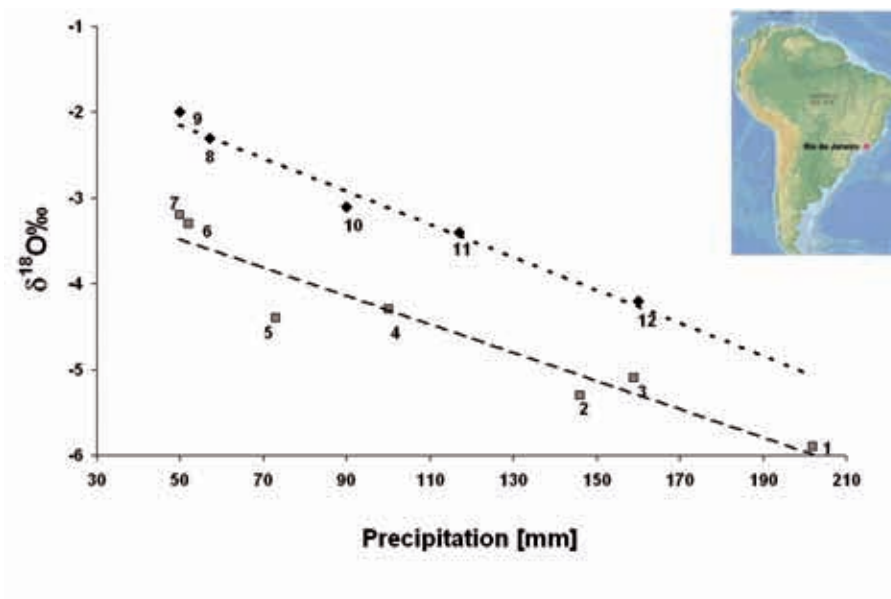


FIG. 14. Amount effect in Rio de Janeiro, after [13].

The Earth's rotation causes separation of the high pressure belt into divergent spiraling anticyclone cells. The compensating back flowing air produces northeasterly and southeasterly trade winds, which converge in the equatorial area, and is therefore also known as the Intertropical Convergence Zone (ITCZ) [15]. As these winds converge, moist air is forced upward. This causes water vapour to condense, or be 'squeezed' out as air cools and rises, resulting in a band of heavy precipitation around the globe. This band is not stationary and shows a strong seasonal behaviour, always being drawn toward the area of most intense solar heating, or warmest surface temperatures.

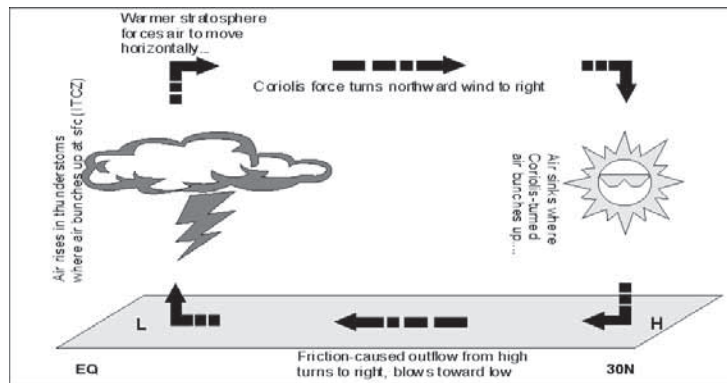


FIG. 15. Sketch of the Hadley Cells.

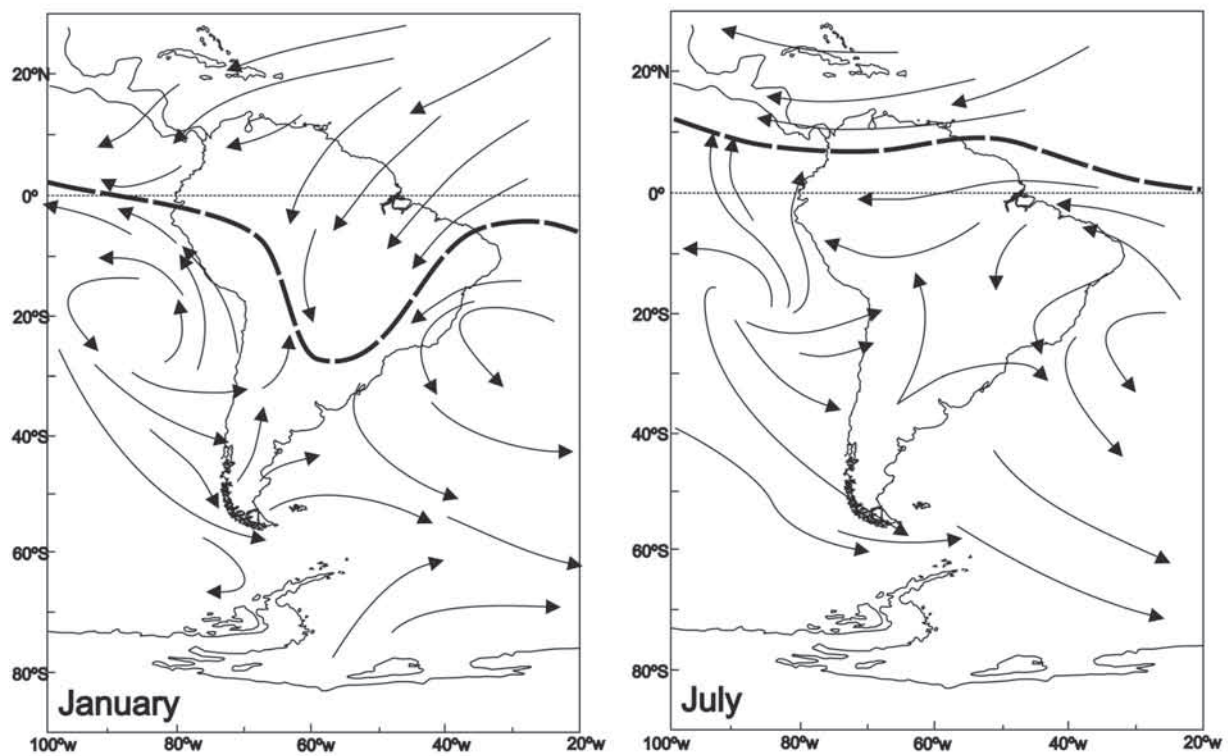


FIG. 16. Seasonal displacement of the Intertropical Convergence Zone, cited in [5].

During the austral winter (July) it is displaced lightly to the North (parallel to the Equator) up to 8°N. During the Austral summer (January) the ITCZ shifts southwards, making a strong inflexion over the continent reaching up to 30°S, between 50°W and 60°W. (Fig.16) [5].

When it shifts southwards, it provides the synoptic conditions for a great increase in precipitation. These conditions produce an amount effect that is recorded with some delay in the stable isotope composition of the Río de la Plata. Therefore, more negative $\delta^{18}\text{O}$ and $\delta^2\text{H}$ values are observed in the months of May–June, overdue ca. 4 months with respect to the southern movement of the ITCZ due to an average transit time of the river water from its head to its mouth.

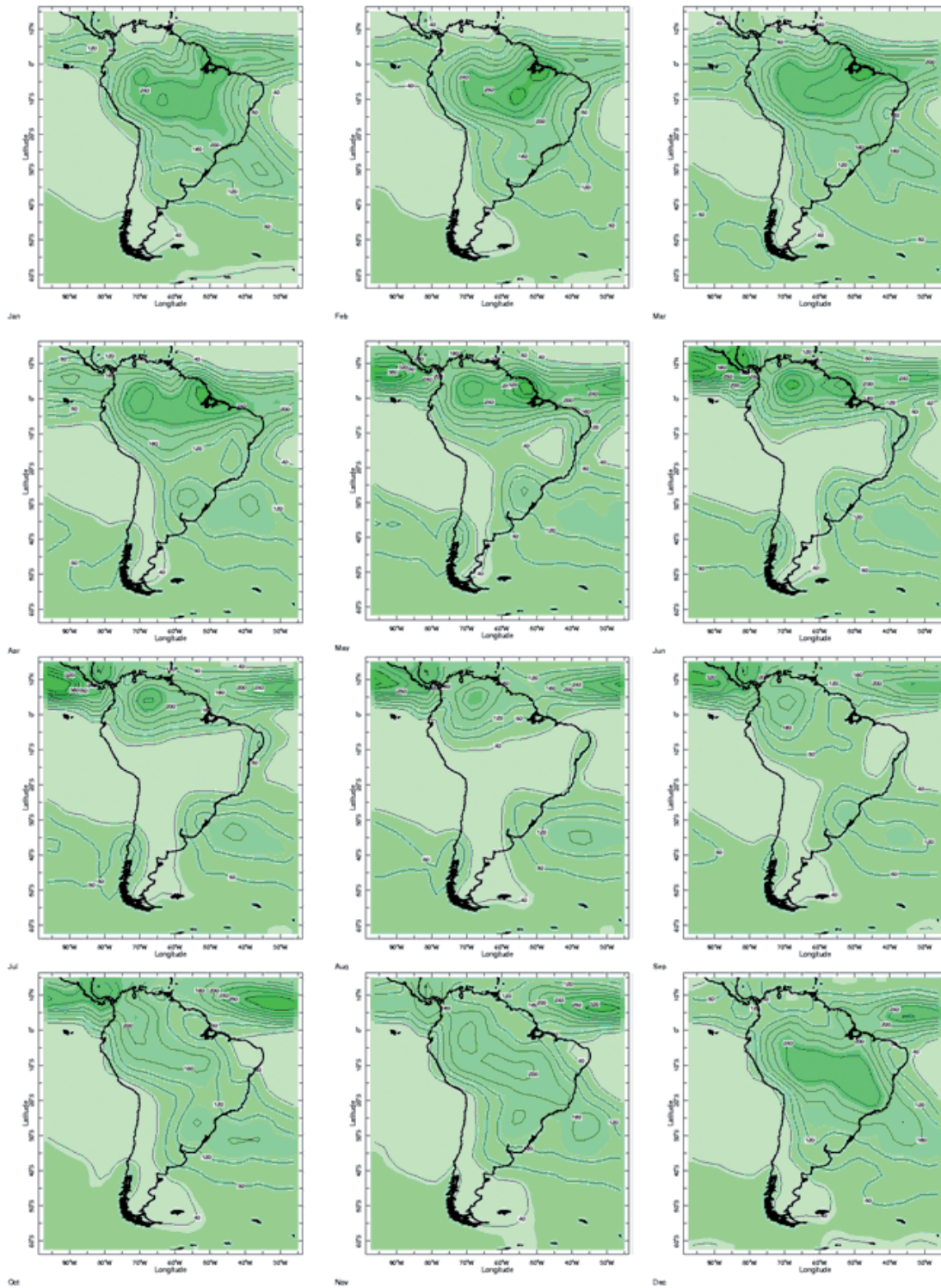


FIG. 17. ITCZ and rain distribution at the catchment areas [16].

A more detailed distribution of precipitation amount and ITCZ position is given in Fig. 17 [16]. These plots evidence dry periods for July–August (reflected in the November values) and humid periods in December–January, producing the isotopic composition observed in May.

4.3. El Niño Southern Oscillation (ENSO)

ENSO is a generic name for oceanic-atmospheric coupled cyclic phenomena which significantly change meteorological conditions around the globe. When associated to an ocean temperature increase, we refer to it as 'El Niño', conversely when ENSO is linked to an ocean temperature decrease, we refer to it as 'La Niña'. In addition, neutral (or normal) events are referred as 'Non Niño-Non Niña' episodes. ENSO phenomena are defined for the Pacific Ocean at 30°S but they have induced consequences at the global scale known as 'teleconnections'.

The El Niño episode of 1997–1998 was associated with a dramatic alteration in the global pattern of tropical rainfall and deep tropical convection, as indicated by above normal rainfall across the eastern half of the tropical Pacific and by significantly below normal convection across Indonesia and the western equatorial Pacific. The combined zonal extent of these rainfall anomalies covered a distance of more than one half the circumference of the earth.

Selected impacts associated with these warm episode conditions included:

- (1) Excessive rainfall across the eastern half of the tropical Pacific;
- (2) Significantly below normal rainfall and drought across Indonesia and the western tropical Pacific;
- (3) Below normal hurricane activity over the North Atlantic during August–October, with a simultaneously expanded region of conditions favourable for tropical cyclone formation over the eastern subtropical North Pacific;
- (4) Excessive rainfall and flooding in equatorial eastern Africa during October–December;
- (5) A dramatic eastward extension of the South Pacific jet stream to well east of the date line during June–December, which resulted in enhanced storminess across south-eastern South America and central Chile;
- (6) Abnormally dry conditions across the Amazon Basin, Central America and the Caribbean Sea. Both phenomena are coupled with atmospheric circulation producing anomalies in the trade winds.

When a warm ENSO (El Niño) take place, southward movement of the ITCZ is pronounced and reaches lower latitudes than in normal or cold episodes (enhanced ITCZ). Under these conditions, winds capture more recycled vapour from the Amazon. On the other hand, when a cold ENSO (La Niña) occurs, southward movement of the ITCZ is limited or interrupted, leading to a decrease in the amount of precipitation, which can produce drought in many cases. The climate over large parts of South America is strongly influenced by the El Niño/Southern Oscillation. During warm episodes, drier than normal conditions are generally observed across north-eastern South America during July–March, while enhanced precipitation tends to be observed throughout south-eastern South America during November–February [17], and throughout central Chile during the austral winter [18]. Also, above average temperatures are typically observed along the west coast of South America from May to April [17]. During the very strong 1997 warming episode, all of these conditions were prominent aspects of the South American climate.

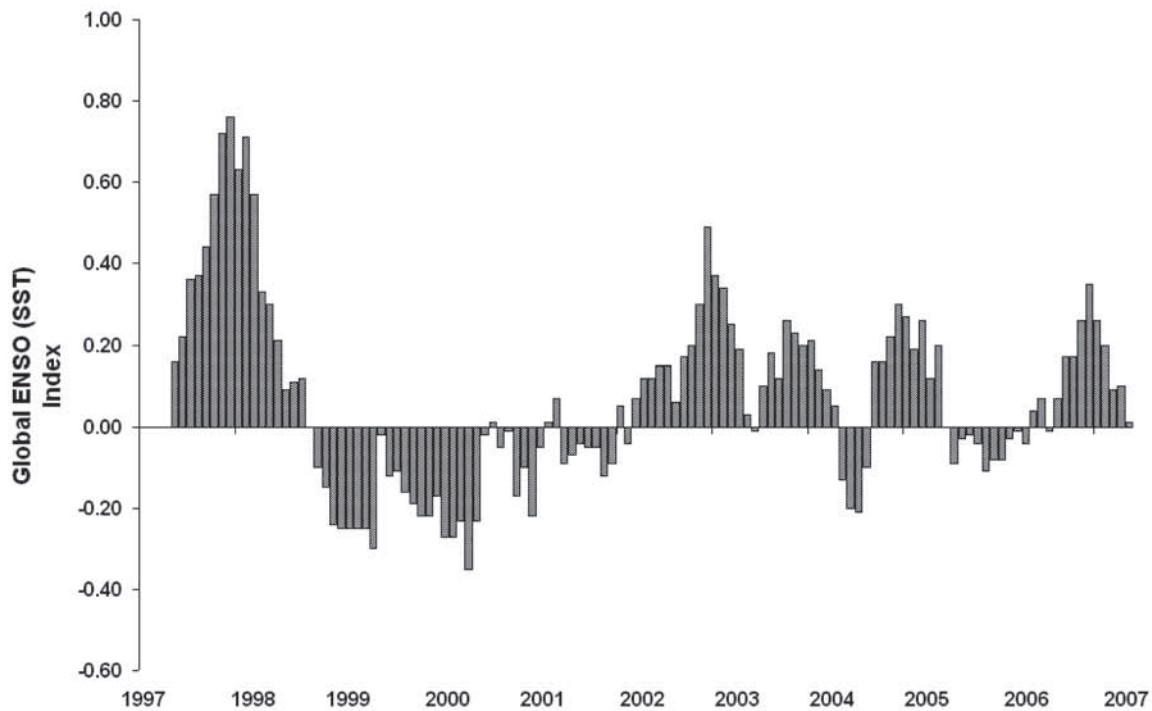


FIG. 18. ENSO index for the period 1996–2007 [19].

The Global Sea Surface Temperature ENSO Index (Global SST ENSO Index) is used to measure the state of the ocean during ENSO phenomena. This ENSO index is the average SST anomaly equatorward of 20 degrees latitude (north and south) minus the average SST poleward of 20 degrees, and it captures the low frequency part of the El Niño/Southern Oscillation phenomenon (Fig.18) [19].

In an early work [3], good correlation was found between El Niño episodes and an increase in Paraná River discharge. Flooding events produced by the Paraná River in May 1998 occurred in response to the strongest El Niño phase of the twentieth century [4].

5. DEUTERIUM EXCESS AND THE ENSO

Changes in the ratio between ^{18}O and ^2H are caused by the different diffusion rates of water species $^2\text{H}^1\text{H}^{16}\text{O}$ (mass 19) and $^1\text{H}_2^{18}\text{O}$ (mass 20) during evaporation. The differential diffusion rate for the above molecular species produces kinetic fractionation. The kinetic factor for this process is related to ocean temperature, moisture and wind strength, among other causes [20].

Figure 19 shows the correlation between the ENSO index and d-excess. During El Niño episodes, river waters show high d values, reaching up to 18‰ in 1997–1998. Conversely, during La Niña, lower d-excess values were observed, reaching up to 1‰ in 2006.

The warmer ocean surface during El Niño increases the kinetic factor and thus evaporation occurs far away from equilibrium conditions. In this case, d-excess values are larger than those in which the process takes place under equilibrium conditions. A colder ocean surface can lead

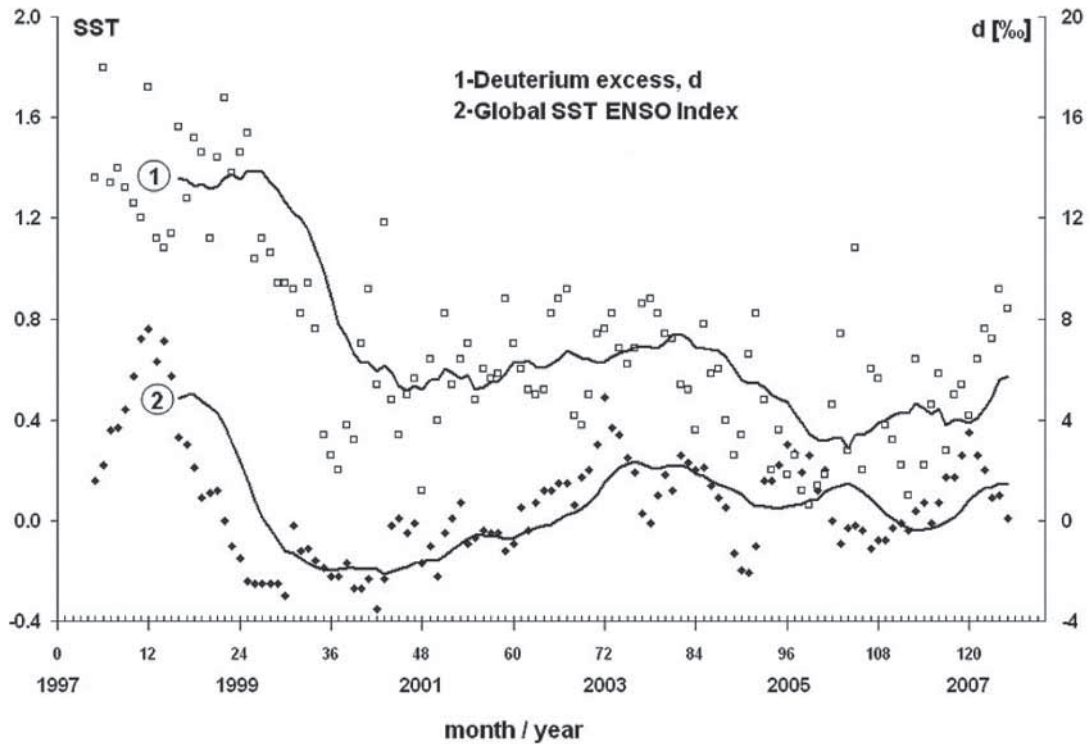


FIG. 19. Twelve month moving average for (1) deuterium excess and (2) the ENSO Global Index (SST). Both signals show a similar general pattern shifted by about 4 months despite all the potential factors that could modify isotopic composition along the river path (≈ 2800 km). Most differences are probably due to variations in transit time from the catchments to the mouth and also to the large number of tributaries whose contribution to the Paraná River change with time. See text for more details.

to a decrease in the kinetic factor; evaporation occurs close to equilibrium and thus d-values approximate zero. However, changes in temperature are not enough to explain the entire variation of d-excess values, although changes in air moisture and wind velocity could also occur. When El Niño forces an enhanced-ITCZ, a large area of Amazon moisture, which is already tagged with exceptionally high d-excess values, is captured. In this way, the ENSO and ITCZ synergise, yielding very high values of deuterium excess.

6. TRITIUM

Tritium concentrations from the Río de la Plata and the Ciudad Universitaria rain collection station have been monitored since 2001 (Fig. 20). It is believed that the most probable source of technogenic tritium in the estuary is water discharge from the cooling system of the Atucha nuclear site. The tritium content of the river reaches peaks of up to 1400 T.U. Rainwater has also tritium concentrations more elevated than expected.

7. CONCLUSIONS

The amount of precipitation defines the isotope composition of precipitation in tropical zones of central South America.

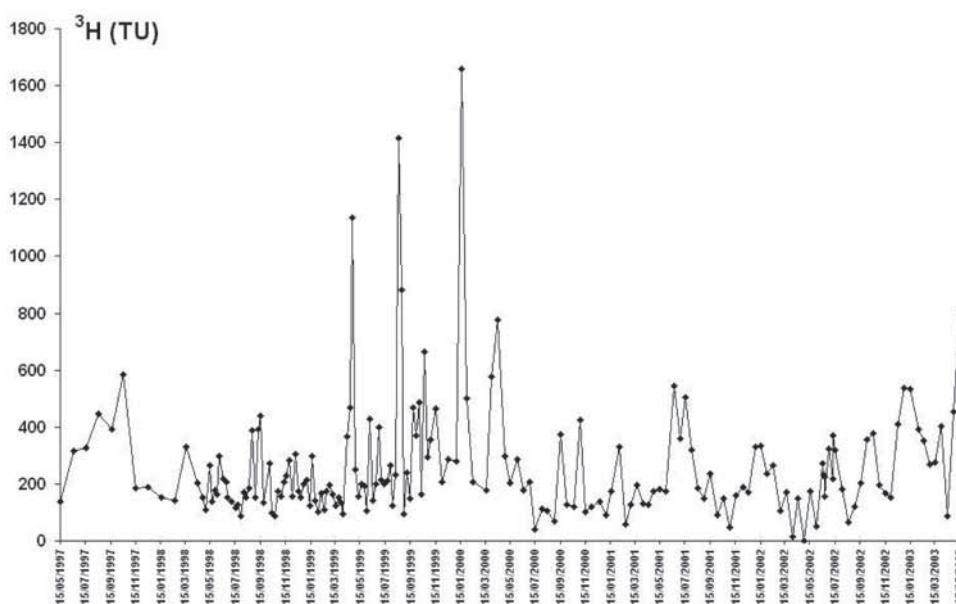


FIG. 20. Tritium values on Río de la Plata in the Ciudad Universitaria station during 1997–2003. Concentrations have been measured by direct counting.

The ITCZ is the main factor controlling the amount of precipitation and thus the isotope composition of the Paraná River, whose catchment area extends over a large portion of South America.

The ENSO phenomena influences the southwards shift of the ITCZ enhancing it (El Niño) or preventing it (La Niña). The ENSO enhanced ITCZ captures Amazon deuterium rich moisture together with marine vapour also deuterium rich lead to deuterium excess values up to 18‰ during El Niño 1997–1998.

This pattern reverts during La Niña onset, i.e. a more reduced zone creating captured Amazon deuterium rich moisture and less significant kinetic fractionation during evaporation under cool conditions. This fact is shown in a dramatic drop after the warm episode of 1997–1998. During 2006 under La Niña conditions, d-excess values reached up to 1‰.

Despite all the interactions with groundwater and physical processes undergone along ca. 2800 km, the Paraná River still reflects all these climatic phenomena at its mouth.

ACKNOWLEDGEMENTS

We are grateful to Ms. Estela I. Ducós for her careful reading of the manuscript and her valuable suggestions. This work was partially supported by grants from the International Atomic Energy Agency (IAEA) within the framework of the CRP “Isotope Tracing of Hydrological Processes in Large Rivers Basin” (INGEIS).

REFERENCES

- [1] UNITED NATIONS ENVIRONMENT PROGRAMME, World Conservation Monitoring Centre (2008), <http://www.unep-wcmc.org/sites/wh/pantanal.html> (accessed on 2008-08-17).
- [2] CLARIN, (2003) <http://old.clarin.com/diario/2003/04/30/um/m-552861.htm>.
- [3] DEPETRIS, P.J., et al., ENSO-controlled flooding in the Paraná river, *Naturwissenschaften* **83** (1996) 127–129.
- [4] CAMILLONI, I.A., BARROS, V.R., Extreme discharge events in the Paraná River and their climate forcing, *J. Hydrol.* **278** (2003) 94–106.
- [5] ROZANSKI, K., ARAGUÁS-ARAGUÁS, L., Spatial and temporal variability of stable isotopic composition of precipitation over the South American continent, *Bulletin de l'Institut Française d'études Andines* **24** 3 (1995) 379–390.
- [6] CERNE, B., et al., Análisis de la composición isotópica del agua de lluvia en la Argentina subtropical durante el experimento SALLJEX. IX CONGRESMET, “Tiempo, Clima, Agua y Desarrollo Sostenible”, Buenos Aires (2005) CD-ROM.
- [7] PANARELLO, H.O., DAPENÑA, C., “Stable isotope composition of the Rio de la Plata estuary: an attempt to relate to meteorological variables”, III South American Symposium on Isotope Geology, Pucón, Chile (2001) CD-ROM.
- [8] COLEMAN, M.L., et al., A rapid and precise technique for reduction of water with Zinc for Hydrogen isotope analysis, *Anal. Chem.* **54** (1982) 993–995.
- [9] PANARELLO, H.O., PARICA, C.A., Isótopos del oxígeno en hidrogeología e hidrología: Primeros valores en aguas de lluvia de Buenos Aires, *Asociación Geológica Argentina, Revista* **39** (1984) 3–11.
- [10] GONFIANTINI, R., Standards for stable isotope measurements in natural compounds, *Nature* **271** 534 (1978).
- [11] ESTADÍSTICA HIDROLÓGICA, SISTEMA NACIONAL DE INFORMACIÓN HÍDRICA (SNIH) DE LA SUBSECRETARÍA DE RECURSOS HÍDRICOS, SECRETARÍA DE OBRAS PUBLICAS, MINISTERIO DE PLANIFICACIÓN FEDERAL, Inversión Pública y Servicios, República Argentina (2007).
- [12] DANSGARD, W., Stable Isotopes in precipitation, *Tellus* **16** (1964) 436–468.
- [13] ALBERO, M.C., PANARELLO, H.O., “Tritium and stable isotopes in precipitation waters from Sudamerica”, *Proc. Interamerican Symposium on Isotope Hydrology (RODRÍGUEZ, C., BRICEÑO, E., Eds)* Bogotá, Colombia (1980) 91–100.
- [14] SALATI, E., MATZUI, E., Isotopic Hydrology in the Brazilian Amazon Basin, *Proc. Interamerican Symposium on Isotope Hydrology, Bogotá, Colombia* (1980) 11–120.
- [15] MOOK, W.G. (Ed.), *Environmental isotopes in the hydrological cycle: Principles and applications*, Vol. I, Chapter 1, *The Global Cycle Of Water*, Paris: UNESCO (2001).
- [16] http://iridl.ldeo.columbia.edu/expert/SOURCES/.NOAA/.NCEP/.CPC/.CAM5_OPI/.original_version/.climatology/.prcp (accessed on 2008-05-28).
- [17] ROPELEWSKI, C.H., HALPERT, S., Global and regional scale precipitation patterns associated with El Niño/Southern Oscillation, *Mon. Wea. Rev.* **115** (1987) 1600–1626.
- [18] ACEITUNO, P., On the functioning of the Southern Oscillation in the South American Sector, Part I: Surface climate, *Mon. Wea. Rev.* **116** (1988) 505–524.
- [19] JOINT INSTITUTE FOR THE STUDY OF THE ATMOSPHERE AND OCEAN, UNIVERSITY OF WASHINGTON, Seattle (2008) http://www.jisao.washington.edu/data_sets/globalssenso.
- [20] MERLIVAT, L., JOUZEL, J., Global climatic interpretation of the Deuterium-Oxygen 18 relationship for precipitation, *J. Geophys. Res.* **84** (1979) 5029–5033.

- [21] CRAIG, H., Isotopic variations in Meteoric waters, *Science* **133** (1961) 1702–1703.
- [22] DAPENÑA, C., et al., “El origen de las precipitaciones en el Norte de Argentina y su importancia para el estudio de los sistemas hidrológicos”, II Seminario Hispano Latinoamericano sobre Temas actuales de Hidrología Subterránea, *Actas* 37–46 (2005).
- [23] HALPERT, M.S., ROPELEWSKI, C.F., Surface temperature patterns associated with the Southern Oscillation, *J. Clim.* **5** 5 (1992) 77–593.

SOUTH AFRICAN CONTRIBUTION TO THE RIVERS CRP

S. Talma^a, S. Lorentz^b, S. Woodborne^a

^a Natural Resources and the Environment, CSIR, Pretoria, South Africa

^b School of Bioresources, Engineering and Environmental Hydrology,
University of Kwazulu–Natal, Pietermaritzburg, South Africa

Abstract. This report summarizes activities undertaken by the South African participants of the IAEA Cooperative Research Project ‘Design criteria for a network to monitor isotope compositions of runoff in large rivers’. The project was led by Siep Talma of the CSIR in Pretoria. Simon Lorentz from the University of KwaZulu–Natal in Pietermaritzburg provided the hydrological input. River flow and stable isotope data that were collected during 1968–1974 by the CSIR were digitised and are now available electronically. Nine sampling stations were set up and operated between 2002 and 2006 in the Orange, Thukela and Zambezi catchments. Three sampling surveys were undertaken along the main stretches of the Vaal and Orange Rivers, to illustrate the isotope and chemical variations that were found during monitoring. Data are presented and preliminary conclusions drawn. In the river catchments there is an inverse relation between flow and ^{18}O content, even on a weekly basis. The presence of reservoirs in these rivers disturbs this relation since water is accumulated in reservoirs and isotope patterns become integrated. The controlled release of water from reservoirs breaks the relation between flow and ^{18}O . The relationship between ^{18}O and deuterium indicates some evaporation causing displacement from the local meteoric water line as well as evaporation effects that are generally found for $\delta^{18}\text{O} > -2\text{‰}$. The isotope and hydrological data that have been obtained provide information on which the utility and possibility of future monitoring and investigative projects can be based.

1. PROJECT BACKGROUND

The South African contribution to this CRP originates from early activities of the CSIR environmental isotope group. Between 1968 and 1974, regular sampling and isotope analysis was undertaken on samples from 12 river stations in southern Africa. It was therefore natural that this earlier work from the region contributed to this CRP, which commenced in 2002.

The participation of CSIR in the present CRP was undertaken in order to

- Capture historical data in a database;
- Set up and operate new isotope sampling stations in line with the needs for a future GNIR programme concentrating on larger catchments;
- Evaluate the two sets of data on a sound hydrological basis.

The collaboration of Prof. Simon Lorentz from the University of Natal in the present project was crucial, since he represents the foremost centre of hydrological research in the country and brought in hydrological expertise that was lacking in the past.

2. HISTORICAL RIVER DATA

During the period 1968–1969, Dr Wolfgang Roether, then at Heidelberg University, spent a sabbatical in Pretoria at what was then the Natural Isotopes Division of the National Physical Research Laboratory of the CSIR. During this year, he commissioned a facility for ^{18}O analysis

in water and established a network of individuals who collected river water on a weekly basis from South African river stations representing major drainages in South Africa (Fig. 1). After Roether's departure, this activity was continued by Siep Talma [1]. Some stations were later closed, and a few new ones opened, but towards 1973–1974 this activity was shut down.

2.1. Sampling in 1968–1974

River water samples were initially collected on a weekly basis from eight stations in South Africa (Table 1). Water samples of 250 ml were collected and forwarded to the CSIR laboratory in Pretoria. The collectors were individuals who also regularly measured flow at these rivers on behalf of the South African (governmental) Department of Water Affairs and Forestry (DWA) (Table 1). From 1971 onward three stations (Orange at Oranjedraai, Caledon River and Kornetspruit) in the highlands of Lesotho (the upper reaches of the Orange catchment) were added to the network to amplify details of the rainfall/runoff response. At some time during this time, samples were also obtained for three years from the Zambezi river at Tete in Mozambique, just below the Cahora Bassa dam, which was then under construction. The entire sampling network was discontinued in 1974 because the analytical load became too large.

The ^{18}O analyses were done on weekly samples for the first two years and occasionally for deuterium and tritium (see Table 1 for details). Later in the project, analyses were done less frequently and usually then on monthly composite samples. River flow data were originally obtained from DWA reports, but are now available online [2].

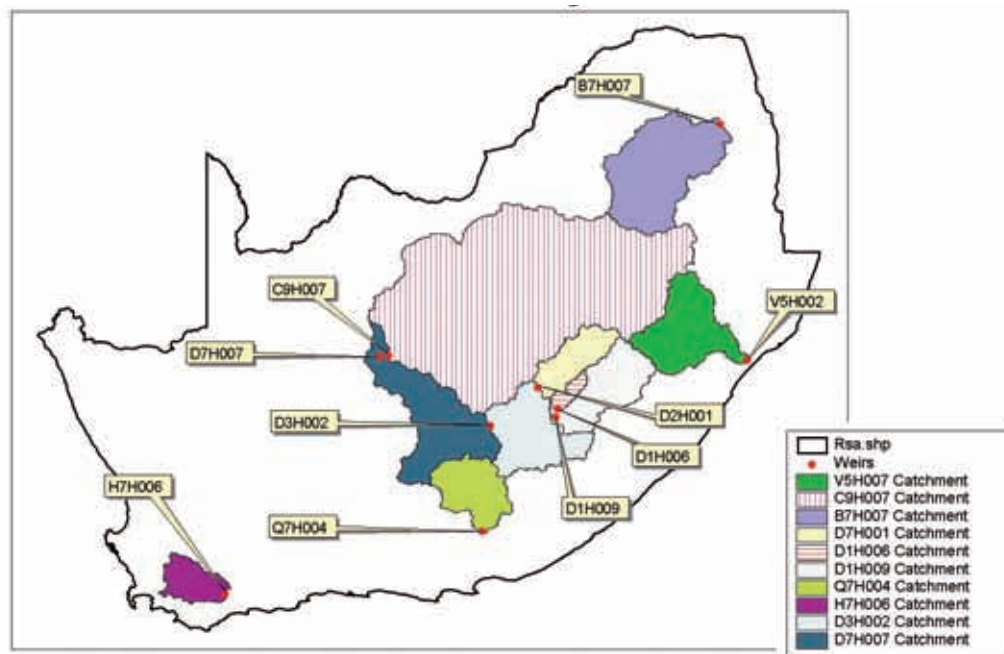


FIG. 1. South African map with catchment boundaries of the areas for which samples were taken during 1968–1974. The catchment numbers refer to the DWA reference numbers used in Table 1.

TABLE 1. SUMMARY OF RIVER DETAILS AND DATA AVAILABILITY OF SAMPLES OBTAINED IN 1968–1974

Catchment	River	Location	Station ref #	Dates	Size km ²	MAR Mm ³ /a	Frequency		
							¹⁸ O	Deut	Trit
Orange	Kornetspruit	Maghallee	D1H006	1971–72	3 014	627	wk		
Orange	Orange	Oranjedraai	D1H009	1971–72	24 870	3 951	wk		
Orange	Caledon	Jammerdrif	D2H001	1971–72	13 315	1 109	wk		
Orange	Orange	Bethuli	D3H002	1968–70	65 380	8 142	wk	occ	occ
Vaal	Vaal	Douglas	C9H007	1968–72	193 765	3 008	wk		
Orange	Orange	Upington	D7H007	1968–72	260 400	12 301	wk		
Olifants	Olifants	Mica	B7H007	1968–72	47 100	2 596	wk		
Thukela	Thukela	Mandini	V5H002	1968–72	28 910	3 804	wk	mon	mon
Thukela	Kl Boesmans	Estcourt	V7H012	1973–74	196	30	wk		
Great Fish	Great Fish	Cookhouse	Q7H004	1968–71	18 490	280			
Breede	Breede	Swellendam	H7H006	1968–72	9 829	2 050	wk		
Zambezi	Zambezi	Tete		1970–73	900 000	81 360	mon		mon

wk — weekly, mon — monthly, occ — occasionally.

2.2. Results from 1968–1974 sampling

The ¹⁸O data show considerable variation on a short term basis and the availability of these historic isotopic data in electronic format enables a comparison with recent data (Fig. 2). General features of the stable isotope pattern are:

- Low ¹⁸O values during the rainy season, more positive during the dry periods;
- Steady ¹⁸O increase with decreasing flow in the dry period;
- Rapid ¹⁸O and flow response to rainfall: all stations are in summer rainfall areas, except Breede River at Swellendam;
- Not all ¹⁸O and D variations (Fig. 3) are due to evaporation; there is also quite some variation along the GMWL;
- Smoothing out of these variations due to the collection of water in reservoirs and release of water due to water demand requirements.

The influence of reservoirs on ¹⁸O patterns can be quite clearly seen in the Orange Bethuli data (Fig. 2). In the winter of 1970, the Gariep dam wall had been completed just downstream from Bethuli and the reservoir started filling up when the rainy season began in September. By December the reservoir must have reached Bethuli (50 km above the dam wall) and from that time onward the stable ¹⁸O plot steadied and became indicative of water mixing that occurred in the reservoir, thereby smoothing out isotope variability from the inflowing water. The same pattern was observed at the Orange at Upington station, located downstream. The Zambezi and Great Fish Rivers, similarly, show a very constant ¹⁸O value throughout the year except for a small lowering during the highflow seasons. This is the same in the Vaal River. All of these rivers contain large reservoirs and the flow in rivers is regulated by demands placed on the water sources.

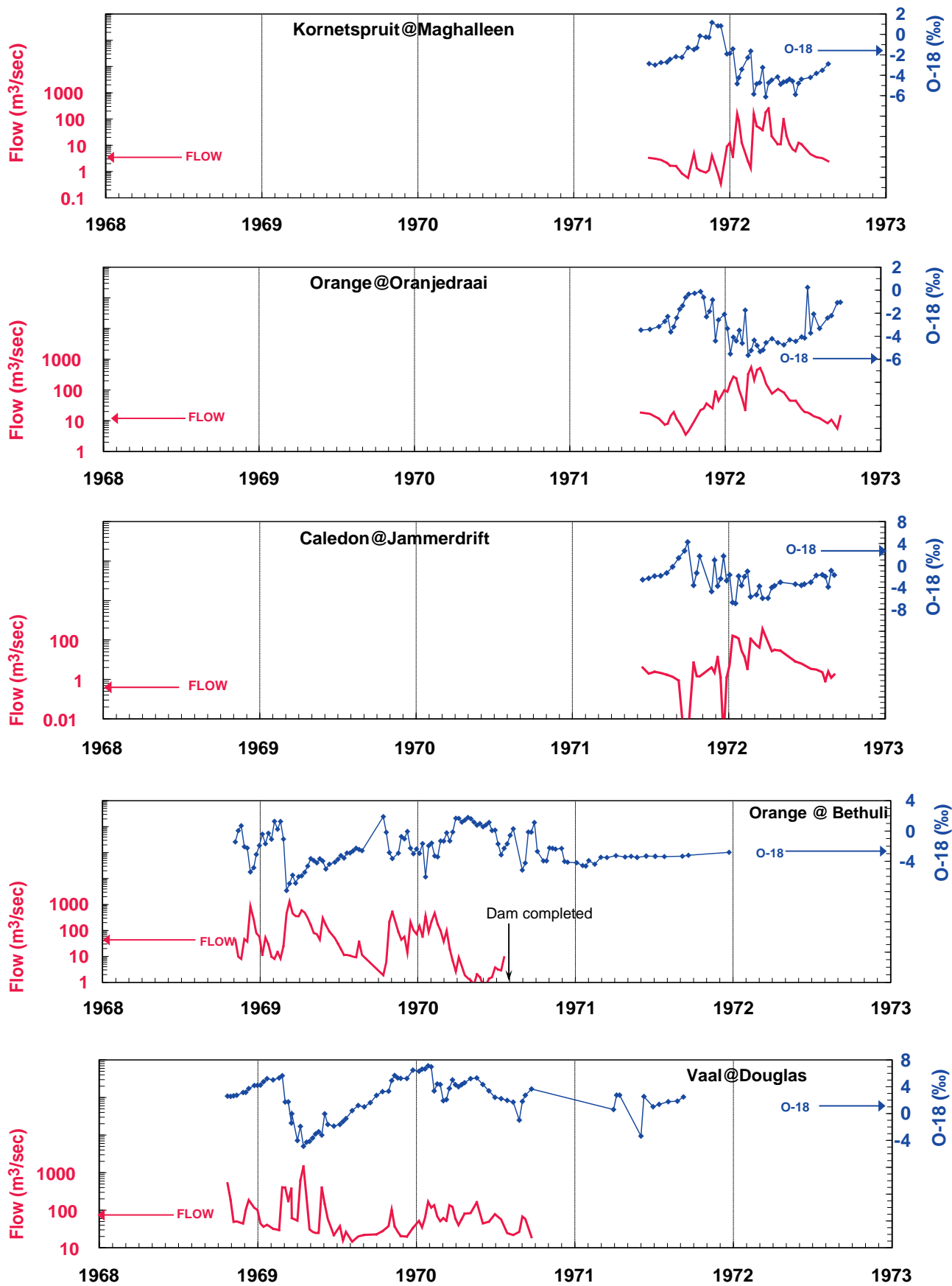


FIG. 2. The ^{18}O and flow plots with time for rivers sampled in 1968–1974. River flows (in cumecs = m^3/sec) are plotted on log scales.

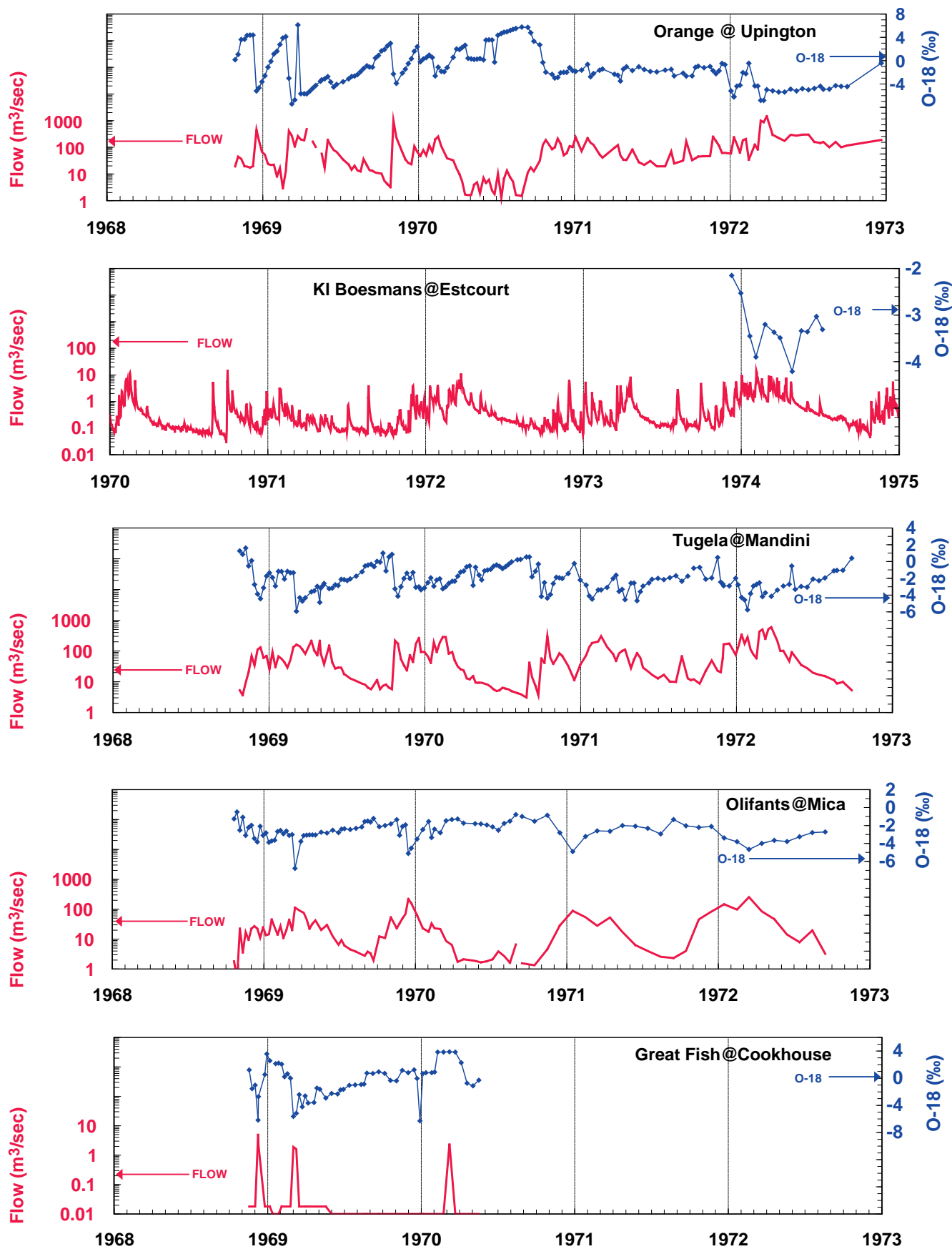


Fig. 2. The ^{18}O and flow plots with time for the rivers sampled in 1968–1974. River flows (in cumecs = m^3/sec) are plotted on log scales (cont.).

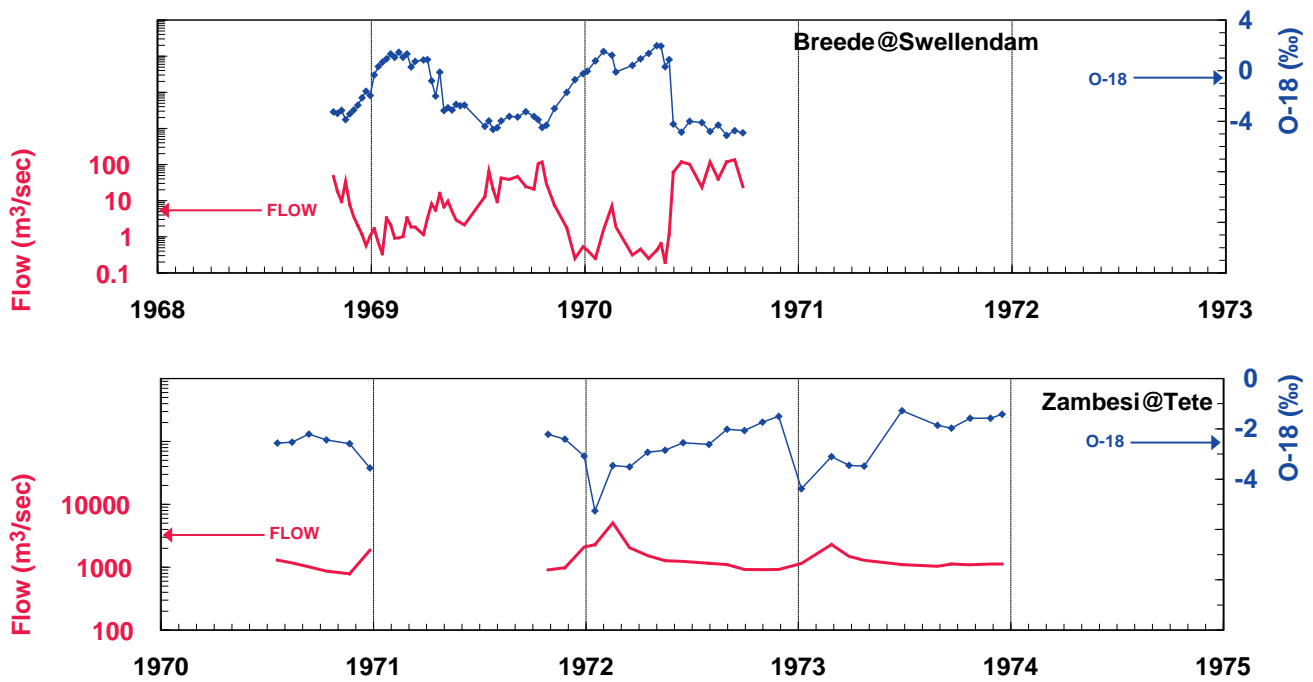


FIG. 2. The ^{18}O and flow plots with time for the rivers sampled in 1968–1974. River flows (in cumecs = m^3/sec) are plotted on log scales (cont.).

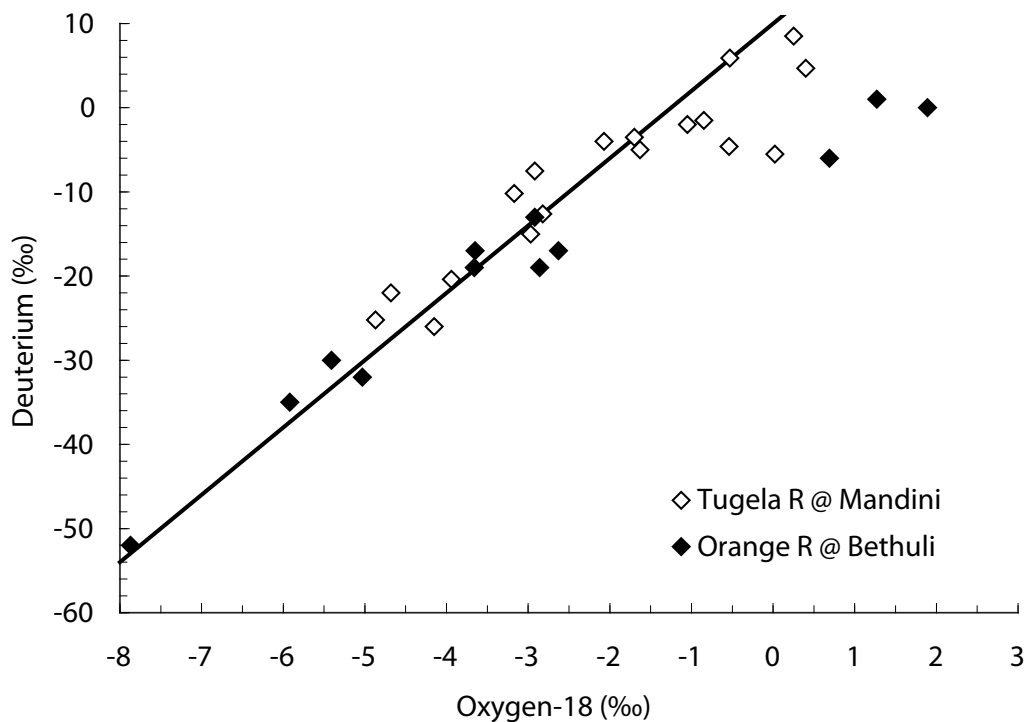


FIG. 3. Deuterium– ^{18}O plot of samples from Thukela and Orange rivers in 1968–1972.

Following this observation, correlation coefficients between flow and ^{18}O were calculated (Table 2) and showed better (negative) correlation for unregulated rivers. To quantify the influence of reservoirs, a ‘reservoir index (RI)’ was calculated as the ratio between the total reservoir size upstream of the sampling station and the mean annual runoff at the station. There

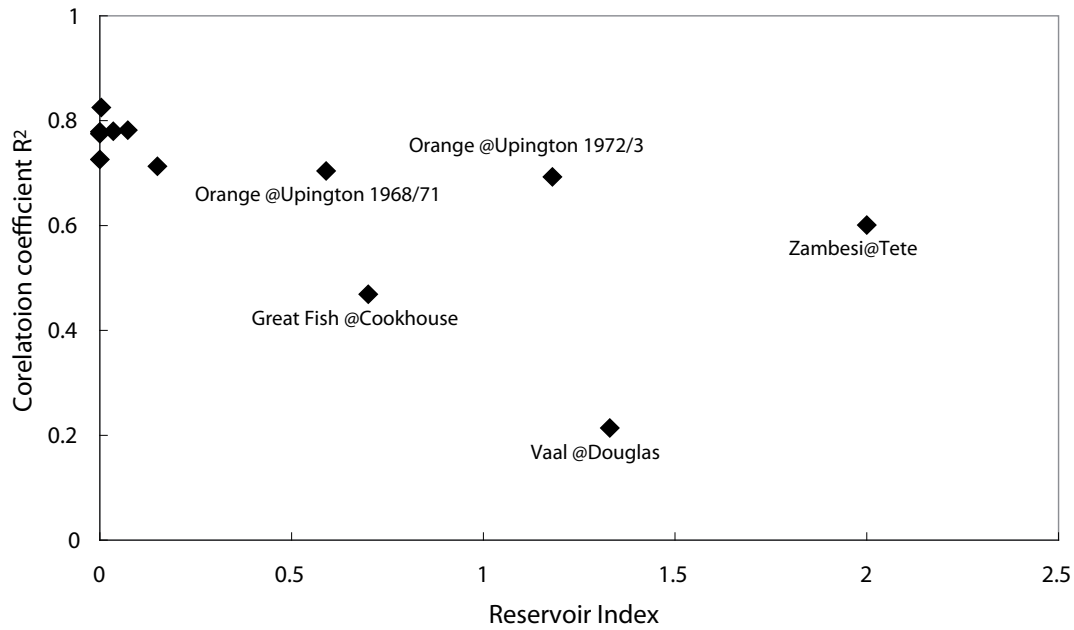


Fig. 4. Plot of the correlation coefficient between log-flow and ^{18}O against the 'reservoir index' above each station.

TABLE 2. CALCULATION OF THE RESERVOIR INDEX AND CORRELATION COEFFICIENT BETWEEN LOG-FLOW AND ^{18}O FOR THE 1968/72 STATIONS

River	Locality	Dates	Catchment area (km ²)	MAR Mm ³ /a	Reservoir Index	R ²
Kornetspruit	Maghalleen	1971–72	3 014	627	0	0.78
Orange	Oranjedraai	1971–72	24 870	3951	0	0.73
Caledon	Jammerdrif	1971–72	13 315	1109	0	0.77
Orange	Bethuli	1968–70	65 380	8141	0.004	0.83
Vaal	Douglas	1968–72	193 765	3031	1.33	0.21
Orange	Upington	1968–70	260 400	12392	0.59	0.70
Orange	Upington	1970–72		12392	1.18	0.69
Olifants	Mica	1968–72	47 100	2615	0.15	0.71
Thukela	Mandini	1968–72	28 910	3804	0.035	0.78
Great Fish	Cookhouse	1968–71	18 490	282	0.7	0.47
Breede	Swellendam	1968–72	9 829	2065	0.073	0.78
Zambesi	Tete	1970–73	900 000	81 360	2	0.60

MAR — mean annual runoff at the station

is some indication that the lower correlation coefficient is associated with increased storage capacity in the catchment (Fig. 4).

2.3. SCOPE/UNEP sampling 1981–1983

An additional sampling run of the Orange River at van der Kloof dam was undertaken between August 1981 and May 1985 as part of a SCOPE/UNEP project to study the transport of carbon

and minerals in the world's major rivers. Sampling was arranged by Prof. Rob Hart, then at Rhodes University in Grahamstown, and the isotope analyses were done at the University of Groningen in the Netherlands [3,4]. The actual data have been made available by Prof. Mook, and the ^{18}O time series is presented in Fig. 5. These data showed very constant ^{18}O content over most of the sampling period with little flow variation. This was a generally dry period and water releases by authorities were minimal. The few deuterium determinations that were made on a representative few samples indicate an exceptionally low D/ ^{18}O slope of 2.2 (Fig. 6).

3. CURRENT PROJECT MONITORING

The routine sampling of rivers under the auspices of the present CRP commenced in the beginning of 2002. Given the mandate of the CRP, stations were selected to sample only the larger catchments of the subcontinent (Fig. 7). In addition, it was intended that sampling stations would be arranged along the same river in order to observe downstream variations (Table 3).

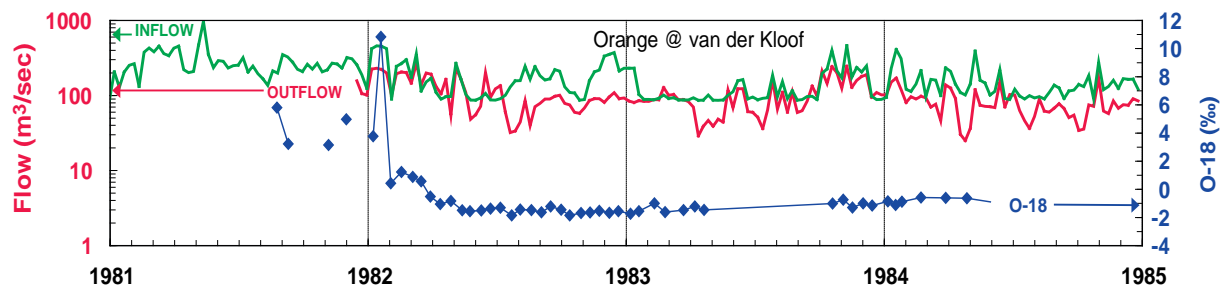


FIG. 5. Oxygen-18 plot with time for the Orange at the outlet of the van der Kloof dam during 1981–1984. (Mook, pers. comm.). Inflow (from the Gariiep dam) and outflow values are plotted on log scales.

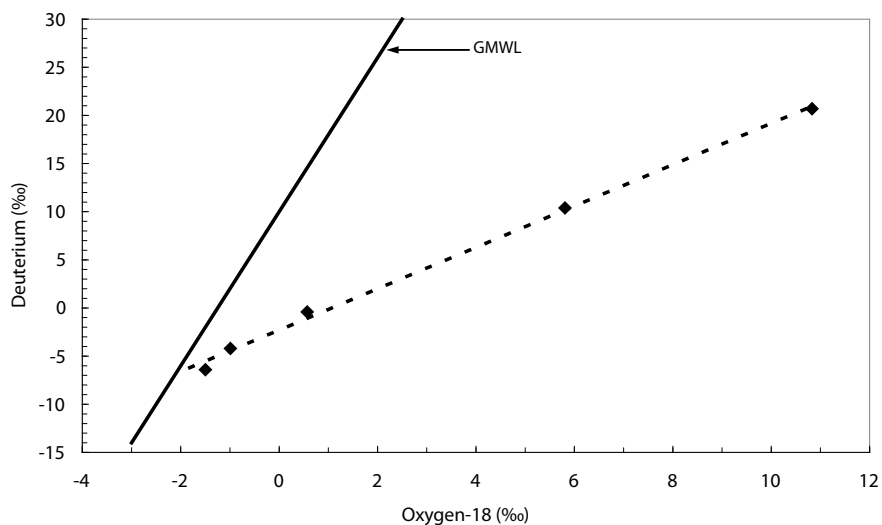


FIG. 6. Deuterium–Oxygen-18 plot of samples from the Orange River at van der Kloof dam during 1981–1984 (Mook pers.comm.). The slope of the evaporation line is 2.2.

3.1. Orange River

The Orange River drains the central part of South Africa (Fig. 8) and is an important water supply source for urban areas [5]. The river originates in the Lesotho highlands (at 2000+ m altitude). This area is characterised by low evaporation (1200 mm/a), high rainfall (>1000 mm/a), shallow soil cover and steep mountain slopes. Some water is retained in the Khatse and Mohale Dams in Lesotho. Flowing towards the Atlantic ocean in the west for nearly two thousand kilometres, the climate is gradually transformed into harsh desert areas where rainfall is less than 50 mm/a, annual potential evaporation is in excess of 3000 mm/a and only occasional floods occur. Other reservoirs in the river downstream are the Gariep Dam and the Van der Kloof Dam, which are used to supply water to meet agricultural needs.

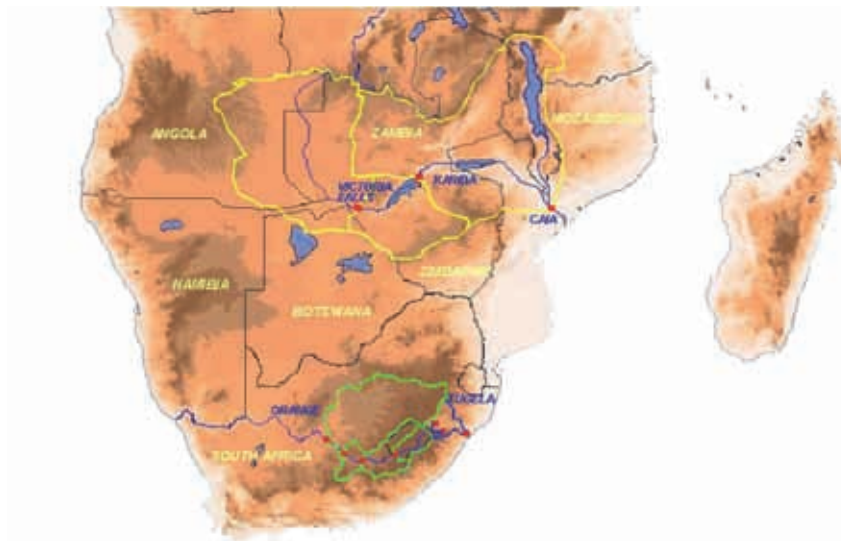


FIG. 7. Map of Southern Africa showing catchments and sampling sites used for the CRP project during 2002–2006.

TABLE 3. DETAILS OF THE RIVER ISOTOPE SAMPLING STATIONS THAT WERE ESTABLISHED FOR THE CRP IN 2002/3. BASIN DATA FROM [5–7]

Catchment	River	Location	Lat South	Long East	Station ref #	Catchment area km ²	MAR Mm ³ /a
Orange	Orange	Oranjedraai	30 20 10	27 21 34	D1H009	24 870	4 000
Orange	Orange	Gariep Dam	30 37 23	25 30 26	D3R002	70 749	8 000
Orange	Orange	Doornkuilen	29 59 28	24 43 28	D3H001	90 209	9 000
Orange	Orange	Upington	29 04 15	23 38 00	D7H007	295 105	12 000
Thukela	Kl Boesmans	Estcourt	29 00 08	29 52 54	V7H012	196	30
Thukela	Thukela	Spioenkop Dam	28 40 52	29 31 00	V1H057	2 452	1 000?
Thukela	Thukela	Mandini	29 08 26	31 23 31	V5H002	28 910	4 000
Zambezi	Zambezi	Victoria Falls	17 55 12	25 47 54	ZGP 26	507 200	33 500
Zambezi	Zambezi	Kariba	16 30 58	28 47 00			

MAR — mean annual runoff at the station.



FIG. 8. Map of the Vaal and Orange River catchments. The synoptic sampling trips were undertaken along the Orange River from the Lesotho highlands to Prieska and then along the Vaal River to the Vaal Dam.

There has been substantial development along the course of the river during the last 40 years [5]. The first dam that was built on the Orange River, the Gariep dam, was completed in 1970 and filled during the 1968–1972 sampling period (Table 4). Subsequently dams were built downstream (Van der Kloof: also for agricultural water) and upstream (Khatse and Mohale: part of the Lesotho Highlands water scheme, [8]). The Vaal River is an important tributary of the Orange River (Fig. 8) and drains the heavily populated Gauteng province. The Vaaldam was completed in 1938 for urban water supply and since the last decade also receives water by interbasin transfer from the Khatse and Mohale reservoirs [8]. Lower down in the Vaal River, the Bloemhof dam has since been built. The middle and lower Orange is therefore a highly regulated river system and water managers have to strike a balance between the demand of water supplies, ecological sustainability and flood control.

Sampling for isotopes in the orange River was arranged at four existing DWAF flowstations (Table 4). Monthly (or fortnightly) samples were collected in 200 ml plastic bottles and sent to CSIR in Pretoria. ^{18}O was analysed routinely and deuterium and chloride analysed selectively (every two months or whenever the ^{18}O content changed markedly). Logistical and staff problems caused some samples to be lost, part of which could be made up from samples collected for the DWAF water quality network.

3.2. Thukela River

In terms of world size, the Thukela (formerly called Tugela) catchment is not large (29 000 km²), yet its water resources are significant in the South African context. The catchment is at present a site of intensive study [9] as well as a new IAEA technical cooperation project. An inter-basin transfer and pumped storage scheme is in operation on the escarpment and further options are presently being studied [10].

The Thukela catchment is bound by the Drakensberg escarpment in the west, where peaks rise up to over 3000 m and rainfall can be as high as 2000 mm/a. The river has a large number of

TABLE 4. DETAILS OF PROJECT SAMPLING STATIONS AND RESERVOIRS IN THE ORANGE CATCHMENT

DWAF station number	Station locality	km down stream	Dams	Capacity (km ³)	Date	MAR Mm ³ /a	RI
			Mohale	0.95	2005	310	3.1
		0	Khatse	1.95	1997	560	3.5
D1H009	Oranjedraai	330				4 000	0.73
		610	Gariiep	5.5	1970	8 000	0.68
D3R002	Gariiep Dam	614					1.1
		736	van der Kloof	3.2	1977	9 000	0.36
D3H001	Van der Kloof	737					1.3
			Vaal	2.54	1938	1 950	1.3
			Bloemhof	1.27	1970		
		925	Vaal/Orange confl				
D7H007	Upington	1300				12 000	1.3

MAR — mean annual runoff at the station.

tributaries (Little Thukela, Klip, Bushman's, Sundays, Mooi and Buffalo Rivers) which all flow eastward, join the Thukela and discharge into the Indian Ocean at Mandini, some 250 km east of the escarpment (Fig. 9).

Although there are a few large reservoirs (Table 5) and numerous smaller ones in the Thukela River system, these are mainly located in the upper reaches of the Thukela River and its tributaries. The total reservoir capacity available in the catchment is 1.0 km³ which represents only 25% of the mean annual runoff. For the most part, the Thukela River remains comparatively unregulated. Apart from the pumped storage system right below the escarpment, other water uses are limited to small town water supplies.

The sampling stations in this catchment were selected to cover a range of situations (Table 6). The station on the Klein Boesmans River at Estcourt is located at the confluence with the Boesmans River and represents typical runoff from a small (196 km²) catchment. The Klein Boesmans River drains important headwater wetlands as well as rural settlements and agriculture. The headwater wetlands were identified in the 1960s as typical of the discharge generating zones of the eastern escarpment and have been the focus of significant hydrological research [9].

Another sampling station is located at the outflow of Spioenkop Dam (completed in 1968) in the foothills of the Drakensberg escarpment. The dam collects water from the escarpment and provides minimum hold-up of water. It is not part of the pumped storage scheme located upstream, but may collect some overflow water from this scheme.

The final sampling station is Mandini, at the river mouth. This station represents the cumulative effects of the entire catchment and was also sampled in 1968/73. The re-sampling undertaken during this CRP has provided an opportunity to compare isotope effects over 35 years.

Samples were collected by personnel from DWAF and forwarded to the Pretoria lab at six monthly intervals.

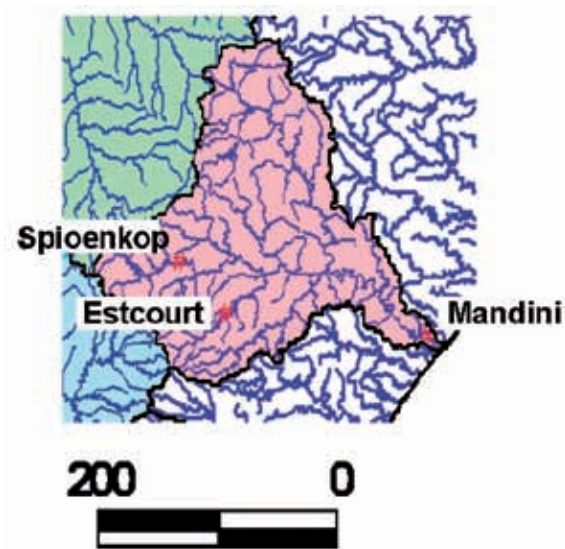


FIG. 9. Map of the Thukela catchment. See Fig. 7 for the regional positioning of this catchment.

TABLE 5. DETAILS OF RESERVOIRS IN THE THUKELA CATCHMENT

Reservoir	Completion date	Capacity (km ³)
Chelmsford		0.20
Craigieburn		0.024
Spienkop	1968	0.27
Wagendrift	Pre-1965	0.058
Kilburn	1982	0.036*
Woodstock	1982	0.38*

* Part of a pumped storage scheme

TABLE 6. SAMPLING STATIONS IN THE THUKELA THAT WERE SAMPLED BETWEEN 2002 AND 2006

River	Locality	Station reference	MAR Mm ³ /a	Catchment area km ²
Kl Boesmans	Estcourt	V7H012	30	196
Thukela	Spienkop dam outflow	V1H057	1000?	2452
Thukela	Mandini	V5H002	4000	28910

MAR — mean annual runoff at the station.

3.3. Zambezi River

The Zambezi catchment (area 1 351 000 km²) is a major feature in central Africa, draining large parts of Zambia and Malawi and smaller parts of Zimbabwe, Mozambique and Angola (Fig. 10). The bulk of the water is derived from the wetlands of Eastern Angola and Western

Zambia, with lesser contributions from the drier areas to the east (Table 7). The catchment consists of grasslands (74%), croplands (20%) and wetlands (8%) [13]. The mean annual runoff from the entire catchment amounts to 106 000 M·m³/a, as set against the cumulative capacity of reservoirs in the catchment of 240 000 M·m³.

The location of sampling stations was determined by access and identifying reliable samplers. In Zimbabwe, two stations were established in the Zambezi River basin: at Victoria Falls (above Lake Kariba) and at the Kariba dam wall, 400 km downstream. Monthly samples from these two stations (Table 7) were collected and forwarded to Pretoria every six months. The Victoria Falls site (ZGP 26) is regularly monitored and flow values are available from 1908 (Fig. 11) showing decadal variations.

Lake Kariba is a large reservoir: It has a capacity of 185 km³, area of 5000 km² and dam wall height of 128 m. During the first visit to the station, samples were collected at Kariba town from dam water at two localities along the wall and at Chirundu 50 km downstream, which is the first publicly accessible point to the river and which represents dam outflow water. The three samples showed the same ¹⁸O content (within ± 0.1‰) and samples from the Kariba dam wall were henceforth taken to represent the outflow value of the reservoir.

We have also managed to obtain a few Zambezi River samples from occasional travellers who crossed the Zambezi river further downstream, below Cahora Bassa dam in Mozambique (at Caia) (Fig. 10). At this station water from the north bank displayed the more enriched ¹⁸O signal of Lake Malawi, draining through the Shire river which enters the Zambezi 12 km upstream from the sampling point. Only samples collected from the south bank at Caia were used.

3.4. Results

Each river station produces a characteristic ¹⁸O and flow pattern that is influenced by conditions and situations upstream. In general, there are ¹⁸O increases towards downstream stations in



FIG. 10. Map of the Zambezi catchment. The sampling stations Victoria Falls, Kariba and Caia are encircled.

TABLE 7. LOCATIONS OF THE ZAMBEZI SAMPLING SITES RELATIVE TO THE MAJOR TRIBUTARIES OF THE RIVER [6]

River	location	Tributary flow (km ³ /a)	Zambezi flow (km ³ /a)	Remarks
Zambesi	Chavuma Falls		18	
Chobe		4.1	33	
Zambesi	Victoria Falls		33	Sampling site
Zambesi	Lake Kariba (cap. 185 km ³)			Sampling site at outflow
Kafue		10		
Luangwa		22		
Zambesi	Cahorra Bassa Lake (cap. 52 km ³)		78	
Zambesi	Tete			Sampling site in 1971/3
Shire		16		
Zambesi	Caia			Sampling site, intermittent
Zambesi	Ocean discharge		106	

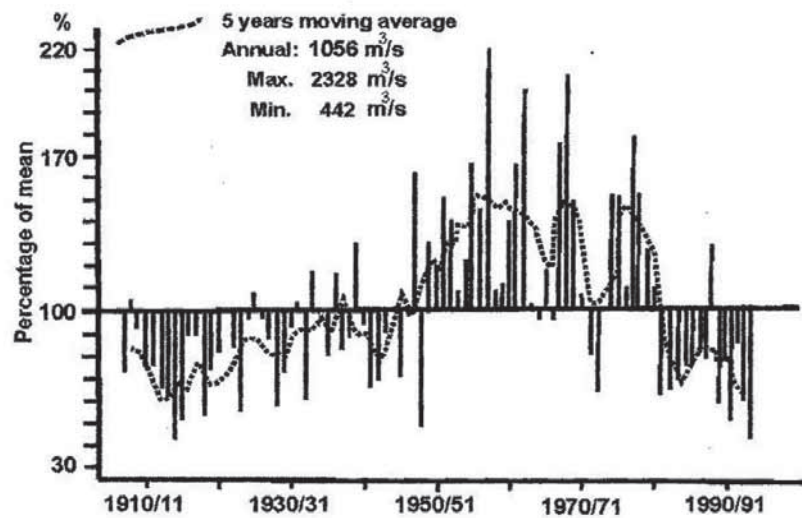


FIG. 11. Zambezi flow variations during the 20th century [11, 12].

each river (Figs 12). Stations may be quite similar with only enrichment occurring downstream, and the presence of reservoirs in-between can change the ¹⁸O and flow pattern significantly (Fig. 13).

In the Orange River, mean ¹⁸O clearly increases from the upstream Oranjedraai station to the Gariiep Dam to van der Kloof Dam, with the highest values at Upington (Fig. 12), located in the arid Northern Cape Province. The latter also contains a contribution from the over-regulated and polluted Vaal River (see Section 4 below). The Oranjedraai station shows

the most variability with lower and more variable ^{18}O during late summer (January–April), when most rains are received in the upper parts of the catchment. This is emphasized in the ^{18}O comparison, and flow for these stations shows the linkage between flow and ^{18}O content (Fig. 13). It can be observed that larger flows in the late summer of 2006 flushed through the entire river system and caused the steady buildup of high- ^{18}O from previous years to be washed out to sea.

In the Thukela catchment, the upstream station in the Klein Boesmans River (upstream) and at Mandini (downstream) show the similar patterns of an inverse relation between ^{18}O and flow that is characteristic of an ‘undisturbed’ river (Figs 12 and 13). Oxygen-18 at Mandini is

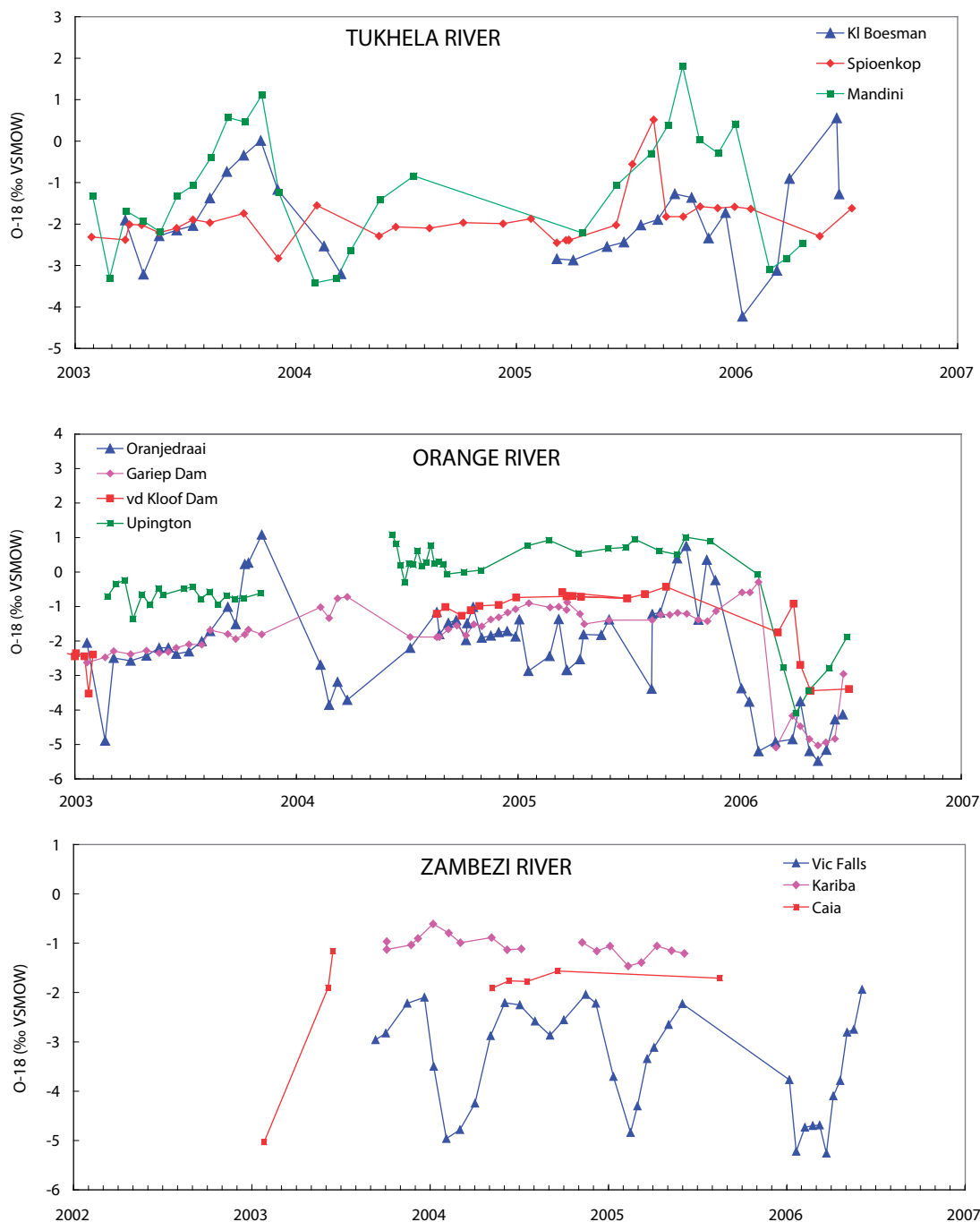


FIG. 12. Oxygen-18 time series from the different catchments for the 2003–2006 period.

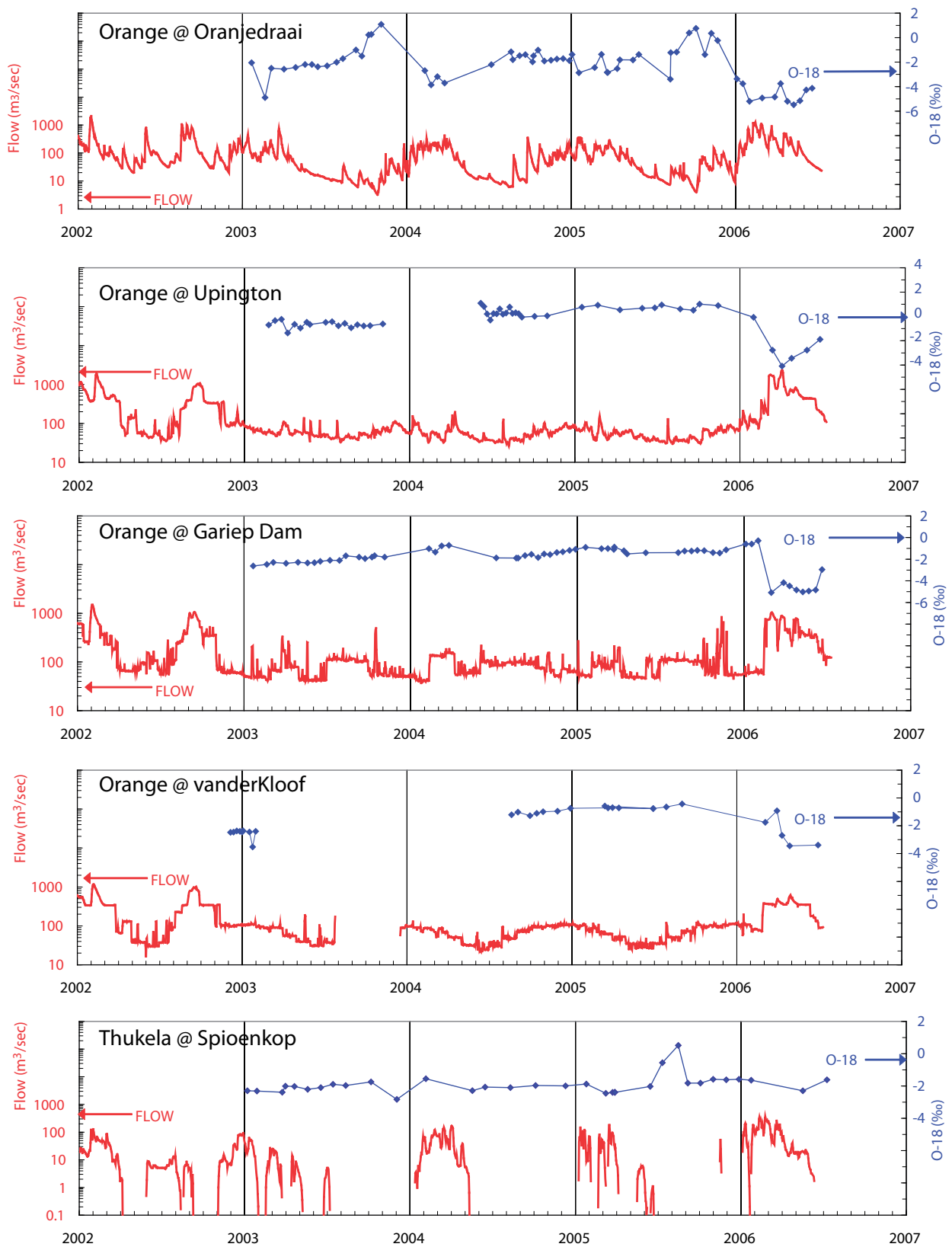


FIG. 13. Oxygen-18 and flow plots with time for the rivers sampled in 2002–2006. Note that river flows are plotted on a log scale and that the scales for both flow and ¹⁸O are different for each river.

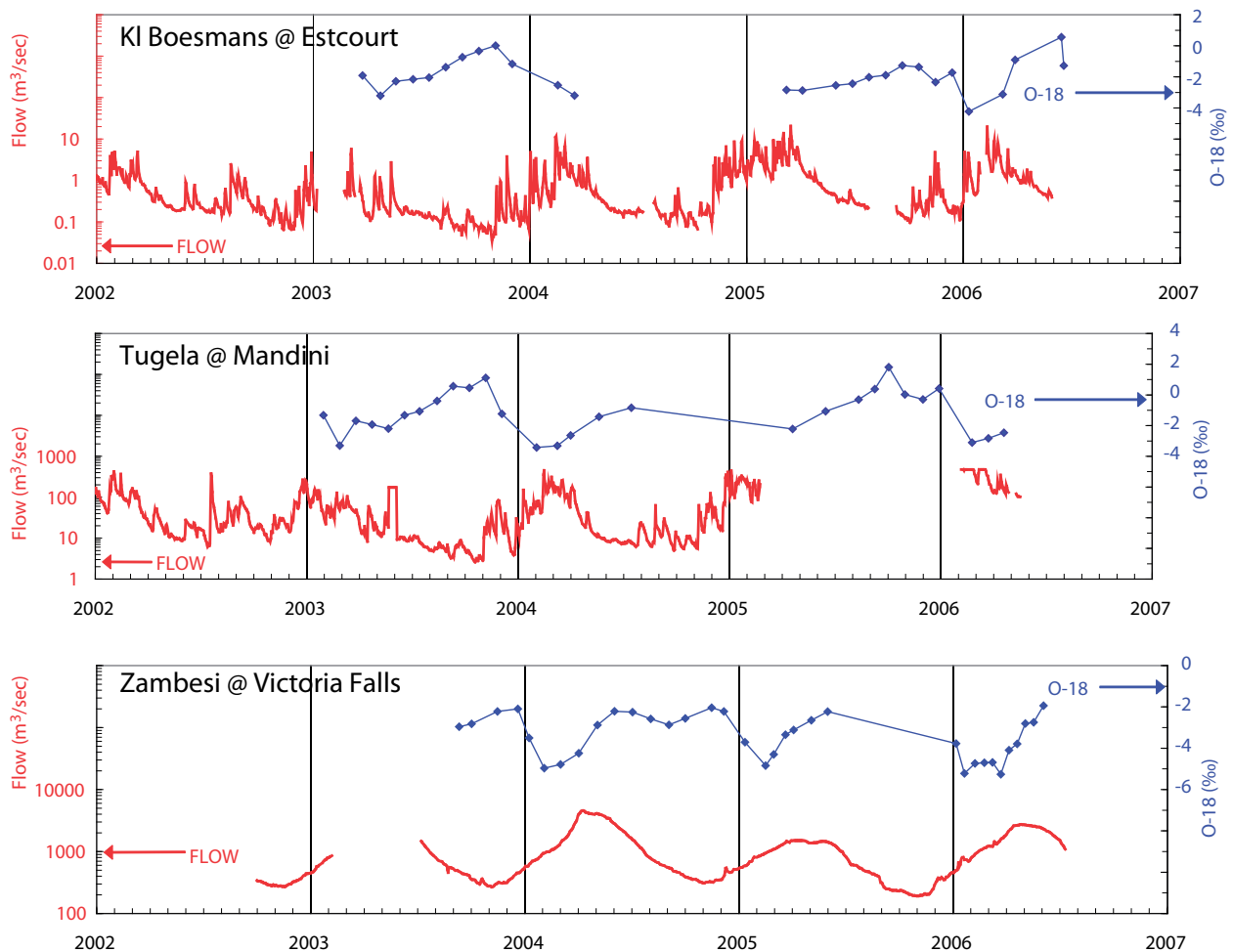


FIG. 13 (cont.). Oxygen-18 and flow plots with time for the rivers sampled in 2002/6. Note that river flows are plotted on a log scale and that the scales for both flow and ^{18}O are different for each river.

however somewhat more positive. The station Spioenkop is right up in the catchment and is fed by transfer from an adjacent catchment, which produces a distorted picture with a fairly smoothed out pattern (Figs 12 and 13).

The various stations along the Zambezi River show the ^{18}O features of a highly regulated river that were also evident thirty years ago. At the Victoria Falls site there is only a dip during the period of maximum flow from January to March (Figs 12 and 13). There is no storage capacity above this site. It is proposed that the very smooth ^{18}O pattern here is due to drainage from the floodplains upstream, which also produce evaporative signals (^{18}O -D variations well below the GMWL, Fig. 14). In contrast to the pattern found in the Thukela and Orange Rivers, the flow peak follows the ^{18}O trough by a few months (Fig. 13). A likely explanation could be that increased rainfall first has to displace a large quantity of evaporated water before the ^{18}O trough reaches the sampling point. An alternative explanation would be that rainfall in the catchment commences at different times. Lake Kariba water shows an extremely smoothed-out pattern, as could be expected from a reservoir three times the size of the mean annual inflow (Table 7). There is a discrepancy, however, in that the ^{18}O content of the Kariba is higher than the mean inflow (Vic Falls) seems to indicate (Fig. 12), yet the ^{18}O -D plot of Lake Kariba water does not show more evaporation enrichment than the inflow water. The limited number

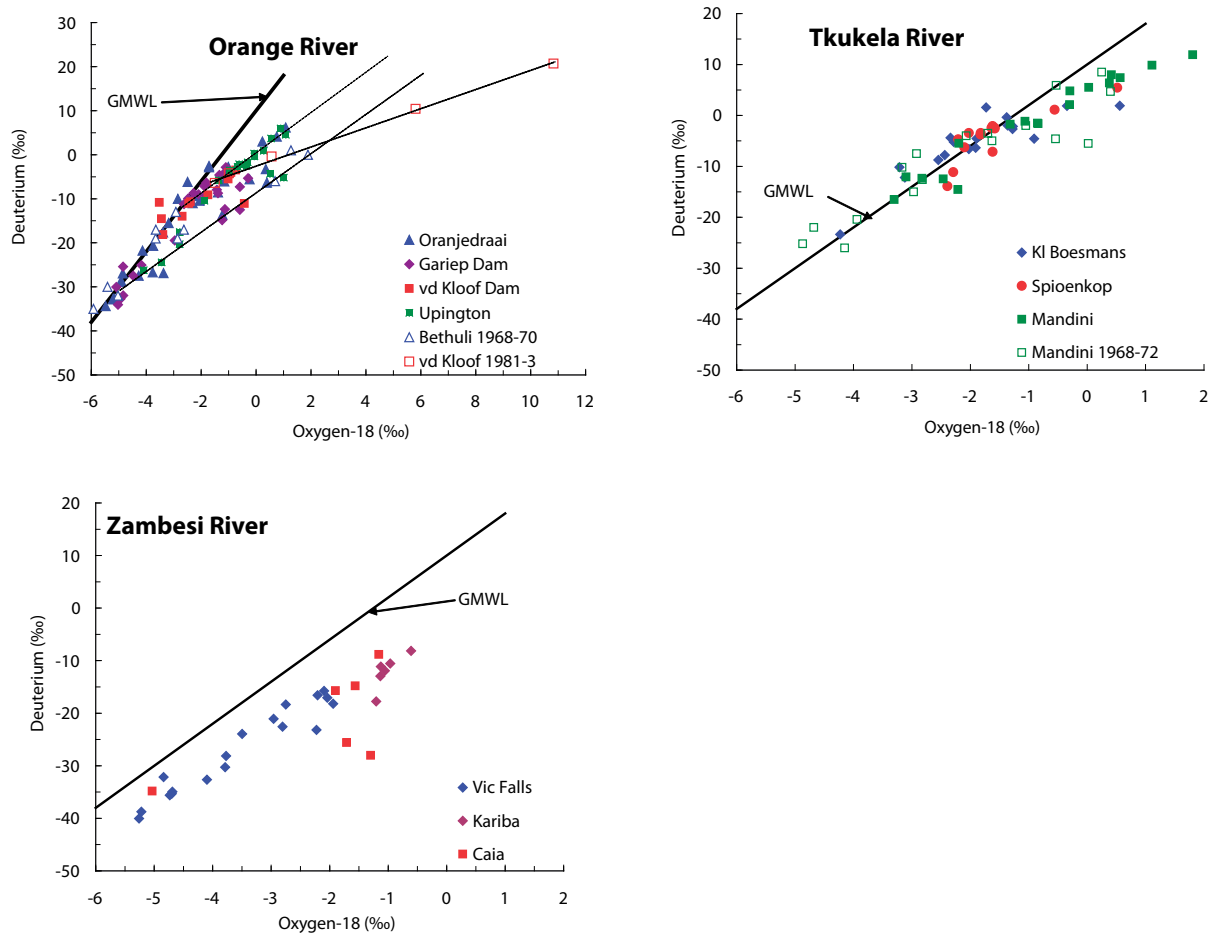


FIG. 14. Deuterium vs. oxygen-18 plots of samples from Thukela, Zambesi and Orange catchments both in 2003–2006 and earlier for comparison. Some possible evaporation lines for the Orange River are indicated.

of samples from Caia (below Lake Cahora Bassa) seem stable but lower than those of Lake Kariba upstream (Fig. 12). There are, however, too many additional water sources in-between (Table 7) to be able to establish any sort of progression. Obviously analyses from other stations need to become available from this vast catchment to explain even the basic patterns found. In particular the upper Zambezi catchment should be a promising research area.

4. SYNOPTIC SURVEYS OF THE ORANGE AND VAAL RIVERS

4.1. Sampling

Three surveys were undertaken along the Orange River for the entire length, from the Lesotho highlands to beyond the confluence of the Orange River with the Vaal. The object of these surveys was to get more information on the development of isotopic patterns by seeing how these change along the course of river flow. Similar sampling was undertaken along the Vaal River at the same time, since the route was more or less on the main road from the base

(Pretoria). Previous work had shown significant isotope and chemical variations downstream along the river [1]. Sampling was undertaken in August 2004 (winter), March 2005 (dry summer) and April 2006 (wet summer). In each of the trips 8 to 15 samples were collected along each river within two days. Some tributaries were also sampled. Sampling points were selected to identify the effects of tributaries and reservoirs along the way. Usually sampling was done at the outflows of reservoirs or at road bridges across the river.

Synoptic river samples were analysed for ^{18}O , deuterium, Cl, SO_4 and EC.

4.2. Results of the synoptic surveys

The general pattern that can be seen (Figs 15 and 16) is that there is a gradual isotope enrichment and salt increase along the stretches of both rivers: more so in the Vaal River than the Orange River. In the Vaal River, these increases are enhanced, since this is a highly utilized river and subject to considerable pollution loads. Winter 2004 and summer 2005 show more enriched effects than summer 2006. Summer 2006 was a high rainfall summer, which explains why both rivers lost the isotope evaporation effects of the previous two years.

Figures 15 and 16 also indicate the location of reservoirs (locally called 'dams') along the river stretches. It can be seen that in some, though not all, reservoirs there is ^{18}O enrichment (van der Kloof, Bloemhof and Gariep dams) due to evaporation. In winter 2004 and summer 2006, the ^{18}O input to Gariep dam was higher than its output (Fig. 15). This is because sampling was done at a period when inflow was momentarily higher than the reservoir due to the reservoir's capacity to store input water integrated over a longer period. It should conceivably be possible to calculate the net evaporation enrichment from the time series of inputs and the water balance of the reservoir. It does not appear that water balance data is sufficiently known for any of these reservoirs.

The ^{18}O -deuterium pattern along the rivers (Fig. 17) is similar to that found in the Orange River at monitoring sites (Fig. 14): all are along the global meteoric water line until $\delta^{18}\text{O} > -2\text{‰}$ above which evaporation occurs.

The behaviour in the Vaal River at its confluence with the Orange indicates that there was some backflow from the (stronger) Orange River into the (weakly flowing) Vaal River. This is indicated by decreasing values during the last few kilometers of the Vaal River (Fig. 16).

The salinity of the Vaal River at its confluence with the Orange is considerably higher than that of the Orange River alone. This is because the Vaal effectively drains the heartland of the country (Gauteng Province) and the water resource is heavily exploited. A sample taken at Prieska in the winter of 2004, 170 km below the confluence confirmed the high salinity. The same high salinity (Cl 16–60 mg/l) has been found on the Orange River at the Upington sampling station.

River data do not, at this stage, indicate the source of gradual ^{18}O and Cl enrichment of the water flowing along its way in those stretches where there are no tributaries adding enriched water.

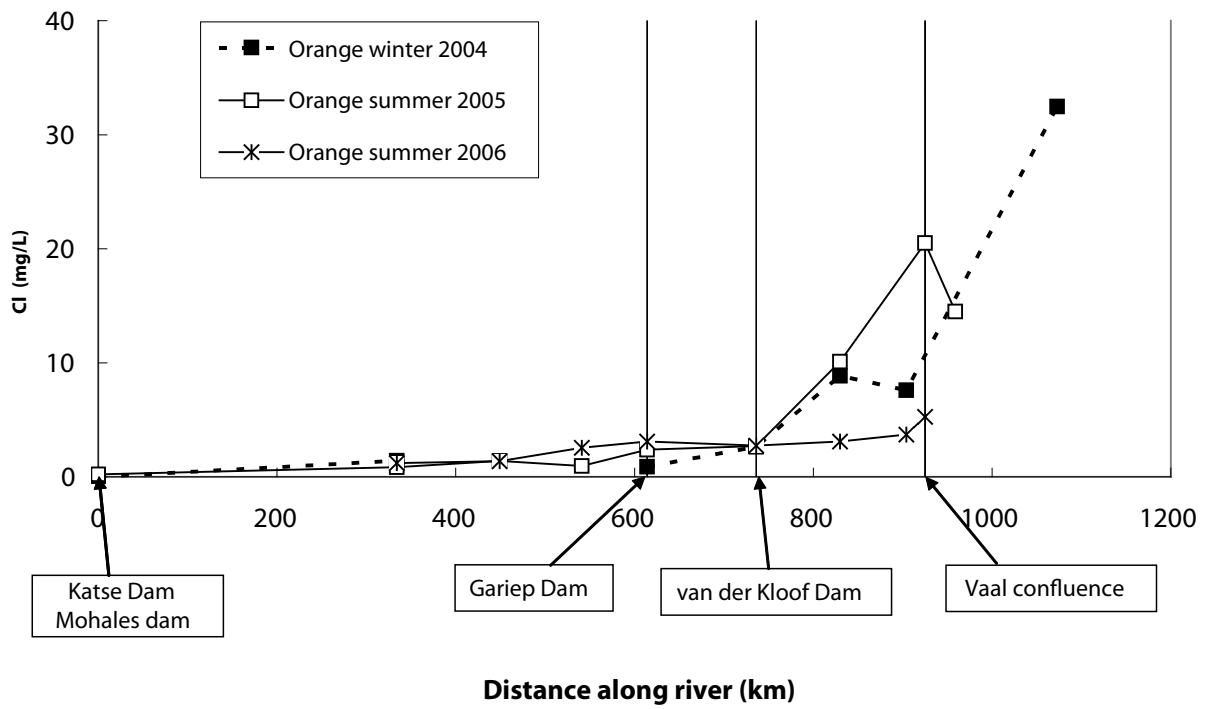
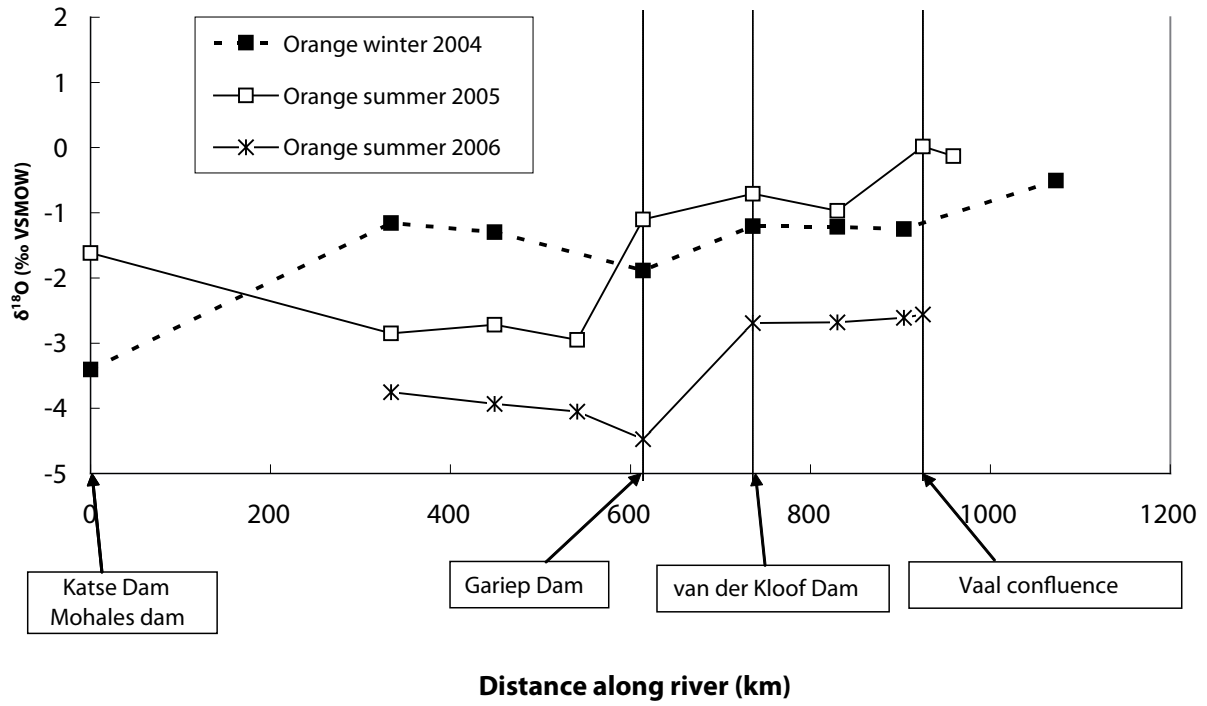


FIG. 15. Plots of ^{18}O and chloride along the Orange River on three occasions.

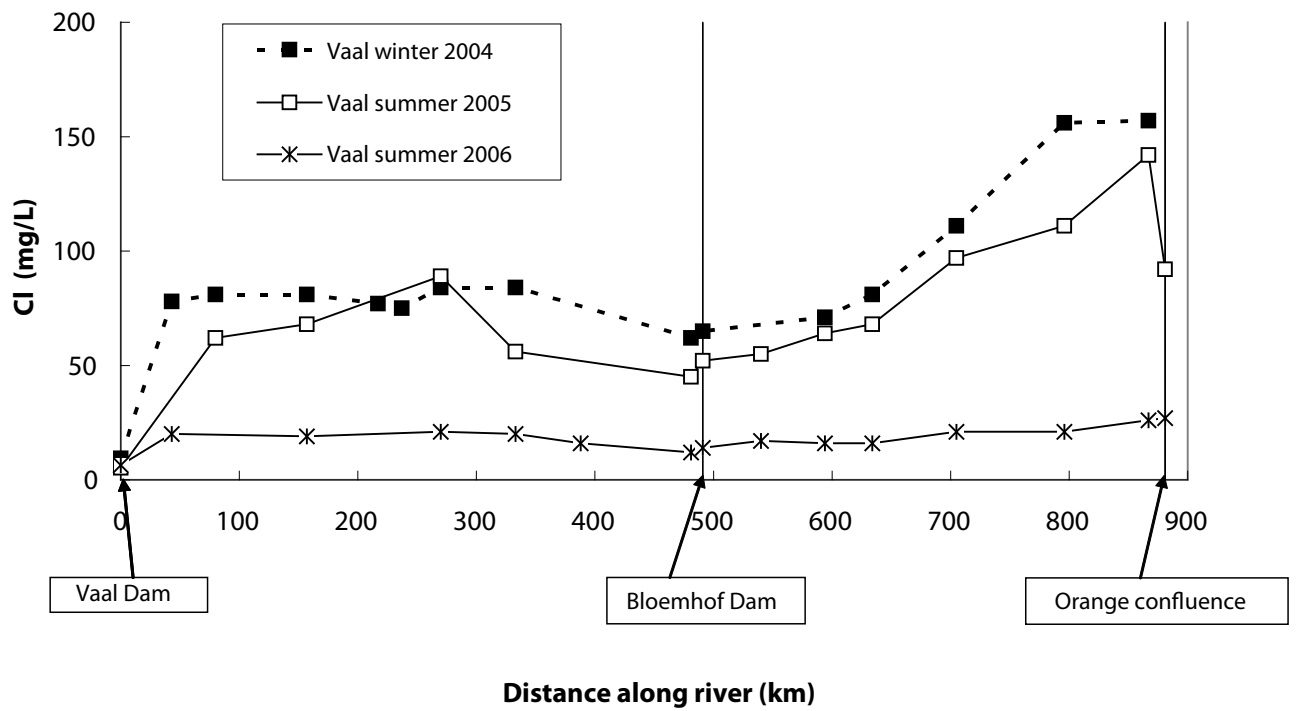
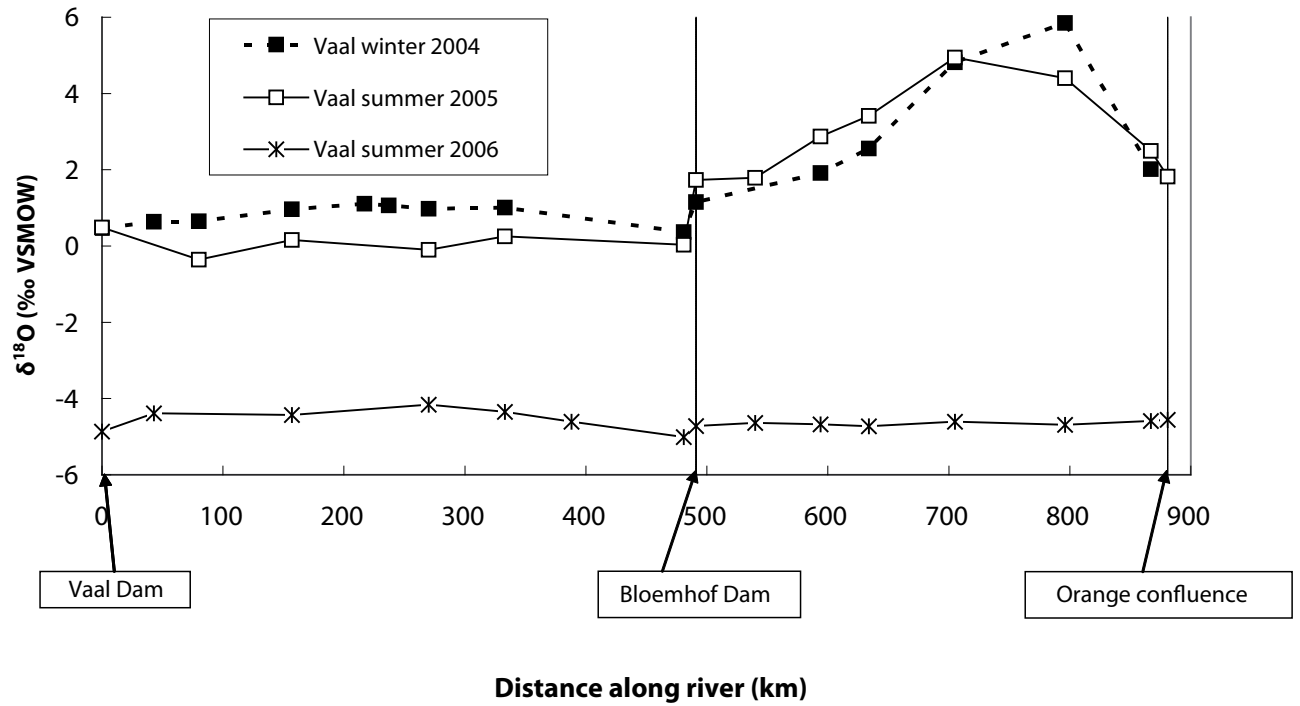


FIG. 16. Plots of ¹⁸O and chloride along the Vaal River on three occasions.

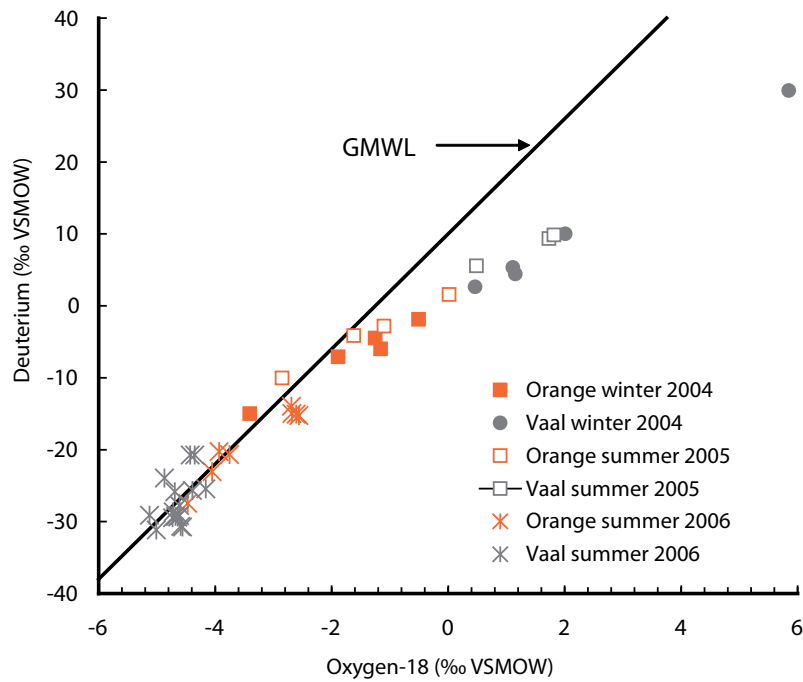


FIG. 17. Oxygen-18 vs. deuterium plot of the Orange and Vaal synoptic river samples.

5. DISCUSSION

5.1. Patterns of isotope variations

There is a consistent saw tooth pattern of ^{18}O (and D) negatively correlated with the flow that is very evident in all unregulated rivers in the region. In 1968–1974, these were the Thukela and Breede Rivers and the Orange River at Bethuli (only until 1970). At present, the Thukela still shows this pattern, but additional minor rivers have not been sampled recently. In most of the rivers that have been sampled the ^{18}O pattern is very stable and mainly influenced by water release practises at any time. It is only during a period of major rainfall (as in Jan–March 2006) that the rivers are purged of the accumulated evaporated water and ^{18}O levels approach that of rain again. In that sense, the mean ^{18}O content of downstream river stations is a reflection of water balance in the catchment. The exception is the Zambezi River, where the ^{18}O and flow variations are slow and the ^{18}O minimum precedes the flow maximum. This suggests some sort of mixing of different water sources in the upper catchment.

5.2. Oxygen-18 vs. deuterium patterns

The ^{18}O –D relation of river water provides a fairly consistent pattern of values more or less along the Global Meteoric Water Line for the lower ^{18}O and D values and an evaporated signal for higher values (Figs 3, 6, 14 and 17). All of the seven African GNIP rainfall stations south of the equator have values of D_{xs} ($=\delta D - 8 \cdot \delta^{18}\text{O}$) between +9 and +15‰ (IAEA 1992). Evaporative enrichment in all of the catchments (except the Zambezi) is therefore small.

For most stations along the Orange River, the starting point for evaporation is at $\delta^{18}\text{O} = -2\text{‰}$ and the slope of the evaporation line is close to 4.6: a value usually found in other evaporating

waters in the region. There is, however, a subset of Orange River data from different stations that would suggest a starting point of around -5‰ (Figs 3, 14 and 17). The flow model is therefore one of rainfall having a $\delta^{18}\text{O}$ value of between -6 and -2‰ flowing downriver, where it is subjected to isotope enrichment due to evaporation. The exception to this pattern in the Orange River is the 1981–1983 data set from van der Kloof dam, for which a slope of 2.2 was found, based mainly on very high $^{18}\text{O}/\text{D}$ levels during the summer of 1981–1982 (Fig. 6). This was an exceptionally dry summer with rainfalls and river flows below normal [2].

In the Thukela River, the same pattern exists as in the Orange, with points along the GMWL and an evaporation line of slope 4.7 originating at $\delta^{18}\text{O} = -2\text{‰}$.

In the Zambezi River, the pattern is not all that clear. Low $^{18}\text{O}/\text{D}$ waters are located on a line parallel to the GMWL and the departure point of the evaporation line is not well defined (Fig. 14). In contrast to the Orange and Thukela Rivers, the D_{xs} of low $^{18}\text{O}/\text{D}$ waters is around $+2\text{‰}$ which suggests some modification after rainfall recharge. This is likely to be evaporation in the upper catchment of the Zambezi (Angola and Zambia), where marshes and flatlands are common. This could also explain the high (6.5) slope of the high $^{18}\text{O}/\text{D}$ water (Zambezi). Mixing of water with different characteristics could explain the variation found.

5.3. Data comparison over 35 years

A comparison of isotope data across the time divide between 1968–1973 and 2003–2006 is mainly influenced by infrastructure developments during that period, different sample frequencies and annual differences in flow rates. Stations for which longer comparison time series are available include the Orange at Upington and the Thukela at Mandini (Fig. 18). Shorter time series are available from the Klein Boesmans at Estcourt and the Orange at Oranjedraai. A comparison can be made between the Orange at Bethuli in 1968–1970 and the Oranjedraai at present. Both sample the river more or less soon after it leaves the Lesotho highlands (Fig. 1).

For the Thukela at Mandini, time series comparison shows qualitatively that the ranges and variations of both flow and ^{18}O have not changed significantly over 35 years (Fig. 18). Even though no hydrological year is the same, overall patterns have not changed in a meaningful way. The Orange at Upington shows that the steady pattern set in at this location after the completion of the Gariiep Dam in 1970 (see also Fig. 2) is still basically the same at present.

The response of stable isotope content to flow changes has similarly not changed significantly since that time for the Thukela as well as for the inflow to the Gariiep dam (be it the station at Bethuli or at Oranjedraai) (Fig. 19). It may be that some of the extreme (high and low) flow occurrences from the period 1968–1972 have not been repeated recently. A more detailed evaluation of the differences should be done at the level of hydrological modelling.

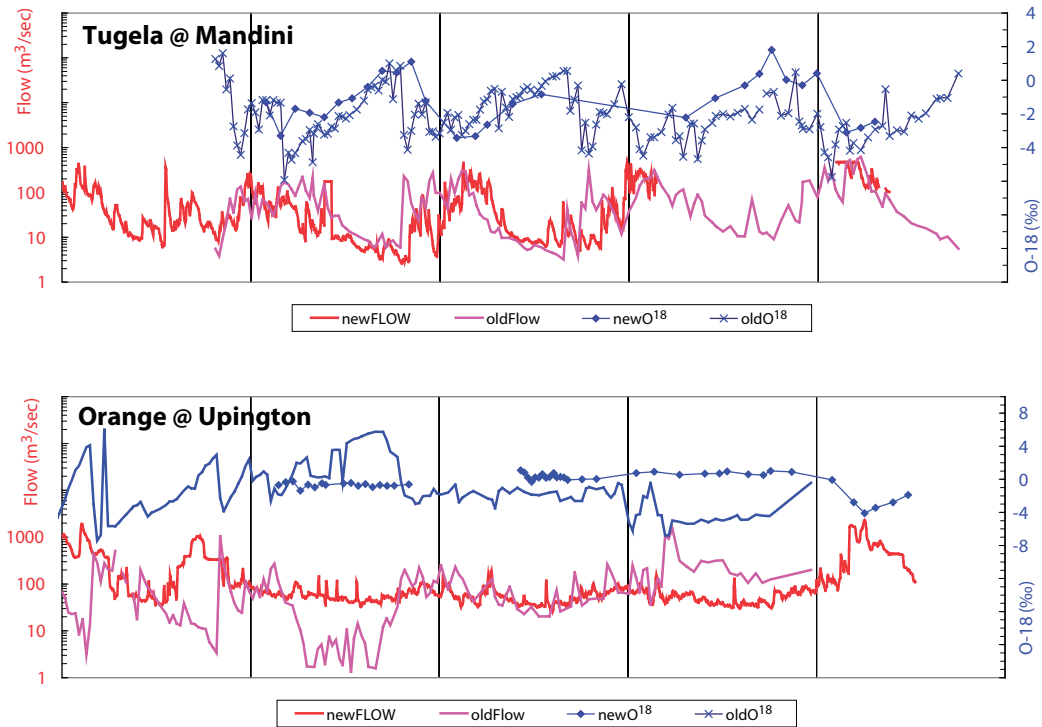


FIG. 18. Comparison of old and recent ^{18}O plots for Thukela (Mandini) and Orange (Upington) Rivers. The X axis denotes a total sampling period of five years.

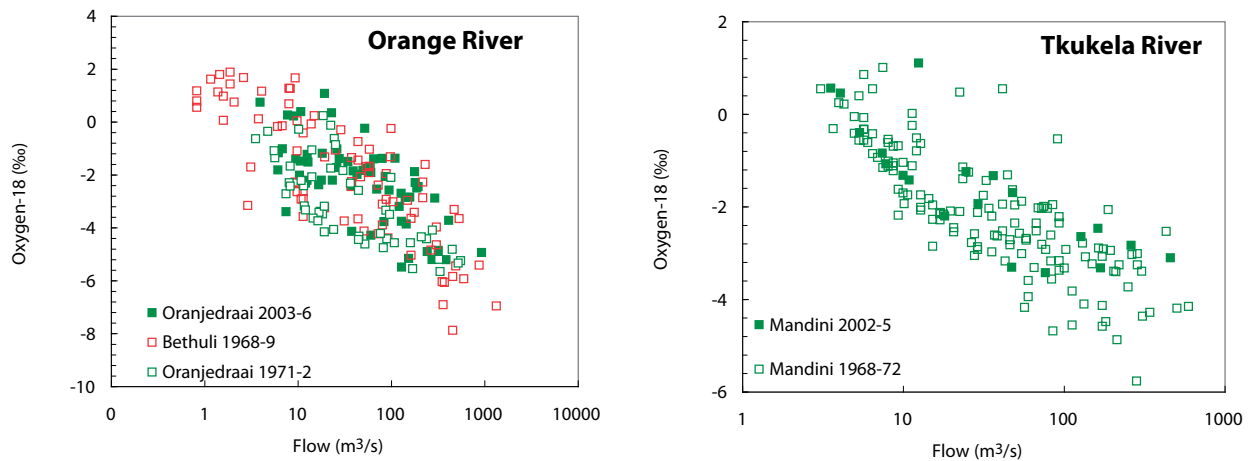


FIG. 19. Comparison of the flow- ^{18}O relationship for the Orange and Thukela Rivers between the sampling periods.

6. RECOMMENDATIONS

6.1. Proposals for future research

Data obtained, both now and in the past, have shown strong variations of stable isotope content with time and flow rate. This implies that using isotope values in rivers as proxy for the isotope composition of rainfall would be invalid here. By the same token, establishing relationships between the isotope composition of rainfall and runoff is likely to yield important hydrological information for each catchment. It was not possible to do this within the present project

because no catchment rainfall isotope data are available. This is a path that needs following and emphasis would have to be placed on stations close to catchment areas.

Much work has been done in South Africa about the effect of forestry on rainfall–runoff relations in small catchments (see review by [14]). No such studies have included isotopes (at least locally) and it would be interesting to establish whether isotope effects in the rainfall–runoff relation are vegetation influenced. If this were the case, then isotope monitoring in or close to headwater catchments can be useful for monitoring land use or environmental change.

Since the residence times of water in the various reservoirs along river traverses can be up to a few years, and the local atmosphere is dry, it might be feasible to do isotope enrichment modelling for those reservoirs that are shallow enough. Study reservoirs would have to be chosen with care to ensure that reliable water balance data are available and will remain available during the course of the experiment. The upper Zambezi catchment would also be a promising research area for evaporation studies. If the shift of the ^{18}O –D line at Victoria Falls is indeed evaporation induced (see Fig. 14 and Section 3.4) then these effects would become visible during synoptic sampling in the right part of the catchment.

Synoptic river data obtained in the present project have shown that isotope and chemical enrichment does not only occur in reservoirs, but also along river stretches with no other apparent inflow (for example the stretch between 500 and 700 km along the Vaal River: Fig. 16). The effect of salinization of rivers due to irrigation practices and the interaction between surface and groundwater have become important questions in this dry region and need to be studied more carefully [15]. GNIR data can be helpful here.

Comparisons of tritium in rainfall and runoff in the Thukela during 1970–1972 [15] show that half the Thukela River water at Mandini consists of water from earlier rainfall seasons. These earlier water contributions can be up to a decade old. This would suggest a very large storage availability within the catchment and much more limited overland flow than is usually assumed. While it is probably no longer possible to use tritium for this purpose, more localised studies can be done using other techniques.

6.2. Proposals for GNIR in southern Africa

The isotope information obtained from sampling stations in the lower reaches of the rivers is very much determined by evaporation and cumulation effects, as well as water release practices in upstream reservoirs. The amount of scientific information that can be derived from monitoring at these stations is probably limited and continuation of these stations should be reconsidered.

The monitoring of streams and rivers above the influence of dams and reservoirs is likely to produce information that can be used for hydrological interpretation. This suggests looking at observations on a longer timescale than the days or week used for standard hydrograph separation. Stations that could be useful here would be those located in the upper Thukela river, as well as in the uplands and lowlands of Lesotho. Similar stations might be found in the headwaters of the Olifants and Breede Rivers in Western Cape. These observations need to be supplemented with rainfall collection within the same catchments.

ACKNOWLEDGEMENTS

We thank S.Phufi, B. Sello, J. van Wyk, S. Montshiwa, C. Hemmings (DWAf South Africa) and E. Madamombe (ZINWA Zimbabwe) for regular river sample collections. Occasional samples from the Zambezi River were collected by travellers J. Weaver, D. Talma and E. Dry. Prof W. Mook kindly made the data from the SCOPE/UNEP project available for comparison. We acknowledge the initiative of, and financial support from, the IAEA's Cooperative Research Programme, through which it was possible to resume sampling in the rivers and revisit historical data.

REFERENCES

- [1] TALMA, A.S., "Stable isotope content of South African river water", Proc. Hydrol. Sci., Symp, Rhodes Univ., Grahamstown, 6–9 September 1987, Vol. 102–112 (1987).
- [2] DEPARTMENT OF WATER AFFAIRS AND FORESTRY, Database of hydrological information, Department of Water Affairs and Forestry (2007), <http://www.dwaf.gov.za/Hydrology/daminfo.htm>.
- [3] MOOK, W.G., The oxygen–18 content of rivers, Mitt. Geol.–Paläont. Inst. Univ. Hamburg, SCOPE/UNEP Sonderband 52 (1982) 565–570.
- [4] MOOK, W.G., (Ed.), Environmental Isotopes in the Hydrological Cycle, Vol. 3: Surface Water, IHP-V, UNESCO, Paris (2000), <http://www.iaea.or.at/programmes/rip/ih/volumes/volumes.htm>.
- [5] DEPARTMENT OF WATER AFFAIRS AND FORESTRY, Orange River project, DWAf (2007), <http://www.dwaf.gov.za/orange>.
- [6] FOOD AND AGRICULTURE ORGANIZATION, Irrigation potential in Africa: A basin approach in Zambezi, FAO (2002), <http://www.fao.org/docrep/w4347E/W4347e0o.htm>.
- [7] CENTRE FOR GLOBAL ENVIRONMENTAL EDUCATION, The Zambesi, CGEE (2000), <http://cgee.hamline.edu/rivers/MA2001/MA2000/guests/archive/keen1.html>.
- [8] LESOTHO HIGHLANDS WATER PROJECT, LHWP (2007), <http://www.lhwp.org.ls>.
- [9] SCHULZE, R., UNESCO HELP project: (2002) <http://www.beeh.unp.ac.za/Thukela>.
- [10] DEPARTMENT OF WATER AFFAIRS AND FORESTRY, Thukela water project feasibility study, DWAf (2001) <http://www.dwaf.gov.za/thukela>.
- [11] SKOFTELAND, E., "Background of water resources in the SADC region", Water resources management in southern Africa — A vision for the future, Conference of SADC Ministers responsible for Water Resources Management, Pretoria (1995).
- [12] UMOH, U.T., "Hydroclimatological approach to sustainable water resources management in semi arid regions of Africa", Water Resources of Arid Areas (STEPHENSON, D., SHEMANG, E.M., CHAOKA, T.R., Eds), Proc. International Conference on Water Resources of Arid and Semi-Arid Regions of Africa, Garborone, Botswana, 3–6 August 2004, Taylor and Francis, London (2004) 389–395.
- [13] EARTHTRENDS, Watersheds of the world: Zambezi, http://earthtrends.wri.org/maps_spatial/maps_detail_static.php?map_select=310&theme=2 (2006).
- [14] SCOTT, D.F., PRINSLOO, F.W., MOSES, G., MEHLOMAKULU, M., SIMMERS, A.D.A., A re-analysis of the South African catchment afforestation experimental data, Water Research Commission, Report No. 810/1/00, Pretoria (2000).
- [15] KIRCHNER, J.O.G., Investigation into the contribution of Groundwater to the Salt load of the Breede River, using Natural Isotopes and Chemical Tracers, Water Research Commission, Report 344/1/95 (1995).

- [16] TALMA, A.S., VOGEL, J.C, Lowered Tritium levels in River Water indicate Significant Storage of Water in a Large Catchment, Isotope Hydrology Symposium, IAEA, Vienna, 19–23 May 2003 (2003).

STABLE WATER ISOTOPE INVESTIGATION OF THE BARWON–DARLING RIVER SYSTEM, AUSTRALIA

C.E. Hughes^a, D.J.M. Stone^a, J.J. Gibson^{a,b}, K.T. Meredith^a, M.A. Sadek^{a,c},
D.I. Cendon^a, S.I. Hankin^a, S.E. Hollins^a, T.N. Morrison^a

^a Institute for Environmental Research, Australian Nuclear Science and Technology PMB 1,
Menai NSW 2234, Australia

² Alberta Research Council, Vancouver Is Technology Park, Victoria BC, Canada

³ Atomic Energy Authority, Nasr City, Cairo, Egypt

Abstract. The Murray–Darling Basin is the largest river basin in Australia and is host to agriculture, recreation, water supply reservoirs and significant biodiversity. Through land use practices and climate change there is the potential for significant disruption to the natural hydrological system of the basin. The Barwon–Darling River, in the upper part of the Murray Darling Basin, is primarily in a semi-arid landscape which is subject to significant evaporation, yet evaporative losses from the river remain poorly described. The stable isotope composition of groundwaters has become widely used over the past several decades as an indicator of the circumstances and geographical locations of aquifer recharge, though applications to surface water budgets have been far less extensive. A global isotopic observation initiative, the Global Network for Isotopes in Rivers (GNIR), focussed in Australia on the dryland Barwon–Darling River system. We report on drought driven isotopic signatures in the Barwon–Darling River during 2002–2007 and estimate that the amount of water lost by the Barwon–Darling River system due to evaporation may be up to 80% during severe drought periods. Runoff ratios have been commonly estimated to be between 0.1 and 1% and there is evidence of groundwater exchange with the river. This work highlights the role of stable water isotopes in assessing the amount of water lost from the river by direct evaporation, and in quantifying groundwater inputs and ungauged losses from the river.

1. INTRODUCTION

Australian inland water resources are especially vulnerable to climatic change and degradation due to a semi-arid climate and a high level of water development and utilization for irrigation and urban water supply. As described in [1], the International Atomic Energy Agency (IAEA) launched a new global isotopic observation initiative for the period 2002–2005, the IAEA Coordinated Research Project ‘Design criteria for a network to monitor isotope composition of runoff in large rivers’ (known as the Global Network for Isotopes in Rivers, ‘GNIR’). In Australia, data collection for the GNIR project is focussed on the Barwon–Darling River in the upper part of the Murray Darling basin (Fig. 1), and involves the application of stable isotope techniques to refine the water balance within the Murray–Darling Basin (MDB) system. This basin is the country’s most important agricultural area, containing about three quarters of Australia’s irrigated crop and pasture land.

ANSTO’s research on the Barwon–Darling River is conducted within the Isotopes for Water Project and has focused on using ¹⁸O and ²H to quantify both natural and development related impacts on the river water balance and water quality. In addition to the GNIR project, outlined by Gibson et al. [1], ANSTO’s work contributes to a number of projects including the IAEA Global Network for Isotopes in Precipitation, the Murray–Darling Basin GEWEX Project, and more recently the IAEA/RCA Coordinated Research Project RAS/8/104 Assessment of Trends

in Freshwater Quality Using Environmental Isotopes and Chemical Techniques for Improved Resource Management. This effort includes the organisation of cooperative networks for monitoring ^{18}O and ^2H of groundwater, precipitation, and evaporation pans as well as river discharge.

Measurement of the stable isotope composition of groundwater has become widespread over the past several decades as indicative of the circumstances and geographical locations of aquifer recharge when compared with the stable isotopes in precipitation of the local area. However, applications to surface water budgets at regional, continental or global scales have only recently been tackled [2–4]. Such regional and continental scale modelling efforts not only require precipitation and groundwater isotope data for validation, but are limited by the availability of surface water isotope data in their ability to model runoff generation.

The stable isotope composition of surface water reflects the integrated effects of rain compositions, modified by the influx of groundwater and enrichment of heavy isotopes ($\delta^2\text{H}$ and $\delta^{18}\text{O}$) in surface waters by evaporation. These isotopes exhibit systematic variations in

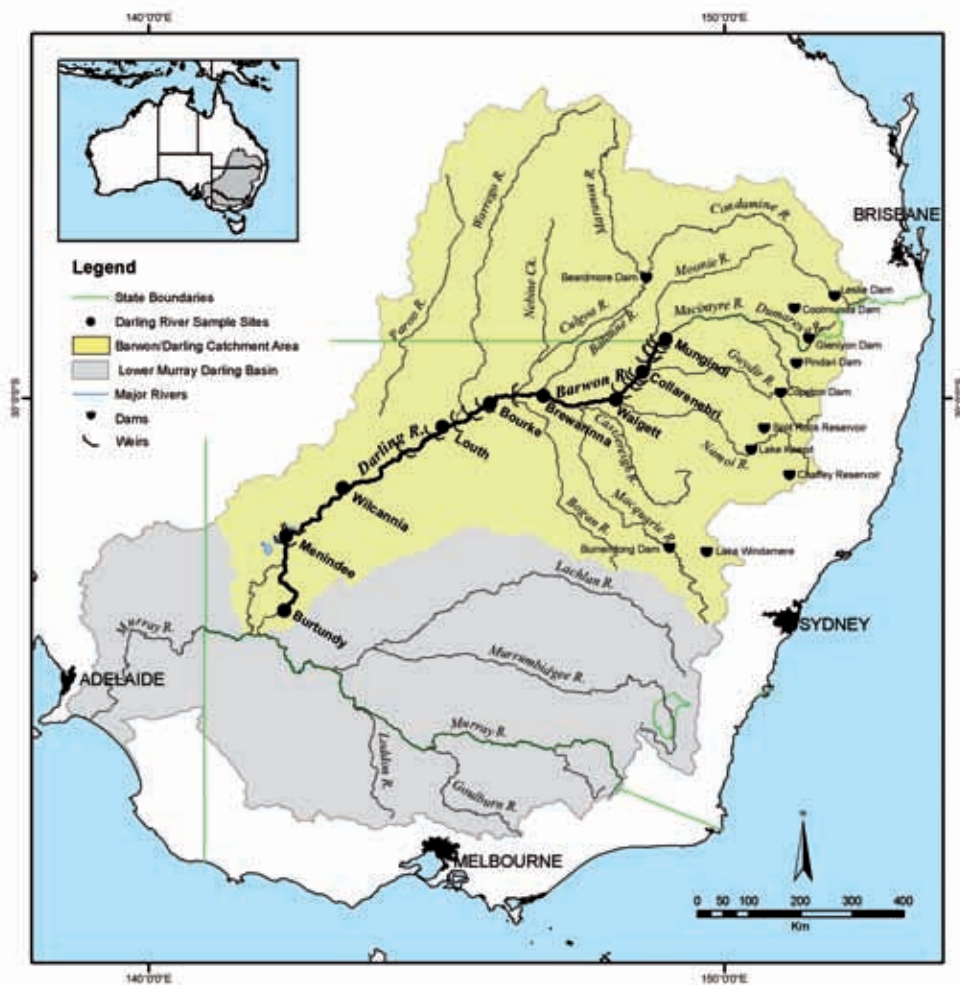


FIG. 1. Location map of the Murray–Darling Basin and the Barwon–Darling River showing position of major weirs and control structures, and location of water gauging and water sampling locations referred to in this report.

the water cycle as a result of phase change and diffusion derived isotopic fractionation (e.g. [5]). Precipitation variability is related mainly to the sources of air masses and their evolution, including temperature dependent equilibrium fractionation. Evaporation increases the proportion of heavy isotope species in surface waters due to additional kinetic isotope effects during diffusion, producing enrichment along so-called 'evaporation lines' of slopes less than the meteoric water line (MWL) [6, 7].

Water transpired by vegetation has approximately the same isotopic composition as root zone soil water and groundwaters [8]. Therefore, this form of return to the atmosphere does not affect the isotopic composition of residual water [9]. Optimal use of irrigation water involves, among other issues, maximising the proportion of water which is transpired rather than evaporated or lost through seepage. Since stable isotope compositions are extremely sensitive to evaporation losses, they offer new insights into this aspect of the catchment water balance and the process of management of water in irrigation areas.

2. BARWON–DARLING RIVER SYSTEM

2.1. Catchment description

The Murray River and its longest tributary, the Darling River, drain about 14% of the Australian continent. Surface runoff, primarily along the Murray River, is controlled by storage reservoirs, weirs, and irrigation canals which contribute to the exploitation of water from the basin. The Barwon–Darling River system is the longest river in Australia with a total length of 2740 km including the MacIntyre and Barwon Rivers [10]. The Darling River Basin area is 650 000 km², about 61% of total basin area, but the river contributes only 17% of flow to the Murray River. The Barwon–Darling River meanders through a dryland plain, with between typically 200 and 500 mm of annual precipitation and 2000 mm of potential evaporation along the main stem of the river. The Murray Darling Basin is fairly flat with elevations to only a few hundred metres above sea level except for at the southeast mountains of the Great Dividing Range, which are the source for a large fraction of water delivered to the catchment. Murray River discharge to the ocean is only about 21% of the basin's average runoff [10] with the Darling River contributing less than a third of this. Simpson and Herczeg [11] estimated that the Darling River discharges less than 1% of precipitation over the catchment, placing it amongst the lowest discharging major rivers (in terms of length) in the world.

Flow along the main Barwon–Darling River stem below Mungindi is highly dependant on episodic rainfall events in higher elevation and rainfall headwater catchments in the north and east of the basin and retains only a very muted natural seasonal maximum flow in summer. Flow variability is very high with the river running dry in some reaches during droughts. Under natural flow conditions the average annual flow at Wilcannia is 3.59×10^9 m³, however diversions and regulatory alterations have reduced annual flows by an average of 40% to 2.15×10^9 m³ [10]. Thoms and Sheldon [12] estimated that for 1997–1998, water diversions constituted 87% of the long term mean annual flow. The headwater catchments of the Barwon–Darling River system contain 11 headwater dams with a full storage capacity of 4.6×10^9 m³. At least 16 main channel weirs control flow along the main Barwon–Darling River channel which has ~120 licensed water extractors, the majority of whom are situated along the Walgett to Bourke reaches of the river (NSW State Water, M. Allen, pers comm. 2007). Water licensees also include a significant number of diversion schemes to irrigate water intensive crops,

primarily cotton. In general, cotton growers and other agricultural users abstract and impound water opportunistically during times of flood, which has had a notable effect on the overall flux and timing of water discharge down the main stem of the river. Storage dams are generally shallow (<5 m deep) and between Mungindi and Wilcannia the total storage capacity is approximately $3 \times 10^8 \text{ m}^3$ (NSW State Water, M Allen pers comm.). At Menindee, 490 km upstream of the Murray River confluence, flood waters from the Barwon–Darling River are diverted into a series of shallow lakes, which are used for irrigation storage. Although impacts of diversions have been generally described, more detailed temporal records of water diversions and water demand during hydrological events are desirable for improving sustainable management of the altered river ecosystem.

For this project, research in the Darling River Basin has focused on a series of nine gauging stations situated along the Barwon–Darling River system from Mungindi to Burtundy (Fig. 1), crossing a distance of over 1000 km, and stretching from the Queensland border to the Darling River's confluence with the Murray River.

2.2. Previous river isotope data from the Murray Darling Basin

The Commonwealth Science and Industrial Research Organisation (CSIRO) provided all of the data on stable water isotopes for the Barwon–Darling River prior to this project. Herczeg et al. [13] provided data for both discharge and deuterium concentrations in the Darling River at Burtundy Weir (1984–1990), showing a strong positive correlation between deuterium and chloride and an inverse correlation with discharge.

Simpson and Herczeg [11, 14] established that the observed enrichment of stable isotopes during summer months (Oct.–March) in the surface waters of the Murray River basin offers the potential to deduce approximate magnitudes of water loss to the atmosphere through evaporation. In run-of-river data, they observed increases in $\delta^2\text{H}$ between the Murray River headwaters (Jingellic) and the mouth of the Murray River channel (Milang) of 31.5‰ in Dec. 1988, 39‰ in March 1989 and 44‰ increase in June 1989. They attributed the increase primarily to evaporation, since transpiration does not cause significant enrichment of $\delta^2\text{H}$ in residual water. They calculated the expected heavy isotope enrichment trend with a model formulation [15] that includes the effects of both exchange flux of vapour and evaporation, using input parameters representative of conditions in the Murray River Basin during the summer. Three sets of calculations were made, for effective mean humidities of 45, 55 and 65%. An approximation was made using the linear part of those curves (less than 50% evaporation), which yielded an enrichment slope for 50% effective mean humidity, of nearly 1‰ change in $\delta^2\text{H}$ for every percent change in the amount of residual water. They suggested that integrated evaporation losses from river surfaces and irrigation diversions in the basin during the months of intensive irrigation from waters contributing runoff to the Murray River represent a major ($40 \pm 15\%$) component of water loss to the atmosphere, similar in magnitude to that transpired through plants.

The El Niño Southern Oscillation (ENSO) phenomenon is crucially important for the climate in the east of Australia. The period 1 January 1979 through 1 March 2008, for example, includes seven El Niño periods covering 10 years (1982–1983, 1986–1987, 1991–1995, 1997–1998, 2002–2003, 2004–2005 and 2006–2007) and five La Niña years (1984–1985, 1988–1989, 1996–1997, 1998–1999, 2000–2001). The $\delta^2\text{H}$ data for Burtundy presented by Herczeg et al (1992) revealed that there was an enrichment of $\sim 75\%$ in river water from late

1984 to early 1988 during the El Niño, while there was little enrichment due to repeated high flows through much of the periods 1984 and 1988–1990, coinciding with two of the La Niña events. The earlier work of Simpson and Herczeg [11] predicted that at least 70% of the water had evaporated during this particular drying period along the Darling River, though this was regarded as an approximation. Run-of-river data for the Barwon–Darling River [1] for early 1991 at the beginning of an extended El Niño period showed that river waters fell along an evaporation line of slope 5.5 with progressive enrichment downstream and clear isotopic impacts from inflowing tributaries.

Analyses based on the current dataset for the Barwon–Darling River have been presented in [17] focusing on the use of monthly isotope data to constrain evaporative enrichment for isotopic water balance calculations and Meredith et al. [18, 19] who use stable water isotopes and major ion chemistry to identify and quantify groundwater–surface water interactions between Bourke and Wilcannia. Clearly stable isotopic enrichment has been shown to have the potential to play an important role in determining the seasonal and geographical variations in evaporation across the basin.

2.3. Previous rainfall isotope data for the Darling River catchment

Hughes and Allison [20] and Hartley [21] published the only rainfall isotope data available for the Darling River catchment. The rainfall isotopic signatures of the main headwater catchment inputs to the Barwon–Darling River system are summarised in Table 1. Rainfall isotope data for Broken Hill to the west of the catchment is also included as it is closest climatically and geographically to the drier SW corner of the catchment. Using the weighted average of the $\delta^2\text{H}$ data for the northernmost three stations and assuming a deuterium excess of 12, as measured for Narrabri and Broken Hill, it can be inferred that the mean stable isotopic composition of precipitation entering the upper Barwon–Darling River system is approximately $\delta^2\text{H} = -30.6 \text{ ‰}$ and $\delta^{18}\text{O} = -5.3 \text{ ‰}$.

2.4. Methods

Surface water samples were collected from nine stations along the Barwon–Darling River approximately monthly from July 2002 to January 2006 (Table 2). At Burtundy, for which weekly samples were collected, there were also a couple of samples collected in January 2002. A number of further samples were collected from other sites during run-of-river campaigns in August 2003, January 2004, January 2006 and January 2007 as well as some additional tributary and reservoir samples.

Routine monthly surface water samples at the 11 sites were collected by the NSW Department of Water and Energy (DWE) as part of their water quality programme and were analysed for EC and major ion chemistry at the DWE Wollie Creek Laboratory. Frozen residual samples obtained by ANSTO were analysed for $\delta^2\text{H}$ and $\delta^{18}\text{O}$ by IRMS at the CSIRO Adelaide Laboratory or INSTAAR at the University of Colorado. In addition, run of river campaigns were conducted on four occasions and for 2006 and 2007 these samples were analysed by the Environmental Isotope Laboratory at the University of Waterloo, Canada.

Discharge, stage and electrical conductivity (EC) data were extracted from PINEENA (2006) which is a database of archived hydrological data published by DWE. Climate data were obtained from the Australian Bureau of Meteorology.

TABLE 1. RAINFALL ISOTOPE DATA FROM OR NEAR THE MURRAY–DARLING BASIN [20]

Station	No of samples	$\delta^{18}\text{O}$ (‰)	$\delta^2\text{H}$ (‰)	Annual rainfall (mm)	Latitude	Longitude	Elevation (mAHD)*
Charleville	31	-	-28.0	605	-26.4139	146.2558	301.5
Toowoomba	35	-	-29.9	1158	-27.5425	151.9134	640.9
Narrabri	27	-5.8	-34.2	679	-30.3154	149.8302	229
Broken Hill	23	-4.71	-25.9	257	-32.0012	141.4694	281.3

* Elevation with respect to the Australian Height Datum.

TABLE 2. BARWON–DARLING RIVER SAMPLE SITES

Sample Site	DWE** Site No.	Frequency	No of samples	Km to mouth	Latitude	Longitude	Elevation mAHD)*
Barwon R at Mungindi	416001	Monthly	33	2020	28.9786°S	148.9899°E	152.93
Barwon R at Collarenebri	422003	Monthly	35	1896	29.5470°S	148.5771°E	135.53
Namoi R at Gunnedah	419007	Monthly	25	2169	30.9736°S	150.2544°E	254.88
Darling R at Walgett (Dangar Br)	422001	Monthly	28	1778	30.0122°S	148.0620°E	118.55
Namoi R at U/S Walgett	419091	Monthly	36	1793	30.0284°S	148.1532°E	-
Barwon R at Brewarrina	422002	Monthly	31	1538	29.9481°S	146.8642°E	106.702
Darling R at Bourke	425003	Monthly	35	1352	30.0537°S	145.9529°E	91.848
Darling R at Louth	425004	Monthly	34	1163	30.5351°S	145.1140°E	83.97
Darling R at Wilcannia Main Channel	425008	Monthly	45	747	31.5601°S	143.3852°E	63.415
Darling R at U/S Weir 32 (Menindee)	425012	Monthly	47	454	32.4372°S	142.3801°E	51.825
Darling R at Burtundy	425007	Fortnightly-monthly	68	124	33.7488°S	142.2633°E	32.404

* Elevation with respect to the Australian Height Datum.

** Department of Water and Energy.

3. RESULTS AND DISCUSSION

Surface water isotope data for the Barwon–Darling, Namoi, Murray and Murrumbidgee Rivers are plotted in Fig. 2. The Barwon–Darling River data reveal a drying trend in time through 2002 and again through 2003, with every station recording a steady increase in the amount of evaporative enrichment as each summer advances. The low flow and rainfall periods of 2002–2003 and late 2004–2005 correspond to El Niño periods with the period 2002–2007 having consistently below average rainfall and above average temperatures for the region. Enrichment of the isotopic composition of rivers can be caused in many basins by inflow from tributaries with much heavier isotope compositions, though this leads to an evolution of the river water along a mixing line which will be close to the local meteoric water line (LMWL) of the basin, and may show little evidence of evaporation. The extent of evaporation

is revealed by plotting the isotopic data in a stable isotope diagram (such as Fig. 2), and observing whether the data plot on a slope is significantly less than the slope of the LMWL, such as a slope of 4–5. Thus, it is important to understand the contribution that variations in the isotopic input of precipitation from various parts of the basin makes to any observed trends in river isotopes. The rivers waters fall predominantly along an evaporation line with a slope of 4.88 with a noticeable increase in enrichment (see run-of-river data in Fig. 3) for successive samples moving downstream for most of the dataset.

3.1. Isotopic trends in relation to flow

Over the four year drought dominated period 2002–2005, five flow events came through the system. The flow volumes of these events estimated at Bourke were: Mar–Apr 2003 ($\sim 1.3 \times 10^8 \text{ m}^3$); Jan–Feb 2004 ($\sim 3.85 \times 10^8 \text{ m}^3$); Mar–Apr 2004 ($\sim 2 \times 10^8 \text{ m}^3$); Dec 2004–Jan 2005 ($\sim 4.8 \times 10^8 \text{ m}^3$); Jul–Aug 2005 ($\sim 2.2 \times 10^8 \text{ m}^3$). During the period 2002–2005, flow at Wilcannia averaged $3.4 \times 10^8 \text{ m}^3/\text{y}$, only 16% of the average flow. Only 35% of the flow at Wilcannia during the period made it past the Menindee Lakes system to the mouth of the Darling River at Burtundy to discharge into the Murray River.

Samples collected from the Menindee Lakes, primarily Lake Copi Hollow, during the drought of 2003–2004 show the most extreme enrichment ($\delta^2\text{H} = +84.4\text{‰}$; $\delta^{18}\text{O} = +16.19\text{‰}$ in April 2004) along a local evaporation line with a slope of 6. This is due to long residence time in

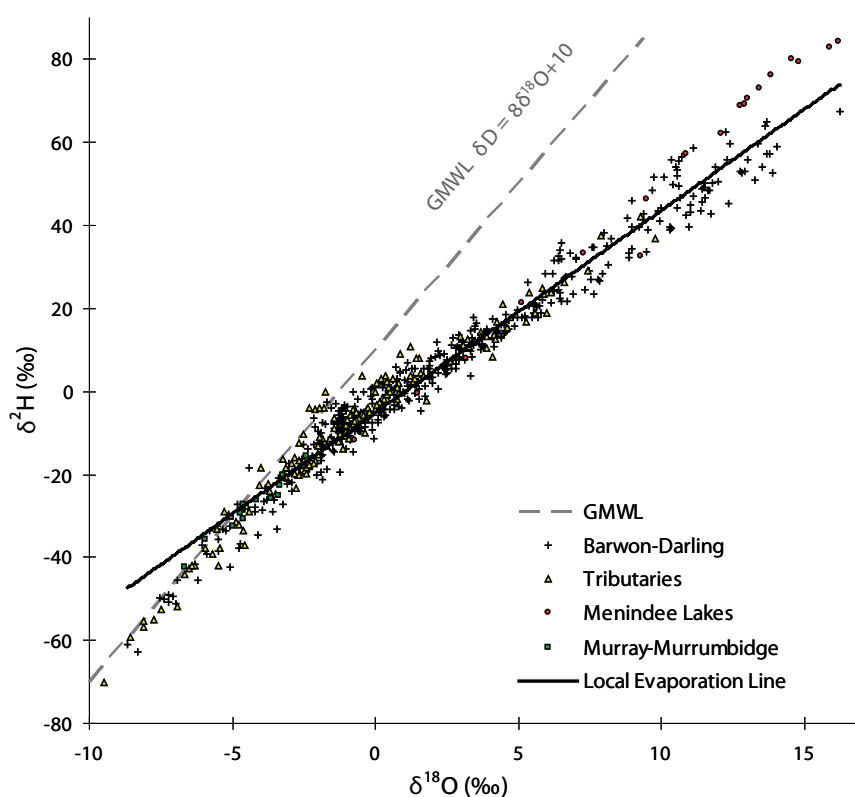


FIG. 2. Plot of stable water isotope data and Local Evaporation Line (LEL) in comparison to the Global Meteoric Water Line (GMWL, [6]) for the Barwon–Darling River system, and other catchment water bodies from 2002 to 2006.

a shallow lake environment. The most enriched Barwon–Darling River waters were seen during the same drought period at Burtundy in February 2004 ($\delta^2\text{H} = +67.4\text{‰}$; $\delta^{18}\text{O} = +16.22\text{‰}$). This extreme enrichment is because the effect of the minor flow of 2003 did not extend past the Menindee Lakes to the downstream sites. This is demonstrated by run-of-river data plotted in Fig. 3, where the August 2003 dataset shows the river isotope values ‘reset’ by earlier flows up until the start of the Menindee Lakes at 550 km upstream. In fact only the flow event of Jan–Feb 2004 passed through the lakes system to have a significant impact downstream.

Tributary river waters are more likely to lie along a meteoric water line and during flow events tributaries may contribute waters with significantly different isotopic signatures. An example of this is the flow event of January 2004 (see run-of-river data in Fig. 3) where the isotope signature at Bourke ($\delta^2\text{H} = -62.9\text{‰}$; $\delta^{18}\text{O} = -8.32\text{‰}$) was significantly more depleted than that of Brewarrina upstream ($\delta^2\text{H} = -28.7\text{‰}$; $\delta^{18}\text{O} = -3.23\text{‰}$) due to an input of depleted water from the normally dry Culgoa River. However, many tributary data still show significant evaporative enrichment. In contrast, the small number of lower Murray–Darling Basin samples collected from the Murray and Murrumbidgee Rivers lie close to the GMWL.

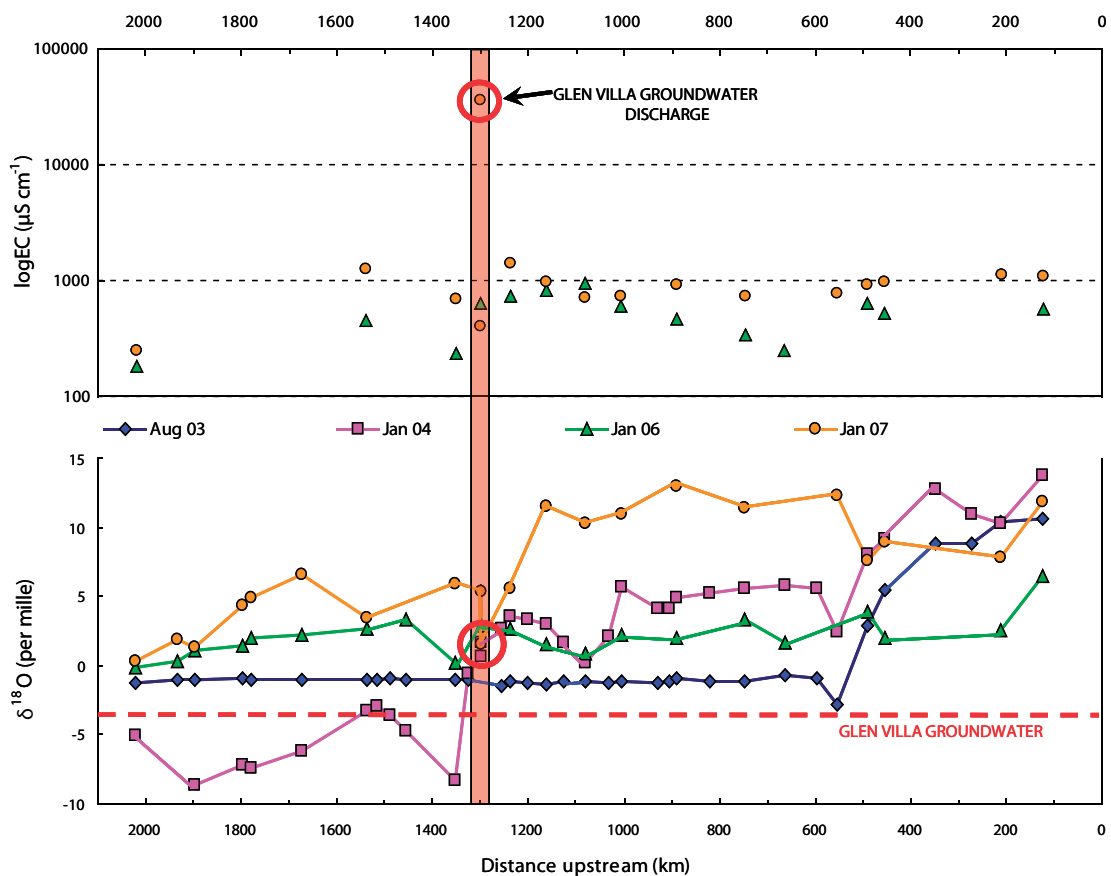


FIG. 3. EC and $\delta^{18}\text{O}$ for run-of-river samples from Mungindi to Burtundy. Red circles indicate high EC and a slight dip in $\delta^{18}\text{O}$ for the Glen Villa site towards the local groundwater value [18, 19]. The distance scale is upstream from the Murray River.

3.2. Enrichment as an indicator of evaporative losses from the system

These data clearly show the cycles of drought driven enrichment between flood events in the Barwon–Darling River system and can be used to establish the degree of evaporation affecting individual reaches of the river. As noted above, an approximation of the amount of evaporation occurring has been made previously by [14] who used $\delta^2\text{H}$ for both the Murray River (covering the entire length over a period of several months in 1989) and the Darling River (data from Burtundy over seven years 1984–1991).

For the dataset from 2002–2005, the stable isotope composition of the Barwon–Darling River during evaporation was estimated based on the methods outlined by [15] using equilibrium fractionation factor coefficients from [22], neglecting salinity and using average values for the period. Relative humidity (45%) and temperature (20°C) were calculated from the daily average BOM data for Walgett, Bourke and Wilcannia for 2002–2005. The composition of atmospheric water vapour δ_A is assumed to be $\delta^{18}\text{O} = -13.55\text{‰}$ [16] and $\delta^2\text{H} = -81.25$ and the initial isotopic composition is assumed to be in the intersection of the GMWL with the LEL (Fig. 2) $\delta^2\text{H} = -28.79\text{‰}$, $\delta^{18}\text{O} = -4.85\text{‰}$. Initial composition is assumed to be very close to the average precipitation composition estimated above. The $\delta^{18}\text{O}$ and $\delta^2\text{H}$ values as a function of fraction of water remaining are shown in Fig. 4 and the fraction of water remaining shown relative to the stable isotope data for the study in Fig. 5.

Fig. 5 indicates that the majority of sites are subject to a significant degree of evaporation with the fraction remaining being between 0.6 and 0.9 for most samples. At the most extreme at Burtundy in February 2004 the fraction remaining was less than 0.25 and the most enriched sample at the Menindee Lakes had a remaining fraction of only 0.2. Under these extreme conditions this represents a cumulative evaporative loss of 75% from runoff to the final discharge point of the river, and losses of up to 80% during impoundment in the Menindee Lakes.

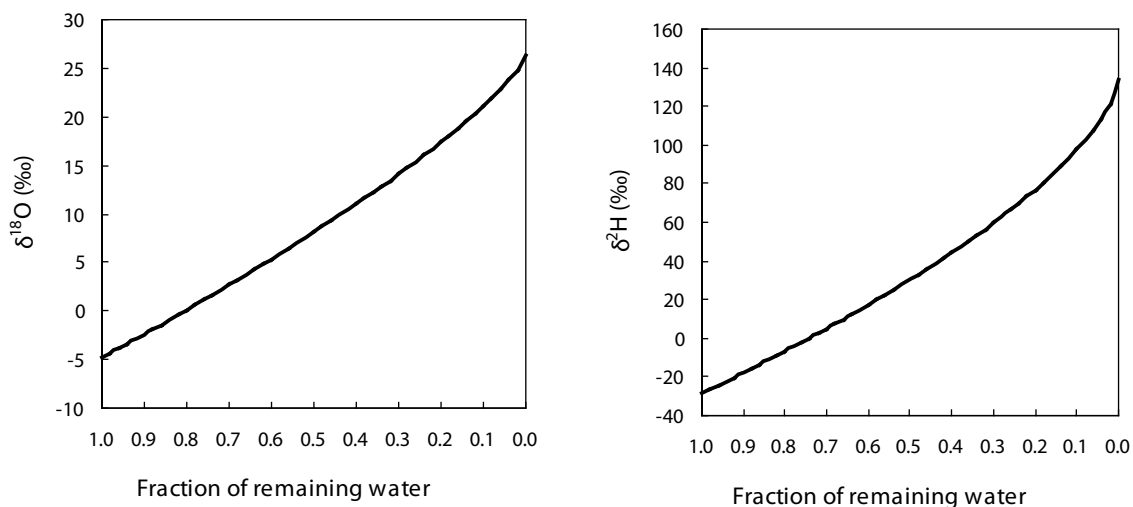


FIG. 4. The $\delta^{18}\text{O}$ and $\delta^2\text{H}$ composition of the Barwon–Darling River as a function of the fraction of remaining water.

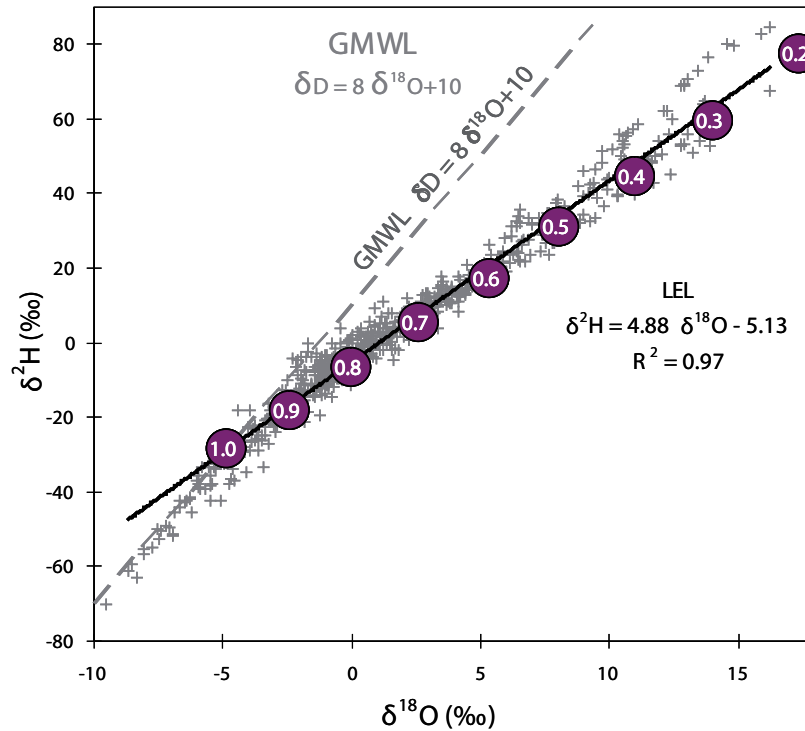


FIG. 5. Fraction remaining along the Local Evaporation Line for the Barwon-Darling River system and tributaries 2002–2005.

3.3. Evidence of groundwater input to the river

The Barwon–Darling River flow is characterized by high flow periods following rainfall in the headwaters followed by gradual drying of the river channel between flow events when the flow is controlled by a series of weirs along its length. During these drying periods groundwater input is suspected along a number of reaches. The most obvious of these is the Glen Villa area below Bourke (EC and stage data shown in Fig. 6), where highly saline groundwater discharge is evident from EC data at zero or low flow. This is most clearly seen in the January 2007 run-of-river $\delta^{18}\text{O}$ and EC data plotted in Fig. 3 which show a significant rise in EC from 398 $\mu\text{S}/\text{cm}$ above Weir 19A (above Glen Villa) to 35752 $\mu\text{S}/\text{cm}$ below the weir. The corresponding $\delta^{18}\text{O}$ dropped from +5.36‰ to +1.36‰ confirming a strong groundwater influence. Groundwater in the Glen Villa area has an average $\delta^{18}\text{O}$ value of -3.5 ‰ [19] and the hydrogeochemical and isotopic mixing processes occurring in this area are further discussed in [19]. Whilst significant, evaporative enrichment of the water is not sufficient to explain the high conductivity levels and there is isotopic and hydrogeochemical evidence of mixing with groundwater at this site (Fig. 3, [19]). There is evidence [19] that at zero flow the groundwater input into the river remains localised and at higher flows the saline waters are diluted and flushed downstream. So the impact on river water quality, which is strongly evident in stagnant reaches at low or zero flow, is also observed in the first flush of a flow event following those periods. Evidence of saline first flush events can also be seen at Bourke, Louth and Wilcannia as well as the Glen Villa study site (Fig. 6).

3.4. Water balance modelling

Further modelling of evaporative isotope enrichment has been carried out as part of this study by [16]. A steady state isotope mass balance using $\delta^2\text{H}$ and $\delta^{18}\text{O}$ was conducted on a monthly

Glen Villa Weir - EC and river level

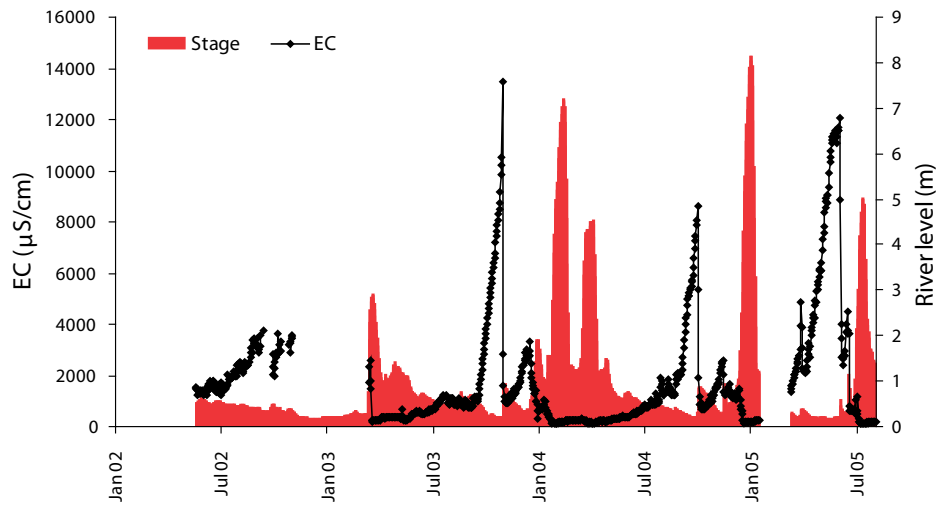


FIG. 6. River stage and electrical conductivity data at Glen Villa [23].

time step from July 2002 to December 2003 on a reach basis with eight reaches between the nine Barwon–Darling River stations shown in Fig. 1 and listed in Table 2. This represents a drying period with one minor flow event.

Modelled evaporation/inflow ratios (Fig. 7) show the progressive evaporation trend prior to the flow event of March 2003. The results also show the potential of the dataset to quantify ungauged gains and losses from the river in terms of groundwater inputs, bank storage losses and irrigation abstraction during flow events. The study estimated that runoff ratios for the period were less than 5.7% and mostly in the range 0.1–1%.

4. CONCLUSION AND ONGOING WORK

The present work has used data from the recent drought in the Murray–Darling Basin to calculate that the amount of water lost by the Barwon–Darling River system due to evaporation may be up to 80% during severe drought periods. This study has also estimated runoff ratios to be commonly between 0.1 and 1% and has shown evidence for groundwater exchange with the river. This dataset shows great potential for assisting in quantification of water balances for the Barwon–Darling River and the Menindee Lakes system, in particular determining rates of evaporative loss, the effect of diversions on the river water balance and zones of groundwater inflow to the river.

In ongoing work the authors also intend to analyse groundwaters along the length of the Barwon–Darling River for stable water isotopes. Stable isotope and hydrogeochemical data are currently being used to construct an isotope mass balance and isotope enabled model (RWSIBal) of the river system that will run on a daily time step. The aim is to enable groundwater gains and losses to be identified with more confidence and to more accurately quantify losses to evaporation. This modelling is being carried out as a collaboration between Cath Hughes (ANSTO), Jeff Turner and Tony Barr (CSIRO Land & Water, WA) and John Gibson (Uni

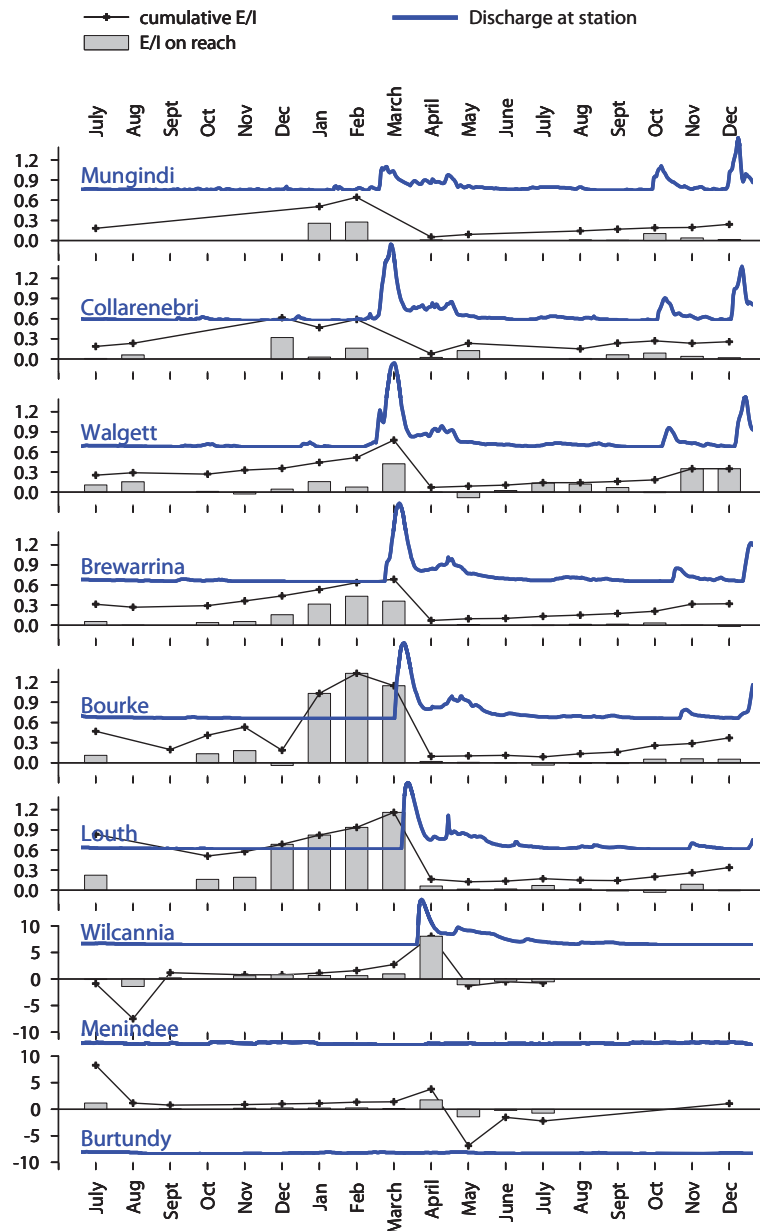


FIG. 7. Derived evaporation/inflow (E/I) ratios and relative discharge rates [16].

Victoria, Canada). Other continuing work includes the installation of an evaporation pan network to improve our ability to characterise atmospheric controls on evaporative enrichment using the method developed by G[17] and the addition of routine rainfall sampling within the catchment. This work is being conducted by Suzanne Hollins (ANSTO) in collaboration with John Gibson as part of the Australian GNIP network.

ACKNOWLEDGEMENTS

We would like to thank the Department of Water & Energy and in particular Principal Hydrogeologist Michael Williams for his support of the project from the outset, John Brayan

from the DWE Wolli Creek Laboratory, for providing the samples for analysis and also their hydrochemistry results for those samples and Richard Cooke for assistance with discharge and EC data. Mick Allen from State Water has been very helpful in providing data and an understanding of catchment irrigation systems. Megan LeFournour and staff from CSIRO, Adelaide provided the bulk of the stable isotope analyses; Bob Drimmie from Waterloo Environmental Isotope Lab, Canada and Bruce Vaughn from INSTAAR for the remainder. Thanks to the IAEA Isotope Hydrology Section for hosting this project especially Tomas Vitvar for constant encouragement. At ANSTO, Nathan Butterworth did lots of work compiling time series data and Barbara Neklapilova and Henri Wong did some of the major ion analyses.

REFERENCES

- [1] GIBSON, J.J., et al., Isotope studies in large river basins: a new global research focus, *EOS* **83**, No 52 (2002) 613–617.
- [2] KENDALL, C., COPLEN, T.B., Distribution of oxygen–18 and deuterium in river waters across the United States, *Hydrol. Proces.* **15** (2001) 1363–1393.
- [3] GIBSON, J.J., EDWARDS, T.W.D., Regional water balance trends and evaporation-transpiration partitioning from a stable isotope survey of lakes in northern Canada, *Glob. Biogeochem. Cycles* **16** 2 (2002) 1026.
- [4] FEKETE, B.M., GIBSON, J.J., AGGARWAL, P., VOROSMARTY, C.J., Application of isotope tracers in continental scale hydrological modeling, *J. Hydrol.* **330** (2006) 444–456.
- [5] DANSGAARD, W., Stable isotopes in precipitation, *Tellus* **16** (1964) 436–468.
- [6] CRAIG, H., Isotopic variations in meteoric water, *Science* **133** (1961) 1702–1703.
- [7] GAT, J.R., Oxygen and hydrogen isotopes in the hydrological cycle, *Annu. Rev. Earth Planet. Sci.* **24** (1996) 225–262.
- [8] ZIMMERMANN, U., EHHALT, D., MUNNICH, K.O., “Soil–water movement and evapotranspiration: Changes in the isotopic composition of the water” *Isotopes in Hydrology*, IAEA, Vienna (1967) 567–585.
- [9] ALLISON, G.B., BARNES, C.J., HUGHES, M.W., LEANEY, F.W.J., “Effect of climate and vegetation on oxygen–18 and deuterium profiles in soils”, *Isotope Hydrology*, 1983, IAEA, Vienna (1983) 105–123.
- [10] MURRAY DARLING BASIN COMMISSION, Murray-Darling Basin eResources (2005) http://www.mdbc.gov.au/subs/eResource_book/chapter1/p2.htm.
- [11] SIMPSON, H.J., HERCZEG, A.L., Salinity and evaporation in the River Murray basin, Australia, *J. Hydrol.* **124** (1991) 1–27.
- [12] THOMS, M.C., SHELDON, F., Water resource development and hydrological change in a large dryland river: the Barwon-Darling River, Australia, *J. Hydrol.* **228** (2000) 10–21.
- [13] HERCZEG, A.L., SIMPSON, H.J., DIGHTON, J.C., Salinity, groundwater and evaporation in the Darling Basin, Murray Darling Basin Workshop, Renmark SA, 27–29 Oct. (1992).
- [14] SIMPSON, H.J., HERCZEG, A.L., Stable isotopes as an indicator of evaporation in the River Murray, Australia, *Water Resour. Res.* **27** 8 (1991) 1925–1935.
- [15] GONFIANTINI, R., “Environmental isotopes in lake studies”, *Handbook of Environmental Isotope Geochemistry*, Vol. 3 (FRITZ, P., FONTES, J.Ch., Eds), Elsevier, New York (1986) 113–168.

- [16] GIBSON, J.J., et al., Evaporative isotope enrichment as a constraint on reach water balance along a dryland river, *Isotopes in Environment and Health Studies*. **44** 1 (2008) 83–98.
- [17] GIBSON, J.J., EDWARDS, T.W.D., PROWSE, T.D., Pan-derived isotopic composition of water vapour and its variability in northern Canada, *J. Hydrol.* **217** (1999) 55–74.
- [18] MEREDITH, K., HOLLINS, S., HUGHES, C., CENDON, D., STONE, D., “Groundwater/surface water exchange and its influence on stable water isotopic signatures along the Darling River, NSW, Australia”, *Proc. XXXV IAH Congress on Groundwater and Ecosystems* (RIBEIRO, L., CHAMBEL, A., CONDESSO de MELO, M.T., Eds): 17–27 September 2007, Lisbon, Portugal (2007).
- [19] MEREDITH, K.T., et al., Temporal variation in stable isotopes (^{18}O and ^2H) and major ion concentrations within the Darling River between Bourke and Wilcannia due to variable flows, saline groundwater influx and evaporation, *J. Hydrol.* **378** (2009) 313–324.
- [20] HUGHES, M.W., ALLISON, G.B., Deuterium and oxygen-18 in Australian rainfall, CSIRO Aust. Division of Soils Technology. Adelaide, Paper No. 46 (1984) 1–13.
- [21] HARTLEY, P.E., Deuterium hydrogen ratios of Australian rain and groundwater, Masters Thesis, Dept of Civil Engineering, University of New South Wales (1978) 111pp.
- [22] MAJOUBE, M., Fractionnement en oxygène-18 et en deutérium entre l’eau et sa vapeur, *J. Chim Phys.* **197** (1971) 1423–1436.
- [23] PINNEENA, Version 9, New South Wales Surface Water Archive, Department of Natural Resources (2006).

ISOTOPIC TRACING OF HYDROLOGICAL PROCESSES AND WATER QUALITY ALONG THE UPPER RIO GRANDE, USA

J. Hogan^a, F. Phillips^b, C. Eastoe^a, H. Lacey^b, S. Mills^b, G. Oelsner^a

^aUniversity of Arizona, Tucson, USA

^bNew Mexico Tech, Socorro, NM, USA

Abstract. The Rio Grande, like many arid region rivers, exhibits reductions in streamflow and degrading water quality with distance downstream as a result of decreasing inflows, increasing evapotranspiration, and the addition of natural and anthropogenic solutes. Between 2000 and 2006 we conducted biannual synoptic sampling of the Rio Grande from its headwaters in Colorado to ~150 km south of El Paso, Texas (at total distance of ~1200 km) to evaluate how these processes result in the observed basin scale water and solute balances. Because of the synoptic nature of sampling, locations at the headwaters can be classified as representing natural hydrological processes whereas downstream samples represent ‘trend’ sites impacted by regulation and development. In addition, our sampling period coincided with a severe regional drought, allowing us to further evaluate basin response to periods of increasing water stress. We employed multiple environmental tracers, including O/H isotopes, Cl⁻, Cl/Br ratio and a suite of solute isotopes to help identify dominant hydrological processes and the causes of salinization. Using Cl/Br, Ca/Sr, ⁸⁷Sr/⁸⁶Sr and ³⁶Cl/Cl ratios as well as δ³⁴S and δ²³⁴U values, we show that very small (< 1 m³ sec⁻¹) and localized discharge of very old (millions of years) sedimentary brine is the dominant solute input into the Upper Rio Grande. The recognition of a geologic salinity source implies that alternative salinity management solutions, such as interception of saline groundwater, might be more effective than changes in agricultural practices.

1. INTRODUCTION

This is the final report for the Rio Grande component (Agreement USA-12047) of the IAEA Coordinated Research Project focused on ‘Isotopic Tracing of Hydrologic processes in Large River Basins: Design Criteria for a Network to Monitor Isotopic Composition of Runoff in Large River Basins’.

The specific goals of this IAEA CRP are as follows:

- (1) To launch and coordinate a programme for isotope sampling of river discharge and related studies via a network of research institutes worldwide, establishing linkages where appropriate to existing research and monitoring activities undertaken by national counterparts, monitoring agencies, and international research programmes.
- (2) To contribute to the understanding of the water cycle of large river basins by developing, evaluating, and refining isotope methodologies for quantitative analysis of water balance and hydrological processes, and for tracing environmental changes.
- (3) To develop an optimal protocol for operational river water sampling, and to design a comprehensive database to support isotope-based water balance studies, and future monitoring of ongoing environmental changes.

Specific activities of the Rio Grande component of the CRP were listed as follows:

- (1) Compile and review bi-annual synoptic sampling of the Rio Grande (at ~10 km intervals), all major tributaries, and important agricultural drains and canals from the headwaters of Colorado to south of El Paso conducted over the last three years, particularly stable isotopes of water, tritium, and related discharge data.
- (2) Compile and review existing USGS, NASQAN, and Los Alamos isotope data for the Rio Grande and related flow data.
- (3) Conduct weekly/monthly sampling at about 5–10 stations in the Rio Grande basin for isotope analysis during the year.
- (4) Compile and review isotope results and related discharge data.
- (5) Interpret isotope results with respect to water cycle and climate processes.
- (6) Report to IAEA on an annual basis.

In this final report we present a report on activities 1–2 and 4–6. Activity 3 above was planned as an education outreach component of the project, however lack of sufficient collaboration with local schools ultimately resulted in its failure. We are able, however, to present some data collected on a roughly monthly basis from other studies of the Rio Grande to provide context on seasonal variability to our report. In addition tritium is mentioned in relation to activity 1. We are unclear as to why this is here as tritium data was not collected at the time of this agreement and was not part of our research plan from the beginning. Finally, a significant amount of isotopic data was collected related to solute sources and salinization processes which is presented here, as we feel such solute isotopic systems provide complementary information to the more commonly studied water isotopes.

The general outline of this report is as follows. First, we provide a general overview of the climate, hydrology, geology, water quality and important socio-demographic characteristics of the Rio Grande Basin. Next we present a summary of discharge patterns along the Rio Grande during the period of this study specifically focused on response to a regional drought. We will then use this understanding in interpreting stable isotope data to assess the role of water resource management and changing hydrologic conditions in controlling the isotopic composition of river water. Building on this we will present a series of solute isotopic systems addressing the salinity sources that result in Rio Grande salinization. Finally we will end with some concluding remarks about the implications of our study results, lessons learned, and potential for a network to monitor the isotopic composition of runoff in large river basins.

2. THE RIO GRANDE

The headwaters of the Rio Grande are in the southern Rocky Mountains, in the state of Colorado, USA (Fig. 1). Most of the runoff that supplies the river originates as snowfall at elevations of 3000 to 4000 m in the San Juan, Sangre de Cristo, and Jemez mountain ranges. The river flows south through the states of Colorado and New Mexico before turning south–

east to form the boundary between the United States and Mexico and ultimately flowing into the Gulf of Mexico. This study was limited to the northern portion of the drainage basin, down to a point 130 km south of the cities of El Paso and Ciudad Juarez. This point is 1150 km downstream from the river's headwaters. Further downstream the river is frequently dry, although eventually additional tributaries restore perennial flow. The elevation at this point is 1100 m and the area of the drainage basin above it is $\sim 120\,000\text{ km}^2$.

For the purposes of discussion, the study area can be divided into three equal portions which provide contrasting hydrology, salinity and human management characteristics (Fig. 1). The 'upper' portion (0–430 km) is generally mountainous and is the source for most runoff in the basin. The discharge gauge located at Otowi marks the lower end of this region and has the highest average discharge in the study area. In the 'middle' section (430–800 km) the Rio Grande enters a more arid landscape and passes significant areas of irrigated agriculture and the population center of Albuquerque, NM. In general the channel is braided with significant sand bars. The lower end of this section holds Elephant Butte Reservoir, the largest reservoir on the Rio Grande. With a ~ 2.5 year residence time, Elephant Butte imparts a significant imprint on the downstream hydrology (due to highly controlled releases) and isotopic composition (due to significant evaporation). The 'lower' portion (800–1150 km) is highly managed for irrigated agriculture with controlled releases from Elephant Butte Reservoir, a well channelized path for the Rio Grande, and an efficient network of canals and drains.

2.1. Hydrogeologic framework

The relatively linear course of the Rio Grande as it flows south is largely due to structural control by the Rio Grande rift. This is an intracontinental extensional feature similar in origin to the better known East African rifts. Rifting was initiated at ~ 30 Ma and was initially rapid, but has slowed with time [3]. The rift consists of a series of elongate basins that are usually bounded on either side by Precambrian crystalline or Paleozoic sedimentary basement rocks (see Fig. 1). The basins are formed by full or half grabens that are filled with up to 4000 m of alluvial and lacustrine sediment [1, 3]. The grabens are terminated at either end by transform structures that bring basement rocks close to the surface. Fig. 2 shows a schematic cross-section of the basin structure parallel to the course of the river.

2.2. Precipitation and runoff

Although precipitation is as high as 1300 mm a/r over small areas in the mountainous headwaters, the majority of the drainage basin ranges from semiarid to arid. Most of the basin receives less than 300 mm a/r and the driest areas only 160 mm a/r. Summer temperatures are high and over most of the basin potential evapotranspiration varies from 1000 to 2000 mm y/r.

Within the study area, river discharge first increases as tributaries flow in, then decreases, partly because no further significant tributaries join the river, and partly because of evapotranspirative losses from riparian vegetation and reservoirs, as well as irrigation and municipal diversions. At the Colorado–New Mexico border, about 270 km from the headwaters, the mean annual discharge is $17\text{ m}^3/\text{s}$, although the natural flow would be about $40\text{ m}^3/\text{s}$ without agricultural diversions (discharge and water use data are from [6]). The river reaches its maximum discharge of $49\text{ m}^3/\text{s}$ at Otowi, New Mexico, 430 km down the river. This would probably be closer to $70\text{ m}^3/\text{s}$ under natural conditions. At Albuquerque, New Mexico, 550 km down river, the discharge is $44\text{ m}^3/\text{s}$. Above Elephant Butte Reservoir (800 km downstream and by

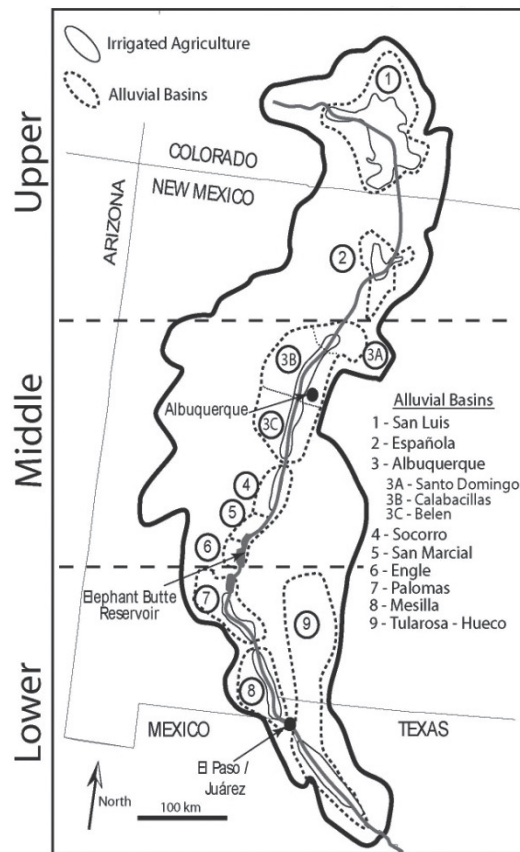


FIG. 1. Map of the Upper Rio Grande outlining the drainage area, river course, irrigated agriculture, population centers and alluvial basins [1] with Albuquerque subbasins [2] that form the Rio Grande rift. For purposes of discussion the basin is divided into three parts.

far the largest reservoir on the river) the discharge amounts to $40 \text{ m}^3/\text{s}$; below the reservoir it is about $33 \text{ m}^3/\text{s}$. The difference is largely attributable to evaporation from the reservoir. At El Paso (1025 km) this discharge has been further reduced to $20 \text{ m}^3/\text{s}$, mostly due to agricultural diversions.

2.3. Water use

There are five major population centers within the drainage basin: Santa Fe, New Mexico (450 km from the headwaters, population $70\,000$), Albuquerque, New Mexico (550 km , population $420\,000$), Las Cruces, New Mexico (950 km , population $75\,000$), and the twin cities of El Paso, Texas (1025 km , population $600\,000$) and Ciudad Juarez, Chihuahua, Mexico (1025 km , population $1\,300\,000$). Most municipal water supply is from wells, but Santa Fe and El Paso do use significant amounts of surface water as well. Use of surface water by municipalities totals about $1 \text{ m}^3/\text{s}$.

Total irrigated area in the basin is approximately $370\,000 \text{ ha}$, of which $260\,000 \text{ ha}$ are in Colorado, near the headwaters of the river. Withdrawals for irrigated agriculture amount to about $70 \text{ m}^3/\text{s}$, of which about half returns to the river. Losses due to open water evaporation (especially from Elephant Butte Reservoir) and riparian evapotranspiration are difficult to quantify, but, based on balancing the various river discharges and consumptive uses given above, are probably about $18 \text{ m}^3/\text{s}$.

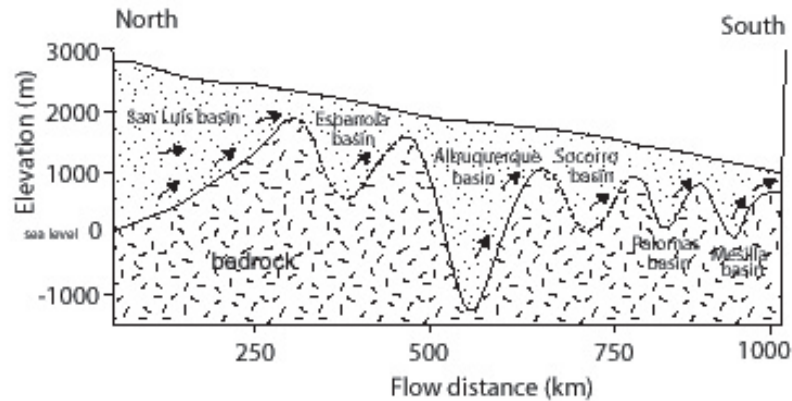


FIG. 2. Schematic hydrogeologic cross-section of the Rio Grande rift, parallel to the path of the river. Basin fill depth dotted where not well-constrained. Basin structure is based on data from [1, 3-5].

2.4. Water quality

The dissolved solids content of the Rio Grande increases markedly as it flows from its headwaters in Colorado to the southern limit of the study area (Fig. 3). The total dissolved solids content in the headwaters region averages about 40 mg/L. By the time the river reaches El Paso the average value is about 750 mg/L, and at Fort Quitman, south of El Paso, it commonly attains values in excess of 2000 mg/L. Not only the solute concentration, but also the solute burden increase downstream, from about 100 000 tons a/r at Lobatos to about 600 000 tons a/r south of San Marcial. The concentrations of dissolved solids vary seasonally, and during the winter, when base flow is not diluted by reservoir releases of irrigation water, can greatly exceed the average values given above. Water quality in the vicinity of El Paso approaches the limits advised for both irrigation and drinking water use. South of El Paso it is not usable for most purposes except irrigation of salt tolerant crops. Analysis of historical records shows that during periods of extended drought, such as the mid-to-late 1950s, salinity consistently exceeded present day averages. Population, and thus demand on the water resources, has greatly increased since the 1950s, and a repetition of such a long term drought could have disastrous consequences with regard to water quality.

The causes of this prominent increase in salinity with flow distance have never been fully explained. Lippincott [7] laid most of the blame on irrigated agriculture: "The increase in the salinity of the waters of the Rio Grande [is] due to their use and re-use [for irrigation] in its long drainage basin..." Evapotranspiration during irrigation and by riparian vegetation clearly plays a role, but cannot explain the observed increase in solute burden. The work of the Natural Resources Committee [8] and Trock et al. [9] attributed it principally to displacement of natural, shallow, brackish groundwater by infiltrating irrigation water. However, they did not explain the source of the brackish water. Hayward [10] and Wilcox [11] laid more emphasis on increases in the proportion of more soluble salts during evaporation in irrigated soils.

3. SAMPLING PLAN

Studies employing environmental tracers to investigate sources of salinity have been pursued as part of the Rio Grande Basin project carried out through the Center for Sustainability of semiArid Hydrology and Riparian Areas (SAHRA), funded by the US National Science

Foundation. High spatial resolution sampling campaigns (~10 km sampling intervals) were conducted twice per year between the winter of 1999–2000 and the winter of 2001–2002. Sampling was conducted during late summer when irrigation water is released from the reservoirs, and during mid-winter when there are no irrigation releases and flow is minimal. Subsequent to the 2001–2002 winter sampling, similar sampling has been performed, but at a lower spatial resolution. The main tracers employed to date have been $\delta^2\text{H}$ and $\delta^{18}\text{O}$ in the water molecule, Cl^-/Br^- , $^{36}\text{Cl}/\text{Cl}$, $^{87}\text{Sr}/^{86}\text{Sr}$, $\text{Sr}^{2+}/\text{Ca}^{2+}$, and $\delta^{234}\text{U}$. Most of the results given below have been presented and discussed by [12–15].

4. RIVER DISCHARGE AND THE RESPONSE TO DROUGHT

Most main stem and tributary gauging stations are operated by the US Geological Survey (USGS) with several additional gauging stations in Colorado operated by the Colorado Division of Water Resources (DWR). We used daily discharge values reported in the National Water Information System (NWIS) and Colorado DWR online databases [16, 17]. The Middle Rio Grande Conservancy District (MRGCD) provided us with discharge data for the New Mexico agricultural drains. To evaluate differences between winter and summer discharge, we averaged the mean daily discharge values for the two weeks prior to each sampling event in January and August for each gauging station.

The winter and summer discharge patterns for the upper and middle portions of the study area vary in a predictable manner as a result of natural hydrology and river management. In contrast the lower region is entirely controlled by releases from Elephant Butte Reservoir. In the winter, average discharge values in the upper portion do not change significantly (Fig. 4). Whereas in summer, average discharge decreases from Del Norte (104.1 km) to Alamosa (192.8 km) and then remains constant through the end of the reach. Agricultural diversions from the Rio Grande between Del Norte and Alamosa were highly variable among sampling events but averaged approximately 6.2 ± 7.3 cm. Generally, average discharge values are higher in the winter than in summer from Alamosa (192.8 km) to the end of the reach. These differences between winter and summer discharge patterns are largely explained by seasonal river management for agriculture. During the summer, diversions of river water for irrigated agriculture in the San Luis Valley sharply decrease discharge between Del Norte (104.1 km) and Monte Vista

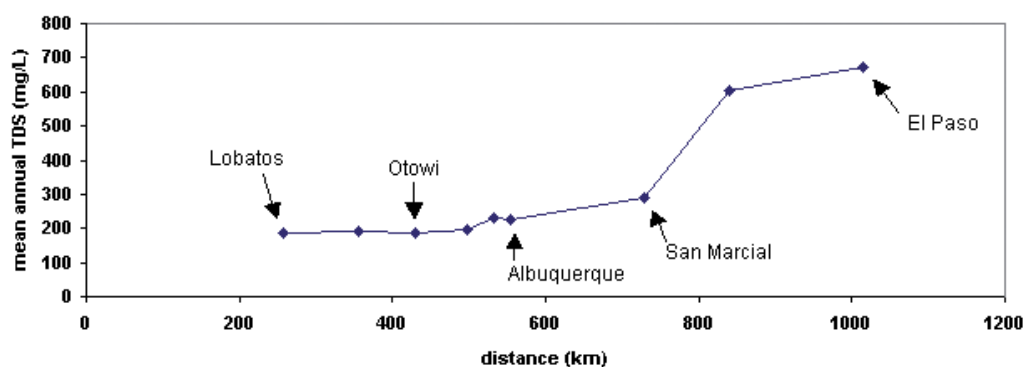


FIG. 3. Variation of mean annual total dissolved solids (TDS) content of the Rio Grande with flow distance (data from U.S. Geological Survey gauging station records). Distances, for this graph and all others, are measured relative to the outlet of Rio Grande Reservoir in Colorado.

(141.2 km) whereas during the winter, the average discharge is fairly constant because there are no agricultural diversions. The mean annual diversions between Del Norte and Alamosa represent approximately $36 \pm 29\%$ of the average flow at Del Norte. Lower average discharge during the summer than in the winter downstream of Alamosa (192.8 km) is likely due to larger amounts of evaporation and transpiration.

Downstream of the Colorado–New Mexico state line the Rio Grande enters a relatively ‘wild’ reach where the overall patterns of discharge are similar in winter and summer. Discharge increases from the beginning of the reach (near Lobatos 256.9 km) to Otowi (430.9 km) from tributary and groundwater inputs in both summer and winter. The average increase in discharge between Lobatos (256.9 km) and Taos (359.6 km) is 5.9 cms in winter and 6.1 cms in summer, which is approximately equal to the sum of average groundwater (4.5 cm) and tributary (1.6 cm) inputs. The Rio Chama substantially augments river flow in summer (+15.4 cm \pm 6.1) and to a lesser extent in winter (+2.9 cm \pm 1.5) between the Embudo (384.5 km) and Otowi (430.9 km) gauging stations. Upstream of the Rio Chama confluence (409.2 km), individual average discharge values are higher in winter than in summer between Lobatos (256.9 km) and Embudo (384.5 km). In contrast, average discharge values are higher in the summer downstream of the Rio Chama confluence.

In the middle section of the study area, there is no significant change in average winter discharge values from Otowi (430.9 km) downstream to San Felipe (496.9 km) as there are no agricultural diversions. On the other hand, during the summer the average discharge decreases significantly from Otowi (430.9 km) to the outfall at Cochiti Dam (471.0 km) and then remains constant to San Felipe (496.9 km). Downstream of Cochiti Dam the Rio Grande enters the Albuquerque basin, a significant urban and agricultural area where there are large differences in summer and winter discharge patterns. In the summer, discharge values decrease sharply downstream of

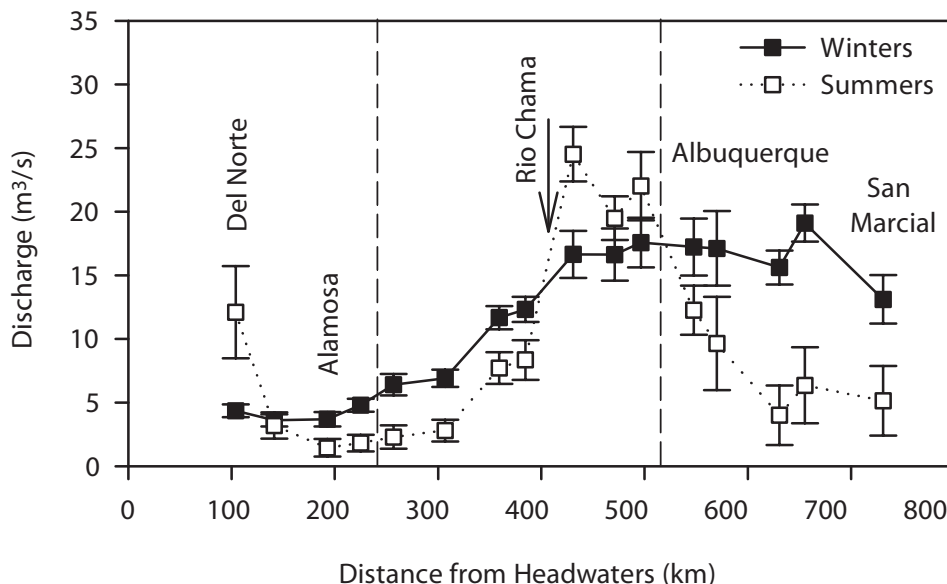


FIG. 4. Mean daily discharge for the two week period preceding sampling in the Upper Rio Grande from Del Norte, CO to San Marcial, NM (upper and middle sections); below this location discharge is controlled primarily by Elephant Butte reservoir releases. Agricultural diversions downstream of Del Norte, CO and Albuquerque, NM decrease summer discharge, whereas the Rio Chama contributes significant amounts of water, especially in summer.

Albuquerque (547.5 km) due to the diversion of water for irrigated agriculture, which removed an average of $11.1 \text{ cm} \pm 2.1$ during summer sampling events (Fig. 5). In contrast, discharge remains nearly constant in winter throughout the reach. Overall, the average winter discharge from Albuquerque (547.5 km) to San Marcial (731.1 km) is significantly higher ($p = 0.002$) than the average summer discharge.

Differences between summer and winter discharge in the middle portion of our study area can be explained by seasonal differences in river management for agriculture, evaporation and transpiration. Diversion of river water for irrigated agriculture at Isleta (570 km) sharply decreases discharge, especially during dry years (Fig. 5). Relatively constant discharge for the middle portion during winters is probably due to the absence of agricultural diversions and decreased evaporation and transpiration. Lower discharge during the summer downstream of Isleta (570.0 km) is likely due to larger amounts of evaporation and transpiration. There is a large riparian corridor between Cochiti Dam (471.0 km) and San Marcial (731.1 km) that has been shown to use substantial amounts of river water during the summer [18]. Despite the seasonal differences in discharge between January and August, larger differences in discharge were avoided by not sampling during snowmelt periods in April and May or during lowest-flow periods in September and October.

The sampling period August 2001–August 2006 represented a relatively dry period within the Rio Grande (Fig. 6). When the two week average discharge for each sampling event was compared to the 30 year average discharge for January and August, almost all the sampling events had lower than average discharge (Fig. 7). Only the winter 2006 sampling event showed average discharge from Lobatos (256.9 km) to San Acacia (655.3 km). Discharge during the summers of 2001 and 2005 was only slightly below average from Lobatos (256.9 km) to Otowi (430.9 km). During remaining sampling events, discharge was 15–95% below the 30 year averages in both January and August. Interannual variations in river discharge are largest downstream of the Rio Chama confluence and likely reflect large scale variations in climate and small scale differences in precipitation and temperature.

4.1. ENVIRONMENTAL TRACERS OF WATER SOURCE AND EVAPORATION

4.1.1. General patterns of isotopic composition with distance

Stable isotopes of oxygen ($^{18}\text{O}/^{16}\text{O}$) and hydrogen ($^2\text{H}/^1\text{H}$) in the water molecule are a commonly employed tool for understanding the origins and circulation of natural waters [19, 20]. The stable isotope content of precipitation at middle and northern latitudes is most strongly controlled by temperature at the time of a precipitation event, with isotopically lighter precipitation being associated with colder temperatures [21]. The only detailed study of precipitation isotopes in the basin is from the mountains surrounding Los Alamos NM [22]. Like much of the southwest USA, the Rio Grande has two periods of isotopically distinct precipitation (Fig. 8), winter precipitation which falls as snow in the higher elevations and a summer ‘monsoon’ period. Inasmuch as most of the runoff for the Rio Grande originates as snow at high elevation, it can be expected to be isotopically light.

One of the most important controls on the stable isotope composition of surface water is evaporation. The heavier isotopic species (H_2^{18}O and ^2HHO) are less volatile than their lighter (and more common) counterparts and thus tend to be retained during evaporation. This causes progressive isotopic enrichment during the process of evaporation. In contrast, transpiration

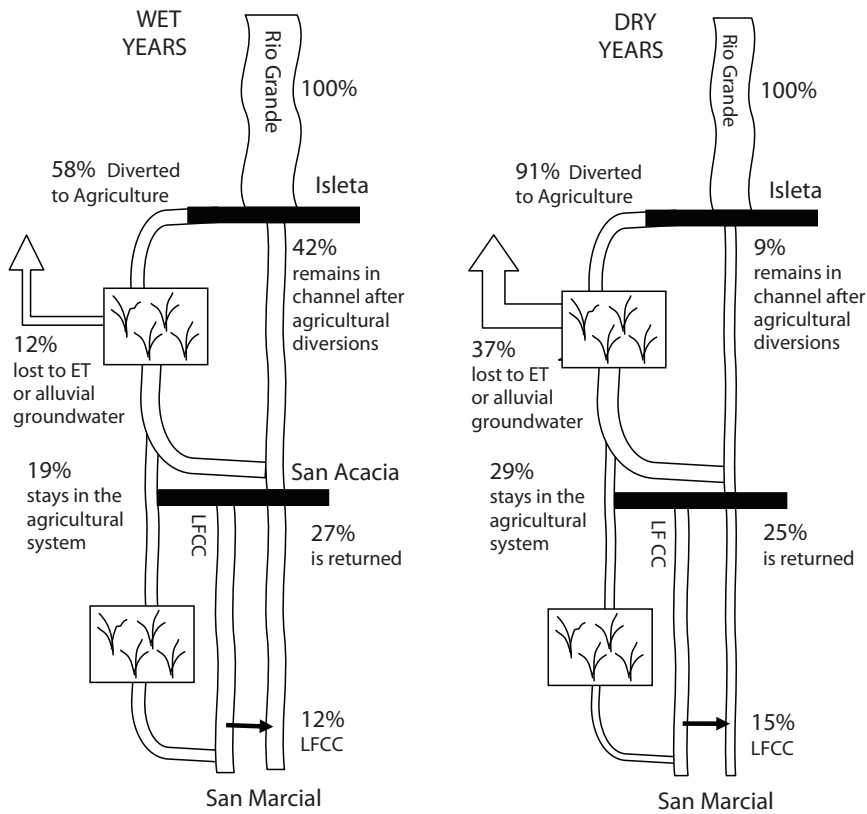


FIG. 5. Schematic diagram of the surface water system illustrating average agricultural diversions and returns for both wet and dry years. Schematic is between Isleta (570.0 km), San Acacia (655.3 km), and San Marcial (731.1 km). LFCC is the Rio Grande Conveyance Channel.

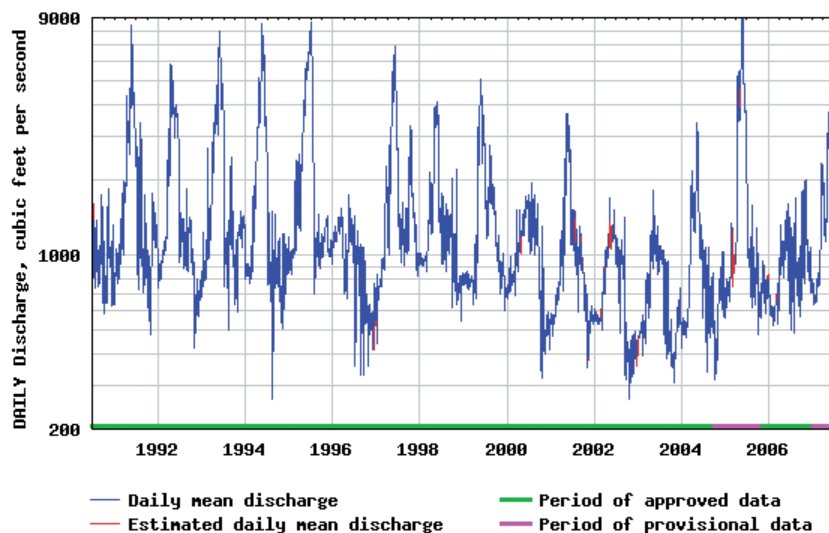


FIG. 6. Discharge of the Rio Grande at Otowi Bridge, 1990–2007, showing worsening drought between 1995 and 2004 and improving, but still below normal conditions, between 2004 and 2007. The dark line indicated long term average discharge for the gauge over the recording period. The Otowi gauge, located at 430 km, marks the boundary between designated upper and lower sections of the Rio Grande and represents the location of maximum river discharge. Graph generated from the USGS NWIS website [17].

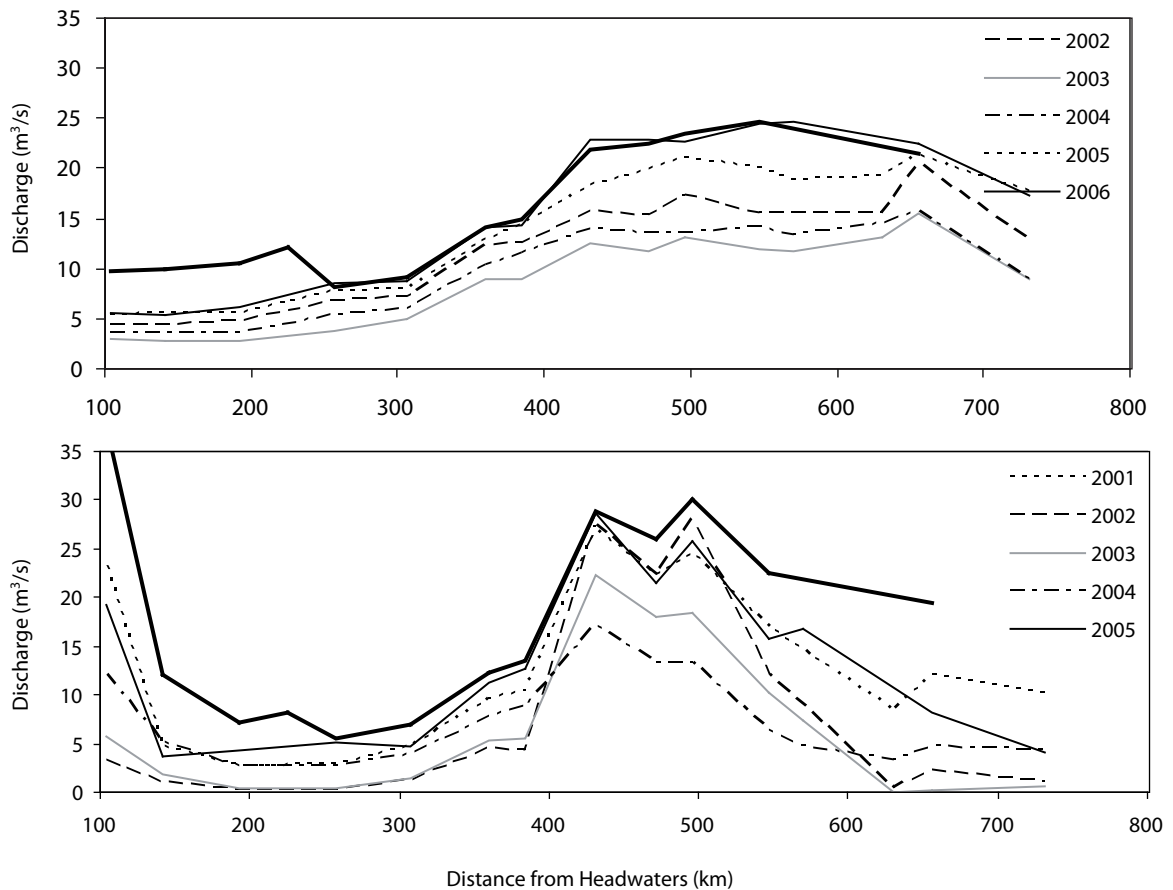


FIG. 7. Two week average discharge values for each gauging station above Elephant Butte reservoir (below this reservoir release control discharge rates) for each sampling event in January (A) and August (B). The bold line indicates the 30 year average discharge for January and August. Note that almost all sampling occurred when discharge was below average.

does not affect the isotopic composition of the residual water because plants transmit water from the soil to the atmosphere without isotopic separation. Measurement of the stable isotope composition of salinized water is a useful method for discriminating the cause of salinity because water that is saline due to evaporation will be isotopically more enriched than source water, whereas water that is saline due to salt addition or transpiration will not change in isotopic composition.

When $\delta^{18}\text{O}$ and $\delta^2\text{H}$ values for the Rio Grande are plotted against each other (Fig. 9), the two isotopes form a linear array with a slope of ~ 5 , which is considered diagnostic of evaporation. As expected, the initial $\delta^{18}\text{O}$ and $\delta^2\text{H}$ are relatively light (-14 and -100 ‰, respectively) and are consistent with winter precipitation for the headwater region [22]. The plot of $\delta^2\text{H}$ against flow distance in Fig. 10 shows obvious trends that correspond to features of the river system. The data for summer 2001 are probably fairly representative of the stable isotope composition of the river during normal summers. The peak in $\delta^2\text{H}$ at about 250 km is largely explained by the inflow of evaporated drainage water from the Closed Basin Project in the San Luis Valley. This isotopically heavy inflow is diluted downstream by isotopically light tributaries. Increasing values between 500 and 800 km are likely due to evaporation from wetted sand bars. The major step in $\delta^2\text{H}$ at 800 km takes place at Elephant Butte Reservoir, which is known to

be the single largest evaporative sink in the entire river system. Downstream of Elephant Butte Reservoir, isotopic composition is surprisingly stable, given the large amount of diversion for irrigation and inflow of return waters in the Mesilla Valley. This may indicate that most water loss in this stretch takes place through transpiration.

A simple Rayleigh distillation model [24] can be used to estimate the degree of evaporation necessary to produce the observed enrichment. Based on the summer 2001 data, and assuming an effective isotopic enrichment factor for ^2H of -89‰ during evaporation, the Rayleigh model indicates that about 35% of the river flow has been evaporated by the time the river reaches El Paso. This differs from the water balance based on gauging that was described above, which indicates that about 75% of the water is lost to evapotranspiration above El Paso. The stable isotope data thus indicate that about half of the river losses are due to evaporation and the other half due to transpiration from irrigated fields and riparian areas.

4.1.2. *Climate related changes in isotopic composition*

The isotopic composition of the Rio Grande responds to both seasonal and interannual climate variability. While we collected data biannually, a study by [23] provides some insight into the seasonal variability of river isotopic composition (Fig. 11). Of note is a clear seasonal increase during the summer months due to increased evaporation and the pronounced decrease during the large spring snowmelt event in 1982.

Of more interest is interannual variability during the course of the recent drought. During the summer, $\delta^{18}\text{O}$ river values show a dramatic increase at the southern end of the San Luis

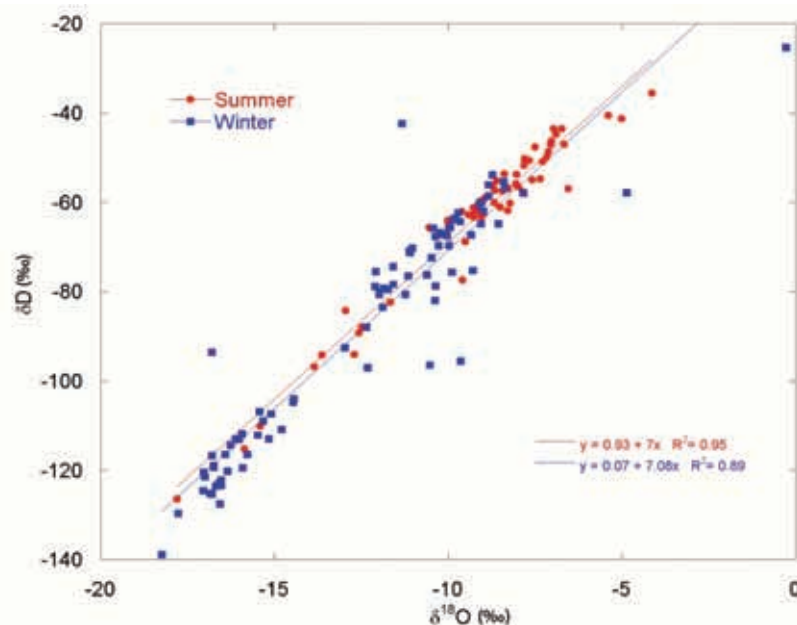


FIG. 8. *Precipitation isotope data for Los Alamos, NM [22]. Samples are separated into winter and summer; the two distinct precipitation periods in the region. This location is representative of precipitation in the mountainous headwater region, the primary source of Rio Grande surface waters. For comparison, the average annual value for Albuquerque precipitation [23], located at a lower elevation on the basin floor, is noted.*

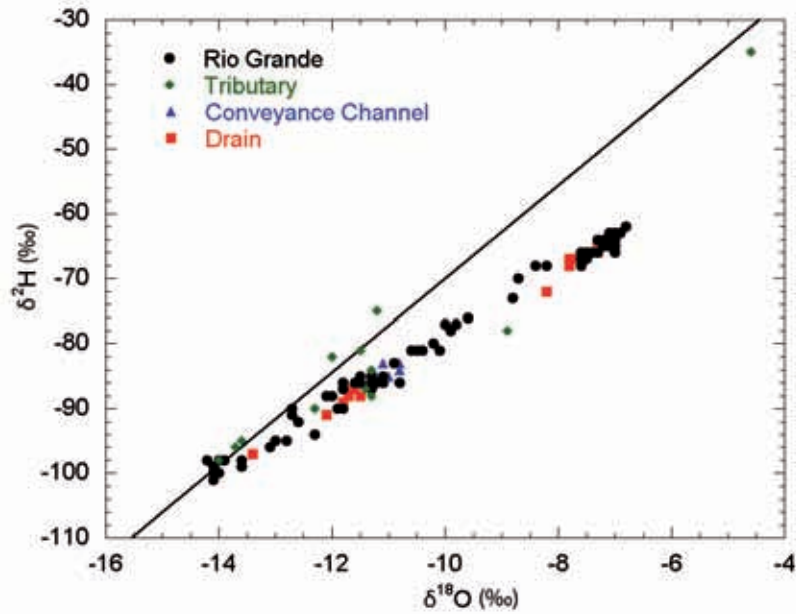


FIG. 9. The $\delta^{18}\text{O}$ versus $\delta^2\text{H}$ for detailed sampling that occurred during the summer of 2001. Samples for the main stem of the Rio Grande plot along a clear evaporation line below the slope of the Los Alamos MWL [22]. Drains and canals associated with the agricultural system plot along a similar trend; in contrast, tributaries plot along the LMWL, with lower elevation tributaries plotting with less negative isotopic values.

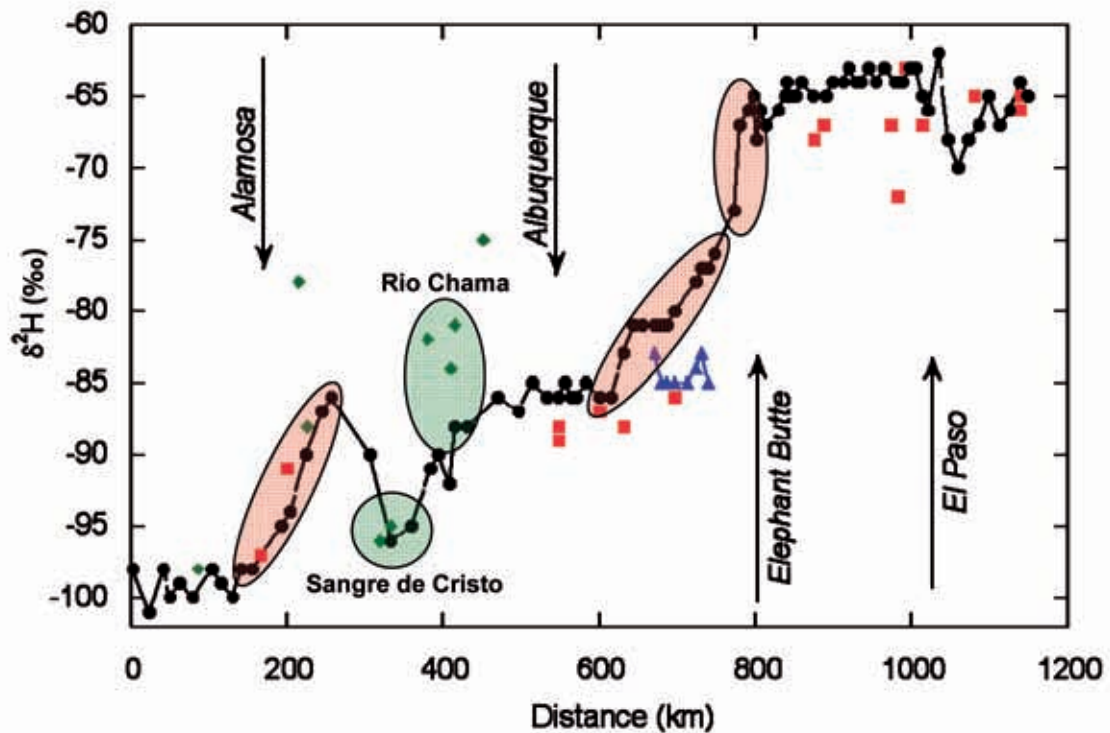


FIG. 10. The $\delta^2\text{H}$ versus distance downstream for detailed sampling that occurred during the summer of 2001. Areas highlighted in red are areas of evaporation whereas areas in green represent tributary inputs. Note that downstream of Elephant Butte Reservoir there is little change (other than a small decrease due to El Paso wastewater returns) in isotopic composition, despite significant transpiration losses associated with irrigated agriculture.

Basin during the drought years 2002–2003 (Fig. 12). This is probably because an increasing proportion of the river is being diverted for irrigation, while the amount of evaporated closed basin water being returned to the river has remained relatively constant. There is also an increase in $\delta^{18}\text{O}$ between northern New Mexico and Elephant Butte Reservoir (Fig. 12), which can probably be attributed to increased evaporation from wetted sands along the Rio Grande. Finally, there is an increase in Elephant Butte and the water discharged from it due to the increasingly unfavorable water balance of the reservoir, which declined to historically low levels during the period 2002–2003. By the end of this period, the reservoir was nearly empty and thus during the relatively large snowmelt year 2005 (Fig. 6) the reservoir filled with relatively ‘unevaporated’ water, resulting in significantly lower $\delta^{18}\text{O}$ values downstream.

The results of our winter sampling, in contrast to summer sampling periods, shows limited variability (Fig. 13). The drought years 2003–2005 do exhibit slightly elevated isotopic values where as the ‘average years’ 2001 and 2006 show lower values. These changes likely reflect a combination of changes in basin water balance with average years having more ‘light’ snowmelt, while dry years bring a higher proportion of ‘heavier’ Rio Chama water; there was also greater relative evaporation during the previous summer.

Finally, it is worth contrasting ‘average’ years 2001 and 2005, ‘dry’ years 2002–2004, and the summer of 2006 when there was a highly anomalous amount of summer ‘monsoon precipitation.’ When $\delta^{18}\text{O}$ versus $\delta^2\text{H}$ for Rio Grande surface water for the middle portion are plotted (Fig. 14) the ‘average’ years 2001 and 2005 plot along the Rio Grande evaporation close to the LMWL, whereas the ‘dry’ years 2002–2004 generally plot further along this trend, indicating greater relative evaporation of these waters. In contrast, the summer of 2006 brought heavy monsoon (summer) precipitation and runoff and thus river samples reflects this input with little evaporation and much heavier values than typical snowmelt waters of the Rio Grande.

4.2. ENVIRONMENTAL TRACERS OF SALINIZATION

To distinguish between saline groundwater discharge and sources associated with irrigated agriculture, we have employed $^{87}\text{Sr}/^{86}\text{Sr}$ and $^{36}\text{Cl}/\text{Cl} \cdot 10^{15}$ ratios and $\delta^{234}\text{U}$ isotopic values, along with the associated solute ratios Cl/Br and Ca/Sr , as environmental tracers. We selected these tracers for three reasons. First, these isotopic and solute ratios are minimally affected by evapotranspiration, and thus are tracers of solute inputs only. Second, in all three systems end member sources are expected to have distinct compositions (Table 1). Finally, the high concentration of potential end members results in mixing relationships with large changes in isotopic values or solute ratios with the addition of small solute fluxes.

4.2.1. Chlorine Isotope

Chloride concentration shows a progressive increase downstream in a distinct series of steps (Fig. 15) The generally conservative nature of chloride and bromide, combined with the distinct Cl/Br ratios (mass/mass) for atmospheric deposition (~ 100) and sedimentary brine (≥ 1000) [25–27], make it an extremely useful tracer. In general, Cl/Br ratios increase from ~ 100 to >1000 , mirroring increasing chloride concentration (Fig. 16) in a stepwise fashion (Fig. 17). Comparing Cl concentration increases to Cl/Br ratios (Fig. 16), it is apparent that the increase in Cl concentration is due to a combination of evapotranspirative concentration and additional solute inputs.

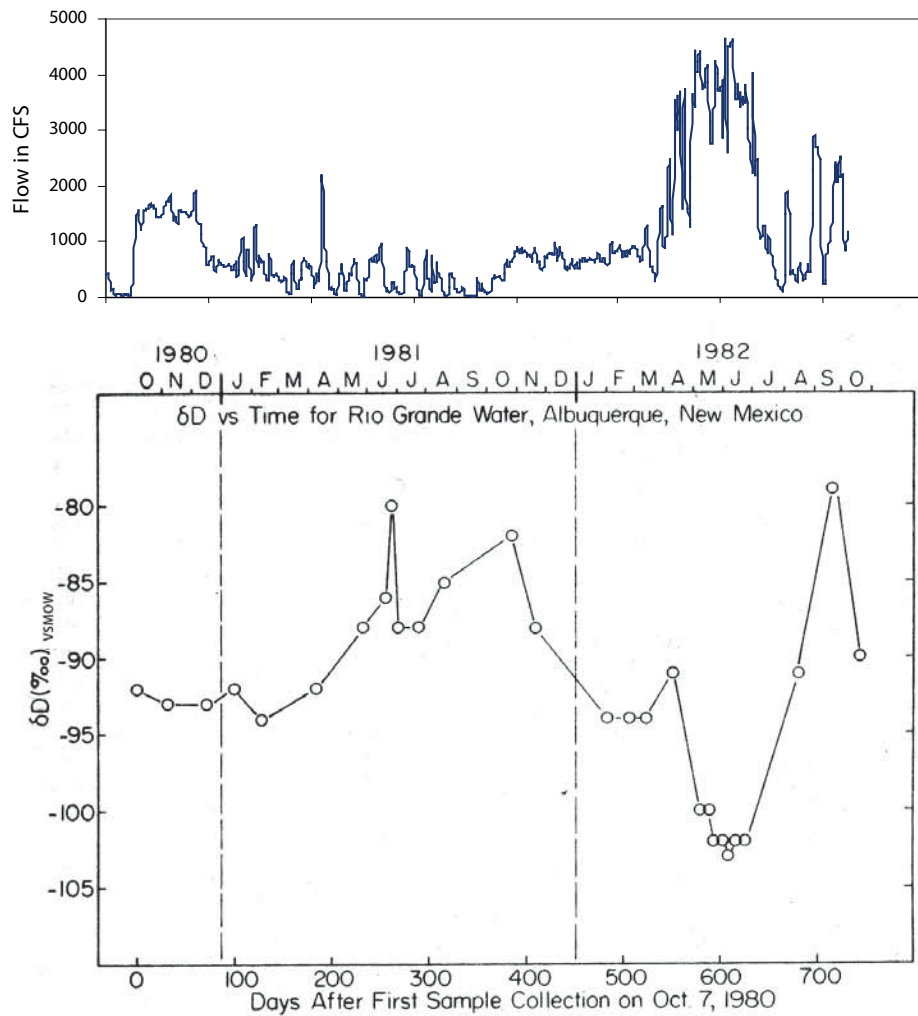


FIG. 11. Seasonal variation in Rio Grande surface water isotopic composition at Albuquerque NM [23]. Note the seasonal increase during the summer months due to increased evaporation and the pronounced decrease during the large spring snowmelt event in 1982.

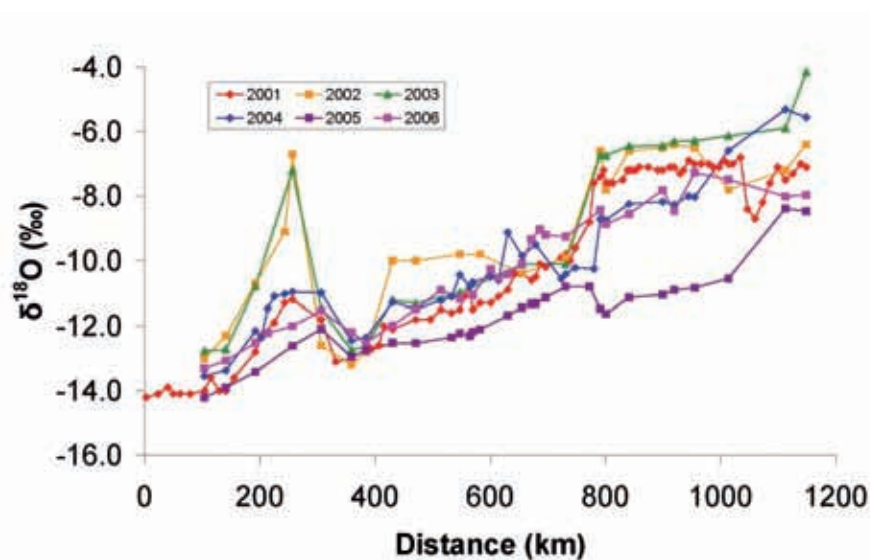


FIG. 12. The variation of $\delta^{18}\text{O}$ with distance down the Rio Grande during the summers (August) of 2001–2006.

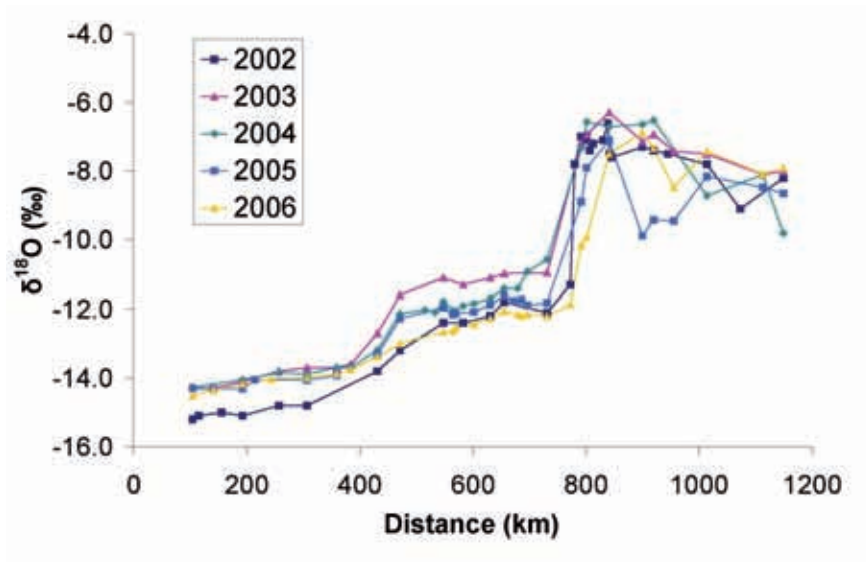


Fig. 13. Variation of $\delta^{18}\text{O}$ with distance down the Rio Grande during the winters (January) of 2002–2006.

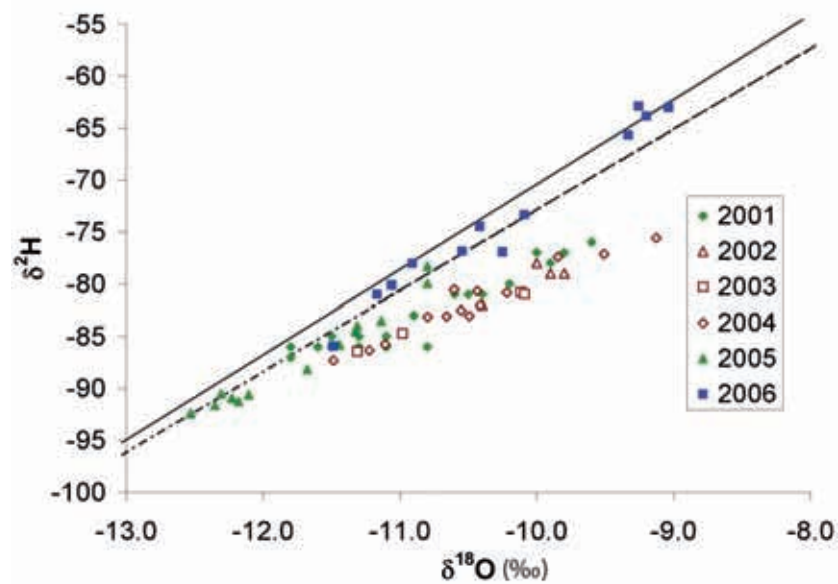


FIG. 14. The $\delta^{18}\text{O}$ versus $\delta^2\text{H}$ for Rio Grande surface water samples collected in the middle portion of the study area. ‘Average’ years (2001 and 2005) are represented by solid markers, ‘dry’ years (2002–2004) by open markers. Note that during the ‘average’ years 2001 and 2005, values plot along the Rio Grande evaporation trend are closer to the LMWL, whereas ‘dry’ years 2002–2004 generally plot further along this trend, indicating greater relative evaporation of these waters. In contrast, the summer of 2006 brought heavy monsoon (summer) precipitation and local runoff, thus river water reflects this input with little evaporation and much heavier values than typical snowmelt waters of the Rio Grande.

Chlorine-36 ratios, measured along the length of the study area, exhibit a decreasing trend from ~2500 in the headwaters to ~100 at the southern end (Fig. 17). Headwater values are consistent with an atmospheric source, but it is important to note that a ^{36}Cl ratio of ~2500 is significantly higher than that in present day precipitation [28], which indicates a component of ^{36}Cl from nuclear weapons testing fallout in these waters. In contrast, the very low ^{36}Cl and high Cl/Br ratios in the lower portion are indicative of a sedimentary brine source. When ^{36}Cl

TABLE 1. ISOTOPIC AND SOLUTE RATIOS FOR POTENTIAL SOLUTE SOURCES AND SELECTED END-MEMBER COMPOSITIONS

End-member	Cl (mg/l)	Cl/Br (wt/wt)	$^{36}\text{Cl}/\text{Cl} \times 10^{15}$	Ca (mg/l)	Ca/Sr (wt/wt)	$^{87}\text{Sr}/^{86}\text{Sr}$	U ($\mu\text{g/l}$)	$\delta^{234}\text{U}$ (‰)
Atmospheric deposition	0.2 to 2*	40 to 200*	700 [†]		430 to 603 [§]	0.709 to 0.713 [§]		
Basalt weathering					100 to 240 [#]	0.704 to 0.705 [#]		
Rio Grande headwaters**	10	100	2500	15	75	0.7096	2	800
Magmatic geothermal sources		250 to 350 ^{††}	1 to 6 ^{††}					
Sedimentary brines		1000 to 10000*	5 to 35 ^{§§}		10 to 50 ^{##}	0.708 to 0.716 ^{***}		
Rio Grande saline groundwaters		400 to 1300 ^{†††}	35 ^{§§§}		20 to 44 ^{†††}	0.7093 to 0.7118 ^{###}		500 ^{§§§}
Saline groundwater end-member****	1000	1300	35	350	33	0.71015	5	500

Note: Concentrations are reported only for end-members used in the mixing calculations. Basalt weathering is not considered to be a major source of chloride, thus associated values are not included. Likewise we report no values for Sr in geothermal waters as values reflect the local rock type (Goff and Gardener, 1994) not a magmatic source. For the emerging U-isotope system, limited data on potential solute sources explains the lack of reported values.

* Precipitation values from Davis et al. (1998) for Nevada and Arizona; [†] Values from Phillips (2000); [§] Values from Graustein and Armstrong (1983); [#] Values from Dugan et al. (1986); ** End-member values based on measured samples from the headwater of the Rio Grande; ^{††} Values from Fehn et al. (1992); ^{§§} Value based on secular equilibrium (Phillips, 2000); ^{##} Values from Banner (1995) and Musgrove and Banner (1993); ^{***} Values from Musgrove and Banner (1993) and McNutt (2000); note individual basins have significantly narrower ranges; ^{†††} Data compiled from Brandvold (2001) and Plummer et al. (2004) using only samples over 500 ppm Cl; ^{§§§} This study, n=1; ^{###} Saline groundwater samples collected by Plummer et al. (2004), measured for this study, n=5; ^{****} For saline groundwater end-member we used the upper end of concentration values compiled from Brandvold (2001) and Plummer et al. (2004) which represent shallow saline groundwaters; saline waters at depth are likely more concentrated. The isotope and solute ratios were selected to be within the observed values for saline groundwaters in the Rio Grande as well as to best fit the observed mixing trend.

ratios are plotted against Cl/Br ratios (Fig. 20A), a clear two-end-member mixing relationship is observed, with all river samples plotting close to the mixing curve. This mixing curve is calculated using Rio Grande headwater values and an estimated higher salinity end member based on groundwaters that are likely a mix of dilute shallow groundwater with a deeper sedimentary brine source (Table 1).

Saline groundwater contributions, while based on the chosen end member, are small, less than 1% of river flow, in the upper part of the study area. In the middle portion of the study area, the saline groundwater contribution increases from 1 to ~5% as the river passes through three large and deep sedimentary basins. Finally, in the lower portion a small increase occurs at the southern end of the Mesilla Basin. South of this, there is a dramatic increase in the percentage of saline groundwater reflecting both saline groundwater discharge from the Hueco Bolson and the diversion of almost all remaining water for irrigated agriculture. Overall, saline groundwater

fluxes appear to be greatest from large and deep alluvial basins (Albuquerque and Tularosa-Hueco [1]) or smaller basins with significant geothermal activity (Socorro, Engle, Mesilla [29]). Note that ^{36}Cl and Cl/Br ratios indicate that this geothermal activity is not the source of the salinity (Table 1) but rather it appears to mobilize the sedimentary brine. Closed — i.e., internally drained — basins (San Luis; Wilkins [1]) and small and/or shallow basins (Española and Palomas [1]) appear to make smaller contributions.

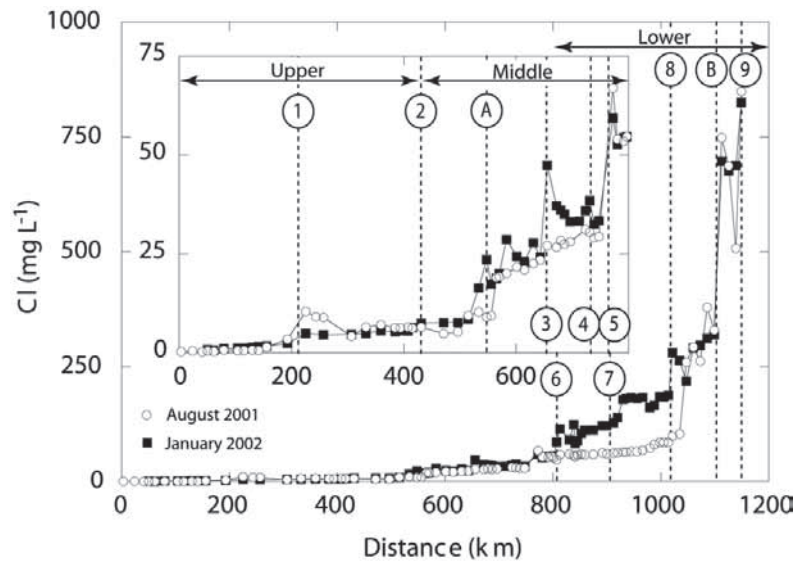


FIG. 15. Chloride concentration versus river distance from the headwaters. Numbers correspond to locations where the Rio Grande exits the southern end of the alluvial basins shown in Fig. 1. Locations marked with letters refer to additional salinity increases not associated with alluvial basin termini. Location (A) is the Albuquerque Wastewater Treatment Plant and location (B) is within the Tularosa-Hueco Basin, see text for discussion.

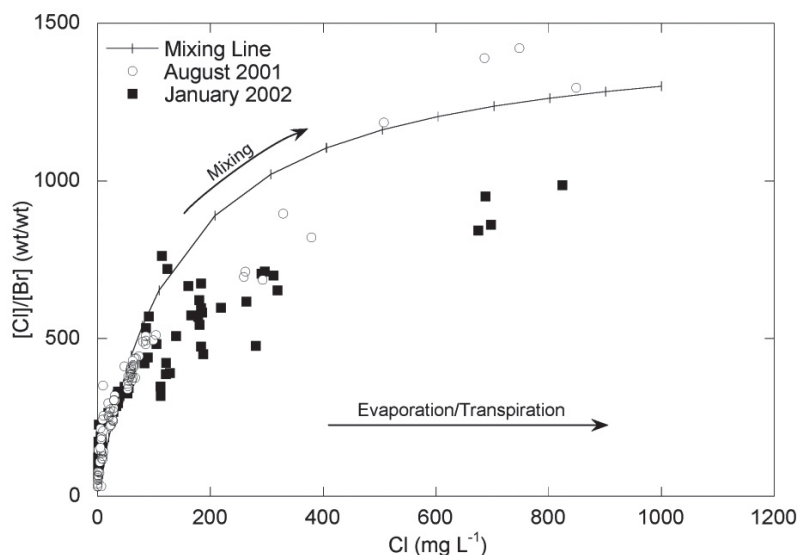


FIG. 16. Mixing plot using Cl/Br ratios vs Cl illustrating the combined effect of evapotranspirative concentration and solute addition, in this case modelled with a high salinity groundwater in explaining downstream salinization. If evapotranspirative concentration were the only factor, the Cl/Br ratio would not change as Cl concentration increased. If mixing was the only important factor, increases would follow the calculated mixing curve (see Table 1 for end members). Data for the Rio Grande are clearly intermediate between these two cases, illustrating their combined effect.

4.2.2. Strontium isotopes

In contrast to Cl/Br ratios, Ca/Sr ratios exhibited a significant change only in the middle portion (Fig. 18), hence $^{87}\text{Sr}/^{86}\text{Sr}$ ratios were measured only for this stretch of the river (400–800 km). In the headwater regions, Sr is likely derived from two sources: atmospheric deposition and mineral weathering (basalt is the dominant lithology through which the Rio Grande flows upstream), both of which are distinct from sedimentary brines (Table 1). As the Rio Grande enters the middle portion, $^{87}\text{Sr}/^{86}\text{Sr}$ ratios are ~ 0.709 and Ca/Sr ratios are ~ 75 , consistent with the mixing of headwater sources with a small contribution of saline groundwater. In the middle section of the river, $^{87}\text{Sr}/^{86}\text{Sr}$ ratios increase while Ca/Sr ratios decrease (Fig. 18). As with the chlorine isotope system, river samples indicate a clear two-end-member mixing relationship (Fig. 20B) between river water entering the middle portion of the study area and sedimentary brine. Mixing calculations indicate that a saline groundwater contribution of between 1% and

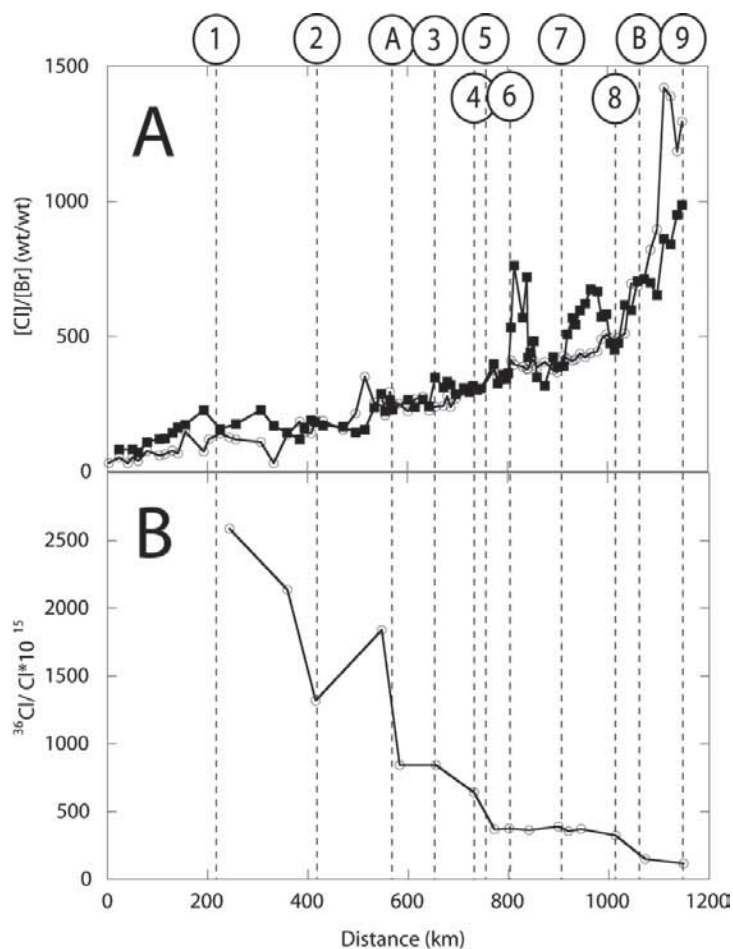


FIG. 17. Chlorine isotope system: (A) Cl/Br ratios and (B) ^{36}Cl versus distance down river. Open circles (\circ) are samples collected in August 2001, whereas solid squares (\blacksquare) were collected in January 2002. Numbers correspond to locations where the Rio Grande exits the southern end of the alluvial basins shown in Fig. 1. Locations marked with letters refer to additional salinity increases not associated with alluvial basin termini. (A) is the Albuquerque Wastewater Treatment Plant and (B) is a location within the Tularosa-Hueco Basin; see text for discussion. In the winter, marked variability is observed in the Cl/Br ratio of the lower Rio Grande as a result of very low flows due to highly restricted reservoir releases. The first increase occurs south of Elephant Butte Reservoir; ratios then decrease at Caballo Reservoir. South of Caballo, Cl/Br ratios increase until a second sharp decrease is observed at the point where El Paso wastewater enters the river.

10% of river flow can explain observed salinity increases in the middle portion of the study area.

4.2.3. Uranium isotopes

Finally, we employed the uranium isotope system. The reactive nature of uranium, as illustrated by both increasing and decreasing concentrations with distance downstream (Fig. 19), limits use of this isotopic system to qualitative interpretation. The $^{234}\text{U}/^{238}\text{U}$ ratio of waters, expressed as the $\delta^{234}\text{U}$ per mil deviation from the secular equilibrium ratio, reflects both the extent of water–rock interaction and residence time. Uranium-234 is preferentially leached from rocks because its crystal site is damaged when ^{238}U decays to ^{234}U , thus groundwater with short residence times and/or strong water–rock interaction typically has high $\delta^{234}\text{U}$ values [30]. If residence time is significant with respect to the half-life of ^{234}U , the $\delta^{234}\text{U}$ value is lowered through the radioactive decay of ^{234}U [30]. The headwaters have high $\delta^{234}\text{U}$ values and low U concentrations, indicative of recent water–rock interaction (Fig. 19) consistent with ^{36}Cl and $^{87}\text{Sr}/^{86}\text{Sr}$ data. In contrast, waters downstream have low $\delta^{234}\text{U}$ and higher U concentration

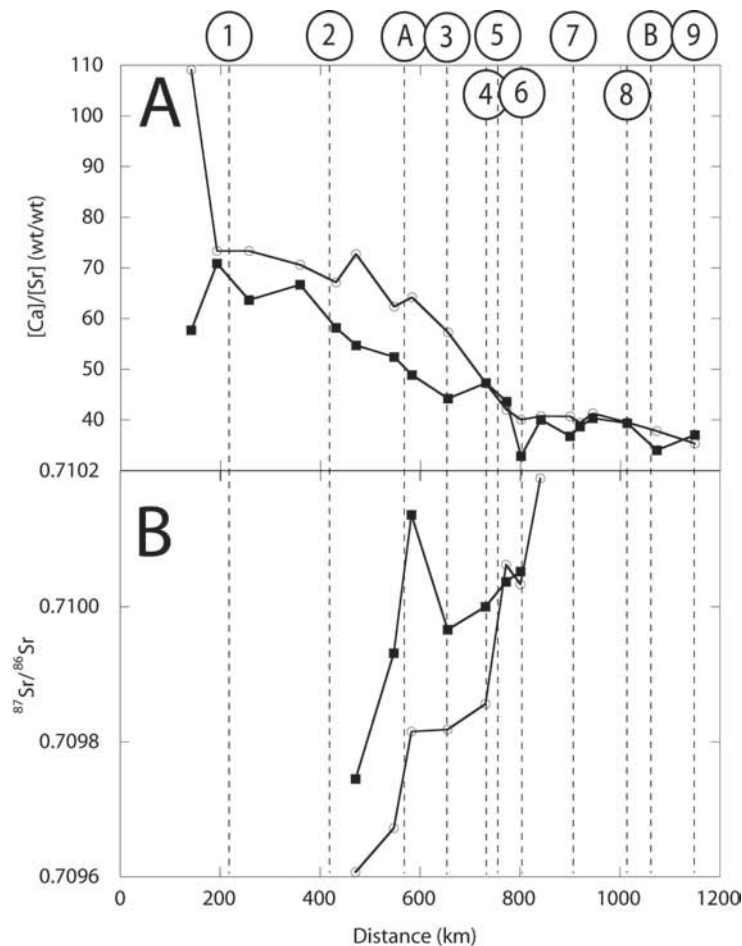


FIG. 18. Strontium isotope system: (A) Ca/Sr ratios and (B) $^{87}\text{Sr}/^{86}\text{Sr}$ ratios versus distance down river. Open circles (\circ) are samples collected in August 2001 whereas solid squares (\blacksquare) were collected in January 2002. Numbers correspond to locations where the Rio Grande exits the southern end of the alluvial basins shown in Fig. 1. Locations marked with letters refer to additional salinity increases not associated with alluvial basin termini. (A) is the Albuquerque Wastewater Treatment Plant and (B) is a location within the Tularosa–Hueco Basin; see text for discussion.

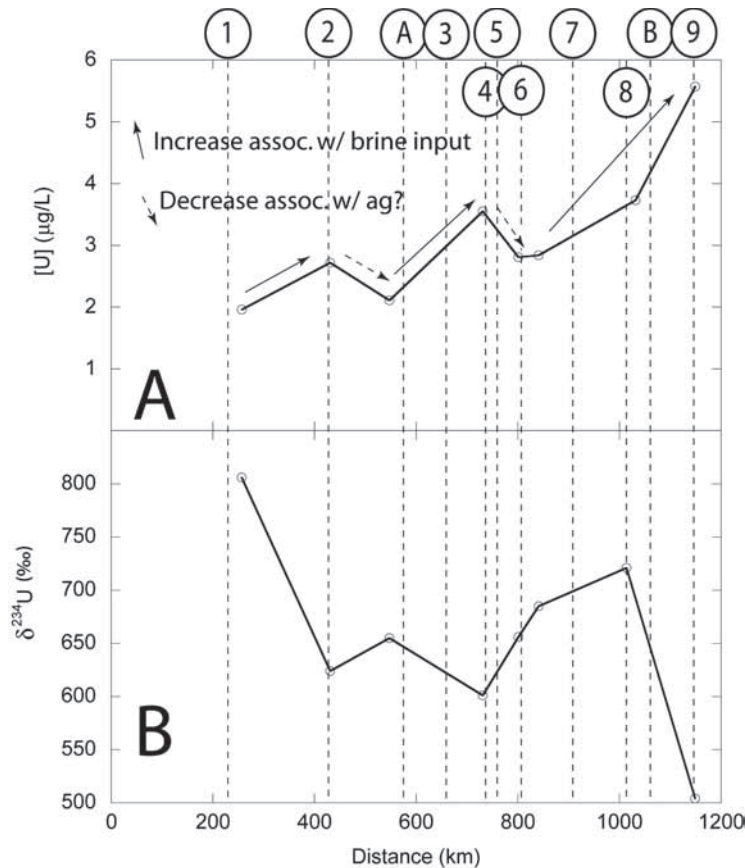


FIG. 19. Uranium isotope system: (A) U and (B) $\delta^{234}\text{U}$ values versus distance down river. Only samples collected during August 2001 (\circ) were analyzed. Numbers correspond to locations where the Rio Grande exits the southern end of the alluvial basins shown in Fig. 1. Locations marked with letters refer to additional salinity increases not associated with alluvial basin termini: (A) is the Albuquerque Wastewater Treatment Plant and (B) is a location within the Tularosa–Hueco Basin; see text for discussion. In the U-profile, note that there are two marked decreases in concentration that reflect the non-conservative behaviour of this solute, likely as a result of removal during application onto irrigated lands (first decrease) or by processes within Elephant Butte Reservoir (second decrease).

values. The data is best explained by two-component mixing (Fig. 20C) in which one end member consists of modern groundwater and surface water and the other is sedimentary brine. The low $\delta^{234}\text{U}$ value and high U concentration of the brine end member could have two possible explanations. The first is that U input is from whole mineral dissolution, in contrast to selective leaching of recoil damaged sites (which would enrich the water in ^{234}U). The second is that the brine water is old, on a time scale of millions of years, given the long half-life of ^{234}U of ca. 245ky [31], leading to a reduction in typically high groundwater ^{234}U excesses [30].

4.2.4. Implications of solute isotopes

The results of all three isotopic systems exhibit mixing relationships between only two end members: Rio Grande headwaters comprised of atmospheric deposition plus mineral weathering and higher salinity groundwater of sedimentary brine origin. This leads us to conclude that discharge of natural saline groundwaters when concentrated downstream by evapotranspiration, is the primary cause of salinity increases in the Rio Grande. Furthermore, the calculated percentages of saline groundwater needed to explain the observed salinity

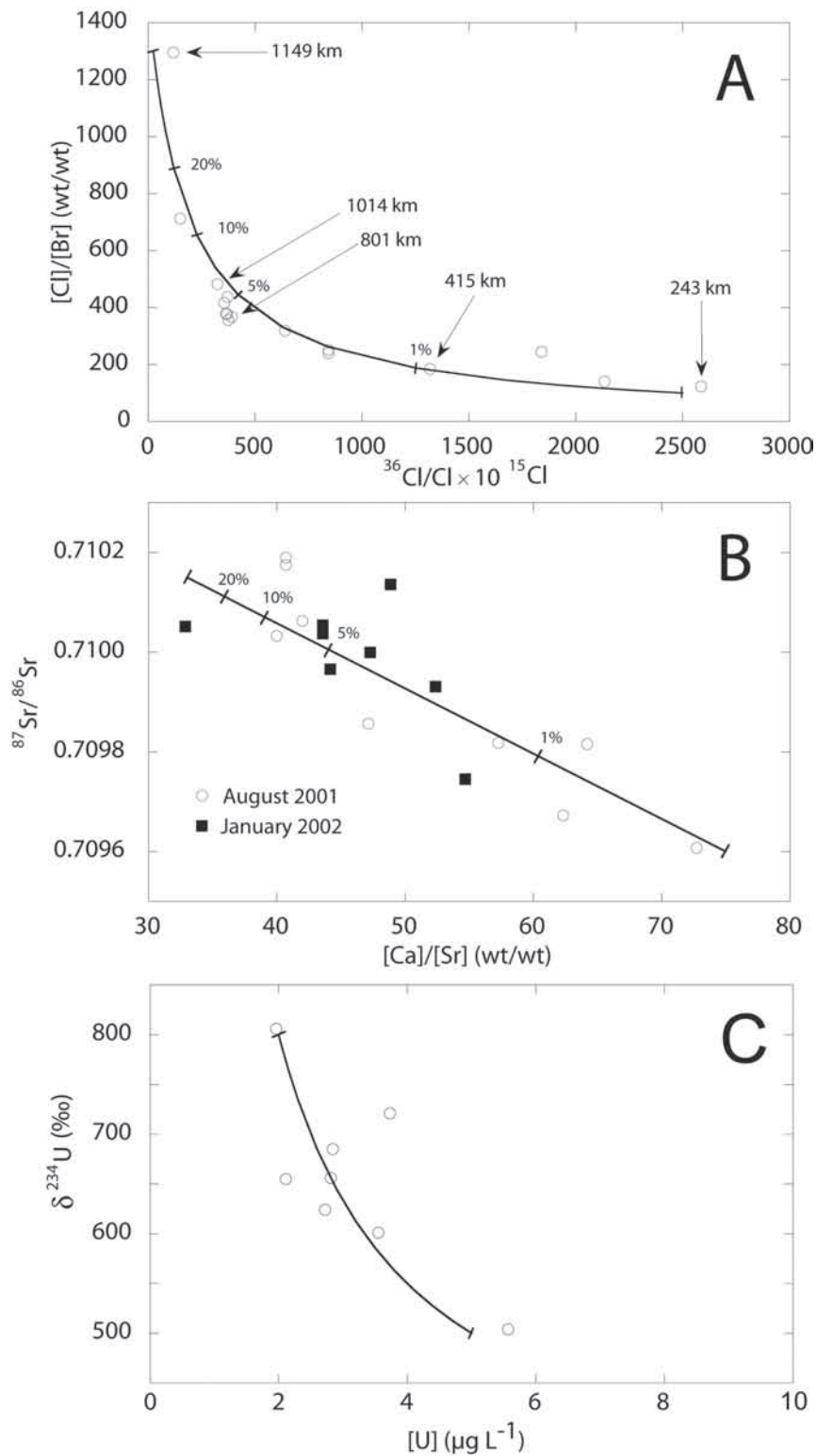


FIG. 20. Isotopic mixing diagrams quantifying saline groundwater discharge: (A) ^{36}Cl versus Cl/Br ratios; (B) $^{87}Sr/^{86}Sr$ versus Ca/Sr ratios; (C) $\delta^{234}U$ values versus U concentration. Mixing lines were calculated using the end members discussed in the text and found in Table 1. Percentages are not included on the U -isotope mixing plot because of its non-conservative behaviour.

increases using different elemental and isotopic systems are relatively consistent. For example, in the middle portion of the river, which includes three distinct inputs, a 5%–10% saline groundwater contribution could explain the observed changes in both Cl and Sr isotope systems. During the summer of 2001, Rio Grande flow was at 24 m³/sec, whereas in the winter of 2002, flow was 20 m³/sec¹. Using these flow rates and our calculated percentage implies a saline groundwater flux of 1–2 m³/sec over this stretch of the river. These values, although uncertain due to a likely range in saline groundwater composition, are broadly consistent with recent discharge estimates from a groundwater model of the Albuquerque Basin [32]. Given that the saline groundwater end member is based on relatively shallow samples that are probably a mixture of shallow groundwater and deep brine, which may be an order of magnitude more concentrated (Table 1), the actual flux of deep brine could be as low as 0.1 m³/sec.

The above observations are significant for two reasons. First, they indicate that brines of geological origin may play a much larger role in the salinization of arid zone rivers than previously suspected. Second, within the Rio Grande they limit the possible role of agricultural return flows as a major factor impacting river salinity. Recognition of saline groundwaters associated with alluvial sedimentary basin brines as a significant factor in river salinization has important management implications. The reduction of agricultural return flows through improved water use efficiency, lining of canals, and even reusing waters are commonly proposed to mitigate salinity increases [33]. The sedimentary brine source identified for the Rio Grande in this study suggests that alternative approaches to salinity management, such as interception wells to capture sedimentary brines, may offer more practical and effective long term solutions for rivers with similar salinity sources.

4.2.5. Salinity response to drought

The Rio Grande Basin has been gripped by drought since the mid-1990s, with the situation worsening substantially during 2001–2004 (Fig. 6). This has afforded an opportunity to examine the dynamic response of the system to changes in water balance. As noted in the previous section, there have been pronounced changes in the isotopic composition of the river water, likewise there have been significant changes in Cl and Cl/Br. The most prominent feature is a region of increased salinity extending from north of Albuquerque to San Marcial. At San Marcial, summer Cl concentrations have gone from 30 to 150 ppm. This is accompanied by an increase in the Cl/Br ratio from 300 to 730. This change partly reflects drastically decreased river discharge, resulting in less dilution of deep groundwater discharge from river runoff. Additionally, during times of drought water is pumped from the drains to maintain flow in the river. However, drain concentrations and ratios have also increased. This can probably be attributed to a decline in the proportion of drain flow derived from irrigation water. As hydraulic heads beneath the agricultural fields in the area decline, a larger proportion of deep saline discharge is probably allowed to flow out. The drought has revealed that there is a delicate balance between saline discharge and irrigation water that under normal conditions is masked by the large infiltration of irrigation water.

Finally, there has been a steady increase of Cl concentration in and below Elephant Butte Reservoir (from 50 to 80 ppm). This, however, is not accompanied by any significant change in the Cl/Br ratio. As described above, this is consistent with the increased evaporative concentration of the river's water as the reservoir declines under drought, but is not consistent with change resulting from increased saline groundwater input.

4.3. IMPLICATIONS FOR GNIR

The results of this study yield several suggestions for the operation of a ‘Global Network of Isotopes in Rivers — GNIR’. First, the isotopic composition of the Rio Grande, and likely most large rivers, is strongly influenced by the human management of water resources as well as natural hydrologic process and climate variability which result in changes to water sources. When interpreting any change in isotopic composition, it is critical that both possibilities be considered.

Second our synoptic sampling approach provides an effective method to understand the relative roles of these processes. While performing biannual synoptic surveys is likely beyond the scope of most GNIR studies, at least one synoptic river survey prior to the development of a fixed station sampling point(s) will aid in understanding both the dominant hydrologic and human processes controlling the downstream isotopic composition of water. Furthermore a synoptic survey would aid in the selection of fixed station sites that are responsive to climate and the human management of both, as is needed for GNIR. The results of such a study would indicate critical hydrologic processes, including changes in the proportion of water sources — such as the percentage of winter snowmelt vs. summer monsoon rains, changes in the relative evaporation of water, which is particularly pronounced during drought, and changes in river management related to the storage and release of waters in reservoirs.

Finally, GNIR should be open to the use of solute isotopes to address water quality issues. In the case of the Rio Grande, the use of solute isotopes to address salinity and salinization proved to be an excellent addition to standard water isotopes. In other basins, issues related to excess nutrients or heavy metals may be of primary concern. In all cases, the fate and transport of these solutes are largely controlled by the same hydrologic and human processes reflected in water isotopes making this an obvious extension with significant public interest.

5. CONCLUSIONS

The Rio Grande is a typical desert river, fed by snowmelt in high mountains at the headwaters and virtually completely consumed by irrigation and other uses along its 1200 km course. Water quality in the headwaters is very dilute and pure, but in the lower part of the drainage basin dissolved solids rise to the point of rendering the river virtually unusable. Not only the dissolved solids content, but also the salt burden, increase markedly along the flow path. The causes of this salinization have never been adequately explained.

We have employed a variety of environmental and isotopic tracers to examine the evolution of water quality in the Rio Grande. The study has been conducted during a period of increasing drought, so dynamics of the system under stress can be examined. Results have shown that salts are introduced into the river at fairly discrete points. Some of these are easily identified as points of wastewater discharge. Others, however, are not associated with any known discharge to the river. Their geochemical characteristics are similar to those of deep sedimentary brines. These brines appear to be leaking upward along faults and other geological structures in the southern portions of the Albuquerque, Socorro, and Mesilla basins.

Changes in agricultural practices have frequently been proposed as a means of improving water quality in the Rio Grande. Our results indicate that, although irrigated agriculture does

cause a significant increase in the concentration of solutes due to evapotranspiration, increases in the salt burden are not related to agriculture. Changing agricultural practices would probably have little effect on salinity, and improvement in irrigation efficiency might even further degrade water quality. The best opportunity for water quality improvement is likely to be identification and interception of brine leakage at the points of discharge.

ACKNOWLEDGEMENTS

This material is based upon work supported by SAHRA (Sustainability of semi-Arid Hydrology and Riparian Areas) under the STC Program of the National Science Foundation, Agreement No. EAR-9876800. We thank the IAEA for including this study in the CRP 'Isotopic Tracing of Hydrological Processes in Large River Basins'.

REFERENCES

- [1] WILKINS, D.W., Summary of the Southwest Alluvial Basins Regional Aquifer: System Analysis in Parts of Colorado, New Mexico, and Texas, U.S. Geological Survey Professional Paper 1407A (1998) 49.
- [2] GRAUCH, V.J.S., SAWYER, D.A., KELLER, G.R., GILLESPIE, C.L., "Contributions of gravity and aeromagnetic studies to improving the understanding of subsurface hydrogeology, Middle Rio Grande Basin, New Mexico", U.S. Geological Survey Middle Rio Grande Basin Study (COLE, J.C., Ed.), Proc. of the 4th annual workshop, US Geological Survey Open File Report 00-488 (2001) 3-4.
- [3] KELLER, G.R., CATHER, S.M., Basins of the Rio Grande Rift: Structure, Stratigraphy, and Tectonic Setting, Geological Society of America Special Paper 291, Boulder, Colorado (1994) 304 pp.
- [4] HAWLEY, J.W., Hydrogeologic cross sections of the Mesilla bolson area, Dona Ana county, New Mexico and El Paso County, Texas, New Mexico Bureau of Mines & Mineral Resources, Open-File Report 190 (1984) 10 pp.
- [5] ANDERHOLM, S.K., Hydrogeology of the Socorro and La Jencia basins, Socorro County, New Mexico, U.S. Geological Survey, Water-Resources Investigations Report 84-4342 (1987) 62 pp.
- [6] ELLIS, S.R., et al., Rio Grande Valley, Colorado, New Mexico, and Texas, Water Resou. Bull. **29** (1993) 617-646.
- [7] LIPPINCOTT, J.B., Southwestern border water problems, J. Am. Water Works Assoc. **31** (1939) 1-29.
- [8] NATIONAL RESOURCES COMMITTEE, Regional Planning: Part VI, The Rio Grande Joint Investigation in the Upper Rio Grande Basin, Colorado, New Mexico, and Texas, 1936-1937, U.S. Government Publishing Office (1938) 566 pp.
- [9] TROCK, W.L., HUSZAR, P.C., RADOSEVICH, G.E., SKOGERBOE, G.V., VLACHOS, E.C., Socio-economic and Institutional Factors in Irrigation Return Flow Quality Control, Robert S. Kerr Environmental Research Laboratory, U.S. Environmental Protection Agency, EPA-600/2-78-174c, Ada, Oklahoma (1978) 136 pp.
- [10] HAYWARD, H.E., "The salinity factor in the reuse of waste waters", The Future of Arid Lands (WHITE, G.F., Ed.), Vol. Publication No. 43, American Association for the Advancement of Science, Washington, D.C. (1956) 279-290.

- [11] WILCOX, L.V., “Analysis of salt balance and salt-burden data on the Rio Grande”, Problems of the Upper Rio Grande: An Arid Zone River, Publication No. 1 (DUISBERG, P.C., Ed.), Socorro, New Mexico, U.S. Commission for Arid Resources, Improvement and Development (1957) 39–44.
- [12] PHILLIPS, F.M., HOGAN, J., MILLS, S., HENDRICKS, J.M.H., “Environmental tracers applied to quantifying causes of salinity in arid-region rivers: Preliminary results from the Rio Grande, southwestern USA”, Water Resources Perspectives: Evaluation, Management, and Policy (ALSHARHAN, A.S. WOOD, W.W., Ed.), Developments in Water Science, v. 50, Elsevier Science, Amsterdam (2003) 327–334.
- [13] MILLS, S.K., Quantifying salinization of the Rio Grande using environmental tracers, M.S. Thesis, New Mexico Institute of Mining & Technology, Socorro (2004) 397 pp.
- [14] OELSNER, G.P., BROOKS, P.D., HOGAN, J.F., Quantifying nitrogen sources and sinks within the Middle Rio Grande, NM, J. Am. Water Resour. Assoc. (2007) in press.
- [15] HOGAN, J.F., et al., Geologic origins of salinization in a semi-arid river: the role of sedimentary brines, *Geology* **35** 12 (2007) 1063–1066.
- [16] COLORADO DIVISION OF WATER RESOURCES, Surface Water Conditions, <http://www.dwr.state.co.us/SurfaceWater/default.aspx>, January 2007 (2007).
- [17] US GEOLOGICAL SURVEY, USGS Water Quality Data for Colorado and New Mexico, <http://waterdata.usgs.gov/nwis/qw>, September 2006 (2006).
- [18] DAHM, C.N., et al. Evapotranspiration at the land/water interface in a semi-arid drainage basin, *Freshwater Biology* **47** (2002) 831–843.
- [19] COPLEN, T.B., HERCZEG, A.L., BARNES, C., “Isotope engineering — Using stable isotopes of the water molecule to solve practical problems”, *Environmental Tracers in Subsurface Hydrology* (COOK, P., HERCZEG, A.L., Ed.), Kluwer Academic, Dordrecht (1999) 79–110.
- [20] GAT, J.R., Oxygen and hydrogen isotopes in the hydrologic cycle, *Ann. Rev. Earth Planet. Sci.* **24** (1996) 225–262.
- [21] DANSGAARD, W., Stable isotopes in precipitation, *Tellus* **16** (1964) 436–468.
- [22] ADAMS, A.I., GOFF, F., COUNCE, D., Chemical and isotopic variations of precipitation in the Los Alamos Region, New Mexico, Los Alamos National Laboratory, LA-12895-MS, Los Alamos, NM (1995) 35 pp.
- [23] YAPP, C.J., D/H variations of meteoric waters in Albuquerque, New Mexico, USA, *J. Hydrol.* **76** (1985) 63–84.
- [24] CAMPBELL, A.R., LARSON P.B., “Introduction to stable isotope applications in hydrothermal systems”, *Techniques in Hydrothermal Ore Deposits* (RICHARDS, J.P., LARSON, P.B., Eds.) Vol. Reviews in Economic Geology, Vol. 10, Society of Economic Paleontologists and Mineralogists (1998) 173–193.
- [25] WHITTEMORE, D.O., Geochemical differentiation of oil and gas brine from other saltwater sources contaminating water resources; case studies from Kansas and Oklahoma, *Environ. Geosci.* **2** (1995) 15–31.
- [26] DAVIS, S.N., WHITTEMORE, D.O., FABRYKA, M.J., Uses of chloride/bromide ratios in studies of potable water, *Ground Water* **36** (1998) 338–350.
- [27] VENGOSH, A., PANKRATOV, I., Chloride/bromide and chloride/fluoride ratios of domestic sewage effluents and associated contaminated ground water, *Ground Water* **36** (1998) 815–824.
- [28] PHILLIPS, F.M., Chlorine-36, “Environmental Tracers in Subsurface Hydrology” (COOK, P., HERCZEG, A.L., Eds), Kluwer Academic Publishers (2000) 299–348.
- [29] REITER, M., Hydrogeothermal studies in New Mexico and implications for ground-water resources, *Environ. and Eng. Geosci.* **5** (1999) 103–116.

- [30] DICKSON, B.L., DAVIDSON, M.R., Interpretation of $^{234}\text{U}/^{238}\text{U}$ activity ratios in groundwaters, *Chemical Geology* **58** (1985) 83–88.
- [31] CHENG, H., EDWARDS, R.L., HOFF, J., GALLUP, C., RICHARDS, D.A., ASMEROM, Y., The half-lives of uranium-234 and thorium-230, *Chemical Geology* 169 (2000) 17–33.
- [32] SANFORD, W.E., et al., Use of environmental tracers to estimate parameters for a predevelopment ground-water-flow model of the Middle Rio Grande Basin, New Mexico, US Geological Survey Water-Resources Investigations Report 03-4286 (2004) 102 p.
- [33] CHHABRA, R., *Soil Salinity and Water Quality*, Brookfield VT, A.A. Balkema Publishers (1996).

CHEMICAL AND ISOTOPIC COMPOSITIONS OF THE EUPHRATES RIVER WATER, SYRIA

Z. Kattan

Department of Geology, Atomic Energy Commission, Damascus, Syria

Abstract. Stable isotope (^{18}O and ^2H) ratios, were measured together with tritium content and major ion concentrations on a monthly basis at 12 stations along the Syrian portion of the Euphrates River during the period January 2004–December 2006. Spatial variations of stable isotope ratios are moderated compared with other large rivers in the world. The concentrations of major ions and environmental isotopes systematically increased with distance downstream, with the sharpest enrichment at Al-Assad Lake. This systematic increase could be explained by: (1) direct evaporation from the river and its tributaries; and (2) drainage return flows of irrigation water via the groundwater system. The isotopic properties of the Euphrates water suggest negligible roles of precipitation and local runoff, compared with evaporation.

1. INTRODUCTION

Stable isotopes ($\delta^{18}\text{O}$ and $\delta^2\text{H}$) are ideal natural tracers that have contributed remarkably to our understanding of the water cycle and related diverse hydrological processes [1–4]. The importance of such isotopes in water studies is due to their properties, as conservative fingerprints of the water molecule, that reflect the cumulative influence of all water modification processes. The isotopic composition of riverine systems has proven to be a useful tool for estimating the mean residence time and storage properties of surface water [5–10]. Changes in the isotopic composition of rivers may also help to better characterize the effect of snowmelt events [11], patterns of river regime and tracing pathways of water flow in small basins [12], as well as quantitative estimates of river flow components, through the so-called ‘hydrograph separation’ method [13–15]. Furthermore, the temporal and spatial variations of river water isotope compositions provide useful information on mixing between different water bodies, effects of input from tributaries, and roles of dams and lakes [16], together with a sensitive evaluation of the influence of terrains, fracture types and evaporation under dry climates [17]. In addition, such isotopes can also be used to study salinity sources [18] and estimate the irrigation return flows [19].

Monitoring of the isotopic composition of large rivers at the continental scale is not an easy task, because of the expansive areas and huge number of water samples required to adequately characterize the geographical distribution of such large systems [18]. Nevertheless, it is well documented from a large number of studies that the isotopic composition of river waters in the headland of large rivers is fairly close to that of local precipitation [9, 18 and 20], and similar to that of rainfall in surrounding areas [21]. Most studies reported a progressive increase in stable isotope composition with increasing distance downstream [18]. The isotopic composition of tropical river waters generally has much smaller scatter than that of precipitation, with more depleted concentrations during the rainy season and more enriched values during the dry season [22]. In the case of small catchments, it was shown that the isotopic composition of most surface and groundwater bodies is constant and rather close to the annual average of local precipitation [21]. In Alpine basins, it was shown that runoff depends strongly on snowmelt that can induce sharp changes in the amount and isotopic composition of discharge [11].

In karstic regions, river waters usually have short transit times, with more pronounced seasonal variations, compared with those fed by groundwater from porous media, where the average residence time is much longer [21]. In moderate climates, it was observed that the evaporation process is generally not too important, unless lakes or large dams considerably affect river flow [23]. Surface evaporation from the Amazon River basin does not have any recognizable effects [24], while evapotranspiration, which is isotopically a non-fractionating process [25], and recirculation of streams and groundwaters to the atmosphere, appear to be essential to the local hydrological cycle [26]. The situation in arid regions is considerably different, because seasonal variations are not caused by changes in the isotopic composition of rainfall in the headlands, but by evaporation from rivers in the lower parts, where rains become less abundant or completely disappear. The enrichment of stable isotopes in arid zone surface waters can be used to gauge progressive downstream water loss through evaporation [19]. For instance, the quantitative evaluation of evaporation in Algerian sebkhas showed that 46% may be lost through this process [27].

Although a large number of isotopic studies were focused on large rivers in many part around the world, few hydrochemical and isotopic investigations [28–30], were devoted to the Euphrates River system. Based on the importance of this large river, especially as a surface water resource, a detailed hydrochemical and isotopic study was proposed to assess the hydrological and geochemical characteristics of this river system. Monitoring of the chemical and isotopic compositions of the Euphrates River in Syria was initiated within the framework of the IAEA coordinated research project (CRP) entitled ‘Design criteria for a network to monitor isotope compositions of runoff in large rivers’, that aims to better understand the water balance and hydrological processes of a number of large river on a global scale. This paper, which discusses parts of the so far obtained results through the monitoring of the chemical and isotopic compositions of the Euphrates River waters during a three years period, aims to demonstrate the overall characteristics of the temporal and spatial variations patterns of the the Euphrates River system in Syrian terretory.

2. GENERAL CHARACTERISTICS OF THE STUDY AREA

Euphrates River, with its basin lands (area = 350 000 km²), is the largest, the longest (entire length = 2900 km) and, to some extent, the most important river in western Asia. This river yields most of its resources from the mountainous regions of eastern Turkey and drains lands belonging to Syria and Iraq, before joining the Arabian Gulf at the so-called ‘Shatt Al-Arab’ (Fig. 1).

The topography of the river basin in the Syrian reach is generally simple, with the presence of a number of small hills near its banks, mainly upstream Al-Assad Lake. The elevation of the Euphrates River course in Syria ranges between 350 m above sea level (m.a.s.l) at Jarablous, and 180 m at Albu-Kamal. The lowest part of the river basin, or the so-called ‘base valley’ is located downstream below 200 m.a.s.l. The slope of the river course averages 0.25 m/km [31, 32].

Climatically, the Euphrates River Basin in Syria ranges from semi-arid to arid with increasing aridity downstream. The climate upstream (i.e. near the Syrian–Turkish border) is nearly identical to that of semi-arid zones, and gradually becomes more arid or desert-like. The winter season is usually cool (5–10°C) and rainy, and the summer is warm (30–45°C) and almost



FIG. 1. Location map showing the Euphrates River system.

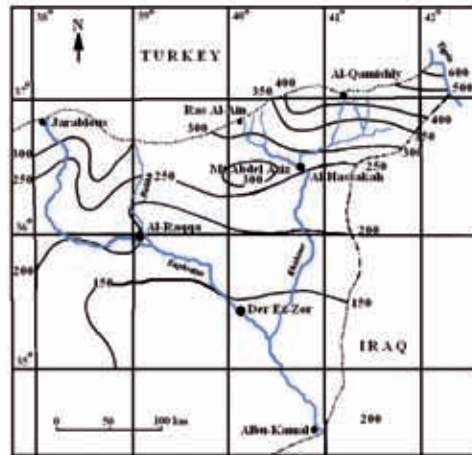


FIG. 2. Distribution of precipitation in north-eastern Syria.

entirely devoid of rainfall. The mean annual air temperature increases from north to south, and varies between 18°C in Jarablous and 20°C in Albu-Kamal, where aridity becomes accentuated.

Mean monthly rainfall decreases from north to south, ranging during the rainy season (October to May) from 20 to 60 mm in Jarablous, and from 5 to 30 mm in Albu-Kamal. The amount of mean annual precipitation ranges from 350 mm (Jarablous) to less than 130 mm in the arid interior lands near the Iraqi border (Albu-Kamal), with an intermediate value (160 mm) at Deir-Ezzor (Fig. 2). The mean annual precipitation over the entire Euphrates River Basin in Syria is around 240 mm [32].

The mean annual value of relative air humidity varies between 56% (Jarablous) and 47% (Deir-Ezzor), and declines to less than 44% (Albu-Kamal), the lowest registered value in the country. The highest value of mean monthly relative air humidity (60–70%) is generally observed during the cool period (December–January), while the lowest (25–30%) occurs during the warmest months (July and August). Potential evapotranspiration generally exceeds rainfall, and ranges from 1300 to 2600 mm, with a mean annual value of close to 2100 mm [29].

3. SURFACE WATER HYDROLOGY

The entire Euphrates River Basin covers lands belonging to three countries: Turkey (110 000 km²), Syria (70 000 km²) and Iraq (170 000 km²). This river, which traverses a length of around 675 km in Syria, flows within a depression structure, filled generally with Paleogene (argillaceous limestone), Neogene (gypsum, silty clays, sandstone, siltstone, clays, and pebbles) and Quaternary (pebbles, gravels, loams and sandy loams) deposits [33]. The alluvial aquifer, composed primarily of gravels and larger pebbles at the bottom and finer alluvial sediments (loams and sandy loams) at the top, is the most important water bearing system in this basin [32].

The recharge zones of the Euphrates River and its main tributaries are mainly located in Turkey, and thus approximately 94% of its discharge originates from this country. Most river inflow occurs between April and June, and is caused by the melting of accumulated snow on the highlands. The mean annual discharge of the Euphrates River at Jarablous station prior to

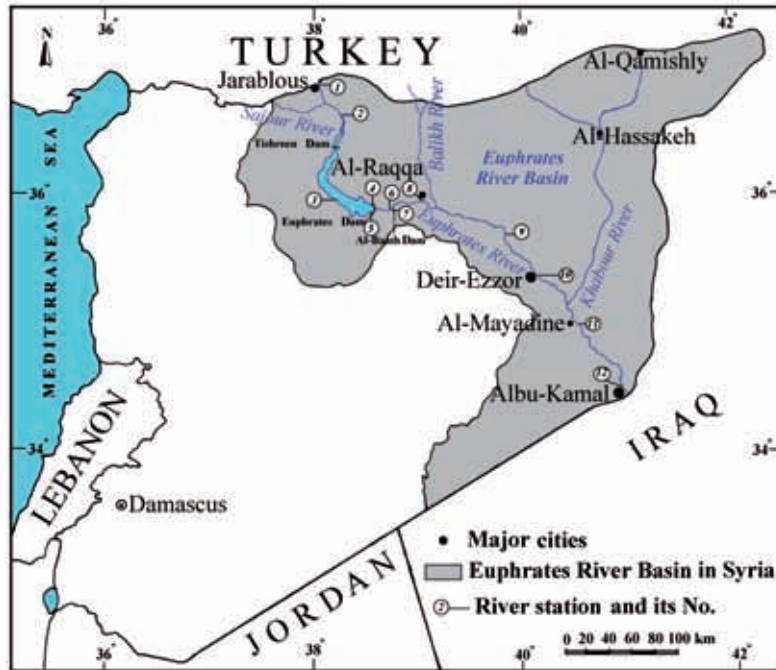


FIG. 3. Location map of the Euphrates River Basin in Syria showing different sampling sites along the river course.

the 1960s was $\approx 735 \text{ m}^3/\text{s}$ [31]. During the last few decades, river discharge has been controlled by Turkey through a treaty that fixes the minimum annual river discharge for both Syria and Iraq at $\approx 500 \text{ m}^3/\text{s}$.

The hydrographic network of the Euphrates River, which covers about one-third of Syrian territory (Fig. 3), is represented by three main tributaries: the Sajour (length about 48 km and average discharge $\approx 3 \text{ m}^3/\text{s}$), the Balikh (length $\approx 105 \text{ km}$ and mean discharge $\approx 6 \text{ m}^3/\text{s}$), and the Khabour (length $\approx 400 \text{ km}$ and mean discharge $\approx 50 \text{ m}^3/\text{s}$). As a result of overpumping and the resulting decline in the groundwater table upstream from the Khabour River, this tributary has become completely dry during the last dozens of years [34].

The hydrological regime of the Euphrates River is artificially controlled by about 20 large dams with 17 hydroelectrical power stations, which were constructed across its course in Turkey. In Syria, only three smaller dams (Tishreen, Euphrates and Al-Baath) were built, with the aim of preventing major flooding and generating electrical power. The establishment of the Euphrates Dam, with its large lake (length $\approx 75 \text{ km}$), serves to regulate, to some degree, river discharge downstream.

Variations in the average monthly discharge of the Euphrates River at five different Syrian gauging stations during the study period (2004–2006) are shown in Fig. 4. The average monthly discharge at the Syrian–Turkish border ranges between 450 and 973 m^3/s , with several peaks during winter and summer periods, and obviously lower registries (250–875 m^3/s) at the Syrian–Iraqi border. Similar temporal patterns in river discharge can be observed for the upstream stations of Jarablous and Tishreen Dam. Downstream of the Euphrates Dam, river discharge trends have a different evolution, and thus temporal discharge patterns at the monitored stations (Al-Baath Dam and Albu-Kamal) are similar and generally identical to

outflow discharge from the Euphrates Dam. Average annual discharge during the study period was ≈ 687 and ≈ 555 m^3/s at Jarablous and Albu-Kamal, respectively.

4. SAMPLING AND ANALYTICAL METHODS

More than 25 sampling campaigns were undertaken in the study area during a three year period from January 2004 to December 2006. Water samples were collected on a monthly basis from 12 sites distributed along the Euphrates River course in Syria. The first sampling site was selected in Jarablous, close to the Syrian–Turkish border, while the last sampling site was selected in the Albu-Kamal area, close to the Syrian–Iraqi border (Fig. 3). Unfortunately, four water samples were missed at each site during the sampling period.

Water samples were generally collected in three rinsed plastic bottles, and immediately after returning back from the field, all samples were preserved in a refrigerated room ($T \approx$ below 5°C) until the time of analysis. A small bottle of 50 mL was filled for the determination of stable isotopes ($\delta^{18}\text{O}$ and $\delta^2\text{H}$), and subsequently analyzed at the Geology Department of the Syrian Atomic Energy Commission (AECS), by equilibrating a 5 mL subsample with small amounts of separate reference gases (CO_2 and H_2), and analyzing the resulted gases using a Finnigan Mat DELTA^{Plus} mass spectrometer. A second bottle with a volume of one litre was collected for tritium measurement, and the subsequent analyses of this radioactive isotope were performed at the Geology Department of AECS (after electrolysis), using a liquid scintillation counter (Quantulus 1220). Measurement accuracy for $\delta^{18}\text{O}$, $\delta^2\text{H}$ and tritium are ± 0.1 , $\pm 1.0\%$ versus VSMOW, and ± 1 TU, respectively.

A third 500 mL bottle was filled for the determination of major ions (Ca^{2+} , Mg^{2+} , Na^+ , K^+ , Cl^- , SO_4^{2-} and NO_3^-), and related chemical analyses were carried out in the Geology Department of AECS, after the filtration of water samples through a 0.45μ Millipore membrane, using a high

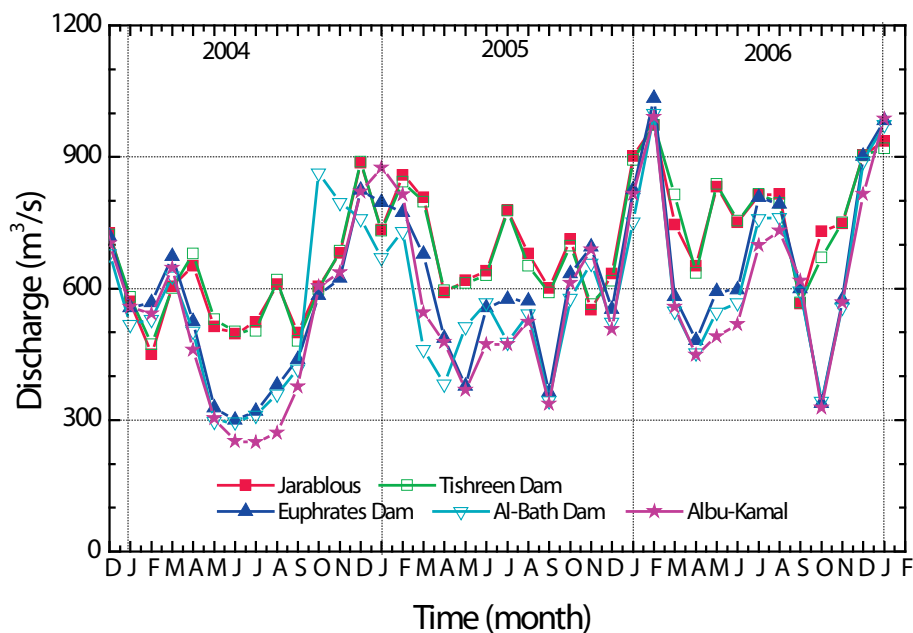


FIG. 4. Temporal variations of average monthly discharge from the Euphrates River at five different stations along the river course between January 2004 and December 2006.

performance liquid chromatography (HPLC) method, with a dual column instrument (model Dionex DX-100), that has an analytical error of less than 1 mg/L. In addition, a number of surface water samples were collected for the determination of silica (SiO₂), and the related analyses were carried out in the Geology Department of AECS, using a spectrophotometer (Hach), delivered with special kits for this purpose.

The water temperature, pH and electrical conductivity (EC), together with total alkalinity (i.e. HCO₃⁻) values of all water samples were measured in the field during sampling. Temperature measurements were carried out using the temperature probe of a WTW conductivity meter (model cond315i) with precision of ± 0.2 °C. The same conductivity meter was also used for the measurement of EC values, with a precision of ±5 µS/cm. Measurements for pH were determined using a WTW pH meter (model pH315i) after calibration with two standard buffer solutions (pH = 4 and pH = 7), with a precision of ±0.01. Total alkalinity values were determined using the volumetric titration method [35] on water samples of 100 mL using a WTW pH315i-meter and 1.6 N sulfuric acid, with a precision of ± 1.5 mg/L.

Quality Assurance procedures, according to the ISO/IEC 17025, are strictly adhered to by all AECS laboratories. Both chemical and isotopic analysis results are periodically verified through participation in different analysis comparison programmes, managed either by the IAEA or other local and international organizations.

5. RESULTS AND DISCUSSION

5.1. Chemistry of the Euphrates River water

Rivers are primarily responsible for the transport of dissolved elements and suspended sediments to the oceans [36]. The study of the chemical composition of river water started early in the second decade of the nineteenth century [37]. Since then a large number of studies have been undertaken in this field all over the world [38–45].

Averages of the physico-chemical parameters of surface water samples collected from the Euphrates River at the different Syrian stations are reported in Table 1. Generally, the data shows that analytical error (σ) related to the chemical balance of water samples is rather small at less than 5%.

The quality of Euphrates River water is generally fresh ($242 < \text{TDS} < 540$ mg/L), with low nitrate concentrations ($\text{NO}_3^- < 5$ mg/L) at all sampling sites. A comparison between the mean chemical composition of Euphrates River water at Jarablous and Abu-Kamal stations and the average chemical compositions of global, arid and semi-arid zone river water [46] shows that river water at both stations is higher than that of average world rivers. The chemical composition of the Euphrates at Jarablous is somewhat comparable with that of semi-arid zone rivers, mainly in terms of magnesium, potassium, and bicarbonate concentrations. However, average chemical composition of the Euphrates at Abu-Kamal is obviously higher than that of arid zone rivers, with the exception that concentrations of calcium, sodium and bicarbonate are similar.

The water chemistry of the Euphrates River in the upper stream essentially reflects the influence of drained lands, largely composed of carbonate rocks. Downstream of the Euphrates Dam,

TABLE 1. MEAN HYDROCHEMICAL DATA OF WATER SAMPLES COLLECTED FROM THE EUPHRATES RIVER DURING THE PERIOD 2004–2006

Site No.	T (°C)	pH	E.C. (µS/cm)	SiO ₂	Na ⁺	K ⁺	Mg ²⁺	Ca ²⁺	HCO ₃ ⁻	Cl ⁻	NO ₃ ⁻	SO ₄ ²⁻	TDS	Mg/Ca	Na/Cl	Ca/SO ₄ (molar ratio)	SO ₄ /HCO ₃	HCO ₃ /Cl	log pCO ₂ (atm)	s %
1*	13.6±3.2	8.30±0.3	360±26	9.9±1.5	15.5±2.2	2.1±0.6	13.7±1.5	34.2±4.5	125.2±18.3	17.4±1.3	2.1±0.6	31.9±2.8	242±20	0.67	1.38	2.61	0.33	4.21	-3.273	4.7
2*	16.5±6.2	8.42±0.3	353±27	8.3±0.9	15.7±2.1	2.0±0.6	13.6±1.3	33.3±4.4	121.8±19.2	17.9±1.4	2.0±0.9	32.1±3.0	238±22	0.68	1.36	2.53	0.34	4.00	-3.389	4.7
3**	18.6±7.5	8.55±0.4	601±375	6.6±2.7	39.3±42.8	2.5±1.2	18.4±7.0	35.2±8.7	110.1±24.7	62.8±86.2	4.9±7.2	70.6±44.1	344±178	0.87	1.06	1.40	0.95	1.75	-3.561	0.1
4**	18.4±5.8	8.54±0.2	414±12	6.4±2.3	21.1±4.1	2.2±0.6	15.6±2.1	32.7±3.3	111.8±18.4	27.4±6.0	2.3±0.5	52.4±6.5	266±29	0.80	1.22	1.50	0.61	2.48	-3.539	1.8
5*	18.4±6	8.49±0.2	403±26	6.4±2.3	21.2±3.6	2.2±0.5	15.7±1.8	33.9±3.9	118.8±18.0	26.5±3.6	1.9±0.5	51.1±6.1	271±22	0.77	1.25	1.62	0.56	2.67	-3.463	2.1
6**	17.1±5.2	8.36±0.2	497±102	8.2±2.5	28.0±6.1	2.3±0.6	19.0±3.6	42.3±10.3	113.3±17.4	29.5±3.4	3.7±2.0	105.4±59.7	343±77	0.75	1.46	1.09	1.23	2.26	-3.368	0.4
7**	17.0±5.2	8.37±0.2	428±14	6.1±2.4	22.1±3.4	2.2±0.5	16.0±1.9	34.5±4.4	111.7±19.0	28.0±2.0	2.3±0.5	56.3±6.0	273±25	0.77	1.22	1.49	0.66	2.33	-3.381	2.8
8*	17.0±5.4	8.32±0.2	464±47	7.3±3.2	26.6±4.6	2.3±0.5	17.1±1.7	37.5±4.3	115.8±19.3	36.2±4.5	2.3±0.8	64.4±12.2	302±29	0.76	1.14	1.44	0.73	1.90	-3.318	2.3
9**	18.1±5.9	8.50±0.2	635±102	6.9±2.2	38.2±10.0	2.7±1.1	21.7±4.2	48.0±9.5	115.7±16.0	52.8±10.9	3.8±0.9	124.5±35.8	407±74	0.75	1.12	0.98	1.37	1.31	-3.498	1.0
10*	18.6±6.3	8.39±0.2	641±123	6.8±2.1	39.8±8.5	2.5±0.8	21.2±3.7	49.7±7.5	120.5±17.1	52.9±10.1	3.4±1.0	123.2±33.7	413±61	0.71	1.17	1.02	1.32	1.37	-3.368	0.5
11*	18.8±6.5	8.29±0.2	727±165	7.0±1.8	50.2±15.4	3.0±1.2	25.2±6.9	55.6±12.4	124.1±18.0	69.8±20.5	4.6±1.6	143.3±45.7	476±97	0.75	1.12	0.99	1.50	1.11	-3.257	0.2
12**	19.5±6.9	8.40±0.3	853±213	7.7±2.5	58.2±17.3	3.4±1.6	28.1±6.8	57.6±14.7	123.2±20.9	86.7±32.4	5.3±5.5	177.2±65.5	540±147	0.81	1.08	0.84	1.83	0.91	-3.368	2.1

* — Water samples were collected during 2004–2006, ** — water samples were collected only during 2004–2005, s — chemical analysis error.

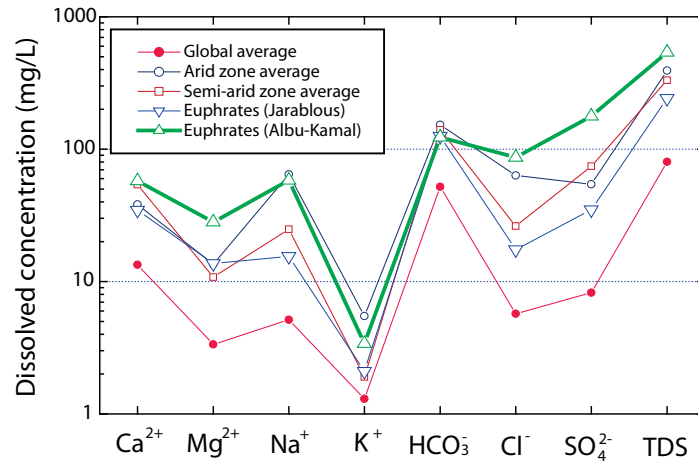


FIG. 5. Comparison between the average dissolved concentrations of the Euphrates River at Jarablous and Albu-Kamal stations and average dissolved concentrations of global, semi-arid, and arid zone river water [46].

river water chemistry becomes more saline, reflecting extensive evapo-transpiration and the influence of dissolution of evaporitic rocks (anhydrite and gypsum), abundantly present in the Neogene substratum outcropping close to the river course.

Silica (SiO_2) is an important chemical species, used essentially for the study of chemical erosion, geochemical weathering and biogeochemical cycles [36]. This ion was measured in Euphrates river water during a one year period from August 2004 to August 2005. The average concentration of SiO_2 in the Euphrates at Jarablous (9.9 ± 1.5 mg/L) is close to the value (10.4 mg/L) provided by Meybeck (1983 [47]) as an average for world rivers, but obviously lower than the value (13.1 mg/L) reported by Livingstone (1963 [48]) for the same water category. The concentration of SiO_2 in the remaining stations was lower than that of Jarablous, ranging around $6-8 \pm 2.5$ mg/L. Relatively low silica content in the lake waters of Al-Assad and Al-Baath reservoirs ($6-6.5$ mg/L) is most probably the consequence of silica consumption by diatoms growth. Similar observations were previously reported for some French rivers [45, 49].

5.1.1. Temporal variations

Figures 6–8 represent temporal variations in water temperature, pH, HCO_3^- , EC, Na^+ , Ca^{2+} , Cl^- , SO_4^{2-} and TDS values at six stations (site Nos 1, 2, 5, 8, 10, 11) distributed along the Euphrates River course in Syria during the period 2004–2006. It can be observed that water temperature follows a cyclic trend, with low values during winter and high temperature ranges during summer (Fig. 6a). The average river water temperature at Jarablous is lowest (13.6 ± 3.2 °C), compared to those of the other downstream stations, which show a gradual increase with distance downstream.

A comparison between river water temperature at Jarablous and Albu-Kamal shows a difference of ≈ 5 °C during winter and clearly higher amplitude (≈ 10 °C) during summer, reflecting the effect of spatial air temperature changes between monitored stations.

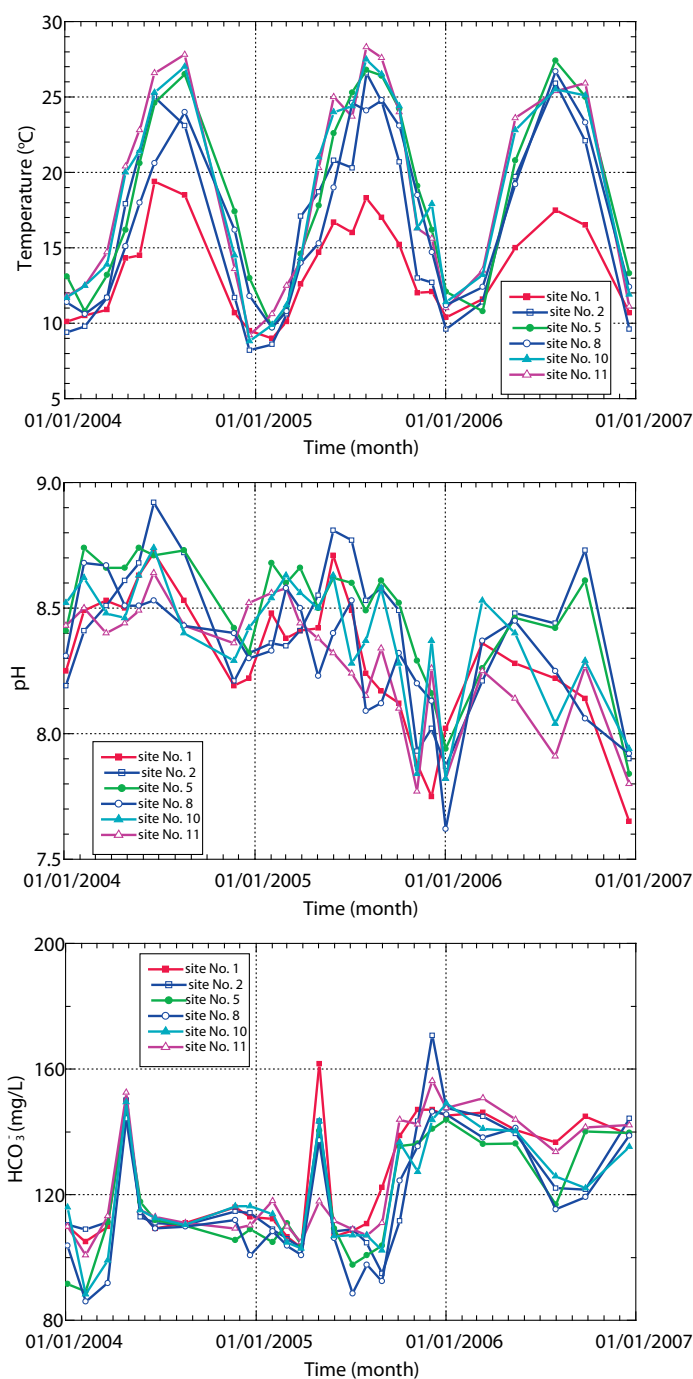


FIG. 6. Temporal variations in water temperature (a), pH (b) and HCO_3^- (c) values at six stations along the Euphrates River course during the period 2004–2006.

The temporal evolution in pH values (Fig. 6b) is marked by a slight increase during May and June, followed by a decrease during November–January, reflecting the variation effect of dissolved CO_2 partial pressure, mostly controlled by consumption of dissolved CO_2 by algae growth and the activity of micro-organisms in this ecosystem [48–50]. The decrease of pH values can commonly explained by the oxidation of organic river water matter, which leads to further liberation of HCO_3^- (Fig. 6c) and H^+ species [51]. Hence, strong correlations which exist between pH and CO_2 partial pressure ($\log p\text{CO}_2$) values ($r = 0.963$), and to a lesser extent

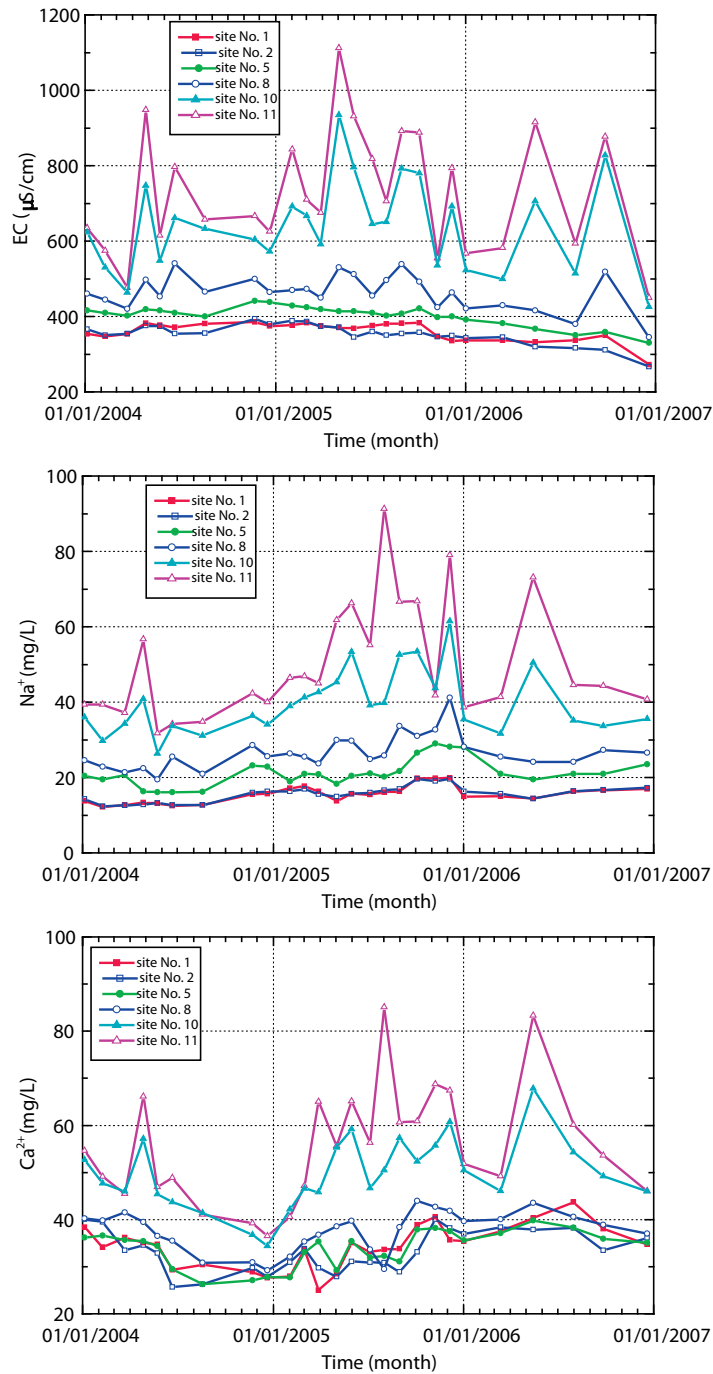


FIG. 7. Temporal variations of EC (a), Na^+ (b) and Ca^{2+} (c) values at six stations along the Euphrates River course during the period 2004–2006.

between pH and bicarbonate concentrations ($r = 0.427$) demonstrate the role of thermodynamic conditions, which control the distribution of carbon species in natural water [52].

Temporal evolutions in EC values, major ions (Na^+ , Ca^{2+} , Cl^- and SO_4^{2-}) and TDS concentrations (Figs. 7–8) are identical, with rather small fluctuations in the upper stations (site Nos 1–8), and more pronounced variations at downstream stations (site Nos 10 and 11). The increase in salinity levels, EC values, and most major ion concentrations in the downstream stations during spring periods is probably the result of groundwater salinization, developed in this area as a consequence of high irrigation rates under arid conditions [30]. The flushing of accumulated

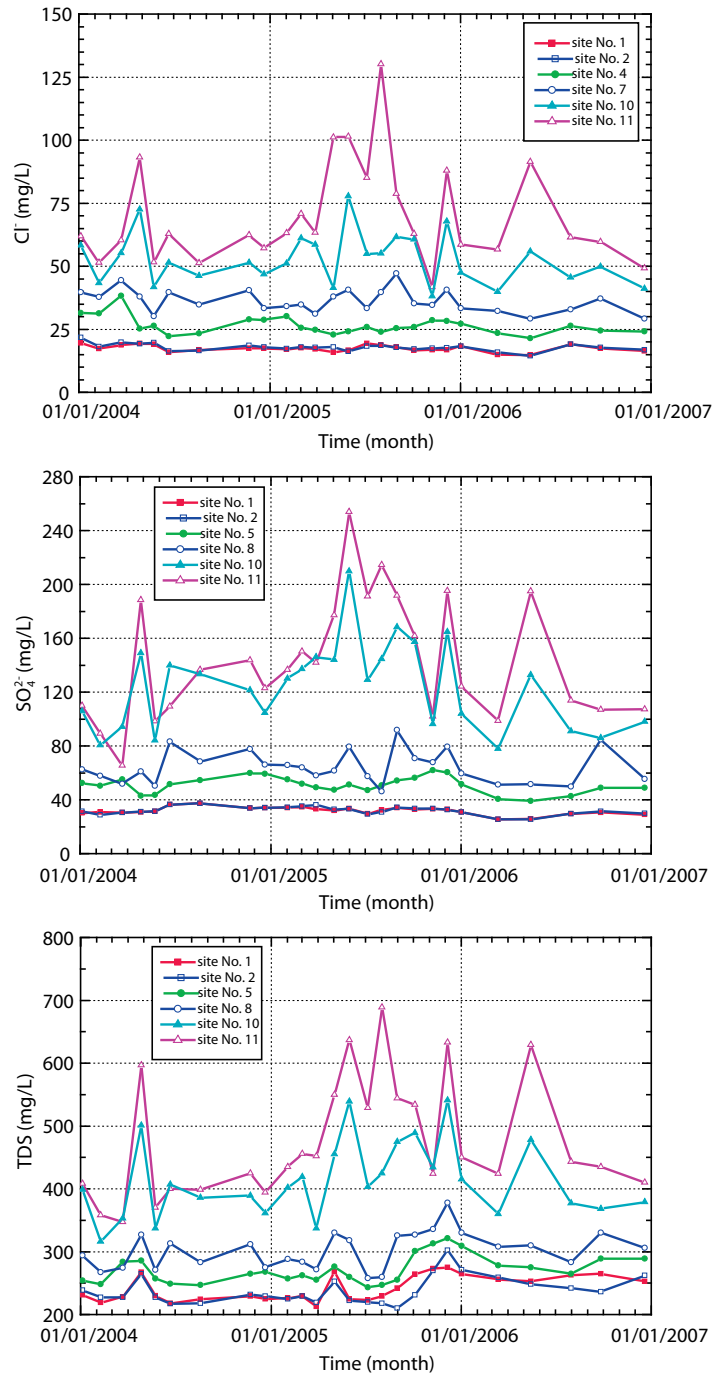


FIG. 8. Temporal variations of the Cl⁻ (a), SO₄²⁻ (b) and TDS (c) values at six stations along the Euphrates River course during the period 2004–2006.

soil salts and mobilization of saline groundwaters into the riverbed can result, describing the so-called ‘drainage return flow’ effect [19, 53, 54].

5.1.2. Spatial variations

Figures 9 and 10 illustrate spatial variations in the average water temperature, pH, SiO₂, major ions, EC and TDS values at different sites along the Euphrates River during the study period. The average river water temperature (Fig. 9a) increases by about 5°C between Jarablous and Al-Assad Lake (13.6 ± 3.2°C) and at Al-Assad Lake (18.4 ± 6°C). As the river flows downstream from the Euphrates Dam, average water temperature values slowly increase by about 1°C. However, a slight decrease in water temperature can be observed for waters at site Nos 6–8, where the river has the potential to receive additional contributions of colder and more saline surface water from different ephemeral tributaries.

The spatial evolution of average pH values along the river path (Fig. 9b) is marked by a slight increase from ≈8.3 to 8.6. The remarkable increase of pH value in Al-Assad Lake water, especially at site No 3, is mostly the result of the consumption of dissolved CO₂ gas by organisms and aquatic plants [47, 49]. Contrarily, the decrease in pH value at site Nos 8 and 11 is most probably due to urban contamination. In all cases, fluctuations in pH value are relatively small, ranging around 8.4 ± 0.3. The spatial evolution of average silica content is rather opposite to that of pH (Fig. 9c). A progressive depletion of silica content from 10 to 6 mg/L can be observed as the river flows from Jarablous towards Al-Assad Lake. The concentration of silica downstream of the Euphrates Dam varies between 6.2 and 7.7 mg/L, with a distinct increase at site No 6 (8.2 ± 2.5 mg/L), most probably because of additional contributions from a different water source more enriched in this ion.

Spatial evolutions of average EC, Ca²⁺, Mg²⁺, Na⁺, Cl⁻, SO₄²⁻ and TDS values along the Euphrates river path show generally similar trends (Figs 9 and 10), with a distinct increase at site No. 3, located in the far southern border of so-called 'Al-Assad Lake'. Lake depth at this site is very shallow (<0.5 m), and its water is probably not well mixed with fresh water entering the lake. The spatial evolution pattern of HCO₃⁻ concentrations has a special trend compared to that of other dissolved ions (Fig. 10a).

With the exception of site No. 3, where the fluctuations of most measured parameters were the highest (highest standard deviation values), it can be observed that standard deviations in EC, most major ions, and thus TDS values, are generally small and increase slightly within the section from Jarablous to Al-Baath Dam (site No. 7). Then, as the river water moves downstream, average EC values, major ion concentrations and TDS values, as well as related standard deviations, progressively increase at a sharp rate. Therefore, the standard deviations of EC, most major ion concentrations and TDS values reach their maximum at site No.12.

While river water salinity doubles within the section from the Euphrates Dam to the Syrian–Iraqi border, chloride concentration increases by a factor of 3. Similarly, the EC value increases between Jarablous and Albu-Kamal by a factor of 2.4. The concentrations of Ca²⁺, Mg²⁺ and Na⁺ increase by factors of 1.7, 2.1, and 3.8 respectively, whereas, Cl⁻ and SO₄²⁻ concentrations increase by factors of 5 and 5.6, respectively. This relative enrichment in Na⁺, Cl⁻ and SO₄²⁻ with respect to other dissolved ions is primarily due to the dissolution and flushing of saline soils, commonly rich in halite (NaCl) and thenardite (Na₂SO₄), minerals present in abundance within the downstream Euphrates valleys, as a consequence of high evaporation rates of irrigation waters [30].

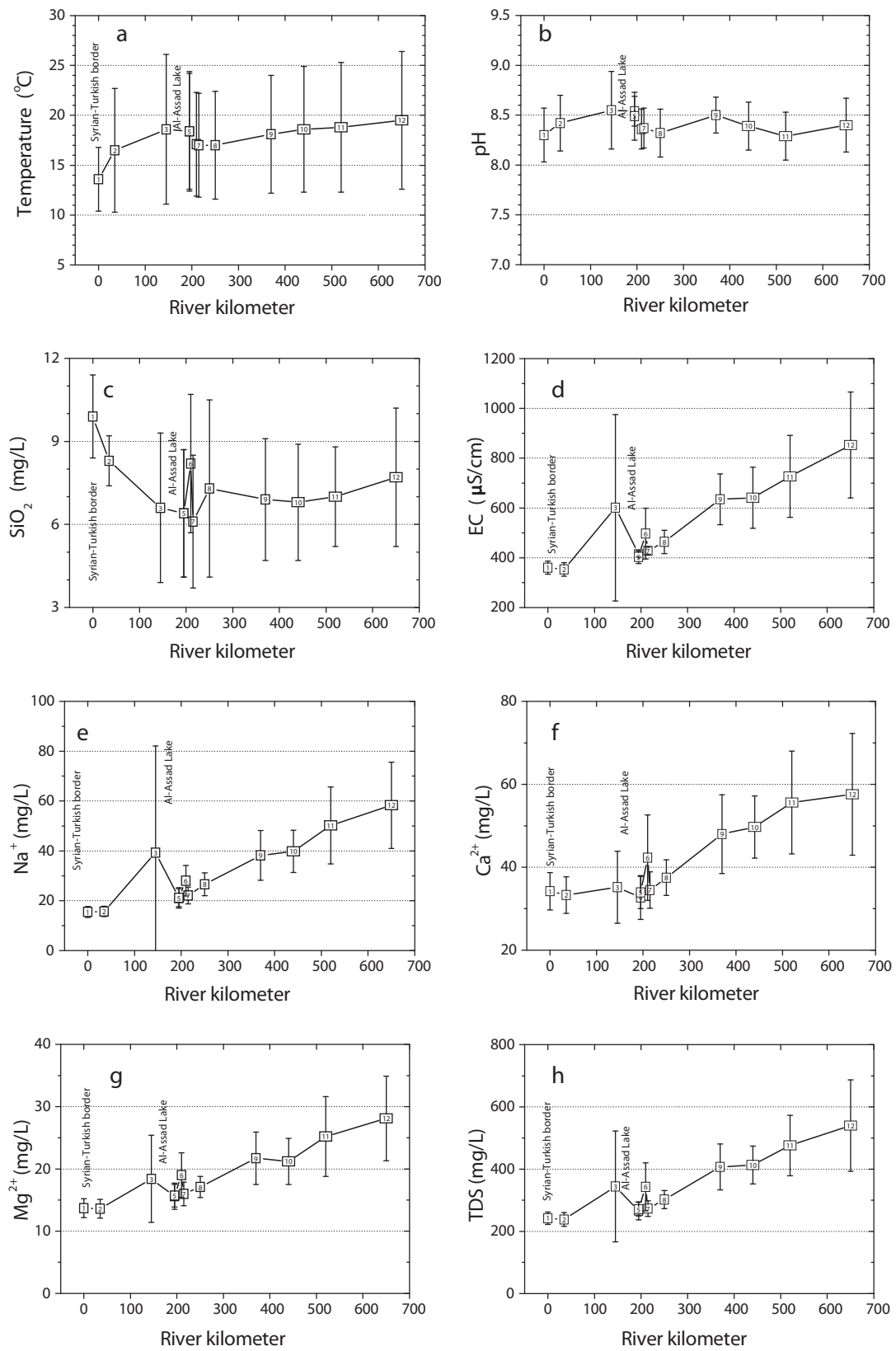


FIG. 9. Spatial variations of averages and standard deviation (error bars) of water temperature (a), pH (b), SiO₂ (c), EC (d), Na⁺ (e), Ca²⁺ (f), Mg²⁺ (g) and TDS (h) values along the different stations of the Euphrates River during the period 2004–2006.

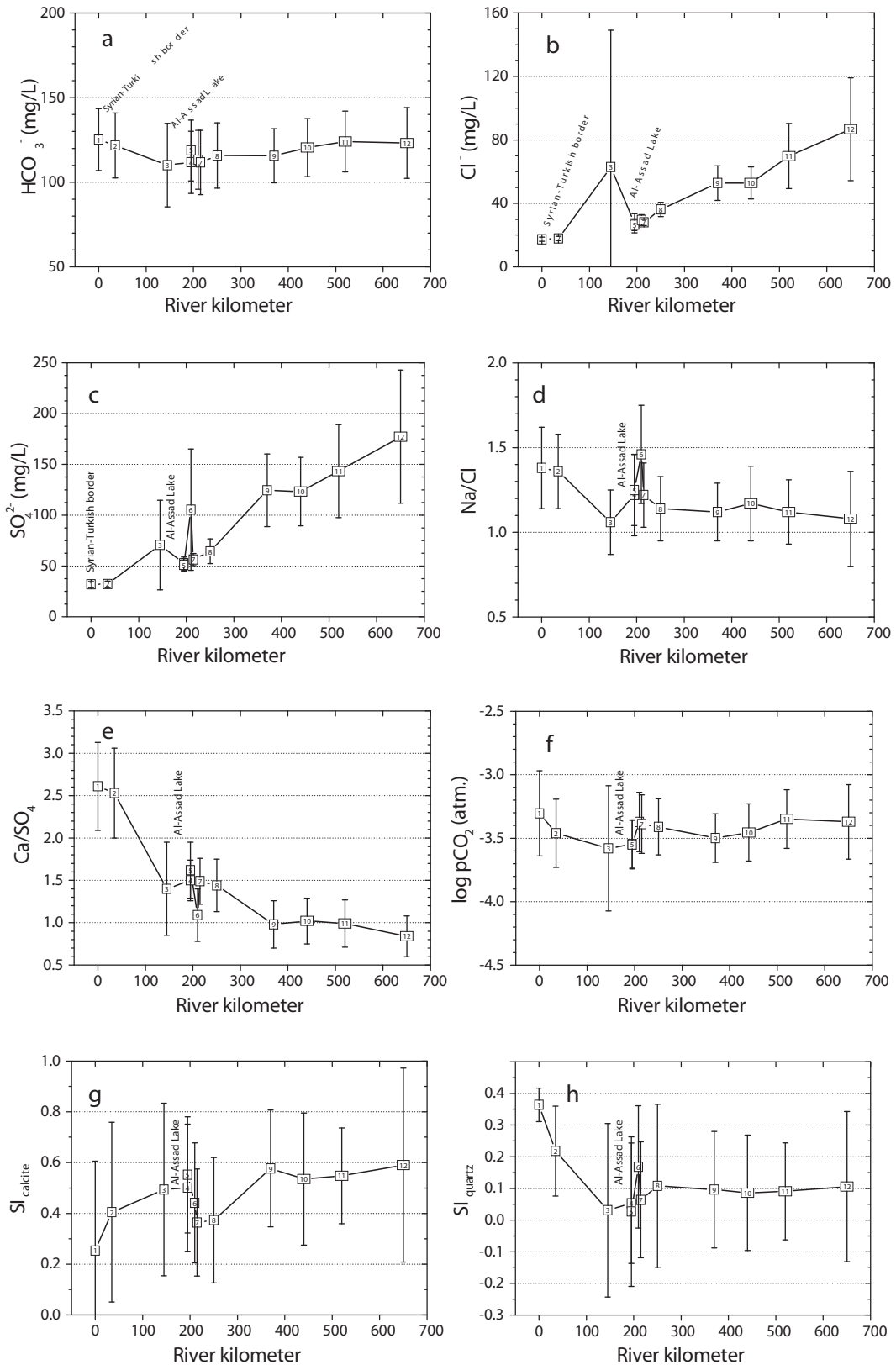


FIG. 10. Spatial variations of average and standard deviations (error bars) of the HCO_3^- (a), Cl^- (b), SO_4^{2-} (c) values, Na/Cl (d), Ca/SO₄ (e) ratios, log pCO₂ (f) and saturation indices: SI_{calcite} (g), SI_{quartz} (h) along the different stations of the Euphrates River during the period 2004–2006.

The determination of ionic ratios (expressed in meq/L) of major ions in water systems is a useful tool to differentiate between different mineralization sources [55–60]. The calculation results of mean ionic ratios (Mg/Ca, Na/Cl, Ca/SO₄, SO₄/HCO₃) of water samples collected from the Euphrates River at different sites during the study period are compiled in Table 1. The data enables one to distinguish between two groups: 1) the river water of the upper first two sites, characterized by a high Ca/SO₄ ratio indicating the carbonate signature of the mineralization, and 2) the river water of the other downstream stations, where this ratio becomes gradually lower with river distance. This group reflects more the influence of evaporation, as well as further salinity input from the dissolution of soluble salts halite (NaCl) and thenardite (Na₂ SO₄), which are accumulated in soil horizons or liberated from the dissolution of local evaporitic rocks (gypsum and anhydrite), and/or saline groundwater input through the riverbed from drainage return flows [19, 30, 54].

Spatial trends in Na/Cl and Ca/SO₄ ratios in function of the river kilometre distance (Figs 10d and 10e) permits detection of a gradual decrease in these ratios as a consequence of the liberation of further amounts of sodium and sulphate, mainly from the dissolution of halite, thenardite, mirabilite (Na₂ SO₄ × 10(H₂O) and bloedite (Na₂Mg(SO₄) × 4(H₂O) in the case of sodium, and from gypsum, anhydrite, thenardite, mirabilite and bloedite in the case of sulphate [30]. The average values of the average partial pressure of dissolved CO₂, together with the saturation indexes with respect to calcite and quartz of all water samples collected from the Euphrates River at the different sites during the study period, were calculated using the WATEQ4F program [61]. Figures 10f–10h illustrate the spatial variations for the above mentioned parameters along different stations of the Euphrates River during the period 2004–2006. The spatial evolution of average partial pressure of dissolved CO₂ is marked by small fluctuations around the value of the atmosphere (log pCO₂ = –3.5), with rather higher values at site No. 6 due to tributary contribution, and lower values at Al-Assad Lake, which

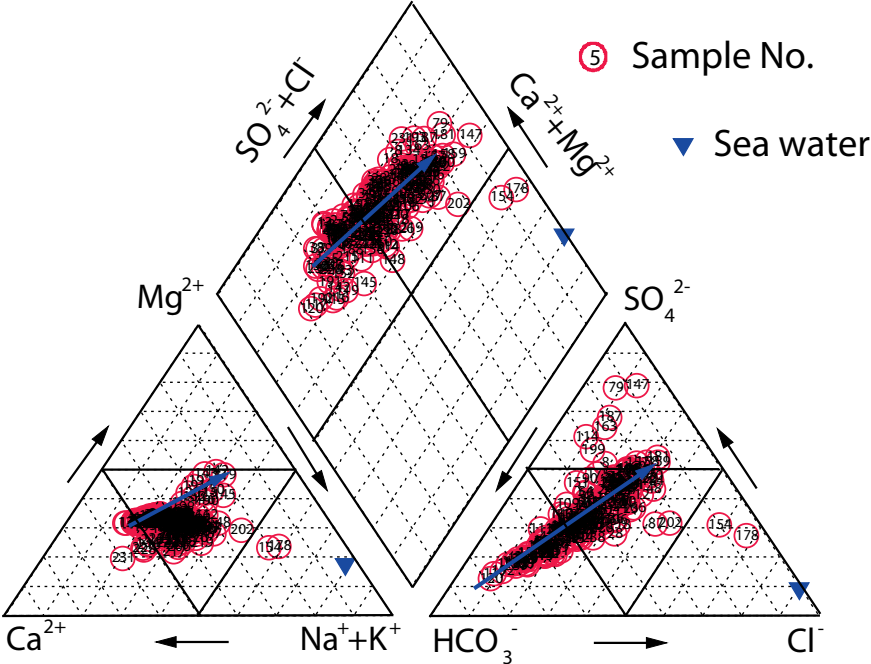


FIG. 11. Piper diagram of surface water samples collected from the Euphrates River during the period 2004–2006.

is susceptible to precipitations of carbonate minerals. Although data shows that river water at all monitored stations is over-saturated with respect to calcite and quartz, opposite evolution patterns can be observed for the saturation indices with respect to calcite (Fig. 10g) and quartz (Fig. 10h), especially within the section containing the upper eight stations. Figure 11 represents a projection of the chemical composition of all water samples collected from the Euphrates River during the period 2004–2006 in the Piper diagram. This plot shows that fresh water samples are usually of a calcium–magnesium and bicarbonate type, and that river water salinity evolves towards a sodium–chloride type or a sodium–sulphate type.

5.2. Stable isotope composition of precipitation

The application of stable and radioactive natural isotopes has become a useful tool in hydrological research, especially in the study of meteoric water, surface water and groundwater. By far the most common isotopes applied are those of the elements hydrogen, oxygen and carbon, which are crucial in the water cycle. The concentration ratios of stable isotopes ($^2\text{H}/^1\text{H}$, $^{18}\text{O}/^{16}\text{O}$) varies depending on the water source and natural processes, such as evaporation and condensation. Radioactive isotopes (^3H , ^{14}C) may provide indications of water sources and the time elapsed since infiltration.

The isotopic composition of meteoric water has been extensively monitored on most continents at regional and global scales [25, 62–66]. Knowledge of the spatial and temporal evolution of the isotopic composition of atmospheric waters as a major input function of most hydrological and hydrogeological systems was successfully used to characterize the behaviour of water resources in terms of recharge origin, replenishment rate, evaporation, mixing process and interconnection between aquifers [3, 21, 25, 67, 68], as well as to predict climatic variations [65, 68].

Results of the weighted mean isotopic composition of rainfall waters collected from two stations in Syria (Jarablous and Al-Raqqa) have been compiled, together with those of three Turkish meteorological stations (Adana, Diyarbakir and Erzurum) in Table 2. The weighted means of the isotopic composition for the different stations were calculated using the following equation [69]:

$$\delta_w = \frac{\sum_i^n [P_i \cdot \delta_i]}{\sum_i^n [P_i]} \quad (1)$$

where

δ_w is the weighted mean isotopic composition of rainfall

P_i is the precipitation amount for the month i

δ_i is the isotopic composition of rainfall for the month i .

Data show that the isotopic composition of rainfall from the two Turkish stations of Diyarbakir (686 m.a.s.l) and Erzurum (1695 m) is depleted in ^{18}O and ^2H by $\pm 1.5\text{‰}$ and $\pm 2.5\text{‰}$, respectively, compared to the mean of the three Turkish stations (Adana, Diyarbakir and Erzurum) which is $\pm 0.5\text{‰}$ and $\pm 1.0\text{‰}$, respectively. The isotopic composition of rainfall from the two Syrian stations (Jarablous and Al-Raqqa) is intermediate between the two Turkish stations, with a depletion in ^{18}O and ^2H of $\pm 1.0\text{‰}$ and $\pm 2.0\text{‰}$, respectively.

The stable isotope composition of rainfall samples collected from the Jarablous and Al-Raqqa stations occupies an intermediate position between the two earlier rainfalls. The value

TABLE 2. WEIGHTED MEAN ISOTOPIC COMPOSITIONS OF RAINFALL COLLECTED FROM TWO STATIONS IN SYRIA AND THREE STATIONS IN TURKEY

Station	Altitude (m.a.s.l.)	Period	$\delta^{18}\text{O}$ (‰, VSMOW)	$\delta^2\text{H}$ (‰, VSMOW)	d (‰, VSMOW)
Jarablous	350	1991–1993	-7.55	-41.5	18.9
Al-Raqqa	250	1991–1992	-6.44	-32.5	19.0
Diyarbakir ^a	686	1966–1968	-9.98	-59.5	20.3
Adana ^a	73	1963–1987	-5.50	-28.0	16.0
Erzurum ^a	1695	1990–1992	-10.18	-63.2	18.2

^aTurkish stations (data from IAEA, 1981 [1]; IAEA, 1992 [64] and Sayin et al., 1994 [70]).

of the deuterium excess (d), which was defined as: $d = \delta^2\text{H} - 8\delta^{18}\text{O}$ [62] highly depends on the relative humidity of air masses at their origin and kinetic effects during evaporation [71, 72]. They can be used to indicate whether more evaporated moisture has been added to the atmosphere (high d value) or whether water samples have been fractionated by evaporation (low d value). Data show that this parameter is significantly higher than 10‰, the value given for global meteoric waters [73]. The highest d values ($d > 19\text{‰}$) are found at stations with higher altitudes. Based on d values, it is possible to distinguish between the following two series: (1) the rains of Jarablous, Al-Raqqa, Diyarbakir and Erzurum stations, which have a d value close to $19 \pm 1\text{‰}$, and (2) the rains of Adana station, characterized by a lower d value ($d \approx 16 \pm 0.5\text{‰}$).

As the isotopic composition of rainwater is the result of interactions between humid marine air masses and dry continental air masses [74], the increasing d value may be attributed to the effect of isotopic exchange with moisture originating from the Mediterranean Sea. This

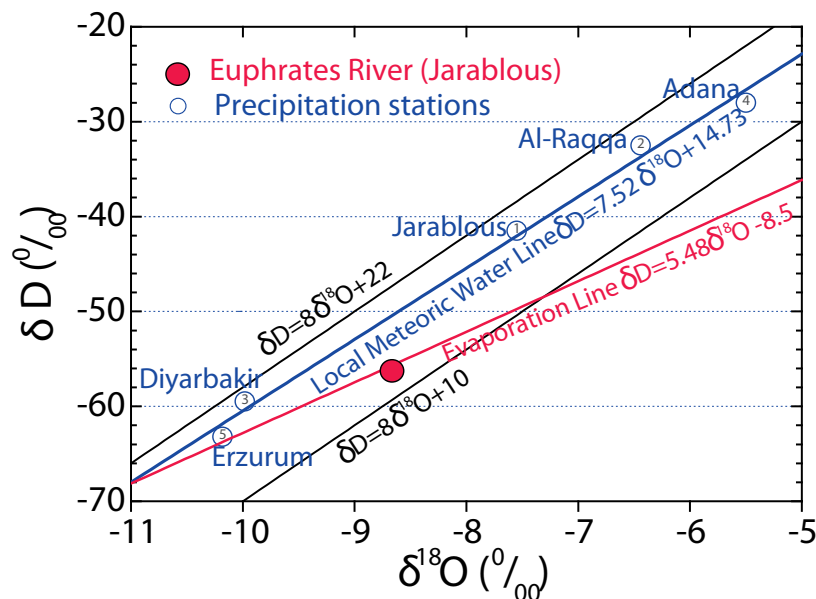


FIG. 12. The relationship between weighted means of $\delta^{18}\text{O}$ and $\delta^2\text{H}$ values in precipitation from different meteorological stations in Syria and Turkey.

moisture is generally characterized by low relative humidity [69, 75, 76], whereas rains with low d values are probably more affected by moisture originating from the Black Sea [34, 70].

Figure 12 shows the relationship between $\delta^{18}\text{O}$ and δD weighted mean values of precipitation from five meteorological stations located in Syria and Turkey. This plot shows that all of the sample points are situated between the Mediterranean meteoric water line (MMWL) defined as: $\delta^2\text{H} = 8\delta^{18}\text{O} + 22$, and the global meteoric water line (GMWL) shown as: $\delta^2\text{H} = 8\delta^{18}\text{O} + 10$.

The equation of the least squares regression line, fitting all the sample points representing selected Syrian and Turkish stations, is shown as:

$$\delta^2\text{H} = (7.52 \pm 0.34)\delta^{18}\text{O} + (14.73 \pm 2.8) \quad (2)$$

with $R^2 = 0.994$ and $N = 5$

This equation is somewhat different from that established for the Syrian meteoric water line (SMWL) by [77, 78]:

$$\delta^2\text{H} = (8.26 \pm 0.37)\delta^{18}\text{O} + (19.30 \pm 2.7) \quad (3)$$

with $R^2 = 0.963$ and $N = 9$

The difference between the two equations is mainly reflected in the low value of the intercept, which is lower in the case of Syrian–Turkish rainfalls ($\cong 15\%$). The decrease in the intercept value is mainly influenced by Adana precipitation, which is characterized by a lower d value ($\cong 16\%$). In all the cases, the estimated intercept value is below the value (22‰) given for the eastern Mediterranean region [75]. The slope of the local precipitation line (7.52) is slightly lower than that (8.17) of the unweighted global meteoric water line, shown as [65]: $\delta^2\text{H} = 8.17\delta^{18}\text{O} + 10.35$. This low slope (7.52) is commonly attributed to the fact that rainfall has undergone a rather small evaporation process under low humidity conditions [69].

5.3. Stable isotope composition of the Euphrates River

The mean isotopic composition ($\delta^{18}\text{O}$ and $\delta^2\text{H}$) of water samples collected from the Euphrates River at 12 stations along its course during the study period are compiled in Table 3, together with the deuterium excess values (d).

5.3.1. Temporal variations

Figure 13 represents the temporal evolutions of $\delta^{18}\text{O}$ and $\delta^2\text{H}$ concentrations, as well as the deuterium excess value of six stations along the Euphrates River during the period 2004–2006. Although, the temporal evolutions of $\delta^{18}\text{O}$ and $\delta^2\text{H}$ concentrations and deuterium excess values were generally not too considerable compared to those of other large rivers, their variations permit the distinction between two water groups:

- (1) The waters of the first two upper stations (site Nos. 1 and 2), which have identical patterns of evolution with a small lag effect, isotopically depleted compositions during summer and autumn and enriched contents from February to May.
- (2) The waters of the remaining downstream stations, which all have rather similar evolution trends, distinctly opposite to that of the first group.

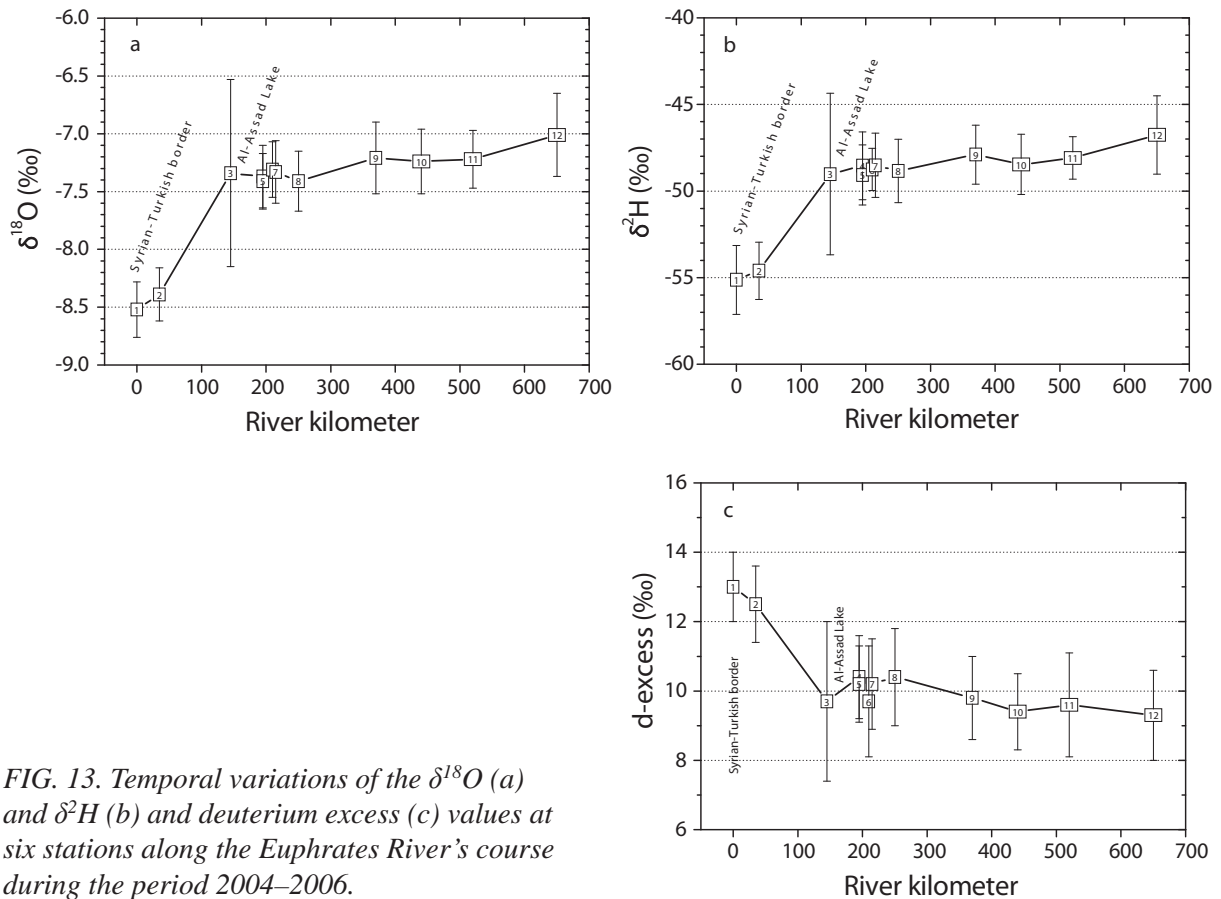


FIG. 13. Temporal variations of the $\delta^{18}\text{O}$ (a) and $\delta^2\text{H}$ (b) and deuterium excess (c) values at six stations along the Euphrates River's course during the period 2004–2006.

TABLE 3. MEAN ISOTOPIC COMPOSITIONS OF WATER SAMPLES COLLECTED FROM THE EUPHRATES RIVER AT 12 STATIONS ALONG ITS COURSE DURING THE PERIOD 2004–2006.

Site No.	Location	$\delta^{18}\text{O}$	$\delta^2\text{H}$ (‰, SMOW)	d	^3H (TU)
1	Jarablous*	-8.52 ± 0.2	-55.1 ± 2.0	13.0 ± 1.0	7.8 ± 0.4
2	Qaraqousak*	-8.39 ± 0.2	-54.6 ± 1.7	12.5 ± 1.1	7.7 ± 0.4
3	Maskaneh**	-7.34 ± 0.8	-49.0 ± 4.7	9.7 ± 2.3	7.7 ± 0.4
4	Euphrates Dam-a**	-7.37 ± 0.3	-48.5 ± 2.0	10.4 ± 1.2	7.7 ± 0.4
5	Euphrates Dam-b*	-7.41 ± 0.2	-49.1 ± 1.7	10.2 ± 1.1	7.8 ± 0.6
6	Al-Mansoura**	-7.31 ± 0.2	-48.8 ± 1.2	9.7 ± 1.6	7.6 ± 0.4
7	Al-Baath Dam**	-7.33 ± 0.3	-48.5 ± 1.9	10.2 ± 1.3	7.7 ± 0.4
8	Al-Raqqa*	-7.41 ± 0.3	-48.4 ± 1.8	10.4 ± 1.4	7.6 ± 0.5
9	Halabieh-Zalabieh**	-7.21 ± 0.3	-47.9 ± 1.7	9.8 ± 1.2	7.5 ± 0.3
10	Deir-Ezzor*	-7.24 ± 0.3	-48.5 ± 1.7	9.4 ± 1.1	7.7 ± 0.4
11	Al-Mayadine*	-7.29 ± 0.3	-48.1 ± 1.2	9.6 ± 1.5	7.6 ± 0.3
12	Albu-Kamal**	-7.01 ± 0.4	-46.8 ± 2.3	9.3 ± 1.3	7.7 ± 0.5

* Water samples collected during 2004–2006, ** water samples collected during 2004–2005.

The difference in isotopic composition between these two groups is clearly small during April and May, and relatively higher during summer and autumn. This isotopic trend is primarily the result of evaporation from the Euphrates River and its related reservoir (Al-Assad Lake). This also includes the portion of evaporated water reaching the riverbed during summer, in the form of drainage return flows.

Similarly, the temporal evolution of deuterium excess values (d) permits the distinction between the above groups: (1) the water at the two upstream stations generally has d -excess values higher than 12‰; and (2) the water at the other downstream stations has distinctly lower d -excess values ($9‰ < d < 12‰$). Although there is a shift of about 3‰ in the d -excess value between these two groups, it is noteworthy to observe that the temporal evolution of this parameter evolves in a similar way. The reason behind low d -excess values in the downstream stations is evidently because of evaporation, mainly from Al-Assad Lake, as water is stored for a long period.

5.3.2. Spatial variations

Figure 14 illustrates the spatial variations in $\delta^{18}\text{O}$, $\delta^2\text{H}$ and deuterium excess (d -excess) average values at different sites along the Euphrates River during the study period 2004–2005. The spatial evolution of $\delta^{18}\text{O}$ and $\delta^2\text{H}$ compositions along the Euphrates River course are identical (Figs 14a and 14b). As the river flows from Jarablous towards Al-Assad Lake, this evolution is represented by a significant increase in isotopic composition ($\approx 1.1‰$ and $\approx 6‰$ for $\delta^{18}\text{O}$ and $\delta^2\text{H}$, respectively). It is noted that the average isotopic composition of Al-Assad Lake (site No. 3) was more or less close to that of the lake at site Nos 4 and 5. Although site Nos 4 and 5 are oppositely located on the end margins of the Euphrates Dam body, the isotopic composition of water was interestingly identical, meaning that the lake water is rather homogeneous and hence has undergone a similar evaporation processes.

Spatial evolutions permit differentiation between the less evaporated water (isotopically depleted) of the river at its entry point from Turkey, and more evaporated water (isotopically enriched), such as the water of Al-Assad Lake. Downstream from the Euphrates Dam, the isotopic composition of the river water exhibits slight enrichment ($\approx 0.4‰$ and $\approx 2‰$ for $\delta^{18}\text{O}$ and $\delta^2\text{H}$, respectively), meaning that the river water is less affected by evaporation than the lake water. This behaviour can also be observed in the spatial evolution of deuterium excess values (Fig. 14c), ranging from 12.5‰ to 13‰ at upstream stations, and fluctuating within 9.3–10.4‰ in the remaining downstream sites, and completely opposites to those of $\delta^{18}\text{O}$ and $\delta^2\text{H}$ values. This spatial evolution reflects without any doubt a high evaporation process from Al-Assad Lake. This process is enhanced by a sharp increase in average lake water temperature, $\approx 5^\circ\text{C}$ higher than compared with that of Jarablous. The large volume of water in the lake (≈ 11.9 billion m^3), and the relatively high mean residence time of water in the lake (≈ 250 days, based on an average river discharge rounded to $550 \text{ m}^3/\text{s}$), together with low deuterium excess values of the lake water ($d < 10.4‰$), support the influence of significant evaporation processes taking place in such an arid environment. The systematic spatial increase of stable isotopic composition results from a combination of the following factors: (1) variations of stable isotope content in rains; (2) the downstream contribution of runoff; and (3) evaporation [18]. The isotopic properties of Euphrates water suggest precipitation and local runoff play a negligible role compared to evaporation.

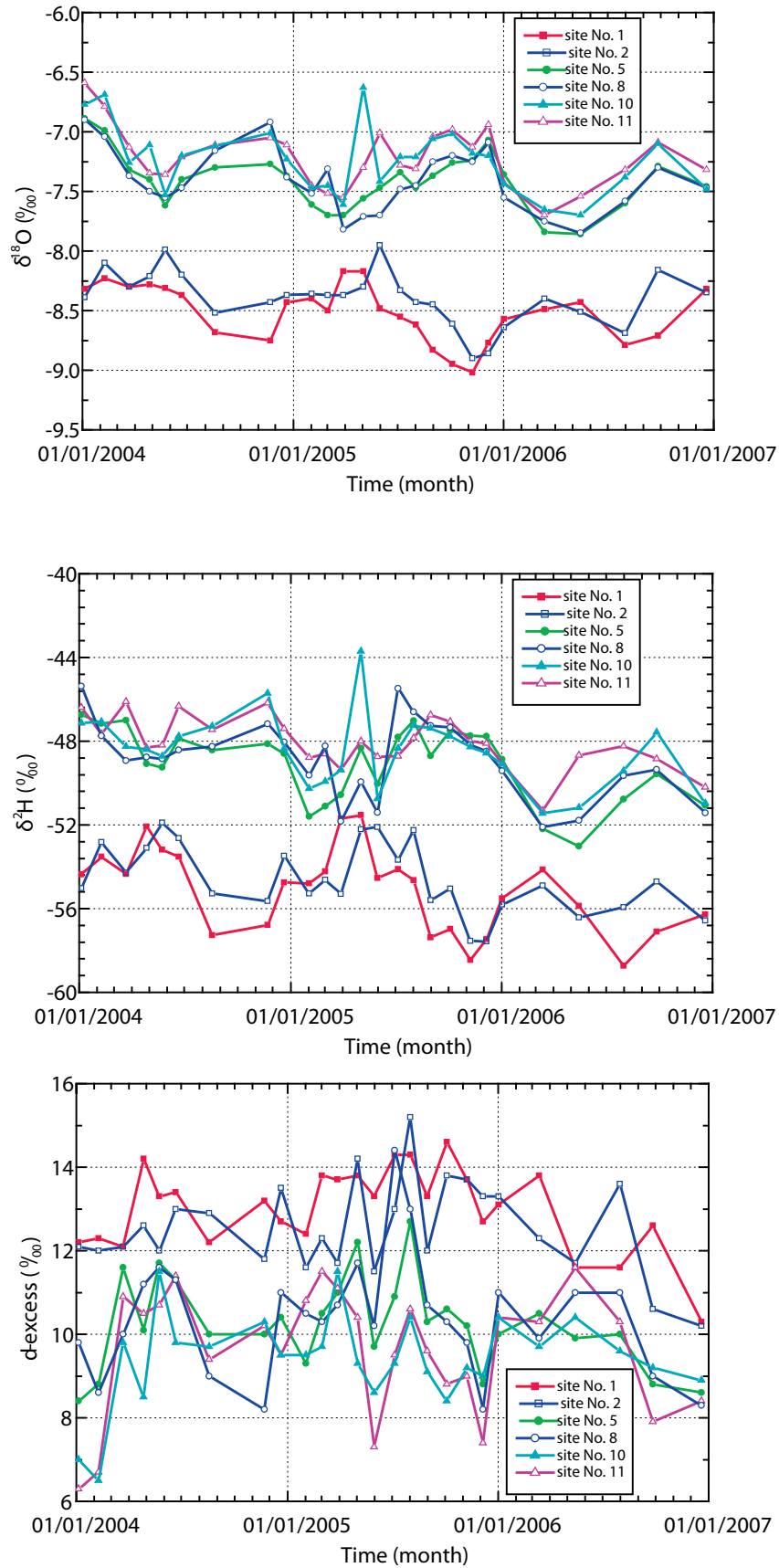


FIG. 14. Spatial variations of the average and standard deviations (error bars) of $\delta^{18}\text{O}$ (a), $\delta^2\text{H}$ (b) and deuterium excess (c) values along the different stations of the Euphrates River between 2004 and 2006.

A comparison of Euphrates River water with other large rivers in the world reveals that the range of stable isotope variations in the Euphrates River is relatively small, compared, for example, with that of the Missouri River in USA, where $\delta^{18}\text{O}$ values vary for instance between -17 and -9‰ [18]. Similarly, the $\delta^{18}\text{O}$ value of the Murray River (Australia) varies from -8.3‰ in the headwaters to $+0.37\text{‰}$ at the river mouth, while that of $\delta^2\text{H}$ changes from less than -51‰ in the headwaters to -1.8‰ in the river estuary [19]. However, vaster ranges (-25.6 to $+10.4\text{‰}$ and -198.3 to $+12.4\text{‰}$ for $\delta^{18}\text{O}$ and $\delta^2\text{H}$, respectively) were reported by Kendal and Coplen (2001, [20]) for a large number of rivers in the USA. The authors showed that rivers with depleted $\delta^{18}\text{O}$ values of less than -20‰ are mostly located in Alaska, Montana and North Dakota, and most rivers with enriched values greater than 0‰ are associated with arid area rivers, such those in Texas and Florida.

5.3.3. $\delta^2\text{H}-\delta^{18}\text{O}$ relationship

Figure 15 illustrates the relationship between $\delta^2\text{H}$ and $\delta^{18}\text{O}$ of all water samples collected from the Euphrates River during the study period 2004–2006, together with projections of the isotopic composition of two water samples collected during 2000 from the Euphrates River at the Syrian–Turkish border and the exit of the Euphrates Dam [79]. The plot shows that all water sample points from all downstream stations (site Nos 2–12) were more enriched with respect to those of the Euphrates at the Syrian–Turkish border (site no. 1). Also, it can be observed that the most enriched water samples belong to Al-Assad Lake (site No. 3) or to stations far downstream (site Nos 10–12).

The water sample points fit nicely a least squares regression line (evaporation line), approximated by the following equation:

$$\delta^2\text{H} = (5.48 \pm 0.11) \delta^{18}\text{O} - (8.50 \pm 0.83) \quad (4)$$

with $R^2 = 0.90$ and $N=276$ (4)

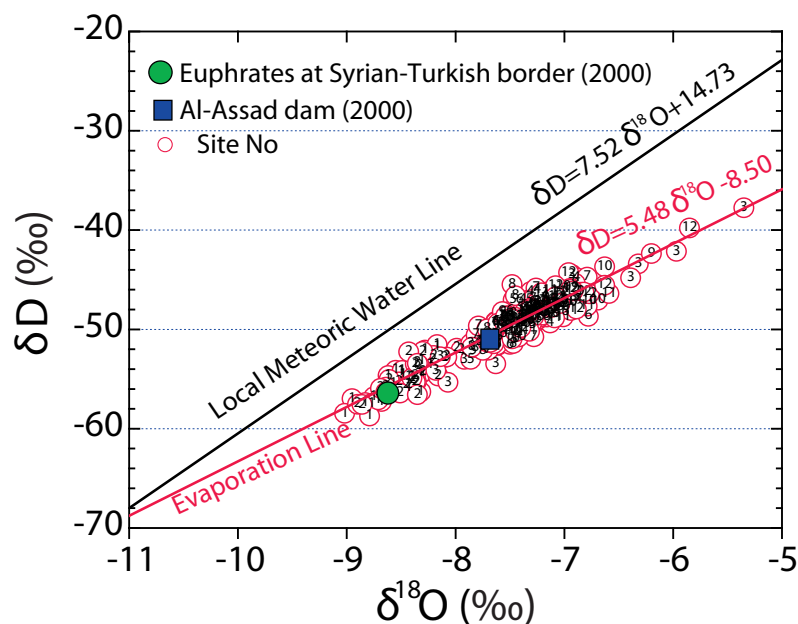


FIG. 15. Relationship between $\delta^2\text{H}$ and $\delta^{18}\text{O}$ of Euphrates River water samples collected from all stations during the period from January 2004 to December 2006.

The slope of this regression line (5.48 ± 0.11) deviates significantly from the value (8) given for the global meteoric water line GMWL [73], and obviously deviates from the more recent value (8.17) given for the unweighted GMWL of most meteoric waters around the world [65]. This slope is also lower than the slope (7.5 ± 0.34 ; Eq. 2) of the least squares regression line, characterizing local meteoric waters over Syrian–Turkish lands (Fig. 12). This means that Euphrates River water was systematically subjected to further evaporation processes after rainfall occurrences. Therefore, the observed $\delta^2\text{H}$ – $\delta^{18}\text{O}$ relationship clearly reflects the importance of water losses through evaporation from Euphrates River waters.

5.4. Tritium content in the Euphrates River

Tritium — with its half-life of about 12.43 years — is the only radioactive environmental isotope that constitutes part of the water molecule. For this reason, it has been largely used as a natural tracer in many hydrological and mathematical simulation studies [80–82]. The mean tritium concentrations of water samples collected from the Euphrates River at different stations along its course during the period 2004–2006 are given in Table 3. The data shows that the mean tritium content of Euphrates River water varies within a very small range (7.5–7.8 TU), noting that the detection limit for the determination of this isotope is below 0.5 TU.

Figure 16 illustrates the temporal variations of tritium content at six different stations along the course of the Euphrates River between January 2004 and May 2006. Accordingly, it can be seen that tritium content mostly ranges within 7–9 TU, with relatively more variations occurring during 2004. The tritium content during 2006 was even lower, below 8 TU.

The tritium content of Euphrates River water is apparently higher than that of actual rainfall (below 5–6 TU). Furthermore, it is even higher than the tritium weighted means (5.5–7.1 TU) of atmospheric precipitation recorded in the country during 1989–1993, with a decline rate of

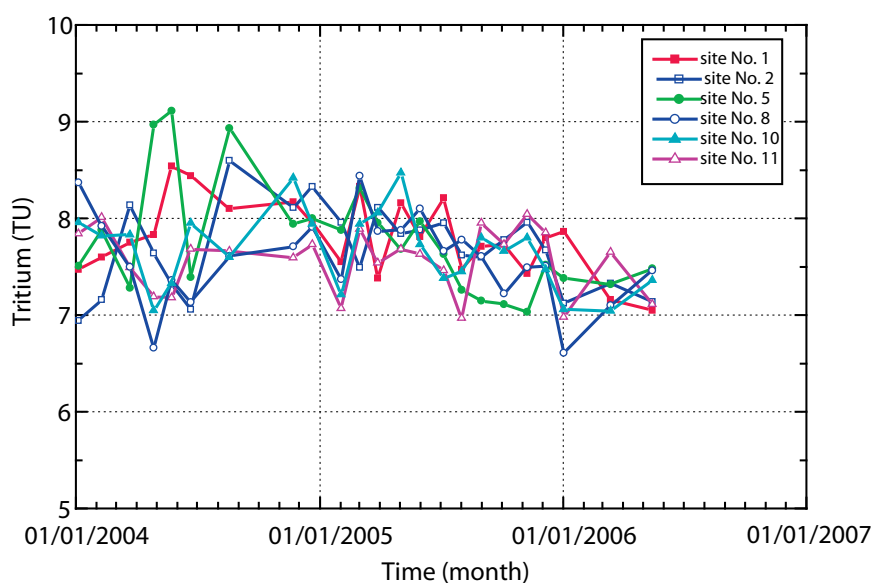


FIG. 16. Temporal variations of tritium content values at six stations along the Euphrates River's course during the period January 2004–May 2006.

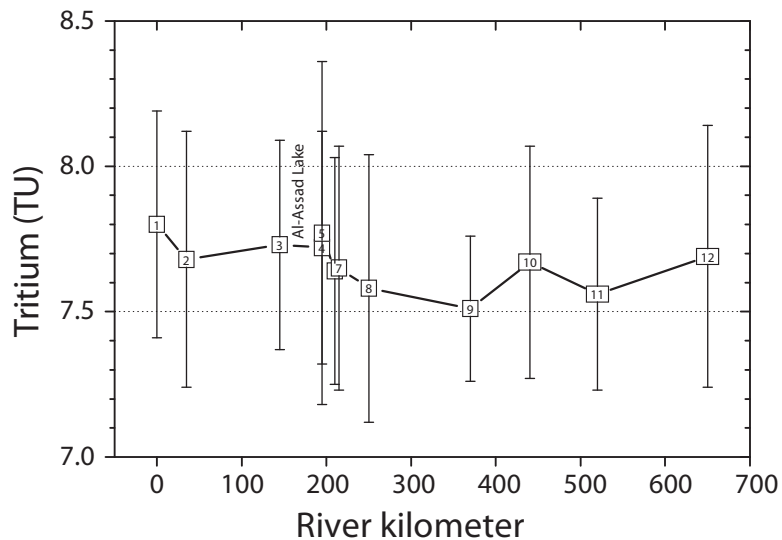


FIG. 17. Spatial variations in tritium content along the different stations of the Euphrates River during the period January 2004 to May 2005.

≈ 0.5 TU per year [83]. The cause of high tritium content in Euphrates River water compared to that of actual rainfall is mostly the storing of river water in divers dams in both Turkey and Syria. It is noted that the earlier atmospheric precipitation, and thus runoff water, was more enriched in tritium concentration as a consequence of nuclear tests conducted in the 1960s [84]. In all cases, it seems that the tritium content of the river water reflects the effect of residence time in the different lakes, mainly Al-Assad Lake, where mean residence time is close to ≈ 250 days.

Figure 17 shows spatial variations in tritium content along the different stations of the Euphrates River during the period January 2004–May 2005. This plot indicates a slight decline in tritium content along the river course. Downstream from the Euphrates dam, the tritium content stays rather constant or displays a slight increase, most probably because of evaporation.

6. CONCLUSIONS

Monitoring of temporal and spatial variations of the chemical and isotopic compositions of the Euphrates River water at 12 stations during the period 2004–2006 has so far led to the following major conclusions:

- The average chemical composition of Euphrates River water is higher than the average for world river waters. It is more comparable to rivers in semi-arid zone rivers, in term of magnesium, potassium, and bicarbonate concentrations, and with that of arid zone rivers in terms of sodium, calcium, chloride and sulphate concentrations. As the river water flows towards its estuary, the chemical facieses changes from a calcium–magnesium and bicarbonate type towards a sodium–chloride type. River salinity increases according to two different rates: the upper seven stations have a low rate, and the remaining downstream stations a relatively higher rate.

- The magnitudes of temporal and spatial variations of stable isotope compositions of the Euphrates River in Syria during the period 2004–2005 were not too considerable, compared with those of other large world rivers. Concentrations of stable isotopes generally increase downstream, with sharp enrichment at Al-Assad Lake, which also exhibits higher fluctuations of the standard deviation values of most parameters. The tritium content of Euphrates River water, higher than that of actual rainfall, changed slightly to around 7.5 TU.
- Isotopic enrichment most likely occurs due to multiple factors: (1) high evaporation rates from the Euphrates River and its tributaries; (2) long residence time of river water in Al-Assad Lake (≈ 250 days) and (3) the contribution of evaporated irrigation water reaching the river in the form of drainage return flows via groundwater discharge.

ACKNOWLEDGEMENTS

The author particularly acknowledges Prof. I. Othman, Director General of AECS, for his support and encouragement. The IAEA organization and, in particular, P.K. Aggarwal and T. Vitvar are deeply acknowledged. The author is also grateful to Drs. W. Rasoul-Agha, C. Safadi and S. Rammah for their views and valuable remarks. Thanks also to Dr. B. Zakkar from the Ministry of Irrigation in Syria for providing discharge data for the Euphrates River, and to Dr. R. Nasser, Head of the Geology Department at the AECS. The technical staff of this department who contributed to this work are gratefully acknowledged for their help in field work and performance of chemical and isotopic analyses of water samples.

REFERENCES

- [1] INTERNATIONAL ATOMIC ENERGY AGENCY, Stable isotope hydrology, Deuterium and oxygen-18 in the water cycle, Technical Reports Series No. 210, IAEA, Vienna (1981).
- [2] INTERNATIONAL ATOMIC ENERGY AGENCY, Isotopes in the water cycle, Past, Present and Future of a Developing Science (Aggarwal, P.K., Gat, J.R., Froehlich, K.F.O., Eds), Vienna, Springer, The Netherlands (2005) 381 p.
- [3] KENDALL, C., MCDONNELL, J.J. (Eds), Isotope Tracers in Catchment Hydrology, Elsevier Science Publishers: Amsterdam (1998) 839 p.
- [4] CRISS, R.E., Principles of Stable Isotope Distribution, Oxford University Press, New York (1999) 254 p.
- [5] MALOSZEWSKI, P., RAUERT, W., TRIMBORN, P., HERRMANN, A., RAU, R., Isotope hydrologic study of mean transit times in an alpine basin (Wimbachtal, Germany), *J. Hydrol.* **140** (1992) 343–360.
- [6] MALOSZEWSKI, P., STICHLER, W., ZUBER, A., RANK, D., Identifying the flow system in a karstic-fissured-porous aquifer, the Schneesalpe, Austria, by modeling of environmental ^{18}O and ^3H isotopes, *J. Hydrol.* **256** (2002) 48–59.
- [7] MALOSZEWSKI, P., ZUBER, A., Lumped parameter models for interpretation of environmental tracer data, Manual on Mathematical Models in Isotope Hydrogeology, IAEA-TECDOC-910, IAEA, Vienna (1996) 9–50.
- [8] VITVAR, T., BALDERER, W., Estimation of mean residence times and runoff generation by ^{18}O measurements in a Pre-Alpine catchment (Rietholzbach, eastern Switzerland), *Appl. Geochem.* **12** (1997) 787–796.

- [9] FREDERICKSON, G.C., CRISS, R.E., Isotope hydrology and time constants of the unimpounded Meramec river basin, Missouri, *Chem. Geol.* **157** (1999) 303–317.
- [10] VITVAR, T., BURNS, D.A., LAWRENCE, G.B., MCDONNELL, J.J., WOLOCK, D.M., Estimation of baseflow residence times in watersheds from the runoff hydrograph recession, method and application in the Neversink watershed, Catskill Mountains, New York, *Hydrol. Proc.* **16** (2002) 1871–1877.
- [11] HERRMANN, A., MARTINEC, J., STICHLER, W., Study of snowmelt-runoff components using isotope measurements, modeling of snow cover runoff. Colbeck SC, Ray M (Ed.), Hanover, Germany (1978) 228 p.
- [12] HERRMANN, A., FINEKE, B., SCHONIGER, M., MALOSZEWSKI, P., STICHLER, W., “The environmental tracer approach as a tool for hydrological evaluation and regionalization of catchment systems”, *Proc. Regionalization in Hydrology*, Ljubljana, IAHS Pub. No. 191 (1990) 45–58.
- [13] DINCER, T., PAYNE, B.R., FLORKOWSKI, T., MARTINEC, J., TONGIORGI, E., Snowmelt runoff from measurements of tritium and oxygen–18, *Water Resour. Res.* **6** (1970) 110–124.
- [14] SKLASH, M.G., FARVOLDEN, R.N., FRITZ, P., A conceptual model of watershed response to rainfall, developed through the use of oxygen–18 as a natural tracer, *Canadian J. Earth Sci.* **13** (1976) 271–283.
- [15] UHLENBROOK, S., FREY, M., LEIBUNDGUT, C., MALOSZEWSKI, P., Hydrograph separation in a mesoscale mountainous basin at event and seasonal timescales, *Water Resour. Res.* **38** (2002) 1–14.
- [16] PAYNE, B.R., QUIJANO, L., LATORRE, D.C., Environmental isotopes in a study of the origin of salinity of groundwater in the Mexicali Valley, *J. Hydrol.* **41** (1979) 201–214.
- [17] ALY, A.I.M., FROEHLICH, K., NADA, A., AWAD, M., HAMZA, M., SALEM, W.M., Study of environmental isotope distribution in the Aswan High Dam Lake (Egypt) for estimation of evaporation of lake water and its recharge to adjacent groundwater, *Environ. Geochem. Health* **15** (1993) 37–49.
- [18] WINSTON, W.E., CRISS, R.E., Oxygen isotope and geochemical variations in the Missouri River. *Environ. Geol.* **43** (2003) 546–556.
- [19] SIMPSON, H.J., HERCZEG, A.L., Stable isotope as an indicator of evaporation in the River Murray, Australia, *Water Resour. Res.* **27** (1991) 1925–1935.
- [20] KENDALL, C., COPLEN, T.B., Distribution of oxygen–18 and deuterium in river waters across the United States, *Hydrol. Proc.* **15** (2001) 1363–1393.
- [21] FRITZ, P., River waters, Stable isotope hydrology, deuterium and oxygen–18 in the water cycle, Technical Reports Series No. 210, IAEA, Vienna (1981).
- [22] MARTINELLI, L.A., GAT, J.R., CAMARGO, P.B., LARA, L.L., OMETTO, J.P.H.B., The Piracicaba river basin: Isotope hydrology of a tropical river basin under anthropogenic stress, *Isot. Environ. Health Stud.* **40** (2004) 45–56.
- [23] GIBSON, J.J., EDWARDS, T.W.D., Regional surface water balance and evaporation–transpiration partitioning from a stable isotope survey of lakes in northern Canada, *Global Biogeochemical Cycles* **10** (2002) 1029/2001GB001839.
- [24] MATSUI, E., SALATI, E., FRIEDMAN, I., BRINKMAN, W.L.F., Isotope hydrology in the Amazonia, 2, Relative discharges of the Negro and Solimoes Rivers through ¹⁸O concentrations, *Water Resour. Res.* **12** (1976) 781–793.
- [25] GAT, J.R., Oxygen and hydrogen isotopes in the hydrologic cycle, *Annu. Rev. Earth Planet. Sci.* **24** (1996) 225–262.

- [26] SALATI, E., DALL'OLLIO, A., MATSUI, E., GAT, J.R., Recycling of water in the Amazon basin: an isotopic study, *Water Resour. Res.* **15** (1979) 1250–1258.
- [27] FONTES, J.C., GONFIANTINI, R., Comportement isotopique au cours de l'évaporation de deux bassins Sahariens, *Earth Planet. Sci. Lett.* **3** (1967) 258–269.
- [28] GERSAR-SCET, Development of the lower Euphrates valley, Technical Report Zone 1, Ministry of Irrigation, Syrian Arab Republic, Damascus (1977) 266 p.
- [29] DOSSO, M., Géochimie des sols salés et des eaux d'irrigation. Aménagement de la basse vallée de l'Euphrate en Syrie, Thèse Docteur Ingénieur, Université de Paul Sabatier, Toulouse, France (1980) 181 p.
- [30] KATTAN, Z., NAJJAR, H., "Groundwater salinity in the Khabour-Euphrates down-streams valleys, Groundwater and Saline Intrusion", *Hidrogeología y Aguas Subterráneas*, Instituto Geológico y Minero de España, Vol. 15 (2005) 565–583.
- [31] UNITED NATIONS DEVELOPMENT PROGRAMME – FOOD AND AGRICULTURE ORGANIZATION, Étude des Ressources en Eaux Souterraines (République Arabe Syrienne), Rapport final, FAO/SF (1966) 17/SYR, 276.
- [32] JAPAN INTERNATIONAL COOPERATION AGENCY, The study of water resources development in the western and central basins in Syrian Arab Republic, Project document, Ministry of Irrigation, Damascus (2002).
- [33] PONIKAROV, V.O., The geology of Syria, Explanatory notes on the map of Syria, Scale 1:500,000, Part II, Mineral deposits and underground water resources, Technoexport, Moscow (1967).
- [34] KATTAN, Z., Use of hydrochemistry and environmental isotopes for evaluation of groundwater in the Paleogene limestone aquifer of the Ras Al-Ain area (Syrian Jezireh), *Environ. Geol.* **41** (2001) 128–144.
- [35] CLARK, I.D., FRITZ, P., Environmental isotopes in hydrogeology. Lewis Publishers, Boca Raton, New York, (1997) 328 pp.
- [36] GARRELS, R.M., MACKENZIE, F.T., Evolution of the sedimentary rocks, WW Norton, New York (1971) 397 p.
- [37] CLARKE, F.W., Data of geochemistry, 5th edition, USGS Survey Bull., No. 770, (1924) 841 p.
- [38] GIBBS, R.J., Mechanism controlling world water chemistry, *Science* (1970) 170 p.
- [39] STALLARD, R.F., EDMOND, J.M., Geochemistry of the Amazon, 2- Influence of geology and weathering environment on the dissolved load, *J. Geophys. Res.* **88** (1983), 9671–9688.
- [40] MARTINS, O., Geochemistry of the Niger River, Transport of carbon and minerals in major world rivers, Part 1 (edit. Degens ET), Hamburg University, SCOPE / UNEP Sonderb. **52** (1983) 397–418.
- [41] KEMPE, S., Impact of the High Dam on water chemistry of the Nile. Transport of carbon and minerals in major world rivers, Part 2, (Degens, E.T., Kempe, S., Soliman, H., Eds), Hamburg University, SCOPE / UNEP Sonderb **58** (1983) 410–423.
- [42] WALLING, D.E., The sediment delivery problem. *J. Hydrol.* **65** (1983) 209–237.
- [43] MEYBECK, M., Les fleuves et le cycle géochimique des éléments, Thèse d'État, Université Pierre et Marie Curie, Paris VI (1984).
- [44] NKOUNKOU, P.R., PROBST, J.L., Hydrology and geochemistry of the Congo River system, Transport of carbon and minerals in major world rivers, Part 4, (Degens, E.T., Kempe, S., Wei-Bin, G., Eds), Hamburg University, SCOPE/UNEP Sonderb **64** (1987) 483–508.

- [45] KATTAN, Z., Géochimie et hydrologie des eaux fluviales des bassins de la Moselle et de la Meuse, Transports dissous et particulaires, Cycles biogéochimiques des éléments, Thèse Ph. D., Univ. Louis Pasteur, Strasbourg, France (1989) 220 p.
- [46] MEYBECK, M., Concentration des eaux fluviales en éléments majeurs et apports en solution aux océans. *Revue Géol. Dyn. et Géogr. Phys.* 21, fasc 3 (1979) 215–246.
- [47] MEYBECK, M., “Atmospheric inputs and river transport of dissolved substances”, Proc. IAHS symposium on dissolved loads of river and surface water quantity and quality relationships, IAHS Publ 141, Germany, Hamburg (1983).
- [48] LIVINGSTONE, D.A., Data of geochemistry (6th edition), USGS, Prof. Paper 440-G (1963).
- [49] MEYBECK, M., Composition chimique des ruisseaux non pollués en France, *Sci. Géol. Bull.* 39 1 (1986) 3–77.
- [50] DERMINE, B., Bilan des charges en nutriments charriés au long du cours de la Meuse belge, Thèse doct., Facultés Universitaires de Namur (1985).
- [51] KEMPE, S., Sinks of the anthropogenically enhanced carbon cycle in surface fresh water, *J. Geophys. Res.* 89 (1984) 4657–4676.
- [52] STUMM, W., MORGAN, J.J., *Aquatic chemistry; An introduction emphasizing chemical equilibria in natural waters*, J Wiley, New York (1981).
- [53] ALLISON, G.B., The relationship between ^{18}O and deuterium in water in sand columns undergoing evaporation, *J. Hydrol.* 55 (1982) 163–169.
- [54] KATTAN, Z., Estimation of evaporation and irrigation return flow in arid zones using stable isotope ratios and chloride mass-balance analysis: Case of the Euphrates River, Syria, *J. Arid Environ.* (2007).
- [55] HEM, J.D., Study and interpretation of the chemical characteristics of natural waters. US Geol Survey Water-Supply Paper, Reston 2254 (1992),
- [56] SCHOELLER, H., Géochimie des eaux souterraines, Application aux eaux des gisements de pétrole, Soci. des Editions ‘Technip’, Paris, (1956) 15 p.
- [57] SCHOELLER, H., *Geochemistry of groundwaters. Groundwater studies- an international guide for research and practice*, UNESCO, Paris, Ch. 15 (1977) 18 p.
- [58] HSU, K.J., Solubility of dolomite and composition of Florida groundwaters, *J. Hydrol.* 1 (1963) 288–310.
- [59] WHITE, D.E., HEM, J.D., WARING, G.A., Chemical composition of subsurface waters, Data of geochemistry (6th ed.), USGS, Prof. Pap. 440-F (1963) p. F1-F67
- [60] ROSENTHAL, E., Chemical composition of rainfall and groundwater in recharge areas of Bet Shean-Harod multiple aquifer system, *Israel. J. Hydrol.* (1987) 329–352.
- [61] PLUMMER, L.N., JONES, B.F., TRUESDELL, A.H., WATEQF- A FORTRAN IV Version of WATEQ, USGS, Water Resour. Invest. 13 (1976) 61 p.
- [62] DANSGAARD, W., Stable isotopes in precipitation, *Tellus* 16 (1964) 436–468.
- [63] GAT, J.R., “The isotopes of hydrogen and oxygen in precipitation”, *Handbook of Environmental Isotope Geochemistry*, (Fritz, P., Fontes, J.C., Eds), Elsevier, New York (1980).
- [64] INTERNATIONAL ATOMIC ENERGY AGENCY, Statistical treatment of data on environmental isotopes in precipitation, Technical Reports Series No. 331, IAEA, Vienna (1992).
- [65] ROZANSKI, K., ARAGUAS, L., GONFIANTINI, R., “Isotopic patterns in modern global precipitation”, *Climate change in continental isotopic records* (Swart, P.K., Lohmann, K.C., McKenzie, J. Savin, S., Eds), *Am. Geophys. Union Monogr. Series*, No. 78 (1993) 1–36.

- [66] GONFIANTINI, R., ROCHE, M.A., OLIVRY, J.C., FONTES, J.C., ZUPPI, G.M., The altitude effect on the isotopic composition of tropical rains, *Chem. Geol.* **181** (2001) 147–167.
- [67] ROZANSKI, K., Deuterium and oxygen-18 in European groundwaters; links to atmospheric circulation in the past. *Chem. Geol.* **52** (1985) 349–363.
- [68] ROZANSKI, K., ARAGUAS, A.L., GONFIANTINI, R., Relation between long-term trends of oxygen-18 isotope composition of precipitation and climate, *Science* **258** (1992) 981–985.
- [69] YURTSEVER, Y., GAT, J.R., Atmospheric waters, Stable isotope hydrology, Deuterium and oxygen-18 in the water cycle, Technical Reports Series No. 210, IAEA, Vienna (1981).
- [70] SAYIN, M., CAN, D., CIFTER, C., The determination of environmental isotope contents of precipitation in Turkey, Report for the co-ordination meeting of a regional technical co-operation project, State Hydraulic Works (DSI), Ankara, Turkey (1994) 1–10.
- [71] MERLIVAT, L., JOUZEL, J., Global climatic interpretation of deuterium-oxygen 18 relationship for precipitation, *J. Geophys. Res.* **84** (1979) 5029–5033.
- [72] GAT, J.R., MATSUI, E., Atmospheric water balance in the Amazon Basin. An isotopic evapo-transpiration model, *J. Geophys. Res.* **96** (1991) 3179–3188.
- [73] CRAIG, H., Isotopic variations in meteoric waters, *Science* **133** (1961) 1702.
- [74] GAT, J.R., CARMI, I., Evolution of the isotopic composition of atmospheric water in the Mediterranean Sea Area, *J. Geophys. Res.* **75** (1970) 3039–3048.
- [75] NIR, A., “Development of isotope methods applied to groundwater hydrology”, Proc. Symp. isotope techniques in the hydrological cycle, Am.Geophys. Union Monogr. Series, No. 11 (1967).
- [76] DINCER, T., PAYNE, B.R., An environmental isotope study of the south-western karst region of Turkey, *J. Hydrol.* **14** (1971) 233–258.
- [77] KATTAN, Z., Chemical and environmental isotope study of precipitation in Syria, *J. Arid Environ.* **35** (1997) 601–615.
- [78] KATTAN, Z., Environmental isotope study of the major karst springs in Damascus limestone aquifer systems: Case of the Figehe and Barada springs, *J. Hydrol.* **193** (1997) 161–182.
- [79] SAJJAD, I., Sustainable utilization of saline groundwater and wastelands for plant production (project No. INT-5.144-9.004-01), Report of an Expert Mission, IAEA, Vienna (2000).
- [80] FONTES, J.C., Dating of groundwater, Guidebook on nuclear techniques in hydrology, Technical Reports Series No. 91, IAEA, Vienna (1983).
- [81] YURTSEVER, Y., Models for tracer data analysis, Guidebook on nuclear techniques in hydrology, Technical Reports Series No. 91, IAEA, Vienna (1983).
- [82] ZUBER, A., On calibration and validation of mathematical models for the interpretation of environmental tracer data in aquifers, Proc. final Research Co-ordination Meeting, IAEA-TECDOC-777, IAEA, Vienna (1994).
- [83] KATTAN, Z., Characterization of surface water and groundwater in the Damascus Ghotta basin: hydrochemical and environmental isotopes approaches, *Environ.Geol.* **51** (2006) 173–201.
- [84] ERIKSSON, E., Stable isotopes and tritium in precipitation, Guidebook on nuclear techniques in hydrology, Technical Reports Series No. 91, IAEA, Vienna (1983).

ISOTOPE INVESTIGATIONS OF MAJOR RIVERS OF INDUS BASIN, PAKISTAN

M. Ahmad^a, Z. Latif^a, J.A. Tariq^a, M. Rafique^a, W. Akram^a, P. Aggarwal^b,
T. Vitvar^b

^a Pakistan Institute of Nuclear Science and Technology, P.O. Nilore, Islamabad, Pakistan

^b Isotope Hydrology Section, IAEA, Vienna, Austria

ABSTRACT

Indus River is one of the longest rivers in the World. It has five major tributaries joining from eastern side, the Bias, Satlej, Ravi, Chenab and Jhelum, while a number of small rivers join the Indus on the west side. These perennial rivers originate from mountains covered with glaciers. Isotopic (^{18}O , ^2H , ^3H) monitoring of these rivers was carried out between 2002 and 2005 to study temporal variations of these isotopes at different control points and to understand water cycles and hydrological processes in the catchments of these rivers. The headwaters of the main Indus River (the Hunza, Gilgit and Kachura tributaries) display the most depleted $\delta^{18}\text{O}$ (-14.5 to -11.0‰) and $\delta^2\text{H}$ (-106.1 to -72.6‰) values due to precipitation at very high altitudes and very low temperatures. Generally these waters have low d-excess, which indicates that the moisture source is the Indian Ocean. The high d-excess in some winter (November–February) samples from the Hunza and Gilgit indicate the dominance of Mediterranean moisture sources. Kachura station has a $\delta^{18}\text{O}$ - $\delta^2\text{H}$ line with a slope of 4 and low d-excess, indicating an evaporation effect in Kachura Lake. The Indus River become enriched in isotopes going downstream towards the Arabian Sea because of contributions from rains at low altitude plains and a baseflow mainly recharged by local rains. At tail stations, evaporation and contribution from baseflow are responsible for isotopic enrichment. Low tritium in some samples also indicates a baseflow contribution of (relatively older groundwater). The Chenab River has the widest variation in $\delta^{18}\text{O}$ and $\delta^2\text{H}$, and the slope of the $\delta^{18}\text{O}$ - $\delta^2\text{H}$ line is 6.1, which is due to the variable contribution of snowmelt at high altitudes and rains at low altitudes. High d-excess in snowmelt and low d-excess in monsoons show that the moisture source in winter is generally western (Mediterranean) and that monsoon conditions predominantly originate from the Indian Ocean. The Kabul River has experiences a wide variation in isotopic values, probably due to variable contribution from the Swat River, which carries snowmelt. High d-excess associated with depleted isotopic values indicates a dominance of Mediterranean moisture sources in winter, while a low d-excess associated with enriched isotopic values, which typically occurs during summer monsoons points to the Bay of Bengal as the major source of moisture. The Jhelum River and its tributaries upstream of Mangla Lake experience enriched $\delta^{18}\text{O}$ and $\delta^2\text{H}$ due to the low altitude of its catchment. Precipitation in the catchment results from Indian Ocean moisture sources, and there is not any significant evaporation effect. Isotopic variations in the river Ravi appears to be mainly due to water diversions from the western rivers through link canals.

1. INTRODUCTION

Water flow in most of the river systems is comprised of two principal components: surface run-off of precipitation and groundwater. Their respective contributions differ in each system and depend on the physical setting of the drainage basin as well as on climatic parameters. Water in a river may thus vary in its isotopic composition, for example large seasonal variations are observed in rivers and lakes in which surface run-off dominates discharge. Isotope signals in river discharge can potentially contribute to a better understanding of the continental portion

of the hydrological cycle, including information such as water origin, mixing history, water balance, water residence time, surface and groundwater exchange and renewal rates, and evaporation-transpiration partitioning. If used in conjunction with more classic hydrologic tools and other chemical techniques, a description of parameters and processes controlling river flow can be obtained. Applications could range from input into a water management programme to model verifications [1, 2]. Stable isotopes also provide information on the source of moisture in rains, especially the monsoon circulation [3].

Pakistan lies between latitudes 24° and 37° north and between longitudes 61° and 76° east. It possesses quite complicated and attractive physiographical features. There are many series of mountain ranges, and areas of deep broad valleys inbetween. This includes the famous valley of the Indus, which has been a cradle of ancient civilization like those of the delta area of the Nile and the valley of the Tigris Euphrates. The Indus River is one of the longest rivers in the world. It has five major tributaries joining from eastern side, which are the Bias, Sutlej, Ravi, Chenab and Jhelum, while a number of small rivers join the Indus on the right side. The biggest is the Kabul with its main tributaries, the Swat, Panjkora and Chitral [4].

All the main rivers of Pakistan are perennial. They originate from the mountains. The physiography and climate of the rivers' catchments vary widely. Going from the catchment of the River Ravi to the Indus River catchment, altitude increases and temperature decreases. In Northern Areas, mountains are covered with glaciers and some peaks are higher than 8000 m and receive snowfall even in summer. The basic source of these rivers is melting snow, rainfall and under certain conditions seepage from the formations. For certain rivers, the source of snow is seasonal which means it falls in winter and melts in summer. From the middle of March until the end of monsoon season in mid July, river water is drawn from melting snow. During monsoon season, rainfall runoff adds to the rivers over and above moisture from melting of snow, so river discharge increases manifold [4].

1.1. Drainage basins

Hydrologically, Pakistan consists of three drainage basins, which are the Kharan Desert and Makran Coastal basins, and the Indus basin in the eastern area, extending from the northeast to the southwest. The Kharan Desert is a closed inland basin which lies in the southwestern part of Pakistan in the province of Blochistan. The major streams in this basin are: the Pishin, Kashkel and Baddo. The water is discharged into shallow lakes and ponds which readily dry because rainfall is low and evaporation is very high. The extreme southwest corner of Pakistan houses the Makran Coastal Basin, which lies to the south of the Kharan Desert Basin. In this basin, several small streams drain individually into Arabian Sea. The main streams of this hydrologic unit are the Desht, Hingol, Porali and Kud. The perennial flow of these streams remains insignificant as the area is a dry desert, but at times rains in their catchment produce flash floods [5].

Among the above-mentioned three hydrological units, only the Indus Basin is of vital importance because of the volume and extensiveness of its water. The Indus Basin watershed spreads over the areas of Pakistan, India, Jammu and Kashmir, Tibet and Afghanistan. The total watershed area of the Indus Basin is 934 000 km², which is larger than the total area of Pakistan (approximately 796 000 km²). Of this area, about 60% lies in Pakistan and the independent part of Kashmir, 15% in Indian-held Kashmir, 10% in Tibet, 8% in India and 7% in Afghanistan. The longest river of the Indus Basin is the Indus River itself. It originates

in the Tibetan plateau north of Mansarwar Lake at an altitude of 5400 m from the Kailas mountain ranges of the Trans Himalayas in the extreme northeast of Pakistan. From its source to the Arabian Sea, where it finally exits, creating a delta near the Thatta area of southwest Pakistan, the Indus River traces a length of about 3200 km. During its journey to the Arabian Sea, it meets a number of rivers which are its tributaries and which include the Gartang, Shyok, Shigar, Gilgit, Hunza, Astore, Siran, Kabul, Haro, Soan, Kurram, Tank Zam, Gomal, Jhelum, Chenab, Ravi, Beas and Sutlej. The Indus River and its tributaries combined together create a gigantic river system called the Indus River System (IRSA) [5].

The rivers of the IRS receive runoffs from both rainfall and snowmelt. The snow line elevations usually varies between 1500 to 4800 m, occasionally rising to 5400 m. The main source of snow is the winter monsoon, while precipitation falls as rain during summer monsoon season. Overlapping of snow melt and rainfall during the summer monsoon season causes high floods in the rivers. The watersheds of the southern rivers — the Sutlej, Beas and Ravi — are the first to be influenced by summer monsoon rains. The upper part of the Indus River Basin receives the least contribution from monsoon rains and the major portion of river discharge is composed of snowmelt. In contrast to other rivers of the IRS, snowmelt runoff in the Indus River is about 70% of the total annual discharge.

1.2. River system

Attention is focussed on large Punjabi rivers, such as the Sutlej, Ravi, Chenab, Jhelum and Indus. The tributaries of these rivers and drains contain effluent from industry, sewerage systems and drainage from Salinity Control and Reclamation Projects (SCARPs), which enter at different locations. A number of link canals are used to transfer water from northern rivers to southern rivers. As a result, isotopic and chemical concentrations in these rivers vary at different locations. Moreover, isotopic fractionation, i.e. the enrichment of heavy isotopes, also occurs due to evaporation, especially in the dry season when discharge is low [6]. Thus, monitoring will be extended to almost all the major dams/barrages/headworks and drainage inlets on the above said rivers in Punjab.

1.2.1. The Indus

The Indus originates from a spring called Singikahad near Mansarwar Lake on the northern side of the Himalaya Range in Kaillas Parbat, Tibet at an altitude of 5900 m above mean sea level. Traversing about 800 km in a northwesterly direction, it is joined by the Shyok near Skardu at an elevation of 3000 m. Flowing in the same direction for another 160 km before it turns round Nanga Parbat, it is joined by the Gilgit at an elevation of 1600 m. The river then flows 320 km in a southwesterly direction to Kalabagh and into the plains at an elevation of about 300 m. Up to Darband, the river still lies in a hilly tract at an elevation of about 700 m. Below Durband near Tarbela, Siran, a small flashy stream rises from the low elevation of 5000 m and drains the alluvial lands of Mansehra, Abbotabad and a part of Haripur before joining the Indus. A further 30 km downstream near Attock, the biggest western tributary of the Indus, the Kabul joins it. The drainage area of this river above Warsak is 67 000 km². The Chitral River is its one of its main tributaries. Below Warsak, another tributary known as the Sawat joins, increasing the total catchment at this site to about 11 000 km². About 8 km below Attock, Harrow, a small stream drains the district of Attock and some parts of the Murree, Hassan Abdal, and Rawalpindi join it. The catchment of this river is about 6000 sq. km up to the G.T. Road. About 12 km above Jinnah Barrage, a stream called the Soan drains the largest and worst eroded areas

of Rawalpindi, Jhelum and Attock districts with a catchment area equal to 12 000 km². Below Jinnah Barrage, the important western tributaries of the Indus are the Kurram, Gomal and Zoab. Dams and barrages on the Indus are: Tarbela Dam, Jinnah Barrage, Chashma Barrage, Taunsa Barrage, Guddu Barrage, Sukkar Barrage and Kotri Barrage.

1.2.2. The Jhelum

The Jhelum is a big eastern tributary of the Indus. It drains areas in the West of Pir Punjal separating the provinces of Jammu and Kashmir. It rises from the spring of Verinag in the North-West side of Pir Punjal and flows in a direction parallel to the Indus at an average elevation of 1800 m. It drains about 6000 km² of alluvial lands in the Kashmir Valley and important sources of water come from glaciers in the north of the valley. At Domel near Muzaffarabad it is joined by its biggest tributary, called the Nelum, which drains about 7000 km² of hilly area lying on the eastern side of Nanga Parbat. This river drains Himalayan ranges between 5000 m and 6500 m high which are perpetually covered by snow and glaciers. Throughout the length of its 240 km, it flows through fairly stable mountains covered by forests. Five miles below Domel, the Kunhar — another tributary of the Jhelum draining the famous Kaghan Valley — joins the river. It drains water from nearly 2800 km² of the area. Its source lies at 5000–5500 m above sea level. One of its tributaries flows through the famous Saif-ul-Malook Lake. From Domel to Mangla at a distance of about 110 km, two streams — the Kanshi and Poonch — join it. Kanshi is a floodwater stream draining eroded areas of the Jhelum and Rawalpindi districts. This stream carries mainly monsoon rain or seepage water. Poonch is an important stream joining the Jhelum about seven miles above Mangla at Tangrot. At Mangla, near the head regulator of the upper Jhelum Canal, the Mangla Dam has been constructed. The Mangla Dam and Rasul Barrage are important water storage and regulators on this river.

1.2.3. The Chenab

The Chenab River originates in the Kalu and Kangra Districts of India's Himachal Pradesh province. The two chief streams of the Chenab, the Chandra and Bagh, rise on opposite sides of the Baralcha Pass at an elevation of about 5000 m. These join at Tandi in Jammu and Kashmir State nearly 3000 m above mean sea level. The river enters Pakistan in the Sialkot district near Diawara Village. It river flows through alluvial plains of Punjab province for a distance of 5500 km and is joined by Jhelum River at Trimmu. A further 65 km downstream, the river Ravi joins it. The Sutlej joins it upstream of Punjnad and finally, about 65 km below Punjnad, it meets the Indus at Mithankot. The total length of the river is about 1200 km, with catchment areas equal to 67 500 km². Of this, 28 000 km² lie in Jammu and Kashmir State, 4500 km² in India and 35 000 km² in Pakistan. The hilly catchment area above Marala Barrage is about 33 000 km². The Chenab has 12 major tributaries: Chandra, Bhaga, Bhut Nallah, Maru, Jammu Tavi, Manawar Tavi, Doara Nullah 1, Doara Nullah 2, Halse Nallah, Bhimber Nallah, Palkhu Nallah and Aik and Bhudi Nallah. The last eight tributaries join the Chenab in Pakistan.

Chenab discharge starts rising in the latter part of May and passes the 1800 m³/s mark in June. High flows, above 1800 m³/s continue until the middle of September, and peak discharge months are July and August. From an irrigation point of view, these are important characteristics of the Chenab. Dependable supplies can be withdrawn when the river is high, from July to September. This river is a lifeline for the Punjab, supplying Marala Barrage, Khanki Barrage, Qadirabad Barrage, Trimmu Barrage and Punjnad Barrage.

1.2.4. The Ravi

The Ravi is the smallest of the Indus's five main eastern tributaries. It rises in the basin of Bangahal and drains the southern slopes of the Dhanladhar. The basin of Bangahal is 100 km in circumference and at an elevation of about 1600 m. Below Bangahal, the Ravi flows through the valley of Chamba in a northwesterly direction parallel to the Dhanladhar range. The river leaves the Himalayas at Baseeli. In the mountainous area, about 200 km long, total drop is 5000 m, or about 25 m per km. Its average slope is therefore 10 m per km. The Ravi enters the river at Chaundh, forming a boundary between India and the state of Jammu and Kashmir for 35 km. After passing through Gurdaspur, it enters the Shkargarh Tehsil of Sialkot. Just after entering Shkargarh, the Ujh River joins it, 63 km downstream of Madhopur. Basantar, another arm, joins the Ravi a little above Jassar Bridge, while the Bein joins downstream of the Jassar bridge, about 100 km from Madhopur. Important headworks on this river include the Balloki and Sidhnai Headworks.

Previously Balloki was adjusted to the Bari Doab Canal; now this headworks also receives water brought by the Marala Ravi Link and Qadirabad Baloki Link Canals. The off-taking Links are No. 1 and No. 2. The Sidhnai, another headwork on this river, receives water through the Haveli and Trimmu Sidhnai Links. The off-taking canals at this site are the Sidhnai Link Canal and Sidhnai Mailsi Link.

1.2.5. The Bias

The Bias is currently the shortest of all the Punjab Rivers. It is only about 400 km long. In the eighteenth century it joined the Sutlej near Harike. Originally it joined the Chenab at Punjnad. The rim station for this river is located at the Mandi plain near Talwara, in Hoshiarpur district, and the Pando and Pong dams have been built over it.

1.2.6. The Sutlej

This river originates in Western Tibet in the Kailas mountain range, near the source of the Indus, the Ganges and the Bramaputra. It flows through the Punjal and Siwalik Mountain ranges and enters the plains of Indian Punjab. The is about 1550 km long with a catchment area of 75 000 km².

2. OBJECTIVES

The overall objective of this project is to contribute to the proposed CRP on the Global Network of Isotopes in Rivers (GNIR), intended to enhance understanding of the water cycle of large river basins and to assess the impact of environmental and climatic changes on the water cycle. To this end, a national network of suitable stations have been established for isotopic and chemical monitoring of river waters in the Indus Basin. The specific research objectives are:

- To study temporal variations of isotopes (²H, ³H, ¹⁸O etc.) and water chemistry at different control points on major tributaries of the Indus River System by collecting water samples periodically and analyzing isotopes and chemical ions;
- To understand water cycles and hydrological processes in the catchments of these rivers;

- To develop a comprehensive database to support future isotope based groundwater studies in the basin on recharge mechanisms, water balance, and monitoring of ongoing environmental changes.

3. METHODOLOGY

Existing data on river discharge, infrastructure, water quality, the inflow drainage system and related literature from different institutes was collected. This information was analyzed and action plans were formulated in order to conduct the study. Sampling sites were selected by PINSTECH, in consultation with the Water and Power Development Authority (WAPDA) and Irrigation Departments (IDs). Sampling station locations, along with their coordinates (longitudes and latitudes), are given below and marked in Fig. 1 [7].

TABLE 1. GEOGRAPHICAL COORDINATES OF SAMPLING SITES IN THE INDUS RIVER

River Indus and Tributaries in Northern Areas	Lat. (N)	Long. (E)
Hunza River at Dainyor (Daintar)	35° 55.3′	74° 22.3′
Indus at Kachura	35° 24.8′	75° 29.7′
Indus River at Besham Qila	34° 56′	72° 53′
Tarbela Dam Reservoir	34° 05.5′	72° 41.5′
Swat River at Chakdara	34° 38.7′	72° 01.7′
Kabul River near Nowshera	34° 0.4′	71° 58.7′
Jinnah Barrage Kalabagh	32° 55.1′	71° 31.4′
Chashma Barrage	32° 26.1′	71° 23.2′
Taunsa Barrage	30° 31′	70° 51′
Punjnad Barrage	29° 21′	71° 01′
Guddo Barrage	28° 24.9′	69° 43′
Sukkar Barrage	27° 40.5′	68° 19′
Kotri Barrage (Hyderabad)	25° 26.5′	68° 19′
River Ravi		
Balloki Headworks	31° 13.3′	73° 51.6′
Sidhnai	30° 34.4′	72° 09.5′
River Chenab		
Marala Barrage	32° 40.1′	74° 28.1′
Khanki Headworks	32° 29′	74° 06′
Trimu Headworks	31° 08.6′	72° 09.1′
River Jhelum		
Jhelum River at Domel	34° 21′	73° 28′
Neelum River at Muzaffarabad	34° 24′	73° 28.7′
Kunhar River at Talhata Bridge	34° 26.6′	74° 21.5′
Jhelum River at Azad Pattan	33° 46.9′	73° 33.6′
Poonch River near Kotli	33° 31.8′	73° 54.8′
Mangla Dam	33° 09.2′	73° 38.3′
Rasool Barrage	32° 40.9′	73° 31.1′
River Sutlej		
Sulemanki	30° 22′	73° 53′

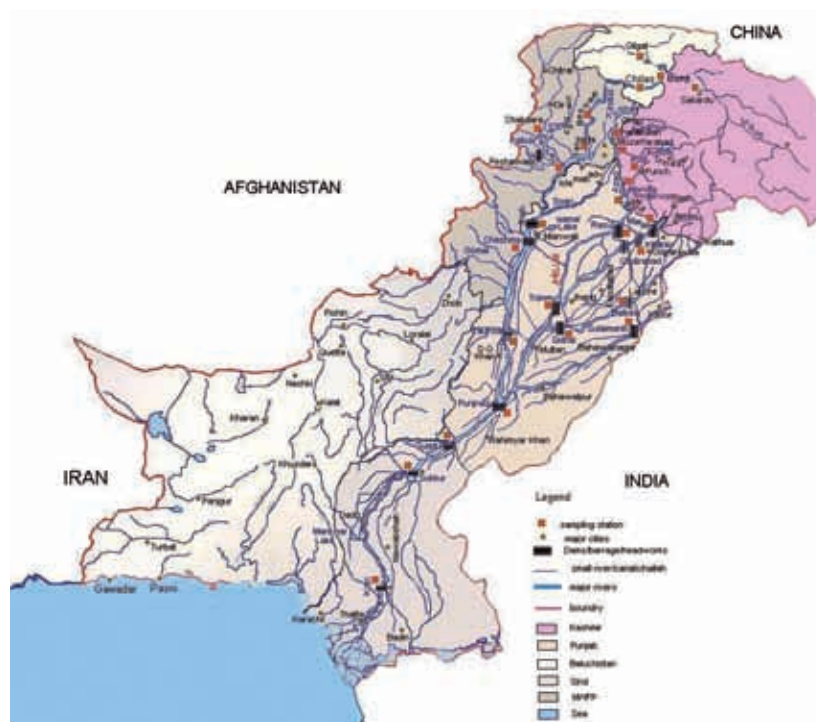


FIG. 1. Map of Pakistan with sampling station locations in the Indus River System.

Sample collecting was carried out through a collaboration with WAPDA and provincial IDs. River samples were collected in brand new, double stoppered, leak proof polyethylene bottles with a one liter capacity from pre-selected sites on a monthly/bimonthly basis. River discharge data of control points was collected.

The $\delta^{18}\text{O}$ and $\delta^2\text{H}$ of the water samples were determined relative to VSMOW using mass spectrometers. The $\delta^{18}\text{O}$ of water was measured using the CO_2 equilibration method [8]. Water samples were reduced to hydrogen gas with zinc shots for $\delta^2\text{H}$ measurement [9]. Measurement uncertainty for $\delta^{18}\text{O}$ is about $\pm 0.1\text{‰}$, while that of $\delta^2\text{H}$ is $\pm 1.0\text{‰}$ [10]. The tritium content of samples was determined by liquid scintillation counting after electrolytic enrichment [11]. The standard error of measurement was in the order of ± 1 TU [12]. Chemical analyses were carried out using: atomic absorption spectrophotometry for Na, K, Ca and Mg; UV-visible spectrophotometry for SO_4 ; titrimetry for HCO_3 ; and ion selective electrode for Cl [13].

4. RESULTS AND DISCUSSION

The $\delta^{18}\text{O}$, $\delta^2\text{H}$ and tritium data were processed to try and uncover different correlations and to prepare histograms, temporal variations and plots, such as $\delta^{18}\text{O}$ vs. $\delta^2\text{H}$, $\delta^{18}\text{O}$ vs. distance from sea, etc. River discharge data collected from the Indus River System Authority (IRSA) were also processed and temporal variations plotted, along with the $\delta^{18}\text{O}$ of samples collected from the same control points. Isotope analysis results are summarized in Table 2.

The head of the River Indus at the highest altitude in the northern areas (Himalayans) shows the most depleted isotopic values. The main source of its tributaries is snowmelt originating

TABLE 2. SUMMARY OF ISOTOPE ANALYSIS RESULTS

Station	$\delta^{18}\text{O}$ (‰)			$\delta^2\text{H}$ (‰)			Tritium (TU)		
	Min	Max	Avg	Min	Max	Avg	Min	Max	Avg
Hunza	-14.5	-11.1	-12.8	-106.1	-72.6	-89.5	15.1	20.3	18.0
Kachura	-14.3	-11.9	-13.0	-102.1	-81.2	-94.4	18.0	21.0	20.0
Gilgit	-13.4	-11.1	-12.1	-95.6	-75.3	-82.8	14.0	19.4	16.9
Besham	-13.1	-9.7	-12.4	-98.9	-69.6	-85.6	13.7	16.2	15.0
Tarbela	-14.2	-10.3	-12.6	-101.7	-71.2	-87.7			
Kabul Riv	-11.7	-6.6	-9.9	-79.8	-43.8	-66.1	14.6	18.7	16.4
Taunsa	-13.5	-8.6	-11.9	-87.9	-54.6	-75.4	10.0	22.1	15.9
Sukkur	-10.5	-7.6	-9.6	-70.4	-48.7	-63.3	14.7	15.5	15.1
Kotri	-10.3	-6.2	-8.6	-69.4	-43.8	-55.2	13.0	16.7	15.1
Chakdara	-9.0	-6.3	-7.6	-58.1	-36.0	-47.0	8.9	11.5	10.1
Noshehra	-11.9	-5.9	-9.3	-79.8	-43.6	-63.3	11.7	22.0	16.5
Baloki	-10.6	-6.4	-8.4	-64.9	-34.1	-51.0	10.0	21.0	15.8
Sidhnai	-10.7	-5.7	-8.5	-76.8	-29.2	-53.1	11.3	22.0	13.8
Marala	-12.8	-5.8	-9.2	-79.5	-35.1	-56.4	6.0	20.0	12.1
Khanki	-10.4	-5.6	-7.8	-65.4	-31.3	-48.2	11.1	20.0	15.4
Trimmu	-13.0	-6.8	-9.7	-79.6	-38.3	-59.4	16.0	25.0	19.8
Punjnad	-10.7	-5.5	-8.8	-72.6	-38.4	-58.3	4.9	21.0	16.4
Kunhar	-8.8	-6.2	-7.5	-58.3	-41.0	-47.9	11.8	15.0	13.0

from glaciers. The most depleted values of $\delta^{18}\text{O}$ and $\delta^2\text{H}$ are found at Hunza, with ranges of -14.5 to -11.6 ‰ and -106 to -84 ‰ respectively. Similarly, the other Himalayan tributaries at Kachura and Gilgit are also depleted in heavy isotopes. At Besham, discharge represents the combined flow of different tributaries in the Himalayas and there is significant variation in the ranges of $\delta^{18}\text{O}$ and $\delta^2\text{H}$ (-13.1 to -9.6 ‰ and -99 to -68 ‰, respectively). This station is at a much lower altitude, and isotopic enrichment can be attributed to the mixing of streams which originate from catchments at a lower altitude with enriched isotopic values. The river Chenab originates from the Jammu and Kashmir area. There are large variations in isotopes at Marala: $\delta^{18}\text{O}$ figures from -14.9 to -5.3 ‰ and $\delta^2\text{H}$ from -95.5 to -32 ‰. Generally, highly depleted values are encountered when there is a large contribution of snowmelt and/or rain from higher altitudes and enriched values are found due to the major contribution of local rains at lower altitudes. The river Ravi, which enters Pakistan from India, originates at a lower altitude. Its $\delta^{18}\text{O}$ and $\delta^2\text{H}$ at the first monitoring point at Baloki varies from -10.6 to -6.4 ‰ and from -65 to -34 ‰, with average values of -8.3 ‰ and -51 ‰. Thus, catchment altitude plays an important role in establishing the isotope indices of these rivers.

The $\delta^{18}\text{O}$ vs. $\delta^2\text{H}$ plot of all samples collected from all rivers is shown in Fig. 2. It shows generally that the Indus is the most depleted in ^{18}O and ^2H in the upper reaches and relatively enriched in the tail stations. River Chenab points are scattered all along the GMWL, displaying wide variation. Ravi River samples fall in the middle, while the river Jhelum is most enriched in ^{18}O and ^2H . At the confluence of the Chenab and Jhelum at Trimmu, some samples are well below the GMWL, indicating an evaporation effect. Sometimes, the river has very low

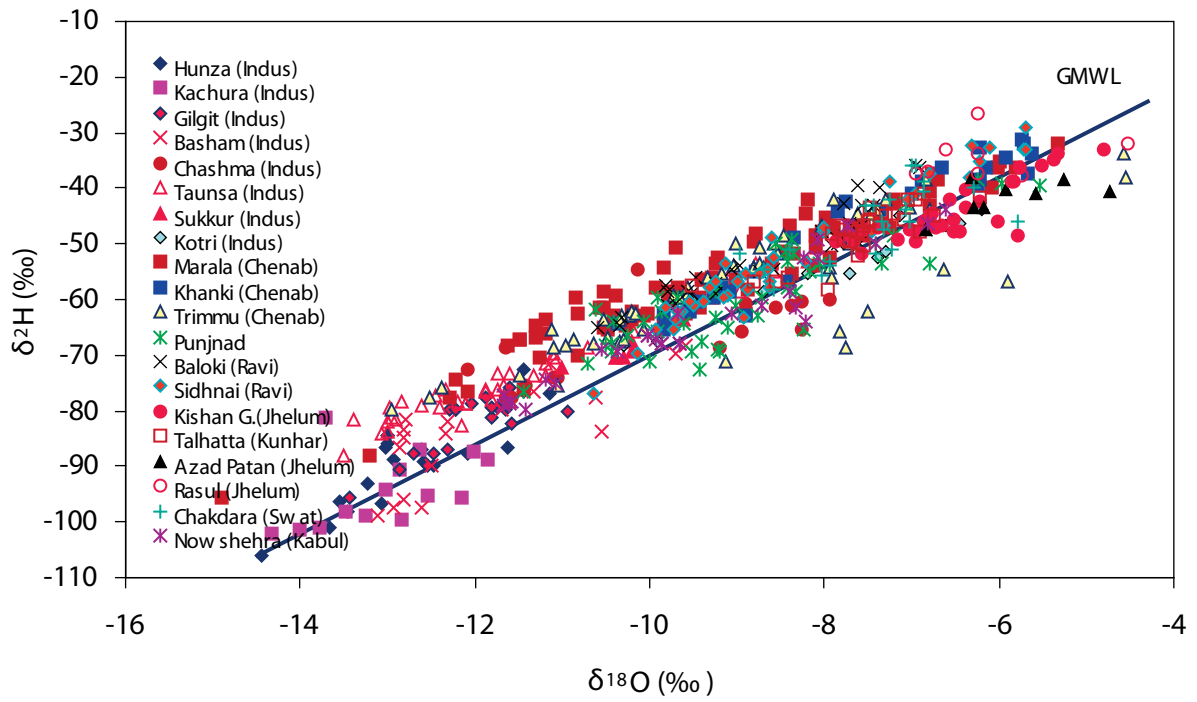


FIG. 2. Plot of δ^2H vs. $\delta^{18}O$ of selected locations at all rivers of Indus River System.

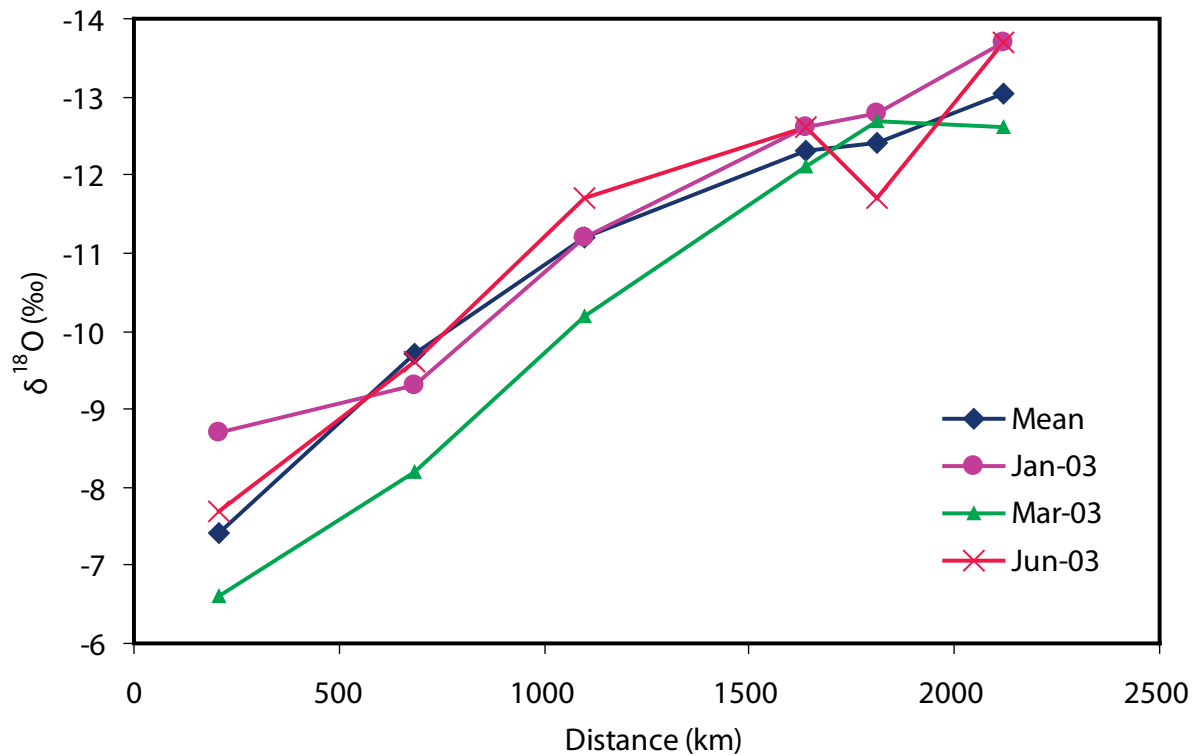


FIG. 3. Plot of $\delta^{18}O$ vs. distance from Arabian Sea of sampling stations at river Indus.

discharge from baseflow, which undergoes evaporation. Two stations — the Nowshwra and Chakdara on the Eastern tributaries the Kabul and Swat Rivers — are also relatively enriched compared to the upper reaches of the Indus river.

The $\delta^{18}\text{O}$ – $\delta^2\text{H}$ correlation has a slope of 6.5 and intercept of -0.1 , which is very different than the Global Meteoric Water Line. Data of individual rivers are discussed below. The $\delta^{18}\text{O}$ plot vs. distance from Arabian Sea for the main river Indus (Fig. 3) clearly indicates enrichment in ^{18}O with decrease in distance. There are three possibilities for enrichment of $\delta^{18}\text{O}$ and $\delta^2\text{H}$:

- The contribution of precipitation enriched in heavy isotopes at low altitudes in the river as it flows towards the sea;
- Enrichment due to evaporation;
- The contribution of baseflow in river discharge, which must be enriched in heavy isotopes due to recharge from local rains.

4.1. Main Indus River

Figure 4 is a $\delta^{18}\text{O}$ vs. $\delta^2\text{H}$ plot of samples collected from Himalayan tributaries and control points of Indus plains. In this plot, samples pertaining to the upper reaches of the river Indus (Hunza, Gilgit, Kachura and Besham) are more negative, while points at downstream stations are more on the enriched side. Although Kachura samples are depleted, they lie below the regression line. Actually, this tributary originates from Kachura Lake and due to its effect these points are shifted downward [14]. A significant number of data points from both areas have a d-excess of more than 20 and lie above the GMWL. These types of waters seem to originate from a Mediterranean source.

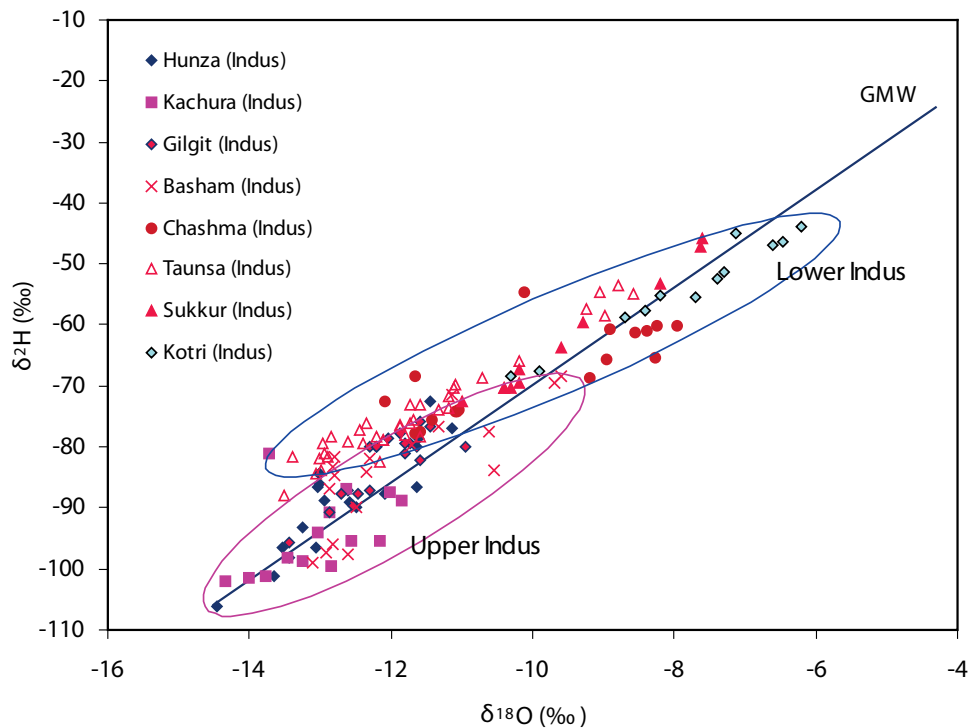


FIG. 4. Plot of $\delta^2\text{H}$ v.s $\delta^{18}\text{O}$ for samples collected from the main Indus River.

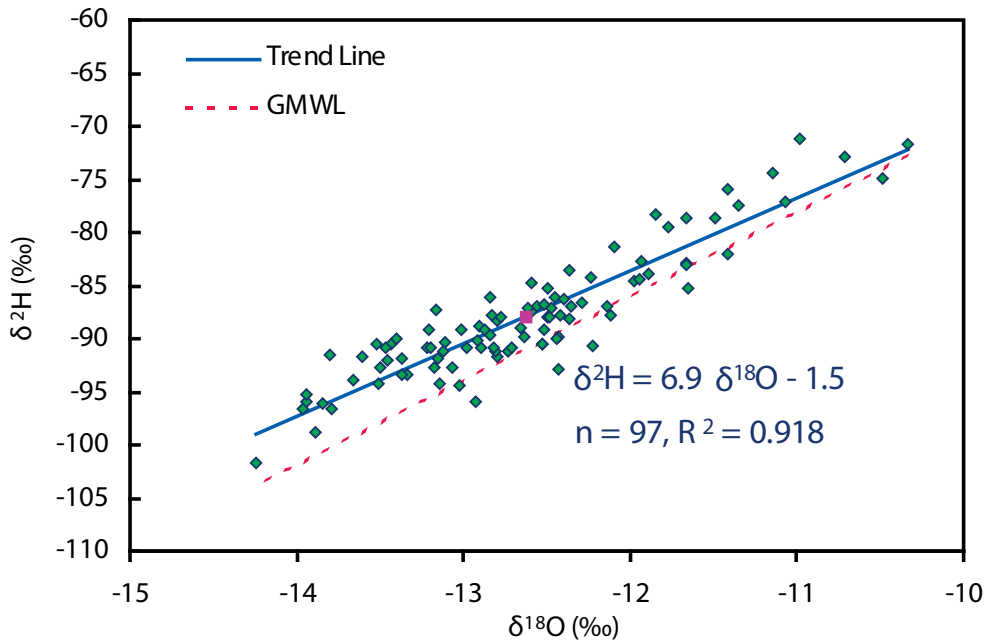


FIG. 5. Plot of δ^2H vs. $\delta^{18}O$ for samples collected from Tarbela Lake.

Figure 5 presents the $\delta^{18}O$ - δ^2H data plot for the river Indus at the Tarbela outlet along with the regression line (RL) and GMWL. The slope of the RL is significantly less than that of the GMWL. Most data points lie above the GMWL. Departures from the point having the most depleted $\delta^{18}O$ and δ^2H values are more than that of points corresponding to enriched samples. Therefore the slope becomes less than that of GMWL. Ahmad et al. determined the d-excess of precipitation for Himalayan Mountains in the northern areas of Pakistan to be 16‰ [15], which is greater than that of low lying areas e.g. 10.9‰ for Islamabad (unpublished data). As mentioned above, highly depleted values are due to the major contribution of snowmelt deposited on high mountains during winter. This suggests that the major source of winter precipitation in these parts of Himalayas may come from Mediterranean Sea; it has a higher d-excess. Temporal variations of $\delta^{18}O$ and the reservoir level of the Indus River at the Tarbela Dam Reservoir outlet are shown for a longer period in Fig. 6. Both parameters show year wise cyclic behaviour. The most depleted $\delta^{18}O$ values are found in August–September, when the reservoir level is generally at its highest and the most depleted values are found during April–May, when the reservoir is at its minimum level. The amplitude of the $\delta^{18}O$ wave varies from 1.5 to 3.8‰ with an average value of 2.4‰. If we consider the d-excess ($= \delta^2H - 8 \delta^{18}O$) of all samples, there is no significant correlation between $\delta^{18}O$ and reservoir level, which means cyclic enrichment is not dominantly due to evaporation effect. The main reservoir input source is snowmelt, which is at its greatest between May and September, when the reservoir becomes full. This snow/glacier melt coming from the high Himalayas is very depleted in heavy isotopes. In the northern areas, snowmelt drained by rivers has an average $\delta^{18}O$ of -13.8 ‰ and a δ^2H of -94 ‰ [15]. Due to the major contribution of snowmelt, $\delta^{18}O$ is most depleted during full/highest level of the reservoir. When the reservoir level is low during April–May, groundwater from nearby areas of low altitude drain into the reservoir; this is strongly enriched compared to the main input. Sajjad et al. found the $\delta^{18}O$ of groundwater around the reservoir to generally be in the range of -7 to -6 ‰ [16]. The $\delta^{18}O$ rain index of this area is also about -6 ‰. Therefore, when the reservoir is low, the contribution of groundwater drained into the input of local rains becomes significant to the increase of $\delta^{18}O$ in the reservoir.

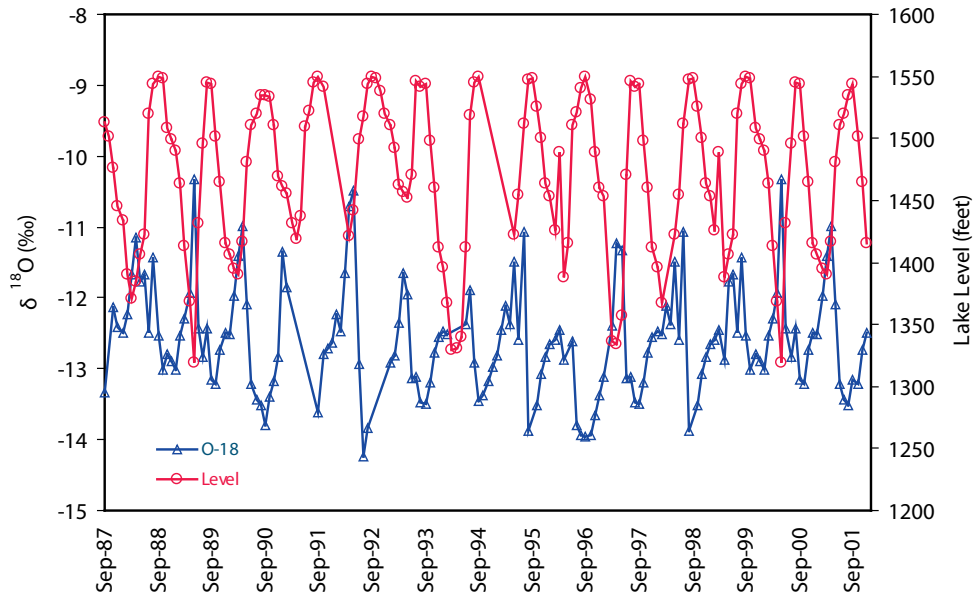


FIG. 6. Temporal variation of $\delta^{18}\text{O}$ and reservoir level of Tarbela lake at Indus River.

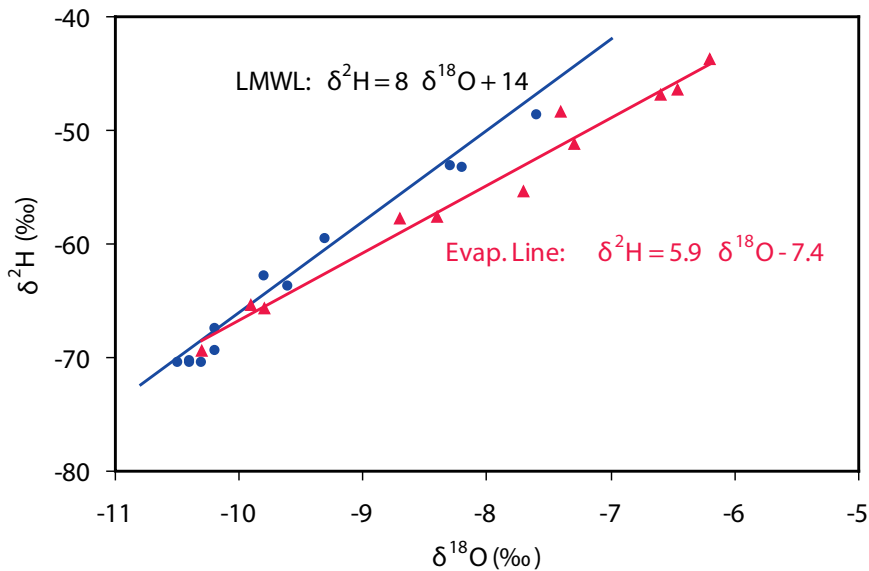


FIG. 7. Plot of $\delta^2\text{H}$ vs $\delta^{18}\text{O}$ of samples collected at Sukkur and Kotri (the last two control points of the Indus River).

The $\delta^{18}\text{O}$ vs. $\delta^2\text{H}$ plot (Fig. 7) of last two stations indicates that all Sukkur data points are plotted on the LMWL, while the data from Kotri (a downstream station) follows an evaporation trend with slope of 5.9. The monthly variation of $\delta^{18}\text{O}$ and discharge of the Indus River at Sukkur and Kotri are shown in Fig. 8. Up to September, downstream discharge from the Sukkur is greater than the upstream discharge of the Kotri, which indicates water losses from this section, possibly due to evaporation and recharge to groundwater. It is possible that for the first six months when discharge is very low evaporation losses are dominant, but during the monsoon period (July–September) river water might infiltrate into the ground. From September to December, the downstream discharge of the Sukkur is less than the upstream discharge of the Kotri, indicating a gain in water discharge. This gain is definitely due to the return flow

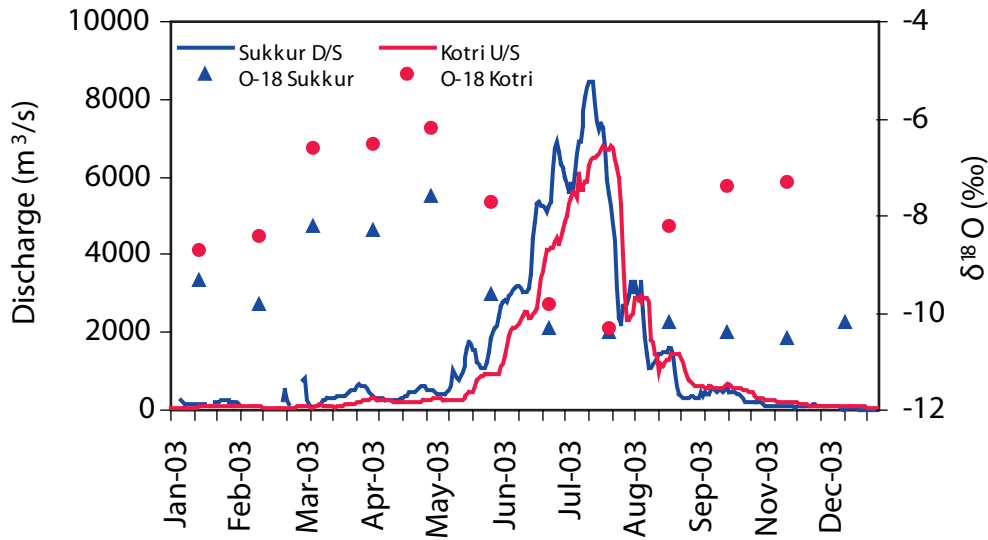


FIG. 8. Monthly variation of $\delta^{18}\text{O}$ and discharge of Indus River at Sukkur and Kotri.

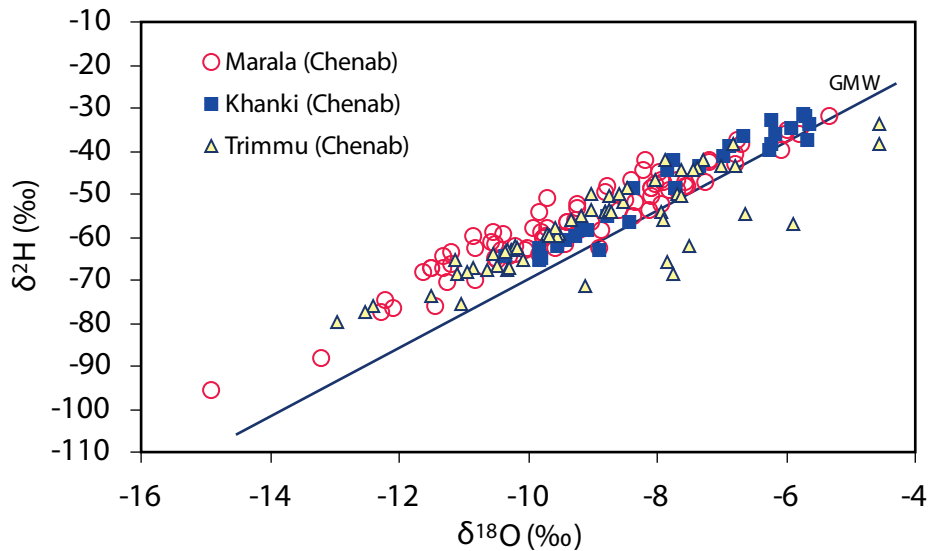


FIG. 9. Plot of $\delta^2\text{H}$ vs $\delta^{18}\text{O}$ of samples collected from Marala, Khanki and Trimmu Barrages.

from the ground into the river. The baseflow may undergo evaporation due low humidity, high surface area and low discharge.

4.2. River Chenab

In $\delta^{18}\text{O}$ vs. $\delta^2\text{H}$ plots (Fig. 9), samples from the Marala, Khanki and Trimmu have similar trends. Almost all the data points lie above the GMWL, and most of the depleted samples ($\delta^{18}\text{O} < -8\text{‰}$) lie above the LMWL, having a slope of 8 and d-excess of 14. The frequency distribution of the d-excess (Fig. 10) of Marala samples has two model classes, indicating a d-excess for most samples of about 15 and 23. A negative correlation between d-excess and $\delta^{18}\text{O}$ (Fig. 11) shows that higher d-excess is associated with depleted $\delta^{18}\text{O}$, which is generally found to be the case in winter precipitation, especially in snowmelt from Mediterranean based moisture sources. In general, summer monsoons originate from the Bay of Bengal, while

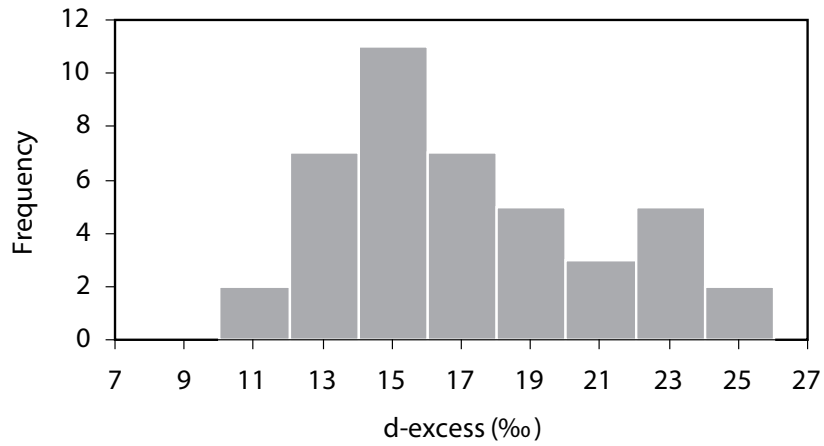


FIG. 10. Frequency distribution of d-excess for samples collected at Marala.

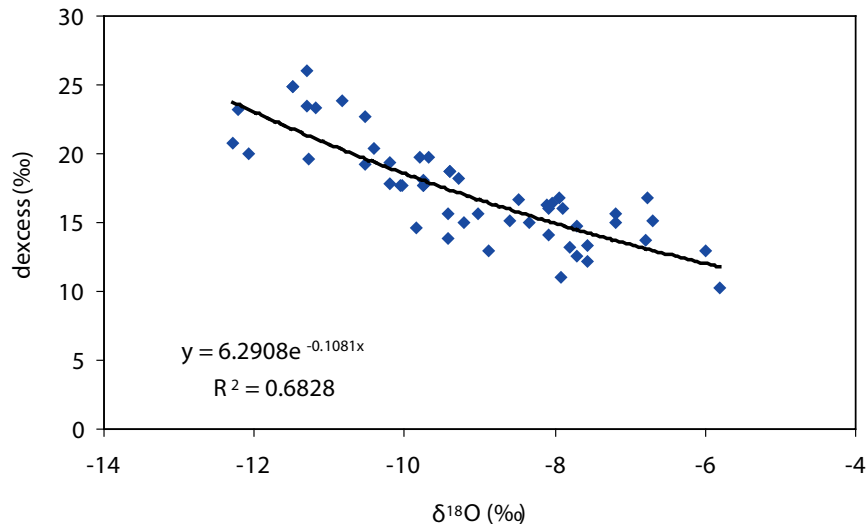


FIG. 11. Plot of d-excess vs $\delta^{18}O$ for samples collected at Marala.

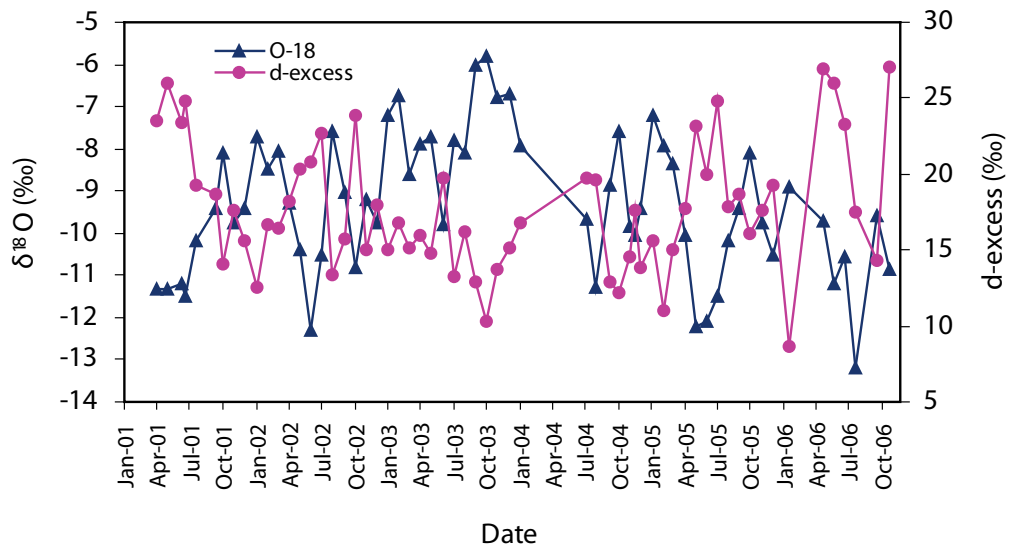


FIG. 12. Temporal variation of $\delta^{18}O$ and d-excess at Marala Barrage.

winter rains result from western disturbances which originate from the Mediterranean [17]. Due to the differing climate at the moisture sources, different isotopic values and d-excesses are encountered. Figure 12 depicts the temporal variation of $\delta^{18}\text{O}$ and d-excess, reflecting mostly depleted ^{18}O and high d-excess during snowmelt period. There is lot of scatter because of different contributions from local rains and snowmelt/rain runoff from higher altitudes.

4.3. River Ravi

Although water from the river Chenab is diverted to the Ravi river upstream of Baloki and although link canals from the Jhelum and Main Indus also contribute upstream of the Sidhnai, water samples collected from Baloki and Sidhnai are still relatively more enriched than those from other rivers. As mentioned above, the catchment altitude of the Ravi river is significantly lower than that of the other rivers. In the $\delta^{18}\text{O}$ vs. $\delta^2\text{H}$ plot (Fig. 13), samples from the Baloki and Sidhnai show similar trends. Almost all data points lie around LMWL. Some of the samples have a higher d-excess due to the mixing of Chenab water, which has very high d-excess during snowmelt.

4.4. Hydrographs and seasonal variations of isotopes

Hydrographs from all control stations at the Main Indus River are provided in Fig. 14, which resembles a mountain. Discharge starts increasing in April due to the contribution of snowmelt and peaks in August due to the added contribution of monsoon rains. After August, it decreases at faster rate. The peaks on the main hump are due to high rainfall events.

Hydrographs of some other stations are included, along with variations of $\delta^{18}\text{O}$. Figure 15 represents the control point of Noshera on the Kabul River, which is a major tributary of the Indus River downstream of Tarbela Dam. The first major rise in discharge takes place from April to June, which seems to be due to snowmelt. The highest peak, which occurs in July, is due to both snowmelt and rains. The $\delta^{18}\text{O}$ is generally low at high discharge because snowmelt coming from higher altitudes is depleted in heavy isotopes, but during July when discharge peaks, $\delta^{18}\text{O}$ is also at its highest, primarily because of the major contribution of local monsoon

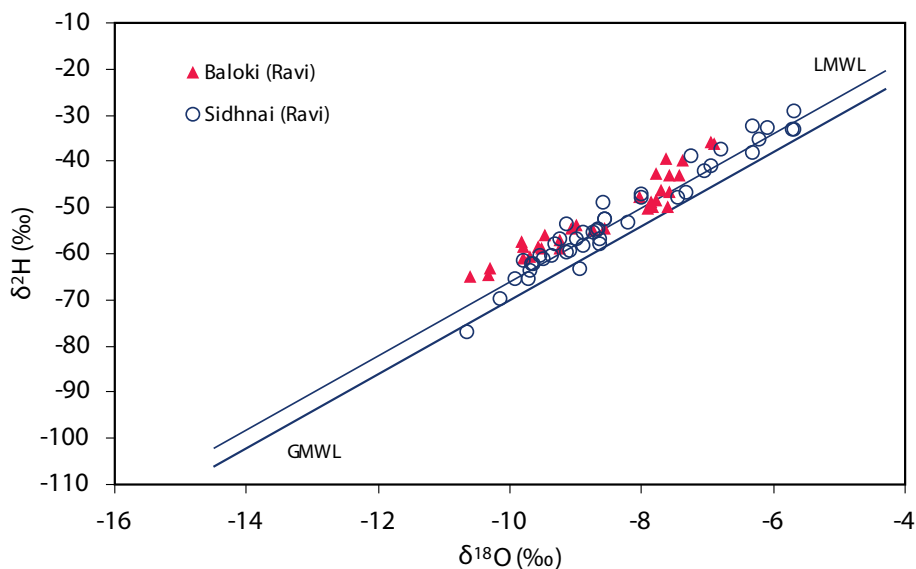


FIG. 13. Plot of $\delta^2\text{H}$ vs $\delta^{18}\text{O}$ of samples collected from the Baloki and Sidhnai barrages.

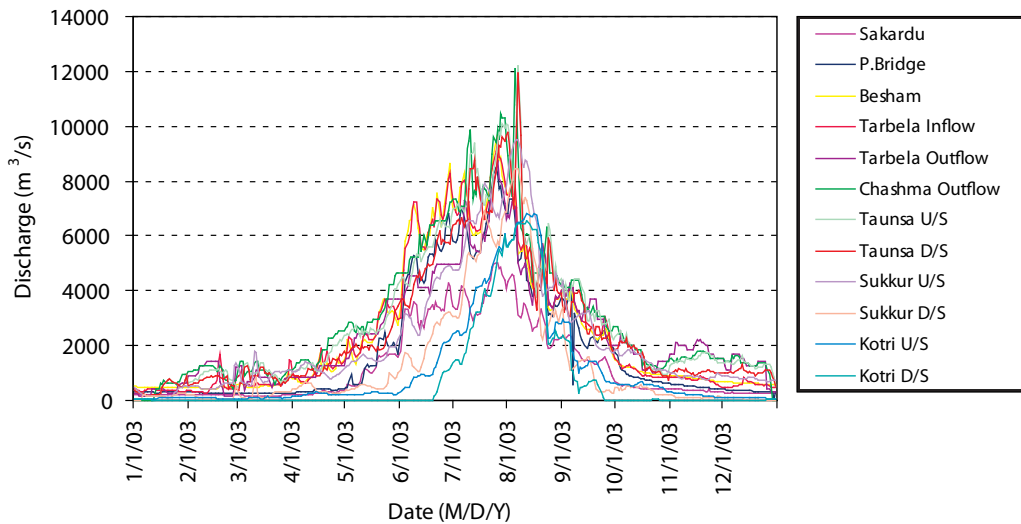


FIG.14. Hydrographs at Main Indus River control stations.

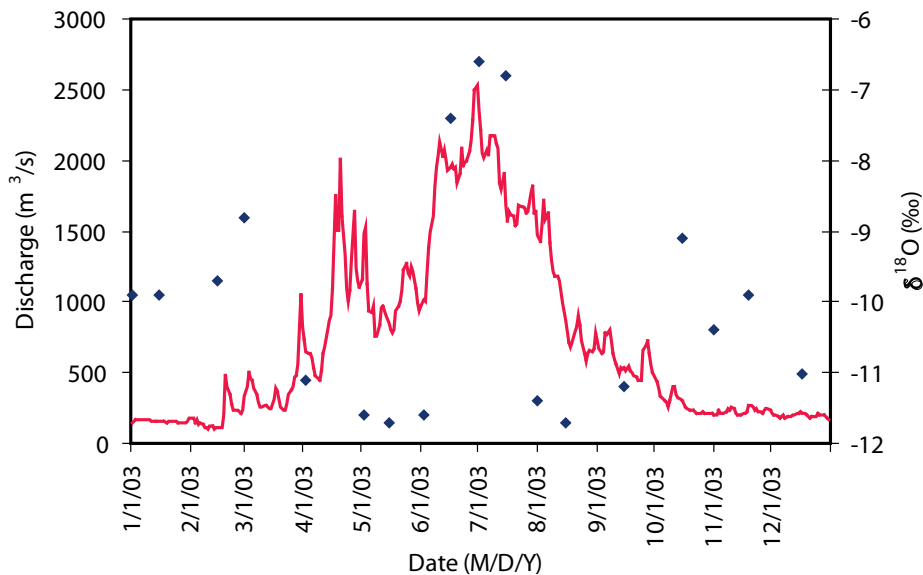


FIG.15. Hydrograph and seasonal variation of $\delta^{18}\text{O}$ in the Kabul River at Noshera.

rain enriched in heavy isotopes. At low discharge, $\delta^{18}\text{O}$ is enriched, possibly due to evaporation and the contribution of local sources from low altitudes such as local rains and baseflow into the river.

Hydrograph and temporal variations at Taunsa, downstream of the Chashma storage barrage, are given in Fig 16. Its $\delta^{18}\text{O}$ increases from January to May, and even with an increase in discharge during the snowmelt period it did not decrease. Actually, most of the snowmelt is stored in the Tarbela Dam Reservoir and the increase in discharge at Taunsa is mainly from the Chashma storage, which might have undergone evaporation and resulted in the enrichment of heavy isotopes. From June to August during peak discharge $\delta^{18}\text{O}$ decreases, reflecting the contribution of snowmelt; at the same time there is no significant increase in $\delta^{18}\text{O}$ after August because water stored in the Chashma reservoir is released at a low flow rate.

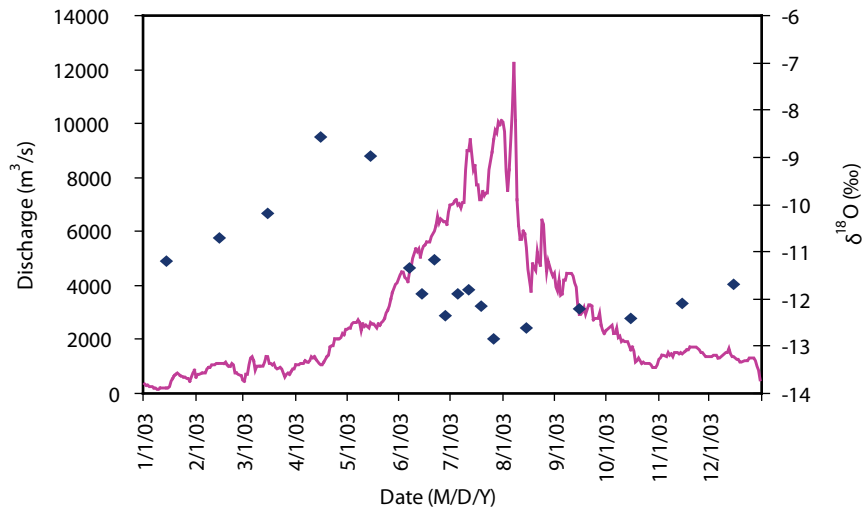


FIG.16. Hydrograph and seasonal variation of $\delta^{18}\text{O}$ at Taunsa, Main Indus River.

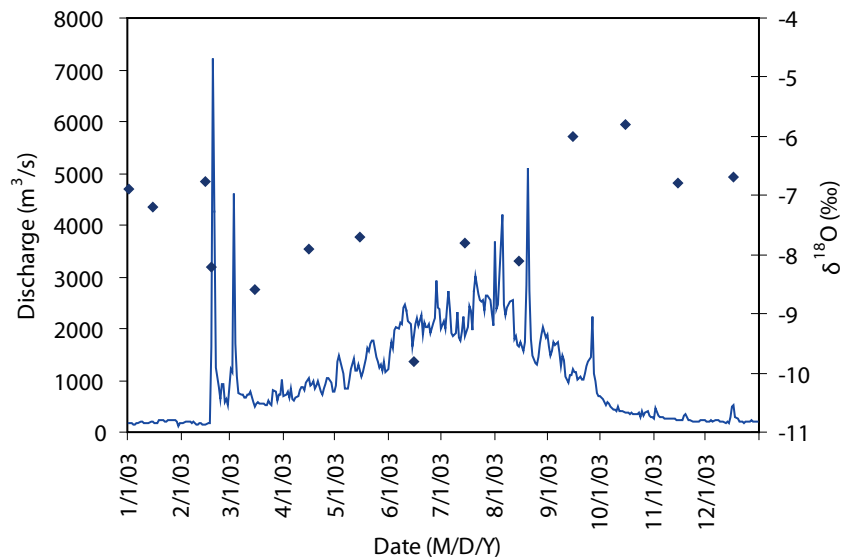


FIG.17. Hydrograph and seasonal variation of $\delta^{18}\text{O}$ at Marala, Chenab River.

Figure 8 provides interesting information about the situation between the Sukkur and Kotri. Up to September the downstream discharge of the Sukkur is more than the upstream discharge of the Kotri, indicating water losses from this area, possibly due to evaporation and recharge to groundwater. For the first six months when discharge is very low, evaporation losses are dominant and enriched ^{18}O is encountered, but during the monsoon period (July–September) discharge is high and due to the contribution of snowmelt (like at Taunsa) and insignificant evaporation, $\delta^{18}\text{O}$ is low. During this period river water may infiltrate into the ground. From September to December, the downstream discharge of the Sukkur is less than the upstream discharge of the Kotri, which indicates a gain in water discharge. This gain is definitely due to the return flow of groundwater into the river. The baseflow may undergo evaporation due to low humidity, high surface area and low discharge. In this case, enriched ^{18}O is found at the Kotri.

Hydrographs with the $\delta^{18}\text{O}$ at Marala for the Chenab River are shown in Fig. 17, while those for the Baloki and Sidhnai at the River Ravi are provided in Fig. 18. Three rivers join just upstream of Marala, and the $\delta^{18}\text{O}$ values may not be representative due to a lack of mixing. Water diverted from other rivers flows into the river Ravi, thus variations in $\delta^{18}\text{O}$ cannot be explained with the hydrographs.

5. CONCLUSIONS

The headwaters of the main Indus River (including Hunza, Gilgit and Kachura tributaries), which are generally comprised of snowmelt, have the most depleted values of $\delta^{18}\text{O}$ (-14.5 to -11.0‰) and $\delta^2\text{H}$ (-106.1 to -72.6‰) due to precipitation entering at a very high altitude and at very low temperatures. Generally these waters have a low d-excess, indicating that the moisture source is the Indian Ocean. The high d-excess of some winter (November–February) samples from Hunza and Gilgit indicates the dominance of the Mediterranean as the moisture source. Kachura station features a $\delta^{18}\text{O}$ – $\delta^2\text{H}$ line with slope of 4 and a low d-excess, indicating an evaporation effect in Kachura Lake. The isotopic values of the Indus River are enriched as it moves downstream towards the Arabian Sea, due to the contribution of rains at low altitude plains and because the baseflow received a recharge contribution from local rains. At tail stations, evaporation and contribution from baseflow are responsible for isotopic enrichment. Low tritium in some samples also indicates a contribution from baseflow (relatively older groundwater).

The Chenab River has the widest variation in $\delta^{18}\text{O}$ and $\delta^2\text{H}$; the slope of the $\delta^{18}\text{O}$ – $\delta^2\text{H}$ line is 6.1, which is due to variable contribution of snowmelt at high altitude and rains from low altitude. The high d-excess in snowmelt and low d-excess in monsoons show that the moisture source in winter is generally western (Mediterranean) and monsoon moisture predominantly originates from the Indian Ocean. Isotope data also reflect the evaporation effect during dry periods.

The Kabul River displays a wide variation in isotopic values, likely due to the variable contribution of the Swat River, which carries snowmelt. High d-excess is associated with depleted isotopic values, while low d-excess is associated with enriched isotopic values, which generally appear during the summer monsoon. Therefore, the slope of the $\delta^{18}\text{O}$ – $\delta^2\text{H}$ line is 7, which appears to be mainly due to the dominance of a Mediterranean moisture source in winter having depleted isotopic values and high d-excesses and moisture from the Bay of Bengal in summer containing relatively high d-excess.

The Jhelum River and its tributaries upstream of Mangla Lake have enriched $\delta^{18}\text{O}$ and $\delta^2\text{H}$ due to the low altitude of their catchment.

Precipitation in the catchment of Ravi river comes from the Indian Ocean, and there is not any significant evaporation effect. Isotopic variation seems to occur mainly due to water diversions from western rivers through link canals.

A reasonable isotope and discharge database for the Indus River System has been established, which will be useful for future surface water and groundwater studies in the basin.

ACKNOWLEDGEMENTS

The present investigation was carried out within the framework of the IAEA Coordinated Research Programme 'Isotope Tracing of Hydrological Processes in Large River Basins' (CRP PAK-12046). Sincere thanks are due to Mr. P.K. Aggarwal and Mr. K.M. Kulkarni for the guidance and suggestions provided during technical discussions. The cooperation between IRSA, WAPDA, Irrigation Departments and the Meteorological Department for the collection of samples and provision of data is highly appreciated. Efforts on behalf of colleagues at the Isotope Application Division, PINSTECH for analysis of samples are thankfully acknowledged.

REFERENCES

- [1] GAT, J.R., Oxygen and hydrogen isotopes in the hydrologic cycle, *Annual Review of Earth and Planet. Sci.* **24** (1996) 225–262.
- [2] FRITZ, P., River Waters, "Stable Isotope Hydrology, Deuterium and Oxygen-18 in the Water Cycle" (GAT, J.R., GONFIANTINI, R., Eds), IAEA Tech. Rep. Ser. 210, pp. 177–210.
- [3] AGGARWAL, P.K., FROELICH, K., KULKARNI, K.M., GOURCY, L., Stable isotope evidence for moisture sources in the Asian summer monsoon under present and past climate regimes, *Geophys. Res. Letters* **31** (2004).
- [4] TARAR, R.N., *Geography and Hydrology of The Indus Basin*, WAPDA, HID-18, Lahore, Pakistan (1982) 1–30.
- [5] AHMAD, N., *Water Resources of Pakistan*, Published by Shahzad Nazir (1993).
- [6] INTERNATIONAL ATOMIC ENERGY AGENCY, *Guide Book on Nuclear Techniques in Hydrology*, Technical Report Series No. 91, IAEA, Vienna (1983).
- [7] SURVEY OF PAKISTAN, *Atlas of Pakistan* Published by Director Map Publication, Survey of Pakistan, Rawalpindi (1985).
- [8] NEHRING, N.L., BOWEN, P.A., TRUESDELL, A.H., Techniques for the conversion to carbon dioxide of oxygen from dissolved sulphates in thermal waters, *Geothermics*, **5** (1977) 63–66.
- [9] COLEMAN, M.L., SHEPHERD, T.J., DURHAM, J.J., ROUSE, J.E., MOOR, G.R., Reduction of water with zinc for hydrogen isotope analysis, *Analytical Chemistry* **54** (1982) 993–995.
- [10] SAJJAD, M.I., *Isotope Hydrology in Pakistan, Instrumentation-Methodology-Applications*. Ph.D. thesis, University of the Punjab, Lahore (1989).
- [11] FLORKOWSKI, T., Low level tritium assay in water samples by electrolytic enrichment and liquid scintillation counting in the IAEA laboratory, "Methods of Low Level Counting and Spectrometry", IAEA, Vienna (1981).
- [12] HUSSAIN, S.D., ASGHAR, G., Programme for TI Programmable calculator for calculation of ^3H concentration of water samples, PINSTECH/RIAD-102 (1982).
- [13] AMERICAN PUBLIC HEALTH ASSOCIATION, *Standard Methods for the Examination of Water and Wastewater*, 6th Edition, APHA, Washington, DC (1985).
- [14] CLARK, I.D., FRITZ, P., *Environmental Isotopes in Hydrogeology*. Lewis Publishers, Boca Raton, New York (1997).
- [15] AHMAD, M., AKRAM, W., HUSSAIN, S.D., SAJJAD, M.I., ZAFAR, M.S., Origin and subsurface history of geothermal water of Murtazabad Area, Pakistan — an isotopic evidence, *Applied Radiation and Isotopes* **55** (2001) 731–736.

- [16] SAJJAD, et al., The sources of groundwater salinization in the Indus basin — An isotopic evidence, PINSTECH Report No. PINSTECH/RIAD-128 (1992).
- [17] AWAN, N.M., Surface Water Hydrology, and Vol: 1, National Book Foundation, Pakistan (1981).

ISOTOPE TRACING OF HYDROLOGICAL PROCESSES IN RIVER BASINS: THE RIVERS DANUBE AND SAVA

N. Ogrinc^a, T. Kanduč^a, N. Miljević^b, D. Golobočanin^b, J. Vaupotič^a

^a Institute of Nuclear Sciences, Vinča, Belgrade, Serbia

^b Vinča Institute of Nuclear Sciences, Belgrade, Serbia

Abstract. Isotope ($\delta^{18}\text{O}$, $\delta^2\text{H}$ and ^3H) measurements in surface waters were used to investigate hydrological pathways and residence times in the River Sava and Danube catchments in Slovenia and in the Belgrade region of Serbia for the period 2004–2006. Precipitation $\delta^{18}\text{O}$ and $\delta^2\text{H}$ values show marked seasonal variations which, although significantly damped, were also reflected in the isotopic composition of surface water. Spatially, the surface water of the River Sava is ^{18}O and ^2H depleted in high mountain areas due to greater precipitation, lower temperatures and higher elevation of the recharge area and are similar to isotopic values observed in the Danube River at Belgrade. In the lower part of the Sava River catchment, $\delta^{18}\text{O}$ and $\delta^2\text{H}$ values are higher and are not significantly different from the sampling stations in Slovenia and Serbia. Exponential flow modelling was applied to provide preliminary estimates of mean residence times (MRT), which varied between 0.8 and 2.2 years. Longer MRT coincides with generally lower mean $\delta^{18}\text{O}$ values in surface water found at the source of the Sava River at Zelenci and the Danube River probably indicating the greater influence of depleted winter precipitation inputs. These data extend our knowledge of Sava and Danube River hydrology vis-a-vis the watershed and demonstrate the utility of isotope tracers in investigating interactions in hydrological processes and catchment characteristics.

1. INTRODUCTION

Rivers are an important link in the global hydrological cycle, returning about 35% of the precipitation that falls over land to the oceans, while at the same time representing the most important source of water for human use. The other two-thirds of the precipitation is evaporated, transpired or infiltrates into groundwater, representing the second most important source of water within rivers. As with all aspects of the water cycle, the interaction between precipitation and surface runoff varies according to time and geography. Surface runoff is affected by both meteorological factors and the physical geology and topography of the land. It can also be diverted by humans for their own use. Isotope monitoring of river water provides an important proxy for the isotopic composition of precipitation and integrates spatial and temporal variabilities in the hydrological cycle [1–5]. Of particular interest is the use of oxygen and hydrogen stable isotopes for constraining residence time, characterizing several different water dynamics within a watershed, including indication of potential inputs (e.g. precipitation vs. groundwater) and for determining mixing and flow paths of water within a system [6–8]. On the other hand, tritium (^3H), a radioactive element characterized by a half-life of 12.4 years with measurable levels in the hydrosphere resulting from nuclear weapons tests, can be used as a transient tracer for following water masses [9–11].

The main objectives of this study were to characterize spatial and temporal variation in $\delta^{18}\text{O}$ and $\delta^2\text{H}$ values of the Sava and Danube Rivers and to make a preliminary estimate of the mean residence time of runoff in the studied rivers catchments. The presented study represents the results of a three year stable isotopic study of the Sava River in Slovenia and the Sava

and Danube Rivers near Belgrade in Serbia and shows the application of $\delta^{18}\text{O}$, $\delta^2\text{H}$ and ^3H measurements as natural tracers which provide potential insight into hydrological cycles which is otherwise unattainable. In addition, this work contributes to the goal of the International Sava River Basin Commission (ISRBC) to ensure cooperation of all parties to realize sustainable water management. Apart from that, it is a crucial test case for implementation of the EU Water Framework Directive — Integrated River Basin Management for Europe (OJ L 327, 2000) for the Danube, the aim of which is to prove that the best possible model for a single system of water management is management by river basin (the natural geographical and hydrological unit) rather than administrative or political boundaries.

2. SITE DESCRIPTION

The Sava River is the largest tributary of the Danube. It is 945 km long and totally drains 95 719 km² of surface area contributing 12% of the Danube watershed area and 25% of the total discharge. The Sava is of great significance to the Danube River Basin because of its outstanding landscape diversity. The Sava is a unique example of a river where some floodplains are still intact, supporting both flood alleviation and biodiversity.

The Sava flows through four countries: 11% of the drainage area belongs to Slovenia, 26.3% to Croatia, 39.8% to Bosnia and Herzegovina and 22.8% to Serbia. There are two sources, both originating in the Alpine mountain area in northwestern Slovenia. The 45 km long Sava Dolinka flows out from the Zelneči spring in Planica mountain at the altitude of 1222 m, near the Italian border. The second source is 31 km long, and originates in Komarča at an altitude of 805 m from the underground source Savica, the water of which comes from the Triglav Lakes Valley, flows into Lake Bohinj and emerges at the other end as a new river — Sava Bohinjka. At the town of Radovljica in Slovenia, both of these springs/streams merge into one: the Sava River. The Sava is a typical meandering river with numerous sharp river bend along its course. The average bottom slope qualifies the Sava as a typical lowland or middle course river. The mean annual temperature changes between 6°C in the upper part and 12.6°C at Belgrade in Serbia. Yearly precipitation follows a descending trend, going from the west to the east and from the higher elevation of the basin to the shallow flatlands. The greatest amounts of precipitation can be observed at the upper flow of the Sava in the Alpine region, where precipitation amounts can reach 2000–3000 mm/year, after which this amount drops to 660 mm/year at the river's mouth. Its average discharge is 84 m³/s in Ljubljana, while at Zagreb it is 255 m³/s, and in Belgrade it is 1722 m³/s. The large retention areas of the Sava are one of the most effective flood control systems in Europe. Their management is seen as an international model for sustainable flood management. The backwater effect of the Iron Gate Dam (Djerdap I) is noticed almost up to the town of Šabac at 105 km during the River Sava's low flow.

The Sava Basin is located in the junction between the southern Alps, the Dinaric Mountains and the Pannonian Plain. In its upper reaches, the Sava Dolinka River drains alpine valleys with carbonate rocks largely of Mesozoic age. In the lower Slovenian Sava, the basin consists of clastics sediments and limestone rocks from the Triassic age. In Croatia, there are mostly alluvial sediments with fertile soil cover. On the Bosnian side, alluvial sandy-gravel deposits are dominant, while the Serbian Sava Basin yields various types of sands, silty clays and gravels. The station is located on the right bank of the Sava river, 14 km southwest of Belgrade where the river merges with the Danube. The location is at the alluvium of the Sava river, the

wideness of which increases upstream from the Danube's confluence. The area is a flood basin characterized by Miocene karst limestone underlined by Mesozoic rocks with great significance as a reservoir of groundwater. Nearby, Makis field (an area of 25 km²) and its surrounding hilly terrain (170–208 mm asl) is an important water protection zone for Belgrade City's drinking water supply. The Danube River sampling point Vinča is located 14 km downstream from Belgrade on the right bank of the River Danube. It is in the vicinity of the one of the largest and most significant prehistoric Neolithic settlements (5200–4200 B.C.) in Eastern Europe. The riverbed is shallow and marshy, connected to its neighbouring terrestrial environment by alluvial forests. Typical fluvial and fluviallake sand-gravelly deposits are approximately 25 m in depth.

3. MATERIALS AND METHODS

River samples were collected monthly at locations along the Sava River; at its source (Zelenci, 46° 29' 48" N, 13° 44' 7" E, altitude 830 m), near the Croatian border (Jesenice na Dolenjskem, 46° 11' 11" N, 14° 06' 09" E, altitude 76 m, 14 km distant from the confluence with the Danube) in Serbia and along the Danube River, at Vinča (44°46'N, 20°37'E, altitude 74 m, 1145 km from its confluence with the Black Sea) in Serbia between 2004 and 2006. Precipitation samples were obtained as monthly composite samples of daily precipitation collected near Ljubljana and in rain gauges at the Belgrade Meteorological Station located at Zeleno Brdo (44°47' N, 20° 32' E, altitude 243.2 m). Samples were stored according to standard procedure, [12] and analysed for isotopic compositions of hydrogen and oxygen. The isotopic composition of oxygen ($\delta^{18}\text{O}$)

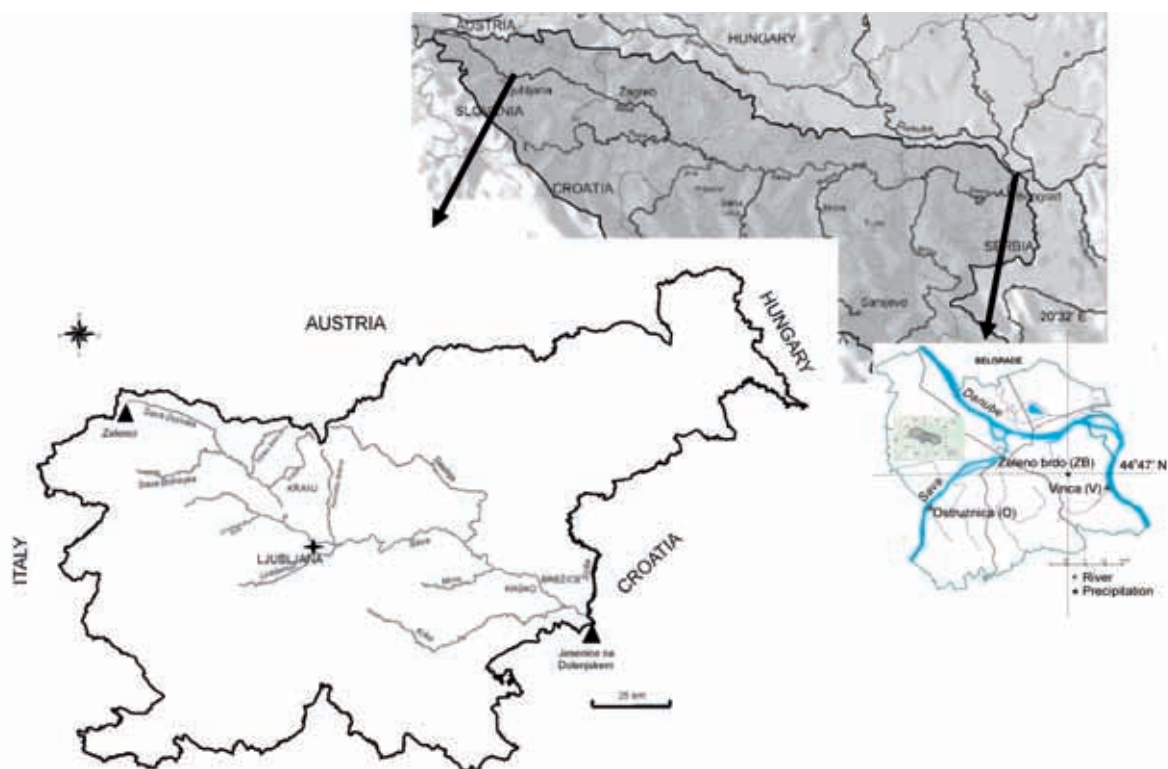


FIG. 1. Sampling locations on the River Sava; Zelenci and Jesenice na Dolenjskem (Slovenia), Jesenice na Dolenjskem (Slovenia) and Zeleno Brdo (Serbia) together with precipitation sampling site at Ljubljana (Slovenia) and Zeleno Brdo (Serbia).

was measured after equilibration with reference CO₂ at 25°C for 24 h [13], while reduction of Cr at 800°C was used to determine the isotopic composition of hydrogen ($\delta^2\text{H}$) in water [14]. Both measurements were performed on a Varian MAT 250 mass spectrometer. Stable isotope results for hydrogen and oxygen are reported using conventional delta (δ) notations $\delta^{18}\text{O}$ and $\delta^2\text{H}$ respectively in permil (‰) relative to VSMOW. Measurement precision was $\pm 0.1\text{‰}$ for $\delta^{18}\text{O}$, $\pm 1\text{‰}$ for $\delta^2\text{H}$.

For ^3H measurements, the majority of distilled water samples were electrolytically enriched and redistilled [15,16]. Six ml of scintillation cocktail was added to 6 ml of sample. Counting was performed on a TRI CARB 3170 TR/SL ultra low-level Liquid Scintillation Counter (LSC, Canberra Packard) with a precision of ± 1.8 TU. All results are expressed in Tritium Units (TU).

Discharge and some basic chemistry data which represent a regular part of the monitoring programme were obtained by the Environmental Agency of the Republic of Slovenia and by the Republic Hydrometeorological Service of Serbia, while regular data on isotopic characteristics of precipitation in Ljubljana is readily available within the framework of the Global Network of Isotopes in Precipitation (GNIP).

4. RESULTS AND DISCUSSION

Precipitation inputs show marked seasonal variation, with winter precipitation (December–May 2004–2006: mean $\delta^{18}\text{O}$ and $\delta^2\text{H}$ values of -11.1‰ and -77‰ , respectively) more ^{18}O depleted than summer and autumn rainfall (June–November 2004–2006: mean $\delta^{18}\text{O}$ and $\delta^2\text{H}$ values of -7.2‰ and -48‰ , respectively) near Ljubljana. Seasonal variations in $\delta^{18}\text{O}$ and $\delta^2\text{H}$ precipitation values were similar near Belgrade in Serbia. Mean $\delta^{18}\text{O}$ and $\delta^2\text{H}$ values were -11.1‰ and -81‰ for the period December–May 2004–2006, while for the period from June to November mean $\delta^{18}\text{O}$ and $\delta^2\text{H}$ values were lower at -8.0‰ and -53‰ , respectively. The large amplitude of isotopic variations in precipitation clearly indicate the complexity of its source as well as the climatic and topography characteristics of the region, which affect the composition of local rain. This follows an approximately sinusoidal, seasonal pattern of precipitation $\delta^{18}\text{O}$ in which winter months are dominated by colder air masses which bring more ^{18}O depleted rain and snow and summer weather systems with more ^{18}O enriched precipitation. The correlation between $\delta^2\text{H}$ and $\delta^{18}\text{O}$ at both stations is high ($r^2 > 0.98$ at Ljubljana and $r^2 > 0.97$ at Belgrade) and Local Meteoric Water Lines (LMWL) [17, 18] are close to the Global Meteoric Water Line (GMWL) [19].

In comparison to precipitation inputs, surface water $\delta^2\text{H}$ and $\delta^{18}\text{O}$ values are generally less dampened. Arithmetic mean, range and standard deviations of $\delta^{18}\text{O}$ and $\delta^2\text{H}$ are shown in Table 1, while seasonal variations of data are graphically presented in Fig. 2. Surface waters also exhibit seasonal differences, being generally ^{18}O depleted during the winter. The effect of the most ^{18}O enriched precipitation was evident in summer $\delta^{18}\text{O}$ values. It can be seen that higher seasonal variability in $\delta^{18}\text{O}$ and $\delta^2\text{H}$ values occurred at Jesenice na Dolenjskem compared to Zelenci, the source of the Sava River, probably due to important sub-catchment variations in hydrological behaviour (Fig. 2). The data at Zelenci reflects the origin of water from snowmelt occurring during spring as well as the elevation effect. The mean $\delta^{18}\text{O}$ and $\delta^2\text{H}$ of -10.10 ± 0.34 and $-68.6 \pm 3.3\text{‰}$ respectively are comparable to the Danube River values from near Belgrade. Higher $\delta^{18}\text{O}$ and $\delta^2\text{H}$ river water values were observed in the lower part of the Sava River in Slovenia, including at the sampling station Jesenice na Dolenjskem, and are

TABLE 1. ARITHMETIC MEAN, RANGE AND STANDARD DEVIATION (SD) OF $\delta^2\text{H}$ AND $\delta^{18}\text{O}$ TOGETHER WITH ESTIMATED MEAN RESIDENCE TIME (MRT) IN THE SAVA AND DANUBE RIVERS AT REPRESENTATIVE SAMPLING STATIONS DURING 2004–2006

Location	River	δD (‰)				$\delta^{18}\text{O}$ (‰)				MRT (yr)
		Mean	Min	Max	SD	Mean	Min	Max	SD	
Zelenci	Sava	-68.6	-74	-63	3.3	-10.10	-10.5	-9.1	0.34	1.76
Jesenice na Dolenjskem	Sava	-60.9	-69	-54	4.9	-9.20	-10.2	-8.4	0.52	0.82
Belgrade	Sava	-63.6	-70	-60	2.8	-9.31	-10.3	-8.4	0.41	1.61
	Danube	-70.4	-86	-61	7.4	-10.02	-10.8	-9.5	0.30	2.24

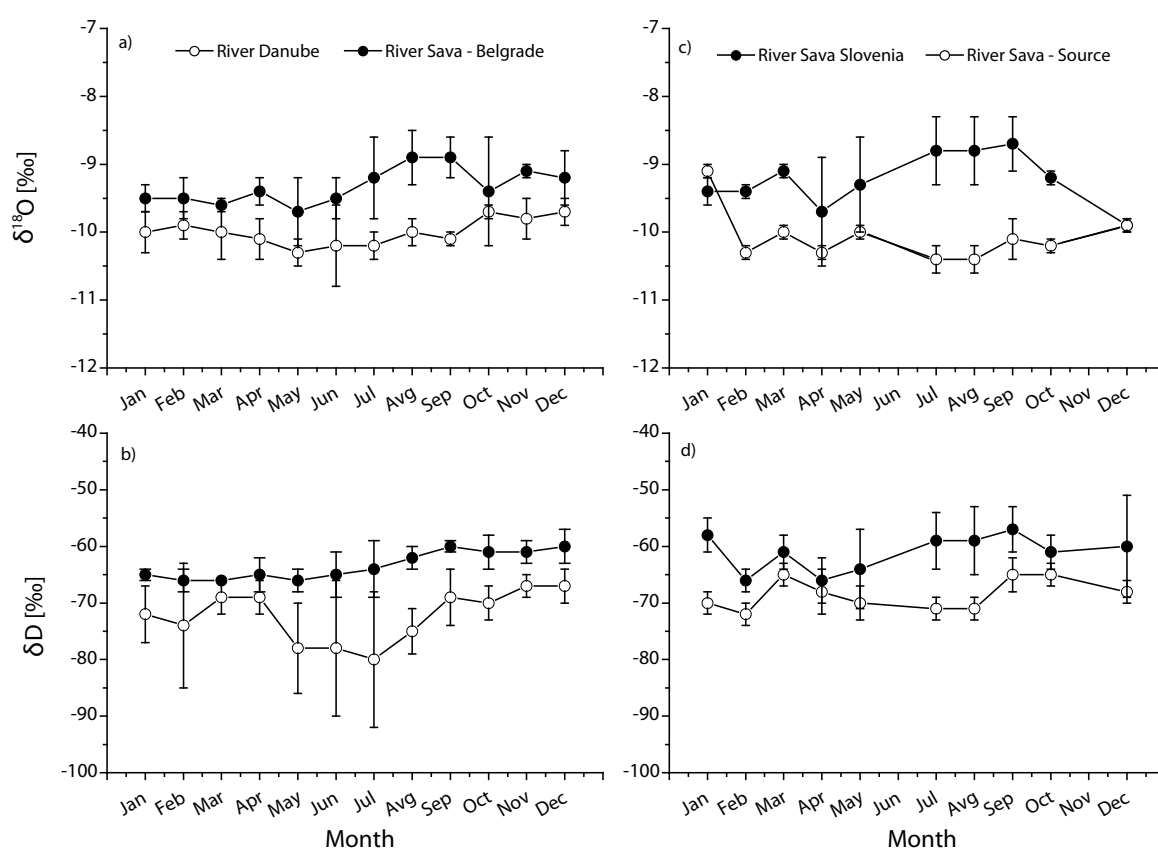


FIG. 2. Seasonal changes in $\delta^{18}\text{O}$ and $\delta^2\text{H}$ values for all sampling stations during 2004–2006.

mostly related to the lower amount of precipitation received in this area [20]. This interpretation is consistent with recharge regimes determined in the Sava River, which change from Alpine high mountain in the upper parts of the catchments to Dinaric Alpine in the lower parts [21].

In the autumn of 2004, $\delta^{18}\text{O}$ and $\delta^2\text{H}$ river sample values approached the weighted mean annual precipitation ($\delta^{18}\text{O} = -8.1\text{‰}$ and $\delta^2\text{H} = -55\text{‰}$) determined over the years 2001–2003 [22]. It seems that this represents the base flow of the Sava River, which integrates the isotopic composition of precipitation over the drainage areas. Poor correlations between $\delta^{18}\text{O}$ values and

river discharge ($r^2 = 0.03$) or temperature ($r^2 = 0.01$) were obtained, suggesting that the factors influencing $\delta^{18}\text{O}$ values of surface waters are multivariate and complex.

The differences in hydrogen and oxygen isotopic composition between the Danube River and Sava water near Belgrade were statistically significant at a level of better than 0.01, using two-tailed tests for the period of observation (2003–2005). Observed differences in isotopic content could be attributed to the integrated isotopic signal of their individual large drainage basins. The δ values weighted by associated discharge values were $-64 \pm 7\text{‰}$ for $\delta^2\text{H}$ and $-9.4 \pm 1.0\text{‰}$ for $\delta^{18}\text{O}$ for the Sava River, and $-73 \pm 3\text{‰}$ and $-9.6 \pm 0.5\text{‰}$, respectively, for the Danube. Clear seasonal variations were observed in $\delta^{18}\text{O}$ and $\delta^2\text{H}$ values for the Sava River with higher isotopic composition found in late summer months (August–September 2004–2006, $\delta^2\text{H} \sim -61\text{‰}$, $\delta^{18}\text{O} \sim -9.0\text{‰}$) and lower composition during spring (April–May 2004–2006, $\delta^2\text{H} \sim -66\text{‰}$, $\delta^{18}\text{O} \sim -9.9\text{‰}$). A good correlation ($r^2 = 0.55$) between $\delta^{18}\text{O}$ values and the river discharge was obtained. This is characteristic for moderate climates with direct surface runoff dominated systems. For the Danube River, seasonal variations were similarly pronounced, but with some lag towards more negative isotopic values during summer months (July–August 2004–2006, $\delta^2\text{H} \sim -82\text{‰}$, $\delta^{18}\text{O} \sim -10.1\text{‰}$) (Figs. 2a, b). This shift in isotopic cycle could be the consequence of the snowmelt contribution which occurs in spring further upstream (at a higher elevation and latitude) in the alpine drainage basin.

Correlations between the river water isotopic compositions and climatic parameters ($r^2 = 0.95$) reveal good agreement between discharge weighted δ values and annual mean water temperatures for the Sava River, whereas they are low ($r^2 < 0.43$) for the Danube. Good agreement between river and precipitation data, especially in the case of the Sava, was observed for amount weighted isotopic composition of precipitation between Belgrade and adjacent UYRUVVM2 WXQED WHDYDDQIQa (the Danube). However, both $\delta^{18}\text{O}$ and $\delta^2\text{H}$ values for the Danube are slightly lower than for those in precipitation. This result could be explained by the fact that large scale mean annual isotopic signatures of precipitation derived from higher elevations are preserved in Danube water. The lower mean temperature of Danube water — about 0.7°C lower than that of Sava water — could be a reason for the noticeable difference in isotopic composition. The close match between mean annual recharge and mean annual precipitation within $\pm 2\text{‰}$ for $\delta^{18}\text{O}$ and $\pm 10\text{‰}$ for $\delta^2\text{H}$ means the two can be considered to have approximately the same isotopic composition where topography is more subdued, rainfall is higher, and evaporation is less important [23]. However, it should be noted that the available dataset is still too small to make a sweeping statement about comparability of precipitation and river δ values in the Belgrade area.

Further, $\delta^{18}\text{O}$ seasonal trends in precipitation and surface water were modelled using periodic regression analysis to fit seasonal sine wave curves to annual $\delta^{18}\text{O}$ variations defined as [24]:

$$\delta^{18}\text{O} = \delta^{18}\text{O}_{\text{ave}} + A[\cos(c \cdot t - \theta)] \quad (1)$$

where $\delta^{18}\text{O}$ and $\delta^{18}\text{O}_{\text{ave}}$ are the modelled and the mean annual measured $\delta^{18}\text{O}$, respectively; A is the measured $\delta^{18}\text{O}$ annual amplitude; c is the radial frequency of annual fluctuations ($0.017247 \text{ rad day}^{-1}$); t is the time in days after the start of the sampling period and θ is the phase lag or time of the annual peak $\delta^{18}\text{O}$ in rad.

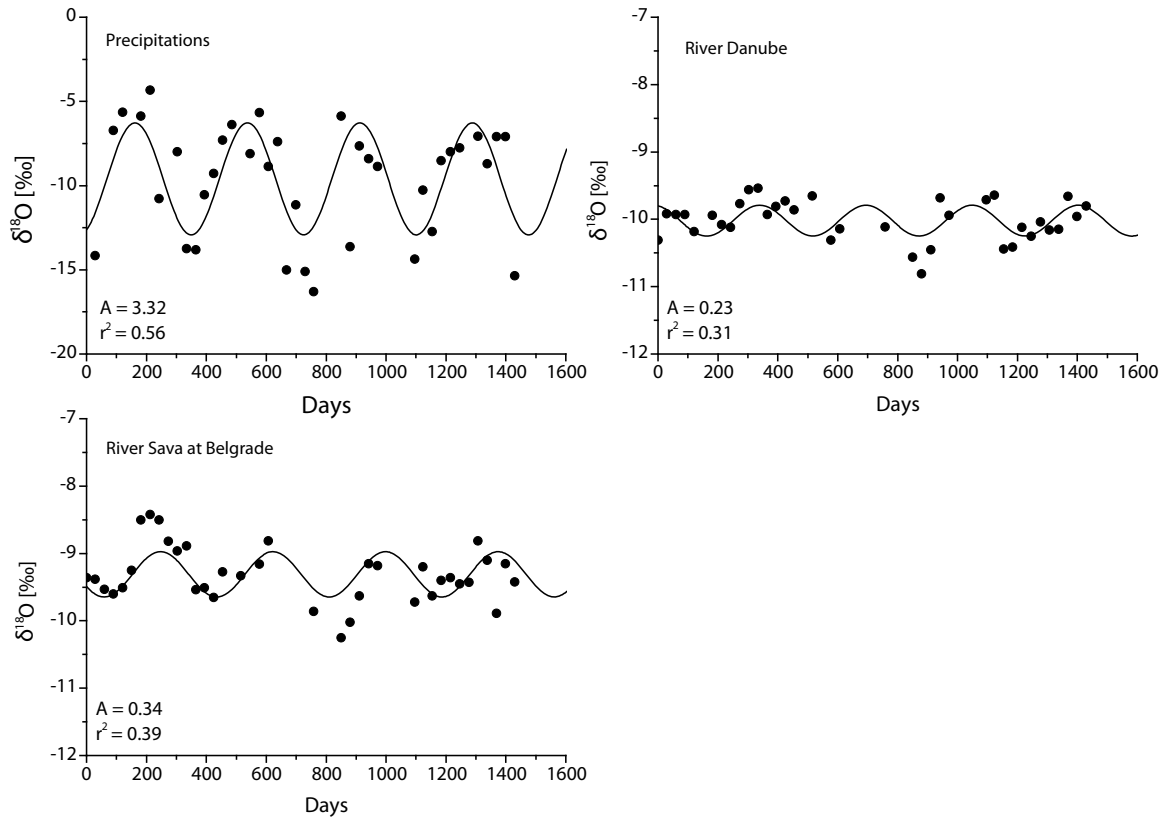


FIG. 3. Fitted annual regression $\delta^{18}\text{O}$ models for precipitation and surface water of the Sava and Danube Rivers at Belgrade between 2004 and 2006.

To estimate mean residence time (MRT) the commonly used exponential model was applied in which precipitation inputs are assumed to mix rapidly with resident water using the following equation [24–26]:

$$\text{MPT} = c^{-1} \cdot [(A_{Z1} / A_{Z2})^{-2} - 1]^{0.5} \quad (2)$$

where A_{Z1} is the amplitude of precipitation; A_{Z2} is the amplitude of the surface water outputs; and c is the radial frequency of annual fluctuation as defined in Eq. 1. It should be mentioned that the results can be taken as preliminary estimates of mean residence time, since the model is relatively simple and the catchments of the Sava and Danube Rivers are more complex. Figure 3 shows the fitted models for annual $\delta^{18}\text{O}$ variations in precipitation and surface water for the Sava and Danube Rivers at Belgrade. Precipitation data are relatively well described using the seasonal sine wave model ($r^2 = 0.56$), which provides a model amplitude of 3.32‰ comparable with other studies [20, 24]. The precipitation data from Ljubljana's sampling station were relatively crudely described ($r^2 = 0.36$) for the 2004–2006 period, but the model described precipitation data quite well for the whole available period 1981–2006 ($r^2 = 0.56$). The estimated amplitude was found to be 2.92‰ and was further used to estimate the MRT in the Sava River in Slovenia [20]. In terms of surface water sampling sites, modeled $\delta^{18}\text{O}$ values show less predictability and lower annual $\delta^{18}\text{O}$ amplitude values, which could be expected for data with the least variable $\delta^{18}\text{O}$ surface water [20]. The model described by Eq. 1 was used to translate results into estimates of mean surface water residence time. The calculated results are collected in Table 1. It should be mentioned that results provide a very general, but useful, indication of the degree of mixing of hydrological sources and thus offer a valuable integrated

assessment of differences in runoff processes in the Sava River catchment. The MRT for sampling stations Zelenci and Jesenice na Dolenjskem were estimated based on precipitation data in Ljubljana and are presented more in detail elsewhere [20]. It is interesting to note that the longer MRT of 1.76 and 2.24 years for the Sava River at Zelenci and the Danube River, respectively coincide with generally more depleted mean $\delta^{18}\text{O}$ surface water than for other sites. This probably indicates the greater influence of depleted winter precipitation inputs. The data at Zelenci and Jesenice na Dolenjskem have good agreement with residence time determined by tritium content. The measured tritium content in the Sava River and its tributaries has an average TU value of 13.7 ± 2.4 , close to the current rainfall value of 7.9 TU, determined at the same time near Ljubljana. These indicate a residence time for the river of approximately two years, and the presence of young waters in the river watershed [17]. A maximum tritium content of up to 122.3 ± 2.0 TU was always determined near the Krško Nuclear Power Plant. However, it has been found that international limits of tritium discharge from nuclear facilities have never been exceeded [27].

5. CONCLUSIONS

The obtained results provide interesting insights into the current understanding of integration of hydrological processes in larger catchments areas. High seasonal variability in $\delta^{18}\text{O}$ and $\delta^2\text{H}$ values was observed in precipitation and is likely to be reflected in the isotopic composition of surface waters. The lower $\delta^{18}\text{O}$ and $\delta^2\text{H}$ values were found at the source of the Sava River at Zelenci are connected to the higher elevation of the recharge area, lower temperatures and greater amounts of precipitation. Similar mean $\delta^{18}\text{O}$ and $\delta^2\text{H}$ values were also observed in the Danube River. Isotopic composition in the lower parts of the Sava River was similar at both locations. The $\delta^{18}\text{O}$ and $\delta^2\text{H}$ values were less negative compared to values at the source of the Sava River at Zelenci, probably due to the lower amount of precipitation. Data for $\delta^{18}\text{O}$ over a three year period revealed the mean water residence time (MRT) estimation using the exponential flow model. The MRT at Zelenci and the Danube River were estimated to be 1.8 and 2.2 years respectively, higher than the MRT estimated for the lower parts of the Sava River. Current results highlight the utility of surface water oxygen and hydrogen isotopes as an analytical tool and could serve as a reference for subsequent studies of Sava and Danube Rivers in areas such as paleoclimatology. It can be concluded that tracer studies such as this are continuing in order to refine our understanding of flow paths and residence time, and to help structure and validate hydrological models on a global scale.

ACKNOWLEDGEMENTS

Part of the project was financially supported by the IAEA under Contract No. 12642 entitled “Chemical and stable isotope investigation of the Sava and Soča Rivers in Slovenia”, and as a part of the CRP “Design criteria for a network to monitor isotope composition of runoff
IQ QJH UYHV 7KHDKWRVDHJUDMXOR 0 U6WMD ä LJRQ 0 U =GIQND UNRYDQG3HMD
Dujmović for technical support and assistance. Special thanks to the staff of the Environmental Agency of Slovenia for their help and the Republic Hydrometeorological Service of Serbia for sample collection.

REFERENCES

- [1] KENDALL, C., MCDONNELL, J.J., Isotope tracers in catchment hydrology, Elsevier Science, Amsterdam (1998) pp. 840.
- [2] YANG, C., TELMER, K., VEIZER, J., Chemical dynamics of the 'St. Lawrence' riverine system: δD_{H_2O} , $\delta^{18}O_{H_2O}$, $\delta^{13}C_{DIC}$, $\delta^{34}S_{sulfate}$, and dissolved $^{87}Sr/^{86}Sr$. *Geochim. Cosmochim. Acta* **60** (1996) 851–866.
- [3] PAWELLEK, F., FRAUENSTEIN, F., VEIZER, J., Hydrogeochemistry and isotope geochemistry of the upper Danube river. *Geochim. Cosmochim. Acta* **66** (2002) 3839–3854.
- [4] GAT, J.R., Oxygen and hydrogen isotopes in the hydrological cycle, *Annual Rev. Earth Planet. Sci.* **24** (1996) 225–262.
- [5] LACHNIET, M., PATTERSON, W.P., Stable isotope values of Costa Rican surface waters, *J. Hydrol.* **260** (2002) 135–150.
- [6] BURNS, D.A., Stormflow hydrograph separation based on isotopes: the thrill is gone — What's next? *Hydrol. Process.* **16** (2002) 1515–1517.
- [7] SKLASH, M.G., "Environmental isotope studies of storm and snowmelt runoff generation", (ANDERSON, M.G., BURT, T.P., Eds) *Process Studies in Hillslope Hydrology* John Wiley, Chichester (1990) 401–435.
- [8] GENEREUX, D.P., HOOPER, R.P., "Oxygen and hydrogen isotopes in rainfall–runoff studies", (KENDALL, C., MCDONNELL, J.J., Eds) *Isotope tracers in catchment hydrology*, Elsevier Science, Amsterdam (1998) 319–346.
- [9] ACHEAMPONG, S.Y., HESS, J.W., Origin of the shallow groundwater system in the southern Voltaian sedimentary basin of Ghana: an isotopic approach, *J. Hydrol.* **233** (2000) 37–53.
- [10] MALOSZEWSKI, P., STICHLER, W., ZUBER, A., RANK, D., Identifying the flow systems in a karstic-fissured-porous aquifer, the Schneeealpe, Austria, by modelling of environmental ^{18}O and 3H isotopes, *J. Hydrol.* **256** (2002) 48–59.
- [11] BOLUNOVSKY, A.YA., BONDAREVA, L.G., Tritium in surface waters of the Yenisei river basin, *J. Environ. Radioactivity* **66** (2003) 285–294.
- [12] CLARK, I., FRITZ, P., *Environmental Isotopes in Hydrology*, Lewis publishers, New York (1997) pp. 328.
- [13] EPSTEIN, S., MAYEDA, T., Variations of ^{18}O contents of water from natural sources, *Geochim. Cosmochim. Acta* **4** (1953) 213–224.
- [14] GEHRE, M., HOEFLING, R., KOWSKI, P., STRAUCH, G., Sample preparation device for quantitative hydrogen isotope analysis using chromium metal, *Anal. Chem.* **68** (1996) 4414–4417.
- [15] FLORKOWSKI, T., Low level tritium assay in water samples by electrolytic enrichment and liquid scintillation counting in IAEA Laboratory, IAEA-SM-252/63 (1975) 335.
- [16] FLORKOWSKI, T., Tritium electrolytic enrichment using metal cells, Low level tritium measurement, Proc. Consultants Meeting, Vienna 1979, IAEA-TECDOC-246 (1981) 133.
- [17] VREČA, P., KRAJCAR BRONIĆ, I., HORVATINČIČ, N., BAREŠIĆ, J., Isotopic characteristics of precipitation in Slovenia and Croatia: Comparison of continental and maritime stations, *J. Hydrol.* **330** (2006) 457–469.
- [18] GOLOBOČANIN, D., OGRINC, N., BONDZIĆ, A., MILJEVIĆ, N., Isotopic characteristics of meteoric waters in the Belgrade region, *Isot. Environ. Heal. Stud.* **43** (2007) 355–367.
- [19] CRAIG, H., Isotopic variations in meteoric waters. *Science* **133** (1961) 1720.

- [20] OGRINC, N., KANDUČ, T., STICHLER, W., VREČA, P., Spatial and seasonal variation in $\delta^{18}\text{O}$ and δD values in the River Sava in Slovenia, *J. Hydrol.* (sent in review 2008).

ISOTOPE COMPOSITION OF MEKONG RIVER FLOW WATER IN THE SOUTH OF VIETNAM

K.C. Nguyen, L. Huynh, D.C. Le, V.N. Nguyen, B.L. Tran

Center for Nuclear Techniques, Hochiminh City, Vietnam

Abstract. As a part of the Research Project entitled: “Design Criteria for a Network to Monitor Isotope Compositions of Runoff in Large Rivers” launched by the International Atomic Energy Agency in 2003, Research Contract No. VIE/12569, entitled “Isotope Composition of Mekong River Flow Water in the South of Vietnam” was accepted to set up a network for monitoring isotope composition in the Mekong river streamflow water in the south of Vietnam. The goal of the project was to understand streamflow–aquifer interactions and other relevant hydrological parameters. The primary results showed a seasonal variation, as well as dependence on local precipitation and river water levels, along with the isotopic composition of two distributaries of Mekong river water. At the same time, a slight change in seasonality of tritium in rivers water and the difference between tritium content in local rainy water and river water were recorded. Although changes in streamflow isotope composition based on season were defined, changes in the isotope composition of Tien and Hau river water is very complicated, being affected by groundwater, precipitation and isotopic (latitude, amount and evaporation) effects. Monitoring must continue on environmental isotopic composition in the future not only at the five existing stations in the south of Vietnam, but also at some stations along the river course outside of Vietnamese territory to collect more isotopic data for the Mekong river basin and thus enhance the study of hydrological processes for Asian rivers (for which few data exist) as well as for the global database.

1. INTRODUCTION

The Mekong is one of the longest rivers in Asia. Originating from high mountains in the northwest of China, the Mekong river flows on to Myanmar, Thailand, Laos and Cambodia, dividing into two tributaries before flowing to the south of Vietnam. In Vietnam, two these tributaries are called the Hau River, which has a flow rate of 20%, and the Tien River, with average flow rate of about 80%. The length of each tributary in Vietnam is about 450 km and both flow into the South China Sea through nine estuaries.

Extending from a latitude of 35° to 9° north with a basin area of about 800 000 km², the Mekong river drains water from different climatic areas. Thus, the isotope composition of river water could reflect the cumulative influence of hydrological processes from precipitation to discharge, including the influence of snow, melting glaciers, dams, lakes, karst terrain, altitude, arid zone evaporation, snowmelt events and tributaries; this can provide information on water origin and residence times, surface–groundwater exchange, precipitation variability, and climate/land use changes because its importance for world river systems.

Previous studies on origin and groundwater dynamics in the Nambo plain (south of Vietnam) applying isotope techniques show that there is a significant difference between the isotope compositions of Mekong river water and that of local precipitation, groundwater and surface water in the area. The seasonal variation in stable isotope composition of Mekong river water was especially observed in its small tributaries. These differences are a good index for hydrogeological studies in the area such as the origin of groundwater, interaction

between surface water and groundwater, recharge mechanisms, as well as the changes in water environment quality.

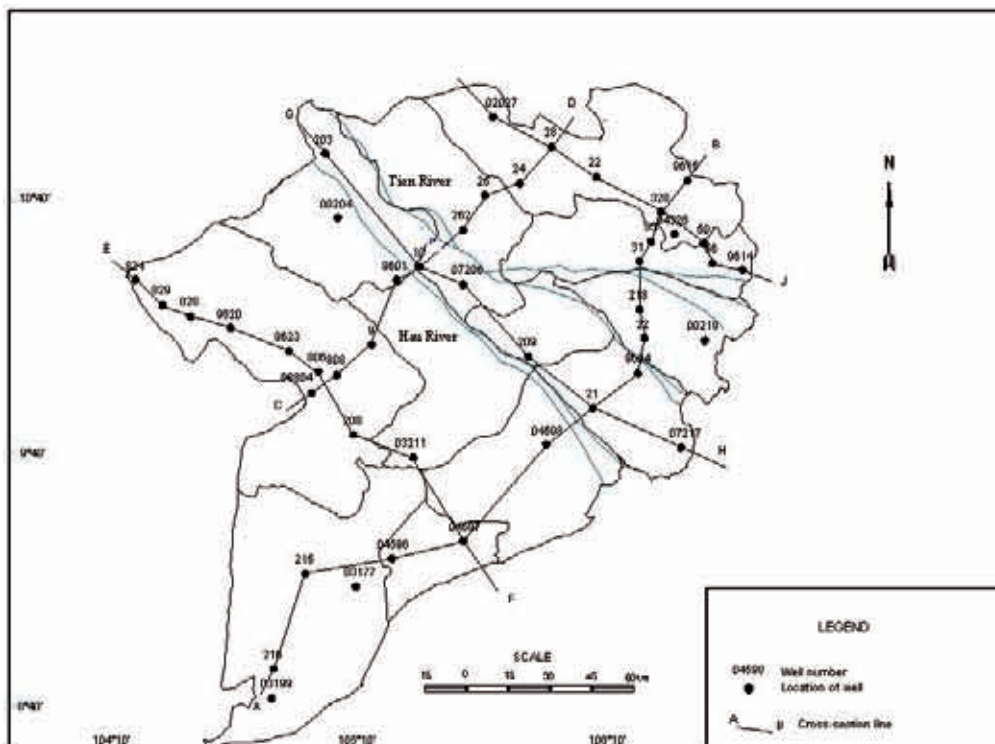
For these purposes, a project to monitor the isotopic composition of Mekong river water was set up starting in 2003. The main objectives are: (i) setting up a network and monitoring the isotopic composition of Mekong River streamflow water in the south of Vietnam to understand streamflow/aquifer interactions; (ii) identification of parameters that should be monitored within the GNIR network of isotopes in rivers basins.

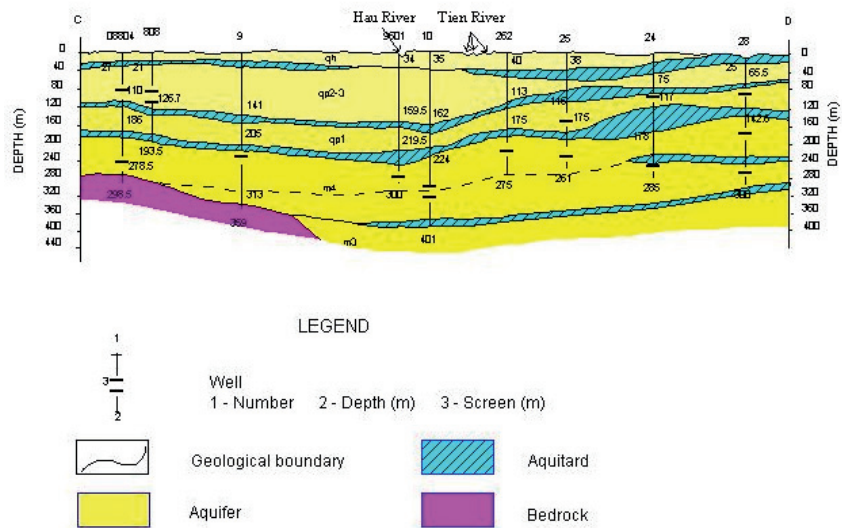
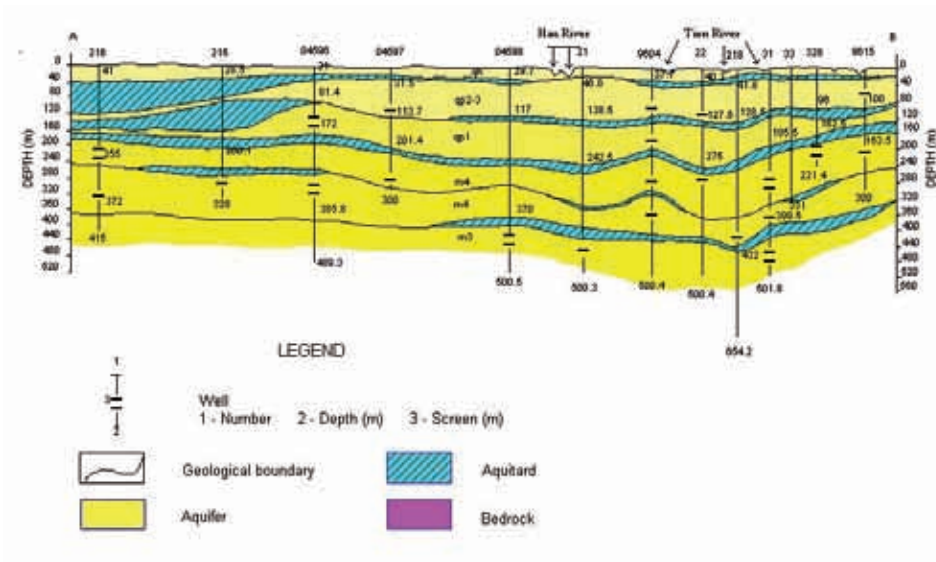
2. DESCRIPTION OF RESEARCH CARRIED OUT

2.1. Collected and compiled hydrogeological documents

The Mekong River derives from mountains in the northwest of China. Flowing through six countries (Cambodia, China, Laos, Myanmar, Thailand and Vietnam), the Mekong River has a basin area of about 795 000 km². With a total length of about 4800 km, Mekong River carries an average water amount of 475.10⁹m³. Most of the river basin is in tropical climate conditions.

Before coursing into the south of Vietnam, the Mekong River divides into two tributaries. In Vietnam, the first tributary is called the Tien River and the second is called the Hau River. The area of basin in the south of Vietnam accounts for 8% of the total river basin and the average water amount glowing is about 11% of the total amount in the Mekong River. Each distributary, from the Cambodia–Vietnamese border to the East Sea, has the length of about 450 km. These tributaries are regulated by Lake Tonlesap in Cambodia. (Data source: *vnm.c.gov.vn*).





Based on hydrogeological studies carried out since 1975, hydrogeological cross-sections of the Mekong Delta area were set up. Among them, two main cross-sections directly related to the monitoring area were compiled. (see Figs 1–3). According to these cross-sections, there could be direct relations between river water and groundwater of the *qh* and *qp₃* aquifers.

Water levels at the three existing hydrological stations along the Tien (MK03) and Hau (MK09, MK11) rivers as well as precipitation data were documented.

2.2. Setting up the sampling network

Based on the topographic and hydrogeological characteristics of the study area, at the beginning a network of 11 sampling points (coded from MK01 to MK11) along the Tien and Hau rivers was set up (Fig. 4) to monitor the isotope compositions of the river water. Afterwards, from

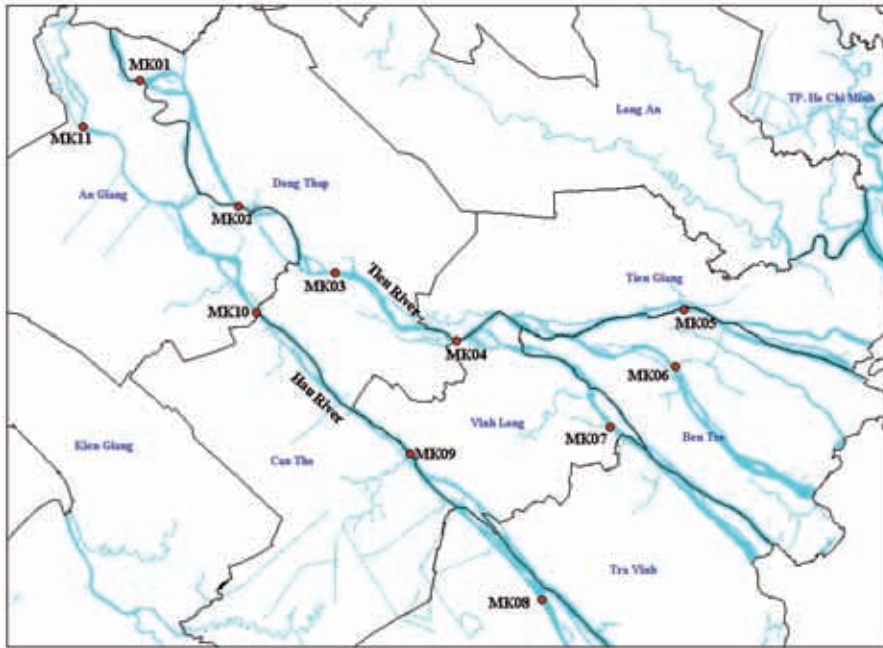


FIG. 4. Network for sampling Mekong River flow water.

Sep. 2004, only five of these have been used for this research, including three sampling points set up on the Tien River (MK01, MK03, MK04) and only two points (MK09, MK11) on the Hau River because the flow rate of the Tien River is of 80% of the Mekong River total flow rate (in the South of Vietnam).

2.3. Sampling and analysis

The area of the Mekong River basin in the South of Vietnam accounts for 8% of the total river basin and has an average of about 11% of the total Mekong river water amount. Collected river water samples are mixed samples. At a sampling point, midstream water has been taken by a submerged pump at different depths and mixed before sampling for analysis. Water samples for ^2H and ^{18}O analysis were taken monthly, while those for tritium were taken every two months. A total of 190 river streamflow samples (for $\delta^2\text{H}$, $\delta^{18}\text{O}$) and 95 samples for tritium were collected. All water samples collected have been analyzed for $\delta^{18}\text{O}$, $\delta^2\text{H}$ and ^3H at the Isotope Laboratories at Institute for Nuclear Sciences and Technology (INST) and the Center for Nuclear Techniques (CNT) in Vietnam. Analysed data is in the database.

3. RESULTS OBTAINED

3.1. Precipitation and river water levels in the monitoring area

Due to the subequatorial climatic conditions there are only two seasons in the South of Vietnam. The wet season lasts from May to October and the dry season from November to April. In the wet season, rain water amounts account for 90–94% of annual precipitation and reach a maximum in September (or October).

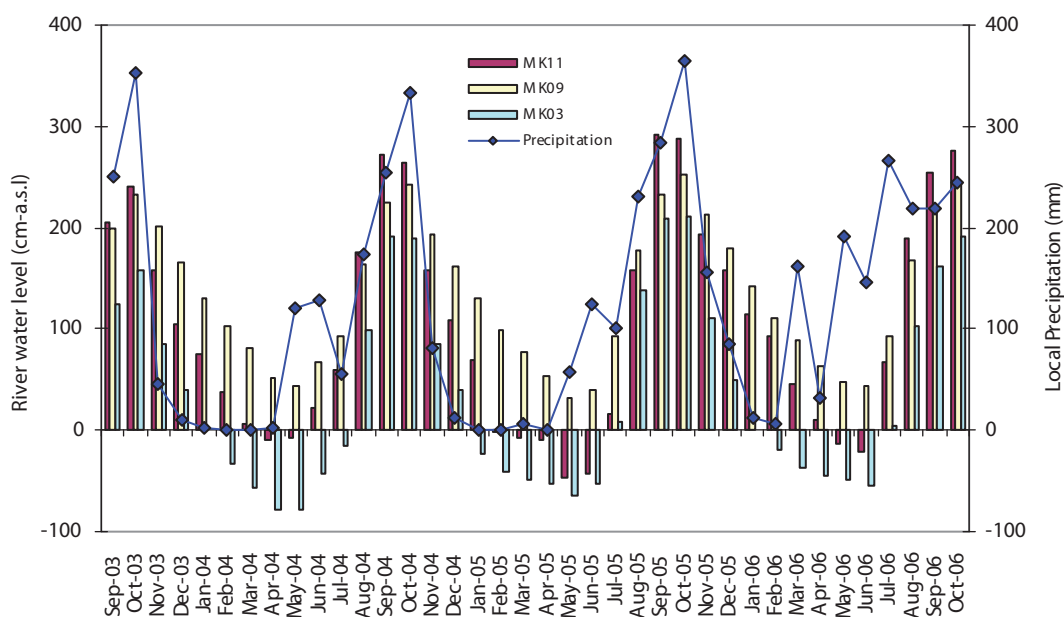


FIG. 5. Monthly precipitation and water levels of the river.

The flow rate measured at MK01 (on the Tien River) is significantly higher than that measured at MK11 for the Hau River. The Vam Nao branch transfers about 25% of the Tien River's water is 'poured' into the Hau River (Data source: Nambo meteoric hydrograph centre).

Precipitation data obtained at the MK10 station as well as river water levels at MK03, MK09 and MK11 are plotted in the figure below.

The variation of river water levels in comparison to local precipitation shows that in the wet season local rain water could be an important component in river water. This means that mixing with local rain water could change the isotopic composition of river water.

3.2. Isotopic composition of river water

The isotopic composition of river water collected from Sept. 2003 to Oct. 2006 along the Tien and Hau Rivers is shown in Fig. 6. Water samples are clustered into two groups. One group is more enriched in heavy isotopes, and includes river water samples collected in the dry season, while the other is more depleted in heavy isotopes and involve water samples taken during the rainy season. Seasonal variation could be defined.

On the other hand, the river water seems to have undergone evaporation. Almost all of the water samples are distributed along the evaporation line.

Variations of ^{18}O and ^2H for all river water samples are presented in Figs 7 and 8.

In general, heavy isotopes in river water are enriched during the dry season (Nov.–Apr.), especially in January, while they become depleted during the rainy season. It seems that ^2H and ^{18}O isotopes are more enriched along the river course. This could be caused by an evaporation effect due to high temperatures in the monitoring area.

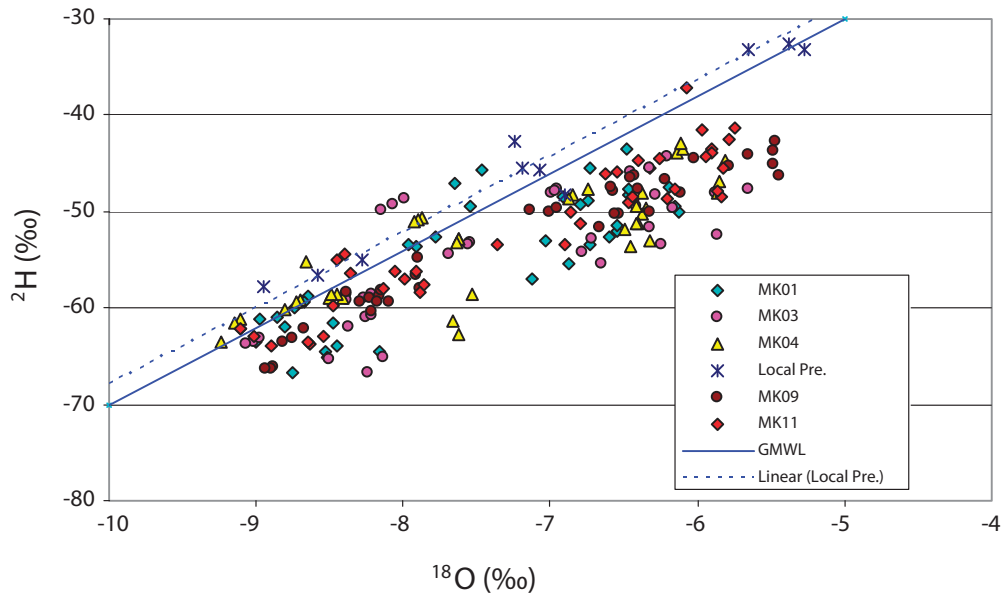


FIG. 6. Relationship between $\delta^2\text{H}$ and $\delta^{18}\text{O}$ at selected stations along the Mekong River.

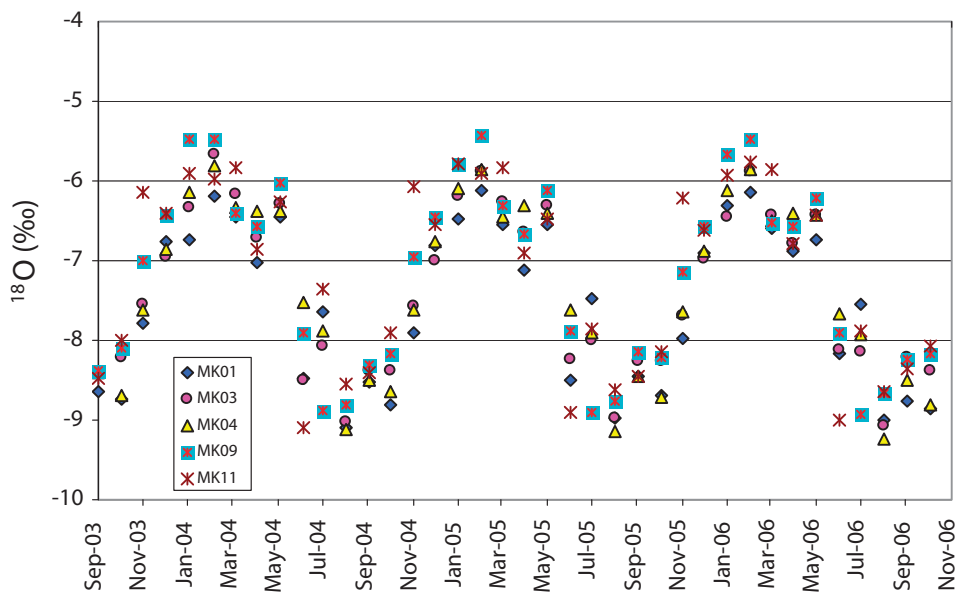


FIG. 7. Variation in $\delta^{18}\text{O}$ over time at selected stations along the Mekong River.

For both rivers, stable heavy isotopes are enriched in July when precipitation is depleted. It could be explained by the fact that precipitation observed in July in monitoring areas is usually lower than for other months of the rainy season.

Figures 9 and 10 present the dependence of $\delta^{18}\text{O}$ and $\delta^2\text{H}$ contents of Tien and Hau river water on local precipitation amounts. These isotopes are enriched in the dry season and become depleted in wet season.

The enrichment of $\delta^{18}\text{O}$, as well as of $\delta^2\text{H}$ in July shows the importance of local precipitation in river water. The enrichment of $\delta^2\text{H}$ in this month is stronger than enrichment of the $\delta^{18}\text{O}$ component.

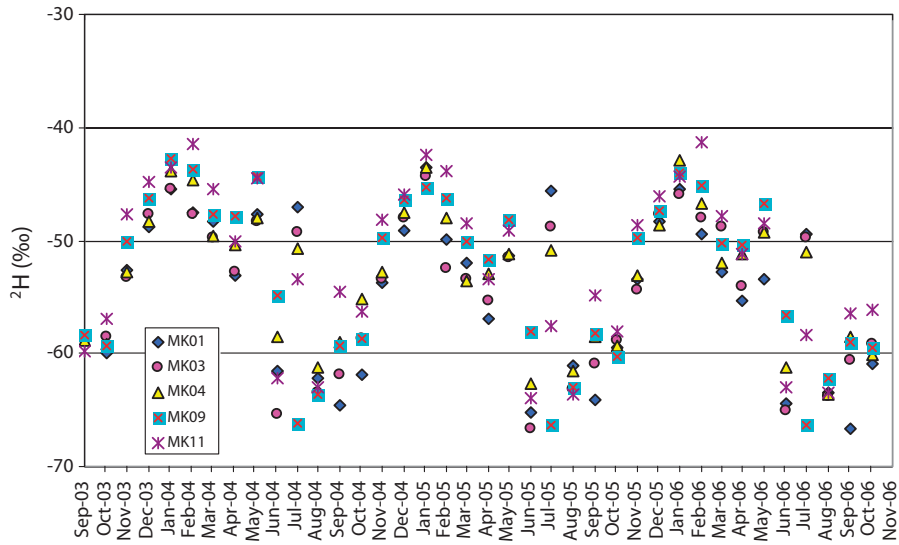


FIG. 8. Variation in δ^2H for time of the Mekong River.

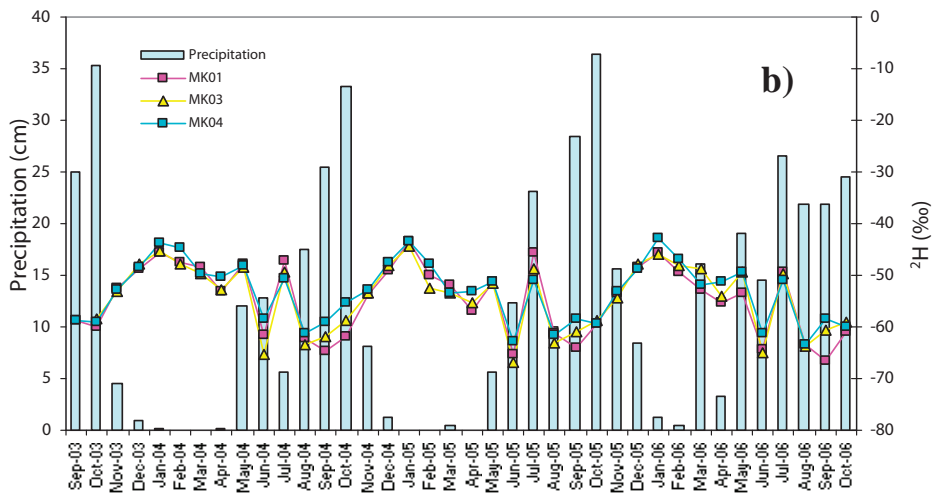
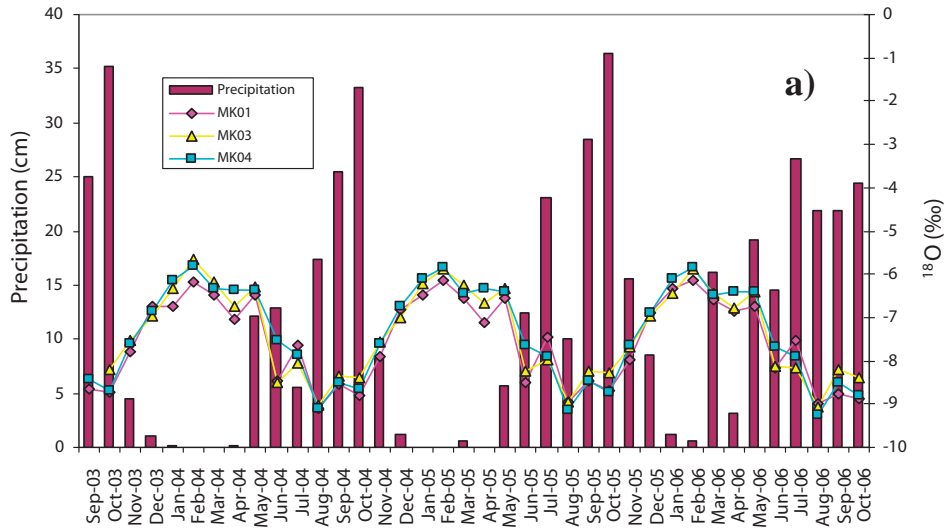


FIG. 9. a) Variation in $\delta^{18}O$ of local precipitation and time for the Tien River. b) Variation in δ^2H of local precipitation and on time for the Tien River.

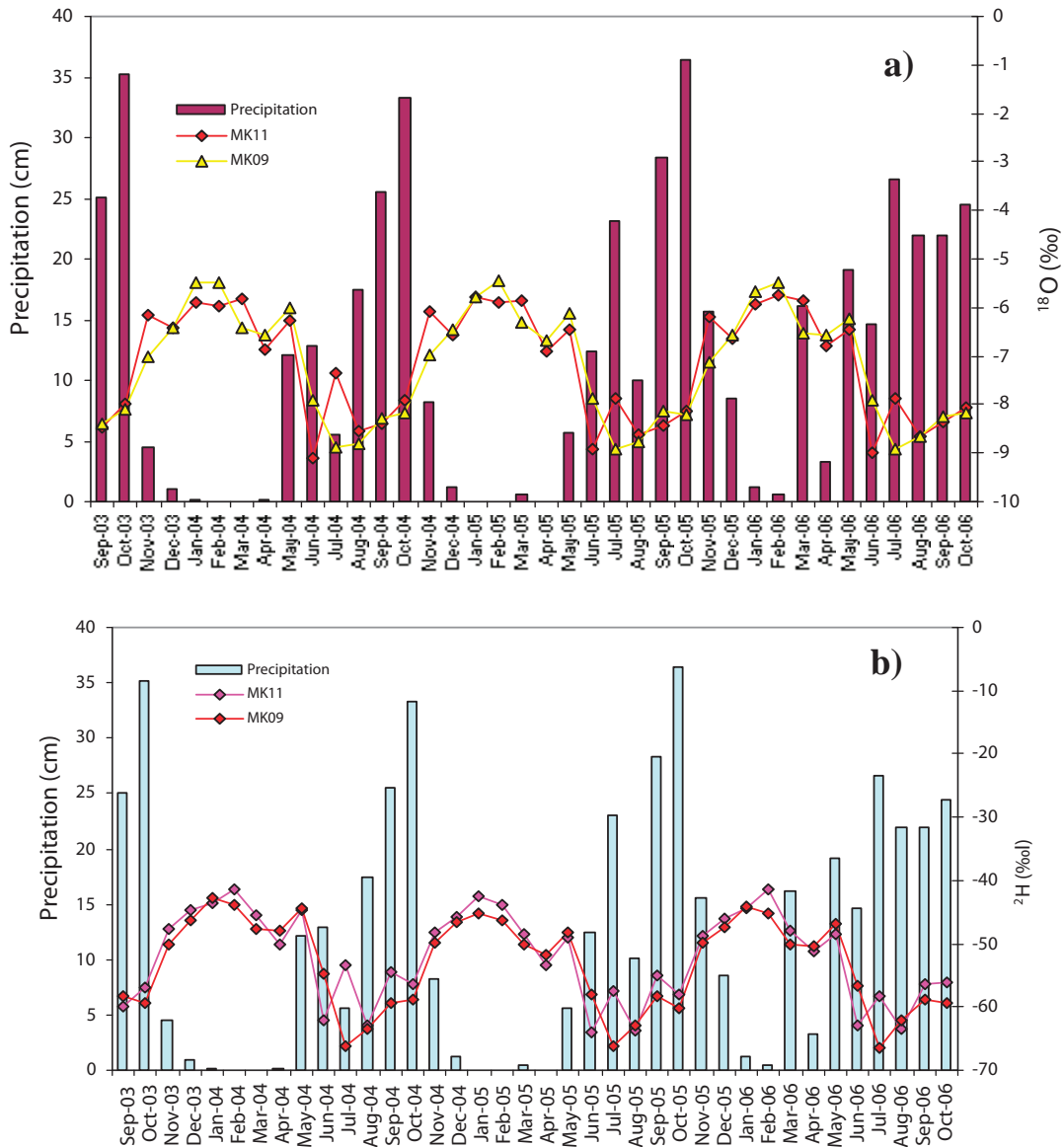


FIG. 10. a) Variation in $\delta^{18}\text{O}$ for local precipitation and time for the Hau River. b) Variation in $\delta^2\text{H}$ for local precipitation and time for the Hau River.

For Tien river, the enrichment of heavy isotopes ($\delta^2\text{H}$ and $\delta^{18}\text{O}$) is very clear, especially for $\delta^2\text{H}$.

The enrichment in heavy isotopes of river water samples collected in July when the amount of rain is low compared to that of other months during the rainy season was observed in the Hau River as well, but the effect is not as strong as in the Tien River (Fig. 10). The difference may be caused by a difference in the flow rate of two these rivers, as described later.

Figures 11–13 show the variations in heavy isotope content for different river water levels and time frames at the MK03, MK09 and MK11 stations.

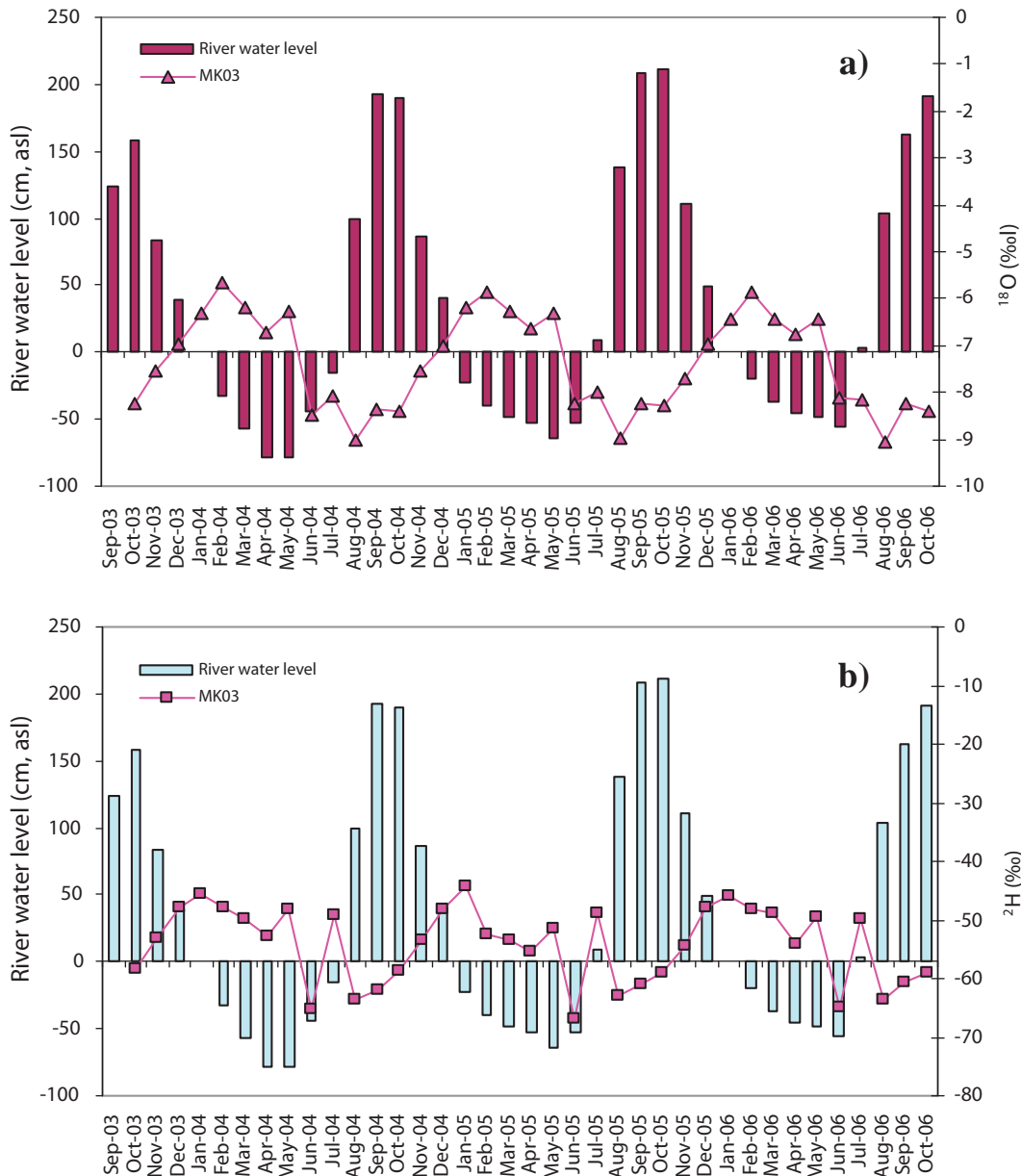


FIG. 11. a) Variation in $\delta^{18}\text{O}$ for river different water levels and times for the Tien River. b) Variation in $\delta^2\text{H}$ in relation to river water levels and times for the Tien River.

At point MK03 along the Tien River, $\delta^2\text{H}$ and $\delta^{18}\text{O}$ values increase when river water levels decrease. This is reasonable because of the dependence of water levels on local rain amounts (see Fig. 5). During the dry season, heavy isotope concentrations in river water increases step by step and are the most enriched in January or February. After that, the river water becomes depleted in heavy isotopes due to groundwater discharge to the river.

In May, the first rains enriched in heavy isotopes fall. Could this be one cause of the increase in heavy isotopes concentrations in river water? In July, the enrichment of $\delta^2\text{H}$ and $\delta^{18}\text{O}$ in river water is explained by a decrease in the amount of rain at the monitoring areas.

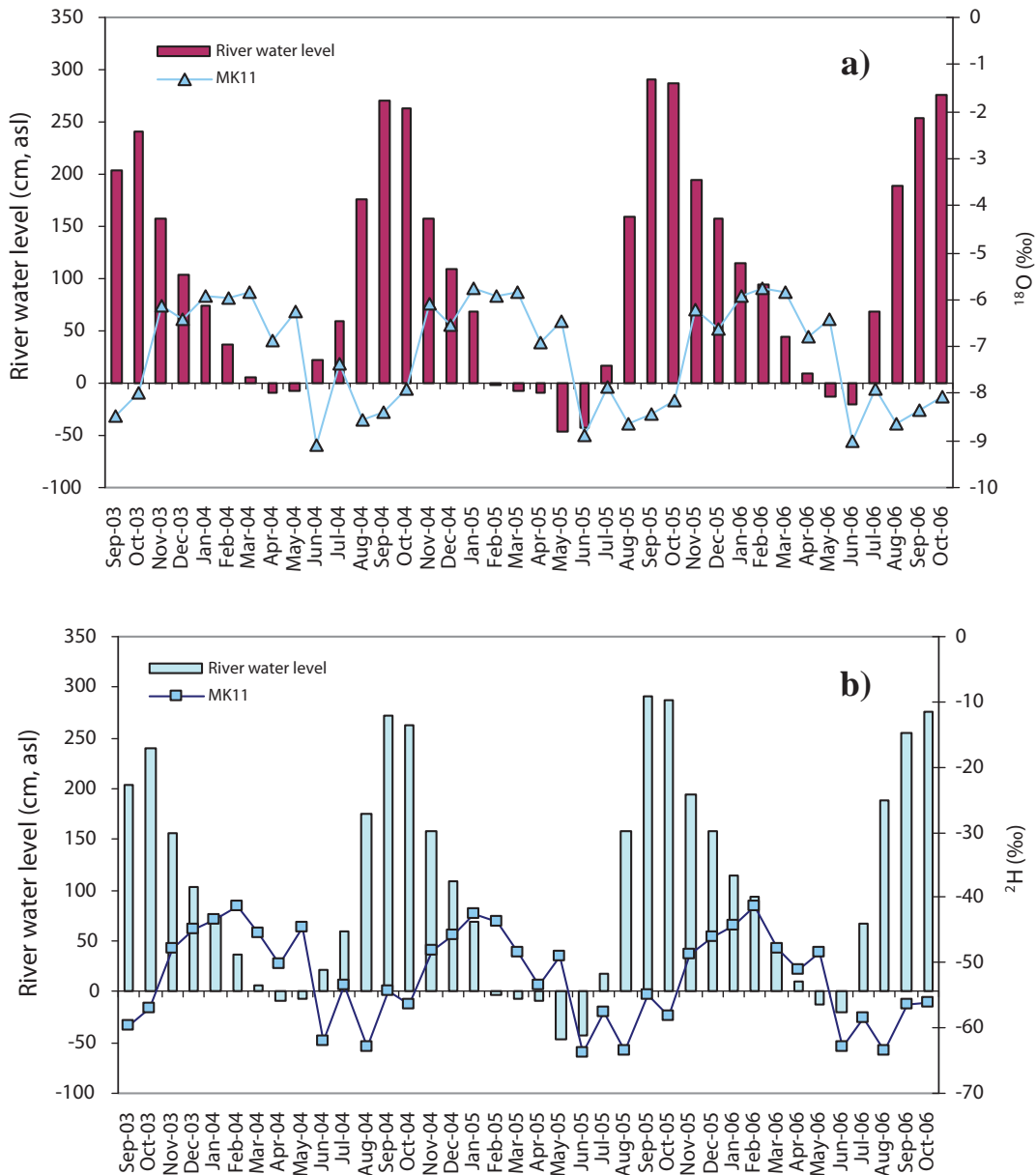


Fig. 12. a) Variation in $\delta^{18}\text{O}$ for river water levels and different times at MK11 for the Hau River. b) Variation in $\delta^2\text{H}$ for river water levels and different times at MK11 for the Hau River.

The $\delta^{18}\text{O}$ (and $\delta^2\text{H}$) of river water are enriched during the dry season, but $\delta^{18}\text{O}$ reaches a maximum value in February, while deuterium reaches a maximum value in January. This phenomenon requires more investigation.

For the Hau River (Figs 12 and 13), variations in levels of isotopic composition are identical: they are enriched in the dry season and depleted in the rainy season.

The enrichment of $\delta^2\text{H}$, $\delta^{18}\text{O}$ in Hau River water in May and July (for MK11 only) was observed once. However, $\delta^2\text{H}$ values at the MK11 were highest in February, while river water at MK09

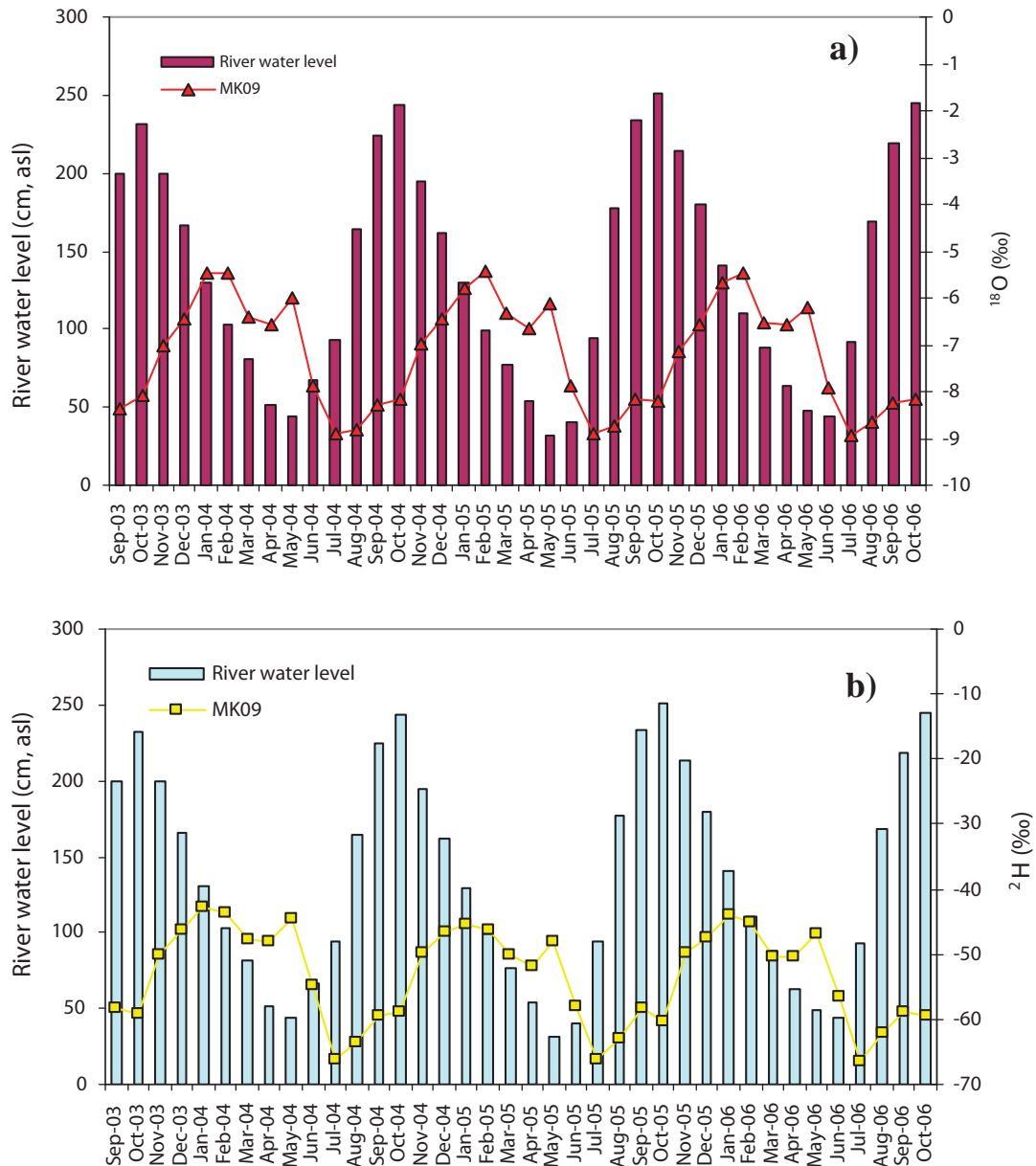


FIG. 13. a) Variation in $\delta^{18}\text{O}$ for river water levels different times at MK09 for the Hau River. b) Variation in $\delta^2\text{H}$ for river water levels and different times at MK09 for the Hau River.

had a maximum deuterium value in January. This could be caused by a strong evaporation effect along the river's course (the same phenomena has been recorded for stations along the Tien River).

Different to other stations, both $\delta^2\text{H}$ and $\delta^{18}\text{O}$ values in river water were at a minimum in July at the MK09 station (see Fig. 13). Is this caused by water being 'poured' from the Tien River to the Hau River through the Vam Nao branch? More study is required.

3.3. Tritium content in river water

Tritium contents in the Tien and Hau Rivers based on time are presented in Fig.14.

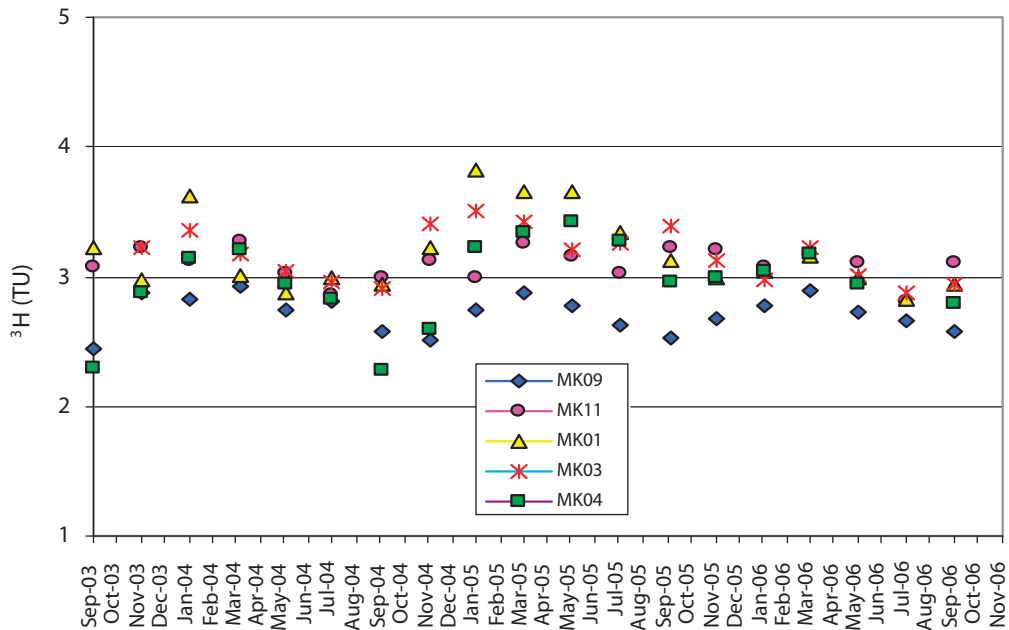


FIG. 14. Tritium content in water of the Tien River.

The tritium content observed in river water over time shows that it seems to change slightly according to season, becoming higher in the dry season when water from high latitude areas with high tritium dominates at the monitoring areas. At the same time, the tritium content of river water is always higher than that in local rain water (less than 2.0 T.U).

Along the river course, tritium content decreases from upstream to downstream. This can be caused by groundwater discharge (which is free of tritium) to the river.

Seasonal changes in tritium, as well as those that occur along the river course, need to be monitored for a much longer time.

4. CONCLUSION

A total of 190 river streamflow samples (for $\delta^2\text{H}$, $\delta^{18}\text{O}$) and 95 samples for tritium were collected. Water samples collected have been analyzed for ^{18}O , ^2H (by IRMS) and ^3H (by LSC after electrolytic enrichment) at Isotope Laboratories at the Institute for Nuclear Sciences and Technology (INST) in Hanoi and Center for Nuclear Techniques (CNT) in Hochiminh City, Vietnam. Analysis accuracy is $\pm 0.15\%$ for $\delta^{18}\text{O}$ and $\pm 1.0\%$ for $\delta^2\text{H}$.

In general, both tributaries (Tien and Hau) of the Mekong River where stable isotopic data was collected show a seasonal fluctuation: heavy isotopes were more enriched in dry season months (from November to April) and became depleted in the rainy season. At the same time, a small divergence in May was observed because of unstableness associated with seasonal change, while more enrichment in heavy isotopes in the river was recorded in July (the rainy season) when local precipitation was isotopically more negative (except at MK09 station). Although seasonal changes in the stream flow of isotope composition are defined, variations in

isotopic composition of Tien and Hau river water is very complicated because it is influenced by groundwater, precipitation and isotopic (latitude, amount and evaporation) effects.

The tritium contents of river water show a small seasonal variation. Tritium content in river waters is always higher than that in local precipitation. This can be explained by the influence of water flowing from higher latitude inland areas where tritium contents are high relative to the monitoring area.

To define residence time and aquifer/streamflow interaction — which would be of importance for studying hydrological processes in Asian rivers (for which few data still exist) as well as for the global database — the Mekong River must continue to be monitored for environmental isotopic composition in the future at a minimum of five existing stations in the south of Vietnam. Parameters that should be monitored within the GNIR network of isotopes in river basins include environment isotopes (^2H , ^{18}O , ^3H) in river water, groundwater and local rain water. It is also necessary to set up some stations along the river's course outside of Vietnam territory to gather more isotopic data regarding the Mekong river basin.

TEMPORAL AND SPATIAL VARIATIONS OF $\delta^{18}\text{O}$ ALONG THE MAIN STEM OF YANGTZE RIVER, CHINA

B. Lu^a, T. Sun^a, C. Wang^a, S. Dai^{a,b}, J. Kuang^c, J. Wang^a

^a State Key Laboratory of Hydrology-Water Resources and Hydraulic Engineering, Hohai Univ., Nanjing, China

^b Flood-control Division, Taihu Basin Authority of MWR, Shanghai, China

^c Hydrology Bureau of MWR, Beijing, China

Abstract. The Yangtze River is the largest river in China, and the third longest in the world. Data on $\delta^2\text{H}$ and $\delta^{18}\text{O}$ isotopes in the river water provide a very useful tool for interpretation of hydrological processes and hydrological cycles related to climate change and anthropogenic activities in a large scale river basin. Since 2003, 170 water samples have been recovered from the first water campaign and regular samples over one year from four stations have been analyzed for $\delta^2\text{H}$ and $\delta^{18}\text{O}$ composition. From upstream to downstream, the isotopic composition of ^2H and ^{18}O gradually increase. The trendline of the first campaign is situated in the middle of the LMWL and the trendline of isotopic $\delta^2\text{H}$ and $\delta^{18}\text{O}$ for one year sampling at four regular stations is in good accordance with the LMWL. Water inflow from tributaries joining the main stem of Yangtze River are one of the main reasons for spatial isotopic variations in the river's water. Results revealed that temporal and spatial variations in oxygen and hydrogen isotopes of water samples along the main stem of the Yangtze River are strongly driven by the isotope patterns in regional precipitation. Secondary signals deriving from the influx of evaporatively enriched waters from several major lakes or reservoirs along the system are also apparent. The peak of river water isotopic temporal variations corresponds well to the boundary marking the beginning or end of annual flooding periods at-site. The peaks and valleys of river water temporal isotopic variations may be a good indicator to mark the split in river water between surface and groundwater water influences at a given location for a water year.

1. INTRODUCTION

The Yangtze River is the largest river in China, and the third largest in the world. The river snakes its way 6397 km from western China's Qinghai-Tibet Plateau to the East China Sea near the city of Shanghai, crossing nine provinces and spanning $90^\circ 33'$ to $122^\circ 25'E$ and $24^\circ 30'N$ to $35^\circ 45'$. Its watershed has an area of about $179.93 \times 10^4 \text{ km}^2$, including approximately 20% of China's total land area and 25% of its total farming land area. About 350 million people live near the Yangtze River and its 700 tributaries.

From its origin to its estuary the river crosses three main physiographic regions in China corresponding to the three main sections, which are upstream, midstream and downstream. From the headwaters to Chongqing, the upstream portion of the river is located on the uplands of the Tibetan Plateau. The downstream portion of the river extends from the mouth of Poyang Lake to the estuary in the lowland region. The portion of the river in between these regions is located on an intermediate step and is referred to as the midstream. The headwaters of the Yangtze are situated at an elevation of about 4876.8 m in the Kunlun Mountains in the southwestern section of Qinghai. In this area, north of the Himalayas at the Yangtze's origin, the Tibetan Plateau has mighty glaciers and continuous snow cover that melt into the river. The famous three gorges are located medium stream, and all four of China's largest freshwater lakes are in the medium and low reaches of the river.

Flood inundation, water shortages caused by environmental pollution, soil erosion and geological disaster are a few of the major issues facing the Yangtze River basin because of intensive human activities and unsuitable land use. To ensure sustainable economic and social development, a better understanding of hydrological processes and the water cycle is very important at the watershed scale. Watershed hydrology requires integrating knowledge of the hydrosphere, biosphere and atmosphere. Previous studies have shown that commonly used hydrological approaches can't completely recognize the intrinsic characteristics and mechanisms of hydrological processes and the water cycle.

River discharge is composed of snowmelt, surface runoff and groundwater seepage, and is a very important link in the global hydrological cycle. It integrates all information on all three disciplines mentioned above and their impact on the watershed. Much valuable information is contained in the isotopic composition of river discharge. Isotopic signatures in river discharge can potentially provide information on how the hydrological cycle is impacted by both climate change and land use. Stable isotope measurements of river discharge are now used in studies of watershed hydrology, for example to describe major flow pathways of groundwater, to trace water mixing history, to determine mean residence time, surface water and groundwater exchange and renewal rates, evaporation–transpiration partitioning, and to split hydrographs. Dansgaard (1964) [1] first proposed use of the value d to characterize the deuterium excess in global precipitation. The value d is defined on a slope of 8, and is calculated for any precipitation sample as $d = \delta^2\text{H} - 8\delta^{18}\text{O}$. On a global basis, d averages about 10. It changes due to variations in humidity, wind speed and sea surface temperature during primary evaporation [1]. The parameter d has been widely used to estimate the impact of global climate changes and anthropogenic activities on large scale water cycles.

The IAEA has accumulated a great deal of isotopic data for rainfall. However, application of isotope techniques to the study of large scale rivers has been limited by a lack of isotopic data on discharge. To support isotope techniques applied at the large scale watershed level, a global research project entitled 'Design criteria for a network to monitor isotope composition of runoff in large rivers' was started in 2002 by the IAEA. 'The isotopic tracing of hydrology processes in the Yangtze River basin' is one cooperative research programme of the project. The main purpose of the project is to better understand the interaction of surface and groundwater, the contribution of the groundwater to stream flow and the water balance, and to identify the impact of human activities and climate change on river runoff.

Apparently, coupling this information into atmospheric GCMs and hydrological models equipped with isotope tracers should improve the accuracy of forecasting basin flooding and improve water resource planning. The measurement of isotopic fluxes and volumetric discharge is very useful for the development, utilization and protection of water resources in large scale watersheds.

2. WATER SAMPLING

The first water campaign combined with a water pollution investigation was carried out by the Environmental Monitoring Center of the Water Resources Committee of the Yangtze River. It took place in January of 2003. Seventy-four water samples were collected for the first water campaign, four samples for each cross-section within Three Gorges Reservoir, a total of 11 transects and one sample per transect not involving the reservoir, totalling 30 transects. At



FIG. 1. Sampling sites for the first water campaign and the four regular monitoring sites (black dots and triangles represent the sampling sites for the first water campaign and for the regular monitoring sites, respectively).

four regular monitoring stations, water was sampled between 8:00 and 8:30 on the first day and 15th day of each month from 1 Oct. 2003 until 3 Sept. 2005. Water samples were taken using the boat measurement method at 0.1 relative depth below the river water surface and at the 0.3 relative width away from the right (or left) bank for each transect of the whole river. The sampling sites are shown in Fig. 1.

All samples were analyzed for $\delta^{18}\text{O}$ and $\delta^2\text{H}$ in the Environmental Isotope Laboratory of the University of Waterloo (Canada) and the Hydrology Isotope Laboratory of IAEA (Vienna), as well as in the Key Laboratory of IGCS (China).

3. RESULTS AND DISCUSSION

3.1. Relationship between runoff and precipitation isotopic compositions

The relationship between $\delta^{18}\text{O}$ and $\delta^2\text{H}$ for precipitation and river water is demonstrated in Fig. 2. As illustrated, the real lines represent the relationship for the first water campaign in January and a few weeks of 2003, as well as for the four regular sampling sites for about one year, starting in October 2003. The corresponding trendline equations are $\delta^2\text{H} = 7.64\delta^{18}\text{O} + 6.93$ and $\delta^2\text{H} = 7.68\delta^{18}\text{O} + 5.61$, respectively. It can be seen that the local meteoric water line (LMWL: $\delta^2\text{H} = 7.62\delta^{18}\text{O} + 8.20$) throughout the whole Yangtze River is mixed; sometimes very close to the global meteoric water line (GMWL: $\delta^2\text{H} = 8\delta^{18}\text{O} + 10$) and sometimes appreciably higher than it [2]. The trendlines for river water along the main branch of the Yangtze River basin are also nearly parallel to the LMWL. This reflects the fact that river water isotopic variations along the main branch strongly depend on precipitation isotope fields. As observed, differences in trend lines for river water are shown as d-excess. This proves the evaporation effect; river water experiences multiple evaporation influences including surface water evaporation and groundwater evaporation after precipitation water is converted into river water, which results in a higher d-excess value for river water than that in precipitation [3, 4].

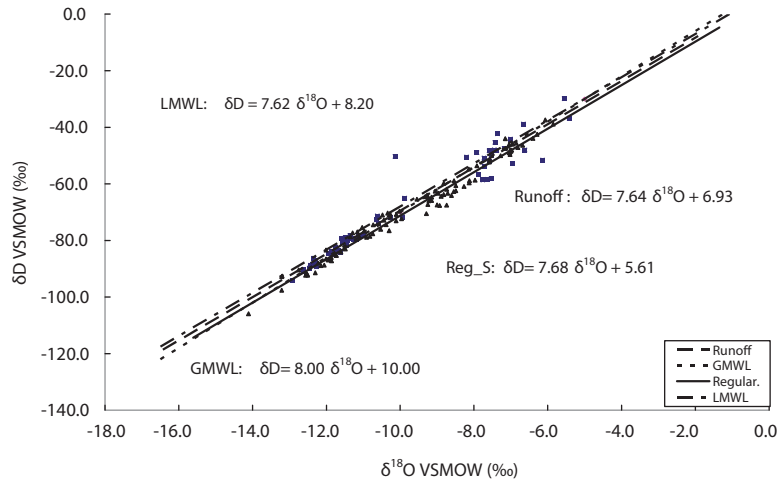


FIG. 2. The $\delta^2\text{H}$ vs $\delta^{18}\text{O}$ relationship of runoff and precipitation isotopes in the Yangtze River.

3.2. Spatial variations of stable isotope ^{18}O

The variation in $\delta^{18}\text{O}$ composition in the first water campaign for a stretch from the headwater along the main stem of Yangtze River is shown in Fig. 3.

As observed, the isotopic composition of the river water progressively increases along the main stem and there are three major peaks in Fig. 3. The increase in $\delta^{18}\text{O}$ along the river course is due to the evaporation effect being enhanced over the long distance. Along the flow path, the isotopic composition of water regulated by lakes or reservoirs is more positive than that of unregulated water in neighbouring sites due to evaporation. Isotopic compositions between former and later cross-sections are obviously different, which also reveals that isotope patterns depend on precipitation isotope fields. The largest $\delta^{18}\text{O}$ peak showing the greatest evaporative enrichment (first $\delta^{18}\text{O}$ peak) is caused by water samples directly collected from Dongting Lake, which may consist of recharge from a rice plant field [5–6]. The results are so because the water sample was collected in the mixing region of Poyang Lake and the main stem of

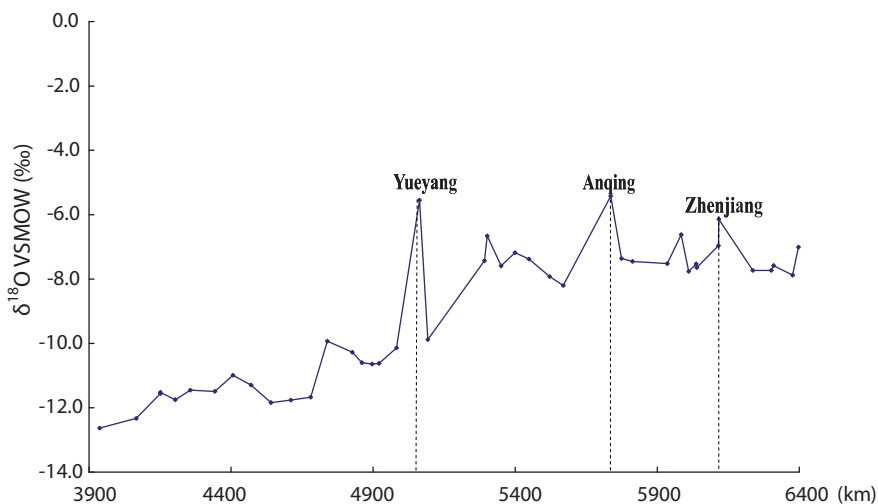


FIG. 3. Variation in $\delta^{18}\text{O}$ contents of the Yangtze River for 3900 km–6900 km from the headwater.

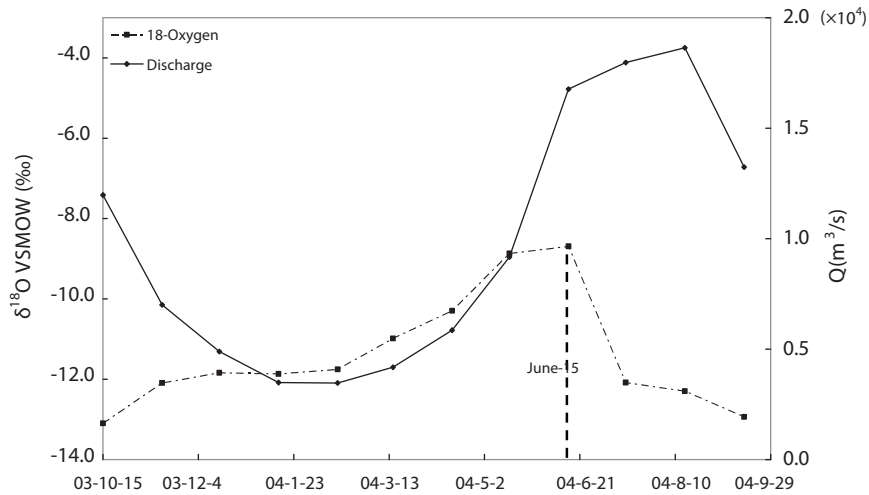


FIG. 5. Weighted $\delta^{18}\text{O}$ and monthly mean discharge change with time at the Chongqing Hydrological Station.

More attention should be paid to the time of the $\delta^{18}\text{O}$ peak, which corresponds closely to the beginning of the flooding period in the corresponding region; June 15 for Chongqing station, and May 15 for Hankou station. This feature could be used to split a water year into flood and the low water periods.

4. SUMMARY AND CONCLUSIONS

Based on the study of stable water isotopes along the main stem of the Yangtze River, the following pertinent conclusions can be drawn:

- (a) Temporal and spatial variations in oxygen and hydrogen isotopes of water along the main stem of the Yangtze River strongly reflect isotope patterns in regional precipitation.
- (b) The influence of lakes and reservoirs on the isotopic composition of the river water can be very large. They directly result in a d-excess values increase.
- (c) Stable isotope composition peaks or valleys for river water are good indicators, splitting water years into flood and low water periods at a given location.

ACKNOWLEDGEMENTS

This study was sponsored by the National Natural Science Foundation Committee of China (NSFC 50379008) and the International Atomic Energy Agency (IAEA-CRP12285), as well as the Hydrology Bureau of the Ministry of Water Resources of China and Hohai University Academician Foundation. The authors would like to acknowledge all those who were involved in the study of water isotopic monitoring along the main stem of Yangtze River.

TABLE 1. ISOTOPE CONTENTS OF THE YANGTZE RIVER, CHINA

Lab No.	Sample Code	Sampling Date	^{18}O (‰VSMOW)	^2H (‰ VSMOW)
49001	A1 (CQ)	2005-1-1	-7.11	-53.67
49002	A2 (CQ)	2005-1-15	-7.83	-57.01
49003	A3 (CQ)	2005-2-1	-7.57	-51.68
49004	A4 (CQ)	2005-2-15	-6.09	-47.07
49005	A5 (CQ)	2005-3-1	-4.13	-38.88
49006	A6 (CQ)	2005-3-15	-6.33	-46.16
49007	A7 (CQ)	2005-4-15	-7.69	-50.93
49008	A8 (CQ)	2005-4-2	-8.3	-51.67
49009	A9 (CQ)	2005-5-1	-8.11	-47.99
49010	A10 (CQ)	2005-5-15	-1.51	-16.21
49011	A11 (CQ)	2005-6-1	-6.69	-40.22
49012	A12 (CQ)	2005-6-15	-5.88	-36.99
49013	A13 (CQ)	2005-7-1	-5.12	-43.2
49014	A14 (CQ)	2005-7-15	-9.36	-59.96
49015	A15 (CQ)	2005-8-1	-8.96	-64.17
49016	A16 (CQ)	2005-8-15	-10.39	-73.57
49017	A17 (CQ)	2005-9-1	-10.28	-69.35
49018	B1 (HK)	2005-1-1	-4.1	-36.46
49019	B2 (HK)	2005-1-15	-5.16	-65.71
49020	B3 (HK)	2005-2-1	-12.08	-86.95
49021	B4 (HK)	2005-2-15	-12.07	-86.83
49022	B5 (HK)	2005-3-1	-11.6	-80.53
49023	B6 (HK)	2005-3-15	-8.97	-68.34
49024	B7 (HK)	2005-4-15	-11.15	-75.64
49025	B8 (HK)	2005-4-2	-8.86	-59.2
49026	B9 (HK)	2005-5-1	-8.4	-64.38
49027	B10 (HK)	2005-5-15	-9.82	-75.69
49028	B11 (HK)	2005-6-1	-3.81	-36.12
49029	B12 (HK)	2005-6-15	-10.63	-77.84
49030	B13 (HK)	2005-7-1	-11.23	-72.38
49031	B14 (HK)	2005-7-15	-10.72	-80.25
49032	B15 (HK)	2005-8-1	-11.39	-79.94
49033	B16 (HK)	2005-8-15	-11.4	-86.79
49034	B17 (HK)	2005-9-1	-13.29	-95.51
49035	B18 (HK)	2005-9-15	-13.32	-98.26
49036	C1 (XLJ)	2004-10-1	-9.87	-69.35
49037	C2(XLJ)	2004-10-15	-10.95	-68.91
49038	C3(XLJ)	2004-11-1	-9.85	-68.3

TABLE 1. ISOTOPE CONTENTS OF THE YANGTZE RIVER, CHINA (CONTD.)

Lab No.	Sample Code	Sampling Date	^{18}O (‰VSMOW)	^2H (‰ VSMOW)
49039	C4(XLJ)	2004-11-15	-10.33	-68.72
49040	C5(XLJ)	2004-12-1	-10.14	-69.01
49041	C6(XLJ)	2004-12-15	-9.47	-69.64
49042	C7(XLJ)	2005-1-1	-9.1	-67.8
49043	C8(XLJ)	2005-1-15	-7.46	-53.75
49044	C9(XLJ)	2005-2-1	-9.8	-68.95
49045	C10(XLJ)	2005-2-15	-9.08	-69.78
49046	C11(XLJ)	2005-3-1	-8.08	-66.91
49047	C12(XLJ)	2005-3-15	-10.37	-69.58
49048	C13(XLJ)	2005-4-15	-7.98	-62.47
49049	C14(XLJ)	2005-4-2	-10.32	-69.55
49050	C15(XLJ)	2005-5-1	-10.16	-69.85
49051	C16(XLJ)	2005-5-15	-6.59	-59.29
49052	C17(XLJ)	2005-6-1	-9.76	-70.1
49053	C18(XLJ)	2005-6-15	-5.25	-56.48
49054	C19(XLJ)	2005-7-1	-9.07	-67.07
49055	C20(XLJ)	2005-7-15	-10.19	-70.2
49056	C21(XLJ)	2005-8-1	-7.71	-55.24
49057	C22(XLJ)	2005-8-15	-9.87	-69.9
49058	C23(XLJ)	2005-9-1	-10.25	-69.67
49059	C24(XLJ)	2005-9-15	-9.45	-67.07
49060	D1(DT)	2004-10-1	-8.97	-63.21
49061	D2(DT)	2004-10-15	-9.97	-68.32
49062	D3(DT)	2004-11-1	-8.41	-62.15
49063	D4(DT)	2004-11-15	-9.26	-66.43
49064	D5(DT)	2004-12-1	-9.16	-64.01
49065	D6(DT)	2004-12-15	-7.9	-57.03
49066	D7(DT)	2005-1-1	-7.7	-55.33
49067	D8(DT)	2005-1-15	-7.75	-51.59
49068	D9(DT)	2005-2-1	-6.13	-44.74
49069	D10(DT)	2005-2-15	-7.26	-47.62
49070	D11(DT)	2005-3-1	-5.52	-37.47
49071	D12(DT)	2005-3-15	-6.23	-36.38
49072	D13(DT)	2005-4-15	-7.44	-44.27
49073	D14(DT)	2005-4-2	-6.83	-42.79
49074	D15(DT)	2005-5-1	-6.75	-42.74
49075	D16(DT)	2005-5-15	-5.51	-34.88

TABLE 1. ISOTOPE CONTENTS OF THE YANGTZE RIVER, CHINA (CONTD.)

Lab No.	Sample Code	Sampling Date	^{18}O (‰VSMOW)	^2H (‰ VSMOW)
49076	D17(DT)	2005-6-1	-6.35	-39.08
49077	D18(DT)	2005-6-15	-6.56	-39.88
49078	D19(DT)	2005-7-1	-6.4	-38.29
49079	D20(DT)	2005-7-15	-7.36	-48.31
49080	17(DN)	2005-5-16	-6.62	-48.69
49081	18(DN)	2005-5-16	-8.57	-58.09
49082	19(DN)	2005-5-16	-8.63	-57.66
49083	20(QJ)	2005-5-17	-7.07	-44.01
49084	21(QJ)	2005-5-17	-8.93	-59.83
49085	16(HK_1)	2005-10-1	-10.48	-72.17
49086	22	2005-10-1	-11.71	-84.07

Note: Flood Forecasting and Water Resources Assessment for IAHS-PUB (Proceedings of the International Symposium on Flood Forecasting and Water Resources Assessment for IAHS-PUB in Beijing, China, September–October 2006). IAHS Publ. 322, 2008 (accepted by IAHS Red Book).

REFERENCES

- [1] DANSGAARD, W., Stable Isotopes in Precipitation, *Tellus* **16** (1964).
- [2] CLARK, I.D., FRITZ, P., Environmental Isotopes in Hydrogeology, Lewis Publishers of CRC Press, USA (1997) 43–61.
- [3] ROZANSKI, K., ARAGUAS-ARAGUAS, L., GONFIANTINI, R., Isotopic pattern in modern global precipitation. Amer. Geophys. Union (1993).
- [4] MARTINELLI, L.A., GAT, J.R., DE CAMARGO, P.B., LARA, L.L., OMETTO, J.P.H.B., The piracicaba river basin: isotope hydrology of a tropical river basin under anthropogenic stress, *Isotope in Environmental and Health Studies* **40** 1 (2004) 45–56.
- [5] ARAGUAS-ARAGUAS, L., FROELICH, K., ROZANSKI, K., Deuterium and oxygen-18 isotope composition of precipitation and atmospheric moisture, *Hydrol. Proc.* **14** (2000) 1341–1355.
- [6] SU XIAOSI, LIN XUEYU, LIAO ZISHENG, WANG JINSHENG, Spatial variations of Isotope ^{18}O , ^2H , and ^3H in Yellow River and the causing factors study, *Geochemica* **32** 4 (2003).
- [7] GIBSON, J.J., et al., Progress in isotope tracer hydrology in Canada, *Hydrol. Process.* **19** (2005) 303–327.

THE ROLE OF LAKES AND RIVERS AS SOURCES OF EVAPORATED WATER TO THE ATMOSPHERE IN THE AMAZON BASIN

L.A. Martinelli^a, R.L. Victoria^a, J.R. Ehleringer^b, J.P.H.B. Ometto^{a,c}

^a Centro de Energia Nuclear na Agricultura (CENA/USP), Brazil

^b University of Utah, USA

^c Centro de Ciências do Sistema Terrestre (CCST/INPE), International Geosphere Biosphere Programme Regional Office (IGBP-RO), Brazil

Abstract. Due its magnitude, the water cycle in the Amazon basin plays a key role in the biogeochemical cycles of the region, as well as affecting regional and global climate. Despite its importance, the Amazon region is under constant pressure because of its natural resources, and deforestation accounts for a major part of this human influence. The continental freshwater system in the region is not highly threatened, although human occupation follows roads and rivers pathways. Several urban and agricultural activities take place by the river's banks. Over the past 30 years, riparian regions have been cleared for agriculture and human settlements, and the floodplains are being intensely used for cattle grazing during the low water season and for fishing during high water, putting at risk highly diverse and abundant fisheries stocks in the region as whole. The floodplains are an important spawning habitat for several species. Thus understanding of biogeochemical and nutrient dynamic of the floodplains is crucial to sustain the ecological health of those systems. Identification of physical process patterns (i.e., evaporation, wind, water current) and sources of water to the floodplains are key to this knowledge. The main objective of this work was to investigate the role of the Amazon floodplains lakes and rivers as sources of evaporated water to the atmosphere.

1. INTRODUCTION

The Amazon is the world's largest continental evaporative basin [1], lying primarily in Brazil; its head waters are in the Andean region of Colombia, Peru, Ecuador and Bolivia, and it has the longest course to the Atlantic Ocean at over 6700 km. The Amazon basin encompasses an area of 6.4 million km², with a precipitation flux of 14.1×10^{12} m³/ar of water into the basin and a final runoff of approximately 6×10^{12} m³/ar [2]. Accordingly, approximately 50%–60% of yearly precipitation returns to the atmosphere via evapotranspiration [3, 6]. Transpiration is the largest component of evapotranspiration flux, and has a clearly recognizable source: the dense vegetation of the region. Evaporation, on the other hand, may be responsible for up to 40% of the evapotranspiration flux [1, 4]. However, distribution of the evaporative flux in the basin among rivers and lakes located in the Amazon floodplain (várzea lakes), and the forest through interception of rain by the canopy is still unclear [1, 5]. Rivers and floodplain lakes were investigated through the CAMREX project and also through monthly sampling over a period of less than one year in a few lakes located in the Central Amazon [5]. At that time, only lake water samples and feeding river waters were collected. Based on this limited data set, we concluded that rivers and, overall, lakes could be an important source of evaporated water to the atmosphere, mainly during the end of falling water and beginning of the rising stage [5]. Moreira et al. [6] indicated that most of the vapour within a primary forest system in the Amazon region is generated by plant transpiration.

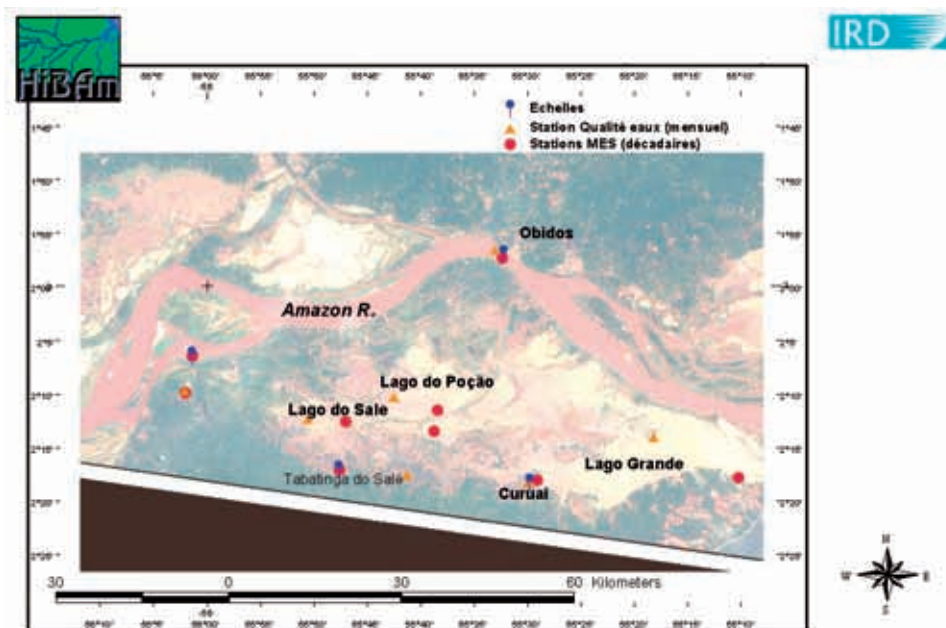


FIG. 2. The Curuai Várzea (floodplain), with major sampling stations.

yearly distribution of radiation and water suspended material content, and it defines rates of primary production in the system. Watershed hydrology and land use are related to the amount of organic matter and the nutrient load brought into floodplain waters through the runoff process, as well as to the dynamic and residence time of water through infiltration, runoff, evaporation, channel flow, and lake storage, among other factors. Thus, answers to questions related to how nutrient and hydrological dynamics take place in the floodplains are crucial to understanding and managing this system.

2. SAMPLING

Samples were taken during the first part of the project with a biweekly frequency for the major water bodies, the Tapajós and Amazon Rivers. The several stations within the Curuai floodplain were sampled once a month, at least, and in key hydrological stages (seasonal changes in water level) every other week. The small rivers draining the forest into the floodplain were sampled every time the lake was sampled. Most sampling was done in collaboration with ERD-France. Rainfall was collected in the floodplain region and per event in the Reserva Nacional do Tapajós (FLONA), a primary forest reserve located approximately 80 km from the Curuai varzea. Water vapour samples were taken within the forest and over the lake surface (about 2 m), using a dry ice slush trapping system. Water samples from rivers and lakes were collected under the surface directly in an oven dry flask. Sampling stations at the Curuai floodplain are shown in Fig. 3.

To determine possible contributions of evaporated water to the atmosphere, slopes of the regression line between $\delta^{18}\text{O}$ and $\delta^2\text{H}$ for river waters and the 'd' values for rainfall and lake water [5] are primarily used. Várzea lakes are not homogeneous water bodies. They receive water from a major feeding river, like the Amazon or Tapajós, as well as from their watershed (small rivers, locally called igarapés). These two water types have distinct isotopic

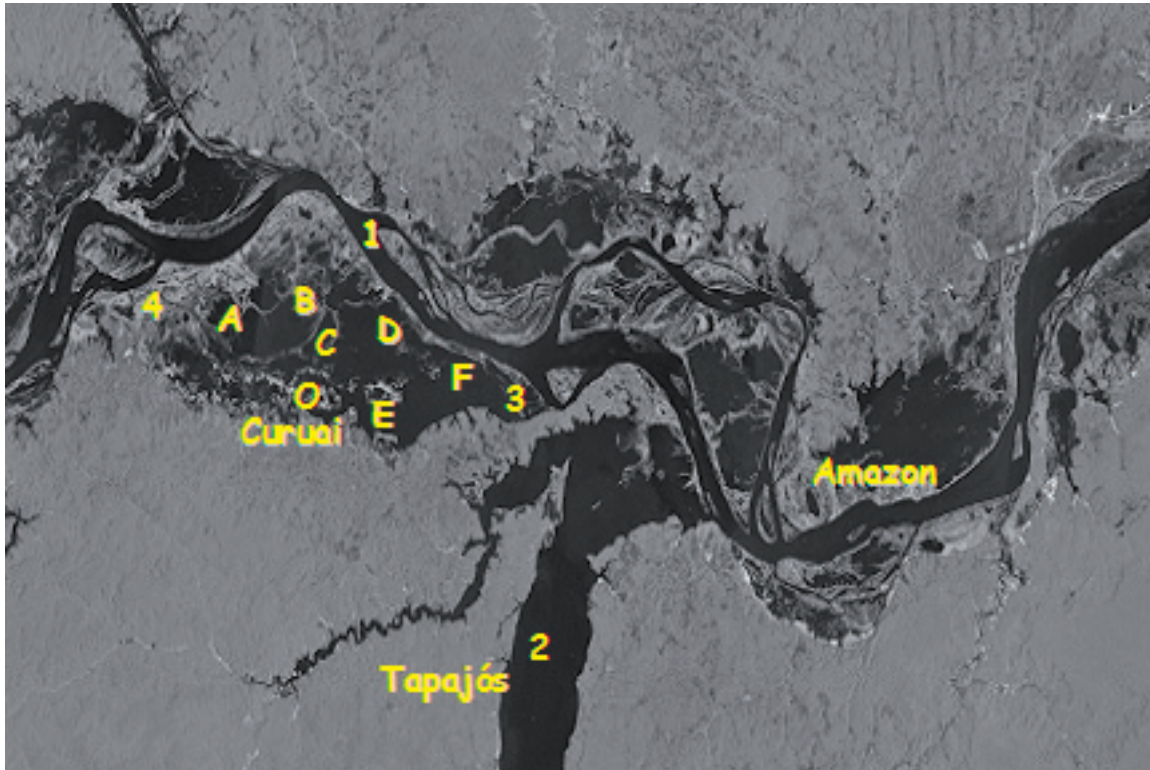


FIG. 3. Study area and sampling sites at: (0) rainfall at Curuai town, (2) Tapajós River, (3) water vapour at Vila do Socorro, (4) stream, (A and B) Lake Salé, (C and D) Lake Poço, and (E and F) Lake Grande do Curuai.

compositions, worsening conditions for classical evaporation studies using isotopes. During the dry season water input is minimum, thus várzea lakes become suitable for classical evaporation studies [1, 9, 10].

3. RESULTS AND DISCUSSION

Figure 4 presents $\delta^{18}\text{O}$ variations in one field campaign in 2002, when water levels started to go down in the floodplain and the upper reaches of the region already presented an evaporation signal (beside two wells samples at -8‰ $\delta^{18}\text{O}$). Figure 4 represents the east–west longitudinal gradient on the x-axis, which follows Amazon river flow, i.e to the east water residence time is higher in the floodplain at this time of the year.

Oxygen isotope seasonal variability and strong evaporation components can be observed in Fig. 5. The model extrapolates point sampling in three periods of the year, represented by side graphs where one can observe Amazon river water level variations and the isotopic values of key elements in the floodplain. Figure 5 represents upper and lower parts of the region and clearly shows substantial isotopic enrichment during the low water period.

Isotopic variability in Curuai Lake is also represented by the $\delta^2\text{H}$ of the stream. Well water did not vary and was always lighter than the stream water for the entire sampling period (Fig. 6).

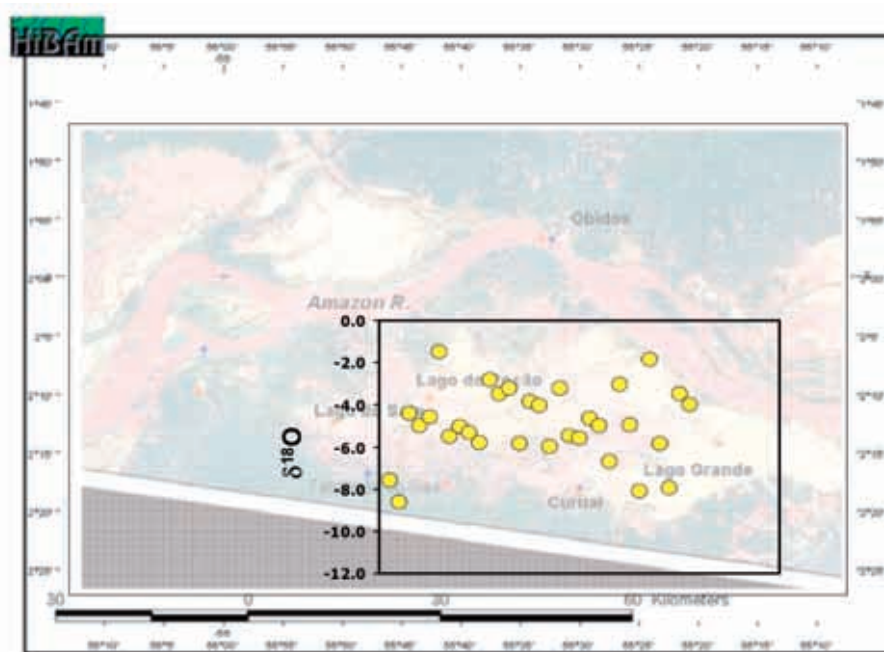


FIG 4. Representation of oxygen isotopic variation throughout the Curuai floodplain over a few days in August 2002. Sampling of the whole system in one day is not feasible.

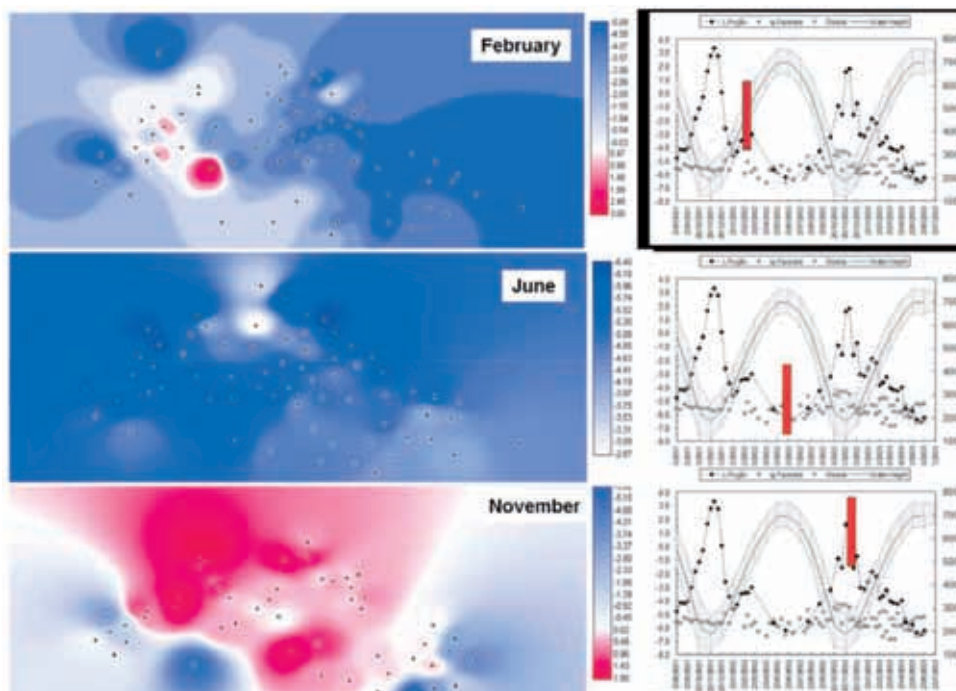


FIG. 5. Representation of $\delta^{18}\text{O}$ in the Curuai floodplain in comparison with xy plots showing water levels in the system.

By contrast, we observed significant variations in the $\delta^2\text{H}$ of lakes during the sampling period. From August to the end of September, the $\delta^2\text{H}$ of the lakes was similar for all lakes. However, from the end of September to end of November, the $\delta^2\text{H}$ of the lakes increased significantly, contrasting with Lake Grande (Fig. 6). The highest increase was observed at Lake Poço, followed by Lake Salé at Tabatinga and São Nicolau. After peak $\delta^2\text{H}$ was reached, the isotopic

composition of water started to decrease up to the beginning of January, staying constant until March–April. The $\delta^2\text{H}$ values of Curuai's Lake Grande behaved differently. The $\delta^2\text{H}$ saw a small decrease from the end of September to the middle of November, then increased significantly at the end of November, maintaining similar values until the end of December, when values started to decrease again (Fig. 6).

The increase in $\delta^2\text{H}$ values of these lakes suggests deuterium enrichment caused by evaporation during the dry season or mixture with an isotopically different water body. Stream and well water had lighter $\delta^2\text{H}$ values than that of the lakes, especially during the dry season (Fig. 2). Therefore, these water bodies were not responsible for the $\delta^2\text{H}$ change observed in the lakes during the dry season. Results from the Amazon and Tapajós rivers are shown in Fig. 7. Curuai lake water clearly shows the Amazon River is the major water source to the floodplain.

Further confirmation of the evaporation effect in the isotopic composition of the lakes can be seen in Fig. 8. The following equations represent rainfall and lake water:

Rainfall

$$\delta^2\text{H} = 7.14 (\delta^{18}\text{O}) + 3.99, r^2 = 0.98 \quad (1)$$

Lake Salé at Tabatinga

$$\delta^2\text{H} = 4.92 (\delta^{18}\text{O}) - 6.70, r^2 = 0.95 \quad (2)$$

Lake Salé at São Nicolau

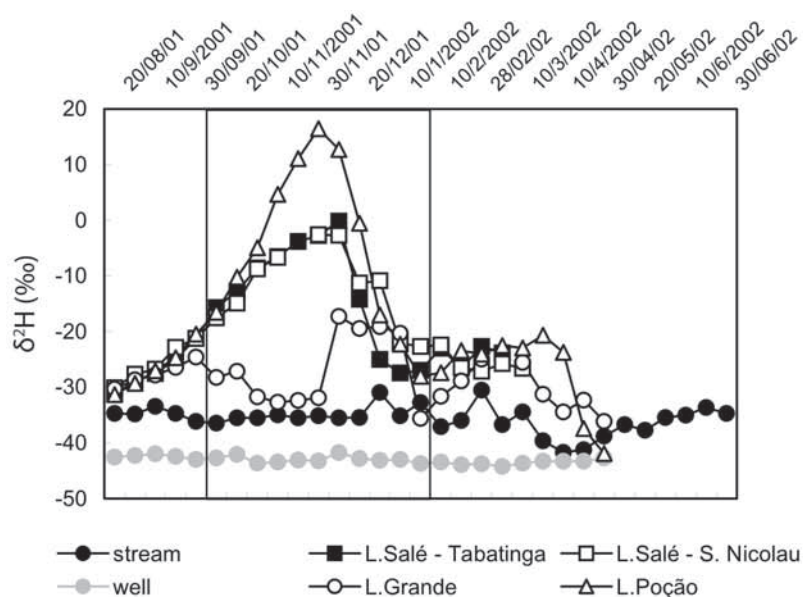


FIG. 6. Temporal variation of $\delta^2\text{H}$ in several water bodies sampled in this study. The box indicates the dry season period.

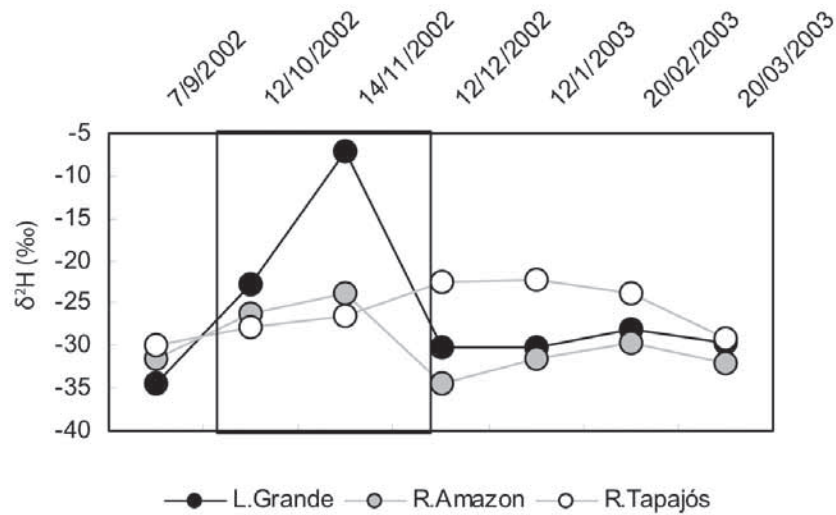


FIG. 7. Temporal variation of δ^2H of the 'Lago Grande do Curuai' and Amazon and Tapajós Rivers. The box indicates the dry period.

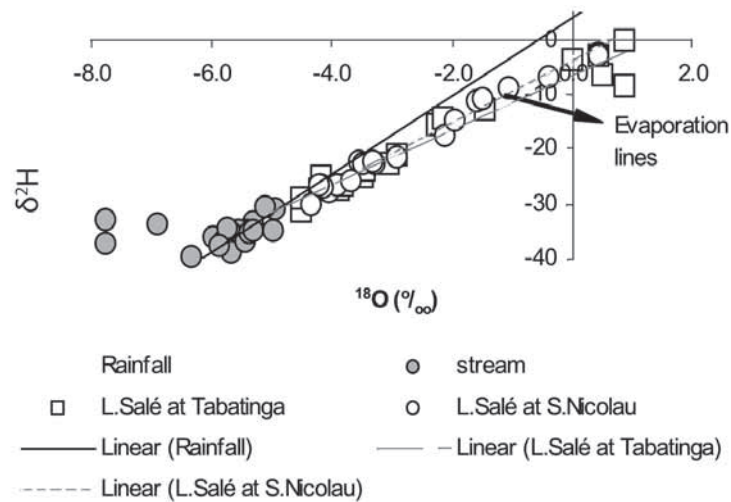


FIG. 8. A plot for δ^2H vs $\delta^{18}O$ in rainfall (only line), as well as the stream and Lake Salé at Tabatinga and São Nicolau.

$$\delta^2H = 5.56 (\delta^{18}O) - 4.19, r^2 = 0.98 \quad (3)$$

The equation yield for both sites sampled at Lake Salé showed a slope < 8 , suggesting evaporation processes affected lake water during the dry season. This was further confirmed by the evaporation lines produced in other regions of the lake (namely Tabatinga and São Nicolau), as presented in Fig. 8.

Values of d_{EXCESS} ('d') below 10 indicate an evaporation process. As can be observed in Fig. 9, seasonal variations of 'd' values point to the strong hydrological fluctuation and decoupling of the floodplains system from the main Amazon river channel. The smallest 'd' values were seen during the low water period, when the highest δ^2H values observed (Fig. 9).

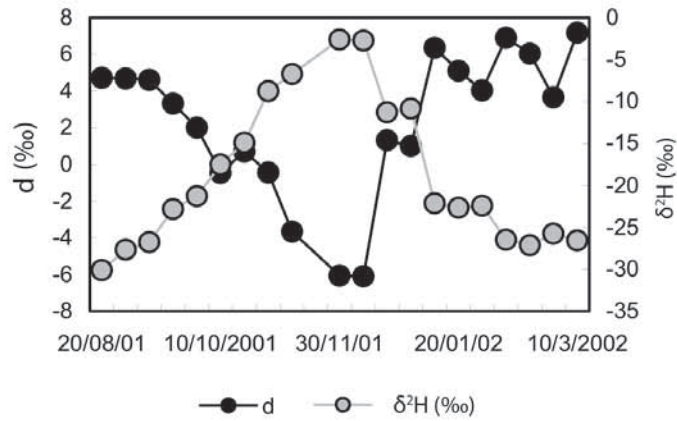


FIG. 9. Temporal variation of 'd' values and $\delta^2\text{H}$ in Lake Salé at Tabatinga and São Nicolau.

3.1. Analysis per reach of the floodplain system

3.1.1. Lake water

In each set of figures to follow we present the temporal variability of $\delta^{18}\text{O}$, the plot $\delta^{18}\text{O} \times \delta^2\text{H}$, and the temporal variability of d_{EXCESS} values and $\delta^2\text{H}$ for lakes Salé at São Nicolau (Fig.10), Salé at Tabatinga (Fig. 11), Poçoão (Fig. 12), and Grande at Curuaí (Fig. 13).

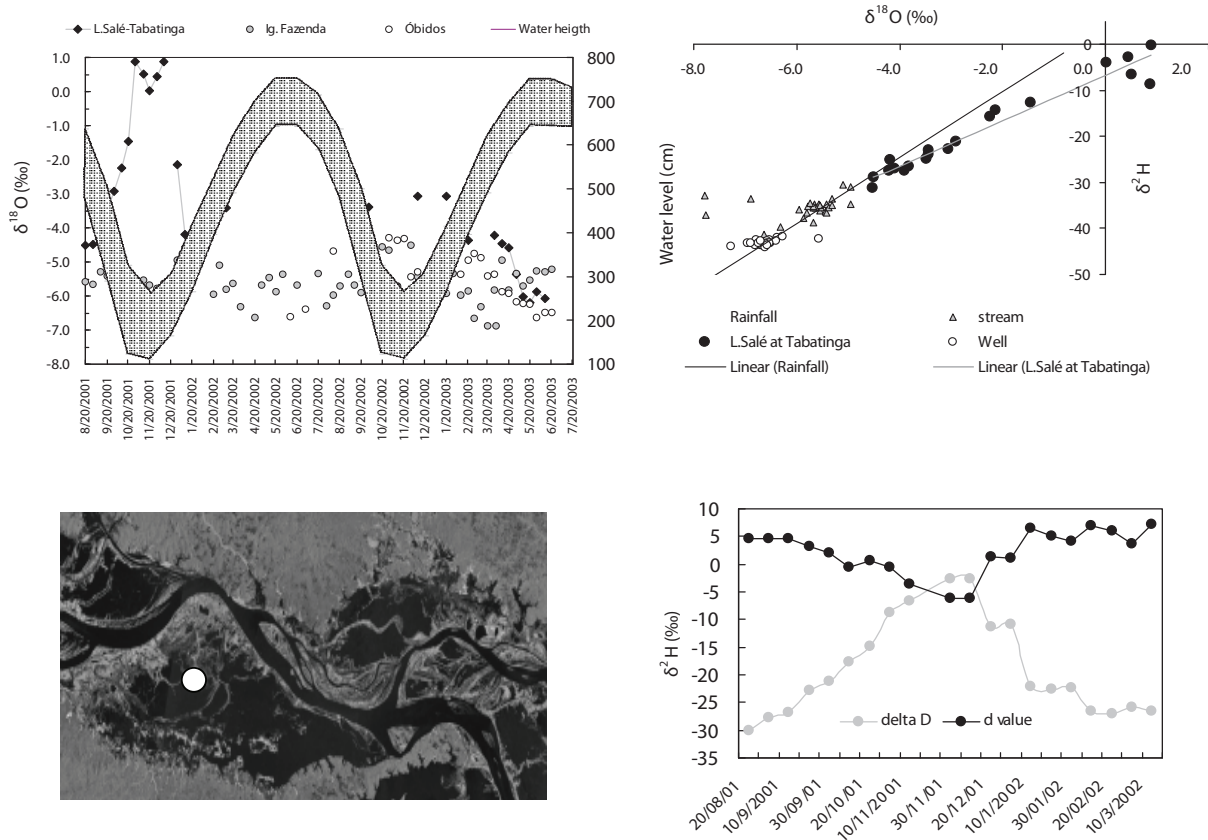


FIG. 10. Temporal variability of $\delta^{18}\text{O}$, the plot $\delta^{18}\text{O}$ vs $\delta^2\text{H}$, and temporal variability of d values and $\delta^2\text{H}$ for lake Salé at São Nicolau.

The $\delta^{18}\text{O}$ values of Lake Salé at São Nicolau increased sharply during the dry season, reaching the highest values at the lowest water level of the Amazon River measured in Óbidos (Fig. 10). This increase suggests that this section of Lake Salé has undergone evaporation during the dry season. During the high water period the $\delta^{18}\text{O}$ of Lake Salé at São Nicolau became similar to the $\delta^{18}\text{O}$ of its water sources (data not shown). This trend is confirmed by the sharp decrease in $\delta^{18}\text{O}$ values of the Lake Salé at São Nicolau during the water rising period, from January to July 2003. The plot of $\delta^{18}\text{O}$ vs $\delta^2\text{H}$ compares lake water with forest stream water and water from a well, which are sources of water to the river. While the water sources plot along the line yielded by rainfall samples ($\delta^2\text{H} = 7.14 \times \delta^{18}\text{O} + 3.99$, $r^2 = 0.98$), water from the lake is plotted along an evaporation line (Fig. 10), with a slope smaller than 8 ($\delta^2\text{H} = 5.56 \times \delta^{18}\text{O} - 4.19$, $r^2 = 0.98$). In addition, the d value of the lake during the dry season decreases to values smaller than 10, indicating that evaporation is affecting the lake.

Lake Salé at Tabatinga followed a similar tendency to that at São Nicolau (Fig. 3). However, $\delta^{18}\text{O}$ enrichment during the dry season of 2003 was not as high in Tabatinga as that at São Nicolau (Fig. 11). As the $\delta^{18}\text{O}$ vs $\delta^2\text{H}$ plot was composed mainly of samples from 2001 to 2002, a clear evaporation line was seen, with the following equation $\delta^2\text{H} = 4.92 \times \delta^{18}\text{O} - 6.70$ ($r^2 = 0.95$). The d values of the lake at that site also decreased to values smaller than 10 during the dry season.

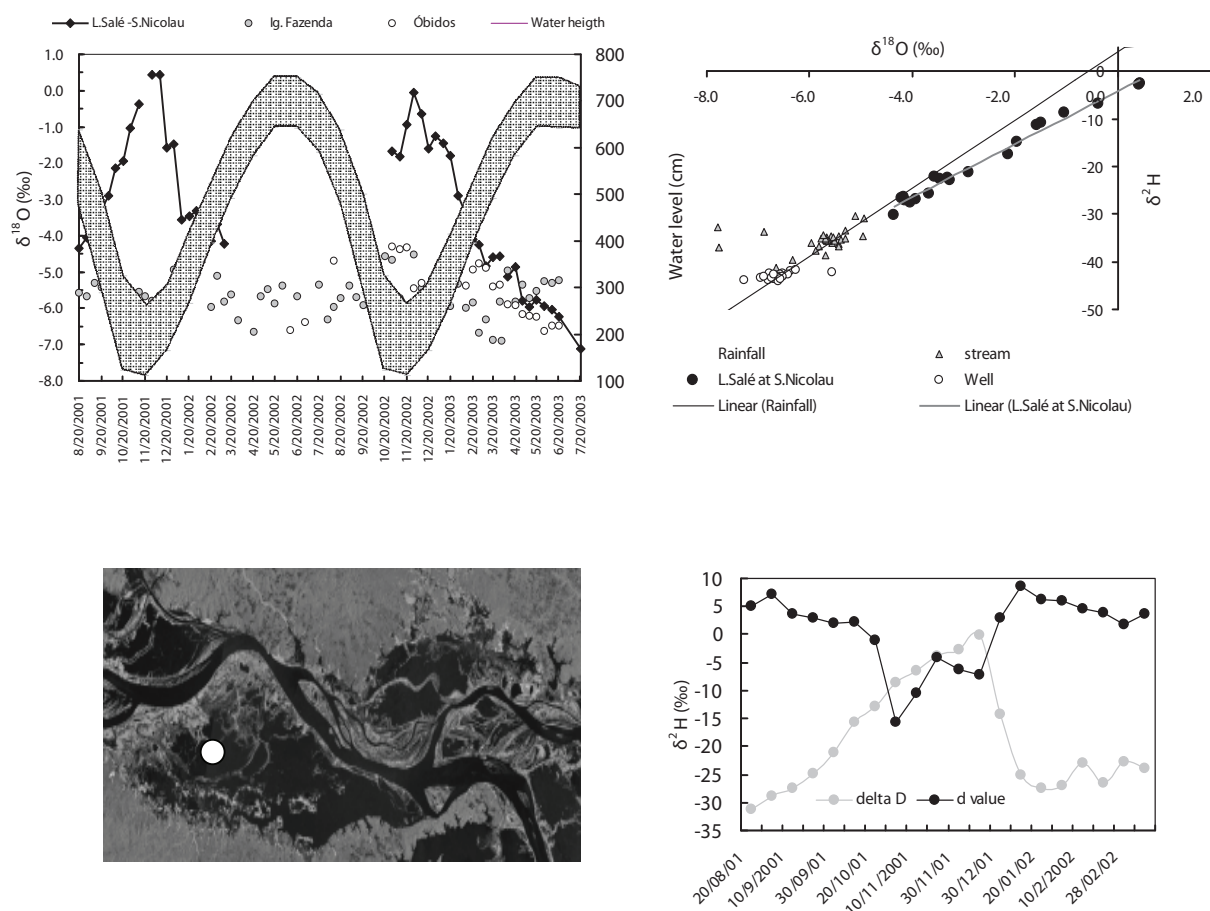


FIG. 11. Temporal variability of $\delta^{18}\text{O}$, the plot $\delta^{18}\text{O}$ vs $\delta^2\text{H}$, and the temporal variability of d -excess values and $\delta^2\text{H}$ for lake Salé at Tabatinga.

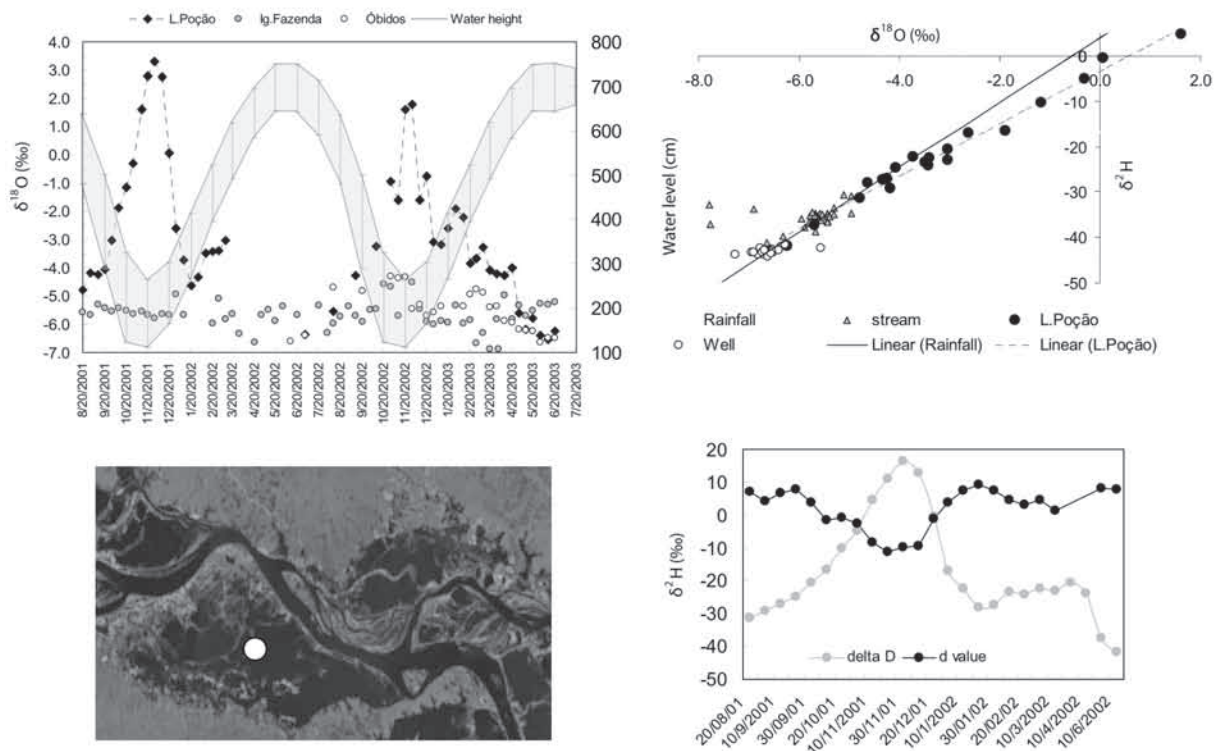


FIG. 12. Temporal variability of $\delta^{18}\text{O}$, the plot $\delta^{18}\text{O} \times \delta\text{D}$, and the temporal variability of d values and δD for the lake Poção.

The greatest $\delta^{18}\text{O}$ enrichment during the dry season was observed at Lake Poção (Fig. 12). From August to November 2001, a 10‰ increase in the $\delta^{18}\text{O}$ values were observed in this lake. The slope of the line $\delta^{18}\text{O}$ vs $\delta^2\text{H}$ was also smaller than 8 ($\delta^2\text{H} = 5.78 \times \delta^{18}\text{O} - 3.34$, $r^2 = 0.99$), and the d -excess value decreased during the dry season, reaching its minimum in November and December (Fig. 4).

Lake Grand near Curuaí is the nearest sampling site connecting the lake to the Amazon River (Fig. 13). At this site, the increase in $\delta^{18}\text{O}$ during the dry season was not so clear as it was for other sampling sites. Minimum $\delta^{18}\text{O}$ values were observed during the rising water period of 2001–2002, not during the minimum level of the river (Fig. 13). The same was observed during the rising period of 2002–2003, but high variability was observed during the river’s minimum level in this period. The plot of $\delta^{18}\text{O}$ vs $\delta^2\text{H}$ did not produce a clear evaporation signal, and the slope of the line was near 6. Finally, the d -excess values during the 2001–2002 dry season decreased only slightly below 10 (Fig. 13). Therefore, this lake site is probably influenced by the connected river; even during the low water period it was not possible to distinguish a clear evaporation signal from the lake.

We have also analyzed isotopic variation within a water column through sampling at several depths; no variability according to water depth was found, suggesting a well-mixed water body. In the Amazon river, isotopic values became heavier downstream, or from west to east, following the outflow of succeeding systems of floodplain, dominated in this stretch by the Curuaí Várzea (Fig. 14). At Tabatinga, the most upstream sampling site, the $\delta^2\text{H}$ value was equal to -58.5% . More than 2000 km downriver, $\delta^2\text{H}$ increased approximately 15‰, reaching -43.8% at Óbidos. The main cause for this downstream increase is the dilution of isotopically

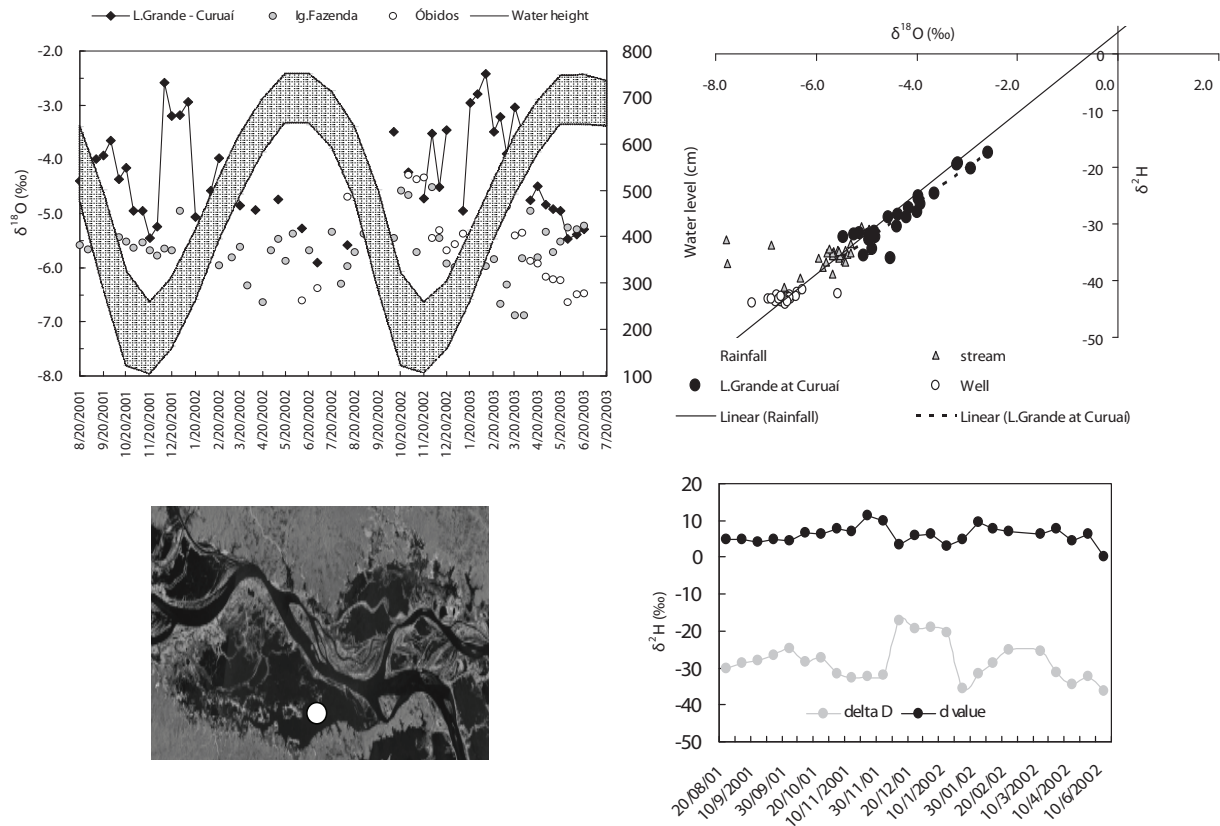


FIG. 13. Temporal variability of $\delta^{18}O$, the plot $\delta^{18}O$ vs δ^2H , and the temporal variability of d -excess values and δ^2H for Lago Grande at Curuai.

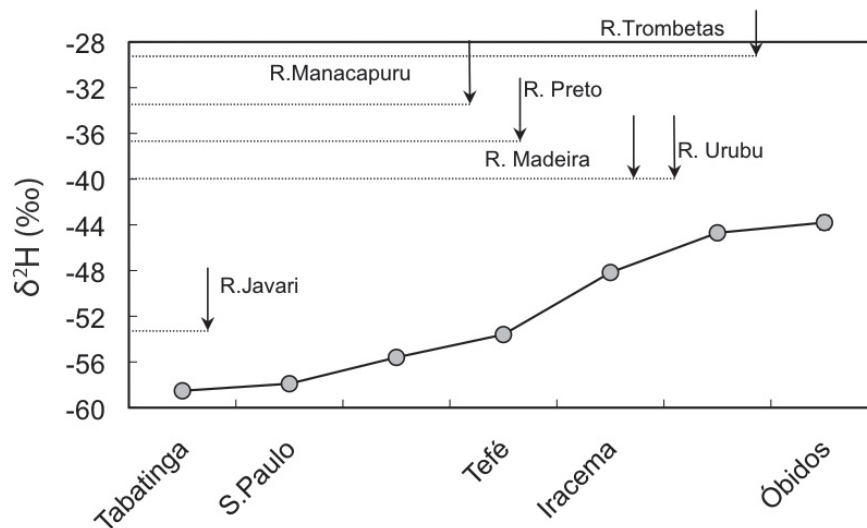


FIG. 14. Downstream variation of δ^2H values along the R.Solimões-Amazon. The arrows indicate the δ^2H values of several tributaries along the river.

light waters from the Andes mountains by isotopically heavier water from the Amazon lowlands (Fig. 14).

3.2. WATER INPUTS TO THE FLOODPLAIN

A compilation of data collected in collaboration with Dr. Bourgoïn showed the isotopic composition of Amazonian precipitation and river waters varying significantly during the hydrological cycle. The isotopic composition of river waters presents limited variations: $-5.8 \pm 0.7\text{‰}$ ($\delta^{18}\text{O}$); $-36.3 \pm 4.3\text{‰}$ ($\delta^2\text{H}$), and isotopic signature becomes impoverished with increasing discharge. Local rainfall shows large annual variations ($\delta^2\text{H}$ from $+30\text{‰}$ to -90‰). Weighted averages are -4.5‰ ($\delta^{18}\text{O}$) and -26.8‰ ($\delta^2\text{H}$), and interestingly the rainfall isotopic signature is out of phase with the pluviograph (enriched during the dry season, and impoverished during the rainy season) due to the mass effect. Groundwater presents a steady isotopic composition signature averaging that of large rainfalls, and surface runoff from the watershed (ie. the stream at Tabatinga do Sale) presents uniform composition throughout the year, probably due to a dominant contribution of groundwater summed to runoff on the forested basin drained by this stream.

3.2.1. Water vapour

Our work also examined water vapour at the mouth of Lake Grande (Fig. 15) and from primary forest in the region (Fig. 16). More depleted vapour is found over the lake surface, compared to vapour over the forest canopy (for comparison the $\delta^{18}\text{O}$ of tropospheric water vapour is presented. This sample was collected during flights over the lake in May 2003). An interesting aspect is enrichment of the water vapour's oxygen isotopic signature both in the forest and over the lake throughout the year 2003. One possible explanation would be a wetter year in 2002, in fact in some locations, such as the Lake Sale in Tabatinga, the $\delta^{18}\text{O}$ of the water is more depleted in 2002 than in the previous year.

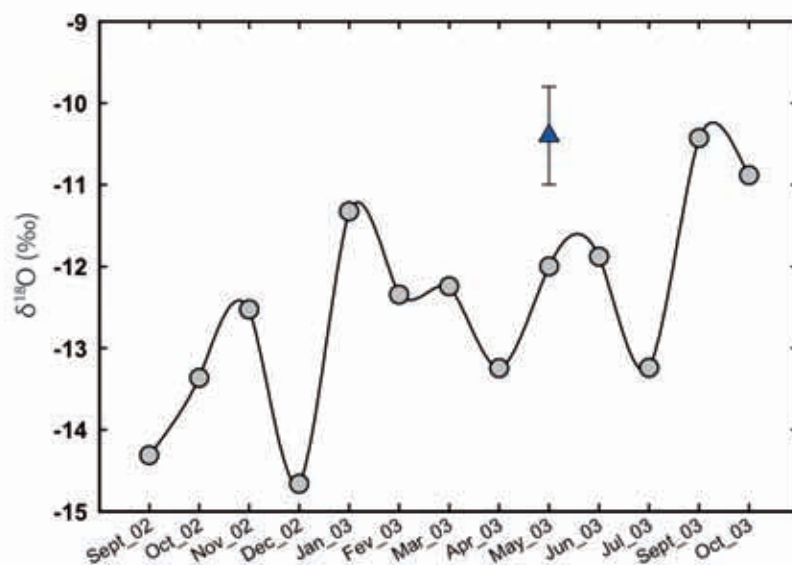


FIG. 15. Isotopic variation of the water vapour ($\delta^{18}\text{O}$) over the Lago Grande do Curuai. The triangle symbol indicates the troposphere water vapor over the Curuai lake region.

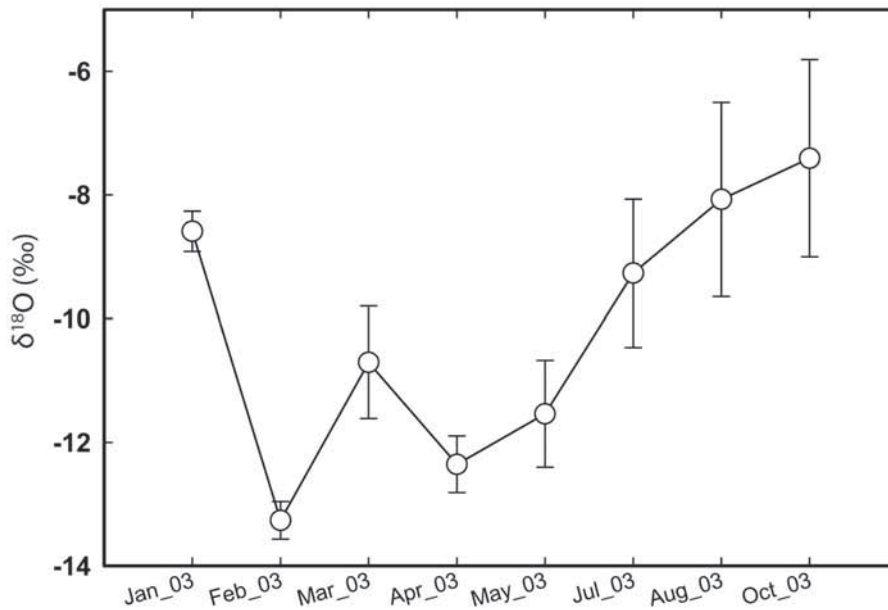


FIG. 16. Isotopic variation of the water vapour ($\delta^{18}O$) over a primary forest in the Satarem region, close to the Lago Grande do Curuai.

3.2.2. Leaf and sap water

Leaves and stems — an important source of atmospheric water vapour in the region — were collected monthly for oxygen isotope analysis. Previous work has shown that in dry periods the contribution of evapotranspiration to atmospheric water vapour can reach 70% in forested canopies, and evaporation associated to transpiration increases during rainy periods due to wetter surfaces (such as those of a leaf). Atmospheric water vapour over the forest increases in $\delta^{18}O$ from the wet to the dry season with a similar pattern for leaf water; contrastingly the $\delta^{18}O$ of stem water is more stable throughout the year.

The $\delta^{18}O$ composition of stem water was near -4‰ , similar to $\delta^{18}O$ values found in the Amazon River (-5.1‰) and Tapajós River (-4.5‰), also collected in September of 2002.

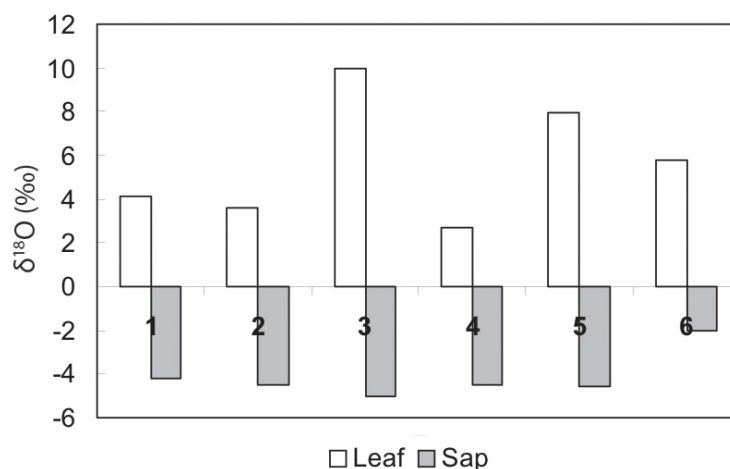


FIG. 17. Values of $\delta^{18}O$ for bulk leaf water and the sap water of plants collected along the shore of Lake Grande in September 2002.

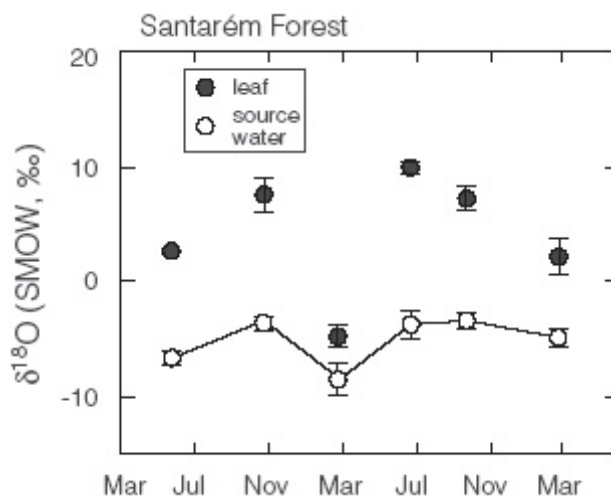


FIG. 18. Isotopic variation of the leaf and stem water vapor for a primary forest in Santarém region.

4. CONCLUSION

The tracing of stable isotopes in the Curuai floodplain proved to be useful in characterizing the spatial and temporal variability of floodplain hydrological dynamics, as well as for the isotopic characterization of water vapour flux to the atmosphere.

Measured isotopic compositions of floodplain waters were compared to values calculated by a coupled hydrological–isotopic simulation model [11]. Contributions from different sources (river, rainfall, groundwater) were constrained by the method. Water fluxes from components that are not easily and directly measured (i.e. watershed runoff, lake evaporation) could be validated using the isotopic geochemistry.

Due to intense evaporation processes in the lakes during the dry season, our results showed that floodplain waters flowing back to the river were generally enriched in stable isotopes (^{18}O and ^2H). This suggests the method is valid to quantify floodplain contribution to main river discharge and its chemical composition during the four main phases of the hydrological cycle.

ACKNOWLEDGEMENTS

We acknowledge Marcelo Moreira and Ecmaz Mazzi from the Centro de Energia Nuclear na Agricultura (CENA/USP), the logistical support provided by the Large Scale Biosphere-atmosphere Programme and the financial support from the International Atomic Energy Agency (IAEA) and the Sao Paulo state science foundation, FAPESP.

REFERENCES

- [1] GAT, J.R., MATSUI, E., Atmospheric Water Balance in the Amazon Basin: An Isotopic Evapotranspiration Model, *J. Geophys. Res.* **96** (1991) 13179–13188.

- [2] RICHEY, J.E., MEADE, R.H., SALATI, E., DEVOL, A.H., NORDIN, C.F., SANTOS, U., Water discharge and suspended sediment concentrations in the Amazon River: 1982–1984, *Water Res. Resour.* **22** (1986) 756–764.
- [3] SALATI, E., DALL’OLLIO, A., GAT, J., MATSUI, E., Recycling of water in the Amazon basin: an isotope study, *Water Res. Resour.* **15** (1979) 1250–1258.
- [4] VICTORIA, R.L., MARTINELLI, L.A., MORTATTI, J., RICHEY, J.E., Mechanisms of Water Recycling in the Amazon Basin: Isotopic Insights, *Ambio* **20** (1991) 384–387.
- [5] MARTINELLI, L.A., VICTORIA, R.L., STERNBERG, L.S.L., RIBEIRIO, A., MOREIRA, M.Z., Using stable isotopes to determine sources of evaporated water to the atmosphere in the Amazon Basin, *J. Hydrol.* **183** (1996) 191–204.
- [6] MOREIRA, M., STERNBERG, L., MARTINELLI, L., VICTORIA, K., BARBOSA, E., BONATES, L., NEPSTAD, D., Contribution of transpiration to forest ambient vapour based on isotopic measurements, *Global Change Biology* **3** 5 (1997) 439–450.
- [7] PAEGLE, H., “Interactions between convective and large-scale motions over Amazônia, The Geophysiology of Amazônia (DICKINSON, R., Ed.) New York, John Wiley (1987) 347–387.
- [8] SHUKLA, J., NOBRE, C., SELLERS, P., Amazon deforestation and climate change. *Science* **247** (1989) 1322–1325.
- [9] MARTINELLI, L.A., VICTORIA, R.L., MATSUI, E., RICHEY, J.E., FORSBERG, B.R., MORTATTI, J., “The use of oxygen isotopic composition to study water dynamics in Amazon Floodplain Lakes”, *Isotope Hydrology Investigations in Latin America, IAEA-TECDOC-502* (1989) 91–101.
- [10] GIBSON, J.J., EDWARDS, T.W.D., PROWSE, T.D., Development and validation of an isotopic method for estimation lake evaporation, *Hydrol. Proc.* **10** (1996) 1369–1382.
- [11] MAURICE BOURGOIN, L., KOSOUTH, P., CHAFFAUT, I., MARTINELLI, L.A., OMETTO, J.P.H.B., “Isotope tracing of the hydrological dynamics of an Amazonian floodplain”, *IV South American Simposium on Isotope Geology, Salvador, Brazil* (2003).

SELECTED PUBLICATIONS RESULTING FROM THE CRP

AHMAD, M., TASNEEM, M.A., TARIQ, J.A., AKRAM, W., LATIF, Z., SAJJAD, M.I., “Isotope characterization of major rivers of Indus basin, Pakistan”, *Isotope Hydrology and Integrated Water Resources Management, Conference and Symposium Papers 23/P, IAEA, Vienna, (2003) 64–66.*

GAT, J.R., *Isotope Hydrology — A Study of the Water Cycle, Series of Environmental Science and Management — Vol. 6, Imperial College Press (2009) 81–106.*

GIBSON, J.J., AGGARWAL, P.K., HOGAN, J., KENDALL, C., MARTINELLI, L.A., STICHLER, W., RANK, D., GONI, R., CHOUDHRY, M., GAT, J., BHATTACHARYA, S., SUGIMOTO, A., FEKETE, B., PIETRONIRO, A., MAURER, T., PANARELLO, H., STONE, D., SEYLER, P., MAURICE-BOURGOIN, L., HERCZEG, A., *Isotope studies in large river basins, A new global research focus, EOS 83 6 (2002) 13–617.*

KATTAN, Z., *Estimation of evaporation and irrigation return flow in arid zones using stable isotope ratios and chloride mass-balance analysis: Case of the Euphrates River, Syria, J. Arid Environ. 72 (2008) 730–747.*

MAURICE BOURGOIN, L., BONNET, M.-P., MARTINEZ, J.-M., KOSUTH, P., COCHONNEAU, G., MOREIRA-TURCQ, P., GUYOT, J.-L., VAUCHEL, P., FILIZOLA, N., SEYLER, P., *Temporal dynamics of water and sediment exchanges between the Curuai floodplain and the Amazon River, Brazil, J. Hydrol. 335 (2007) 140–156.*

MEREDITH, K.T., HOLLINS, S.E., HUGHES, C.E., CENDÓN, D.I., HANKIN, S., STONE D.J.M., *Temporal variations in stable isotopes (^{18}O and ^2H) and major ion concentrations within the Darling River between Bourke and Wilcannia due to variable flows, saline groundwater influx and evaporation, J. Hydrol. 378 (2009) 313–324.*

LORENTZ, S.A., TALMA, A.S., *Isotope Compositions of Runoff in Large Catchments in southern Africa, VIIth Scientific Assembly IAHS, 3–9 April 2005, Foz do Iguaçu, Brazil. (2005) poster.*

LORENTZ, S.A., TALMA, A.S., *Isotope composition of runoff in large catchments in southern Africa, Proceedings 12th SANCIAHS Symposium, Midrand, South Africa. 5–7 September 2005 (2005) CD-ROM.*

OGRINC, N., KANDUČ, T., STICHLER, W., VREČA, P., *Spatial and temporal variations in $\delta^{18}\text{O}$ and δD values in the River Sava in Slovenia, J. Hydrol. 359 (2008) 303–312.*

PANARELLO, H.O., DAPEÑA, C., *Large scale meteorological phenomena, ENSO and ITCZ, define the Paraná River isotope composition, J. Hydrol. 365 (2009) 105–112.*

MICHEL, R.L., *Tritium hydrology of the Mississippi River basin, Hydrol. Proc. 18 (2004) 1255–1269.*

PHILLIPS, F.M., HOGAN, J., MILLS, S., HENDRICKS, J.M.H., “Environmental tracers applied to quantifying causes of salinity in arid-region rivers: Preliminary results from the Rio Grande, southwestern USA”, *Water Resources Perspectives: Evaluation, Management, and Policy (ALSHARHAN, A.S., WOOD, W.W., Eds), Developments in Water Science 50, Elsevier Science, Amsterdam (2003) 327–334.*

LISTO FP PARTICIPANTS

- Argentina
ARG-12038
Mr Hector O. Panarello
Consejo Nacional de Investigaciones Cientificas y Técnicas
Instituto de Geocronología y Geología Isotópica (INGEIS)
Ciudad Universitaria
1428 Buenos Aires
Tel. +54 11 4783 3021
Fax +5411 4784 7798
hector@ingeis.uba.ar
- Australia
AUL-12039
Mr John J Gibson
Australian Nuclear Science and Technology
Organization (ANSTO)
Private Mail Bag 1
Menai, SW N 2234
Tel. +61 2 971 737 09
Fax +61 2 971 792 60
jgi@ansto.gov.au
- Austria
AUS-12040
Mr Wolfgang Papesch
Austrian Research Center Seibersdorf
Environmental Sciences
2444 Seibersdorf
Tel. +43 50550 36 15
Fax +43 50550 36 16
wolfgang.papesch@arcs.ac.at
- Brazil
BRA-12041
Mr Jean Ometto
Universidade de Sao Paulo
Centro de Energia Nuclear na Agricultura (CENA)
Avenida Antonio Carlos 303
Piracicaba/SP EP C 136-
Tel. +55 19 3429 4677
Fax +55 19 3434 9210
jpometto@cena.usp.br
- Canada
CAN-12042
Mr John J. Gibson
National Water Research Institute at W-CIRC
University of Victoria
PO Box 1700 STN CSC
Victoria, BC V8W 2Y2
Tel. +1-250-472 51 37
Fax +1-250 472 51 67
john.gibson@ec.gc.ca
- China
CPR-12285
Mr Jiyang Wang
Chinese Academy of Sciences

Institute of Geology and Geophysics
No1, Hua Yan Li. PO Box 9825
Beijing
Tel. +86 25 37 86 621
Fax +86 25 37 35 375
jywlp@mail.iggcas.ac.cn

France
FRA-12114

Ms Laurence Maurice Bourgoïn
IRD Institut de Recherche pour le Développement
Observatoire Midi-Pyrénées
LMTG - UMR5563 - IRD UR 154
14 Avenue du Professeur Jean Babin
31400 Toulouse
Tel. +33 5 61 33 26 68
Fax +33 5 61 33 25 60
maurice@lmtg.obs-mip.fr

Germany
GFR-12072

Mr Willibald Stichler
GSF-Institute of Groundwater Ecology
Ingolstädter Landstraße 1
85764 Neuhergen
Tel. +49 89 318 72 566
Fax +49 89 318 73 166
stichler@gsf.de

Israel
ISR-12073

Mr Joel R. Gat
Weizmann Institute of Science
Department of Environmental Sciences and Energy Research
76100 Rehovot
Tel. +972 8934 26 10
Fax + 972 3965 21 91
cigatj@wisemail.weizmann.ac.il

Japan
JPN-12044

Ms Atsuko Sugimoto
Hokkaido University
Graduate School of Environmental Earth Science
Sapporo 060-0810
Tel. +81 11 706 22 33
Fax +81 11 706 48 67
atsukos@ees.hokudai.ac.jp

Pakistan
PAK-12046

Mr Manzoor A Choudhry
Pakistan Institute of Technology
Radiation and Isotope Application Division
P.O. Box 107, Islamabad
Tel. +92 51 929 02 61
Fax +92 51 929 02 75
manzoor@pinstech.org.pk

Slovenia
SLO-12642
Ms Nives Ogrinc
Jozef Stefan Institute
Department of Environmental Sciences
Jamova 39
1000 Ljubljana
Tel. +386 1 588 53 93
Fax +386 1 588 53 46
Nives.Ogrinc@ijs.si

South Africa
SAF-12286
Mr Siep Talma
Quaternary Dating Research Unit
Environmentek SIR- C
PO Box B 395
Pretoria 0001
Tel. +27 12 84 13 402
Fax +1 27 12 84 27 740
Stalma@csir.co.za

Syria
SYR-12643
Mr Zuhair Kattan
Atomic Energy Commission of Syria
P.O. Box B 6091
Damascus
Tel. +963 11 611926/7
Fax +963 11 611289
zkattan@aec.org.sy

USA
USA-12048
Ms Carol Kendall
U.S. Geological Survey
345 Middlefield Rd, MS 434
Menlo Park, CA 94025
Tel. +1 650 329 45 76
Fax +1 650 329 55 90
ckendall@usgs.gov

USA-12047
Mr. James Hogan
Hydrology & Water Resources
University of Arizona
P.O. Box B 121001
Tucson, AZ 85721
Tel +1 520 626 29 10
Fax +1 520 621 14 22
jhogan@hwr.arizona.edu

Vietnam
VIE-12568
Mr Kien Chinh Nguyen
Center for Nuclear Techniques
217 Nguyen Trai St. S
District 1
Ho Chi Minh City C

Tel. +84 8 839 58 46
Fax +84 8 836 73 61
tkthn@hcm.vnn.vn

Cost-Free Participants/Observers

Austria

Mr Dieter Rank
University Vienna
Institute of Ecology
Althanstrasse 14
1090 Vienna
Tel. +43 1 4277 534 05
Fax +43 1 50550 6587
Dieter.Rank@univie.ac.at

Ms i-Sook Min
Austrian Research Center Seibersdorf
Environmental Sciences
2444 Seibersdorf
Tel. +43 50550 36 15
Fax +43 50550 36 16
minjisook@naver.com

China

Mr Baohong Lu
Hohai University
College of Water Resources & Environment
Xikang Rd. No.1, Nanjing 210098
Tel. +86 25 83787311
Fax + 86 10 86206396
lubaohong@126.com

USA

Mr Robert L Michel
U.S. Geological Survey
345 Middlefield Rd, MS 434
Menlo Park, CA 94025
Tel. +1 650 329 45 47
Fax +1 650 329 55 90
rlmichel@usgs.gov

Consultants

UNEP/GEMS

Ms Genevieve Carr
UNEP EMSC Water Programme
Place Vincent Massey
351 St Joseph Boulevard
Gatineau, Quebec K1A 0H3, Canada
Tel +1 819 934 55 67
Fax +1 819 953 04 61
genevieve.carr@gemswater.org

USA

Mr Balazs M. Fekete
University of New Hampshire
Institute for the Study of Earth, Oceans and Space
Complex System Research Center, Water Systems Analysis Group
Morse Hall H
Durham, NH 03824
Tel. +1 603 662 02 70
Fax +1 603 862 05 87
Balazs.Fekete@unh.edu

Slovakia

Mr Ladislav Holko
Slovak Academy of Sciences
Institute of Hydrology
Ondrašovecká 16
03105 Iptovský náhon
Tel./Fax +421 44 5522 522
holko@uh.savba.sk



IAEA

International Atomic Energy Agency

No. 22

Where to order IAEA publications

In the following countries IAEA publications may be purchased from the sources listed below, or from major local booksellers. Payment may be made in local currency or with UNESCO coupons.

AUSTRALIA

DA Information Services, 648 Whitehorse Road, MITCHAM 3132
Telephone: +61 3 9210 7777 • Fax: +61 3 9210 7788
Email: service@dadirect.com.au • Web site: <http://www.dadirect.com.au>

BELGIUM

Jean de Lannoy, avenue du Roi 202, B-1190 Brussels
Telephone: +32 2 538 43 08 • Fax: +32 2 538 08 41
Email: jean.de.lannoy@infoboard.be • Web site: <http://www.jean-de-lannoy.be>

CANADA

Bernan Associates, 4501 Forbes Blvd, Suite 200, Lanham, MD 20706-4346, USA
Telephone: 1-800-865-3457 • Fax: 1-800-865-3450
Email: customercare@bernan.com • Web site: <http://www.bernan.com>

Renouf Publishing Company Ltd., 1-5369 Canotek Rd., Ottawa, Ontario, K1J 9J3
Telephone: +613 745 2665 • Fax: +613 745 7660
Email: order.dept@renoufbooks.com • Web site: <http://www.renoufbooks.com>

CHINA

IAEA Publications in Chinese: China Nuclear Energy Industry Corporation, Translation Section, P.O. Box 2103, Beijing

CZECH REPUBLIC

Suweco CZ, S.R.O., Klecakova 347, 180 21 Praha 9
Telephone: +420 26603 5364 • Fax: +420 28482 1646
Email: nakup@suweco.cz • Web site: <http://www.suweco.cz>

FINLAND

Akateeminen Kirjakauppa, PO BOX 128 (Keskuskatu 1), FIN-00101 Helsinki
Telephone: +358 9 121 41 • Fax: +358 9 121 4450
Email: akatilais@akateeminen.com • Web site: <http://www.akateeminen.com>

FRANCE

Form-Edit, 5, rue Janssen, P.O. Box 25, F-75921 Paris Cedex 19
Telephone: +33 1 42 01 49 49 • Fax: +33 1 42 01 90 90
Email: formedit@formedit.fr • Web site: <http://www.formedit.fr>

Lavoisier SAS, 145 rue de Provigny, 94236 Cachan Cedex
Telephone: + 33 1 47 40 67 02 • Fax +33 1 47 40 67 02
Email: romuald.verrier@lavoisier.fr • Web site: <http://www.lavoisier.fr>

GERMANY

UNO-Verlag, Vertriebs- und Verlags GmbH, Am Hofgarten 10, D-53113 Bonn
Telephone: + 49 228 94 90 20 • Fax: +49 228 94 90 20 or +49 228 94 90 222
Email: bestellung@uno-verlag.de • Web site: <http://www.uno-verlag.de>

HUNGARY

Librotrade Ltd., Book Import, P.O. Box 126, H-1656 Budapest
Telephone: +36 1 257 7777 • Fax: +36 1 257 7472 • Email: books@librotrade.hu

INDIA

Allied Publishers Group, 1st Floor, Dubash House, 15, J. N. Heredia Marg, Ballard Estate, Mumbai 400 001,
Telephone: +91 22 22617926/27 • Fax: +91 22 22617928
Email: alliedpl@vsnl.com • Web site: <http://www.alliedpublishers.com>

Bookwell, 2/72, Nirankari Colony, Delhi 110009
Telephone: +91 11 23268786, +91 11 23257264 • Fax: +91 11 23281315
Email: bookwell@vsnl.net

ITALY

Libreria Scientifica Dott. Lucio di Biasio "AEIOU", Via Coronelli 6, I-20146 Milan
Telephone: +39 02 48 95 45 52 or 48 95 45 62 • Fax: +39 02 48 95 45 48
Email: info@libreriaaeiou.eu • Website: www.libreriaaeiou.eu

JAPAN

Maruzen Company, Ltd., 13-6 Nihonbashi, 3 chome, Chuo-ku, Tokyo 103-0027
Telephone: +81 3 3275 8582 • Fax: +81 3 3275 9072
Email: journal@maruzen.co.jp • Web site: <http://www.maruzen.co.jp>

REPUBLIC OF KOREA

KINS Inc., Information Business Dept. Samho Bldg. 2nd Floor, 275-1 Yang Jae-dong SeoCho-G, Seoul 137-130
Telephone: +02 589 1740 • Fax: +02 589 1746 • Web site: <http://www.kins.re.kr>

NETHERLANDS

De Lindeboom Internationale Publicaties B.V., M.A. de Ruyterstraat 20A, NL-7482 BZ Haaksbergen
Telephone: +31 (0) 53 5740004 • Fax: +31 (0) 53 5729296
Email: books@delindeboom.com • Web site: <http://www.delindeboom.com>

Martinus Nijhoff International, Koraalrood 50, P.O. Box 1853, 2700 CZ Zoetermeer
Telephone: +31 793 684 400 • Fax: +31 793 615 698
Email: info@nijhoff.nl • Web site: <http://www.nijhoff.nl>

Swets and Zeitlinger b.v., P.O. Box 830, 2160 SZ Lisse
Telephone: +31 252 435 111 • Fax: +31 252 415 888
Email: info@swets.nl • Web site: <http://www.swets.nl>

NEW ZEALAND

DA Information Services, 648 Whitehorse Road, MITCHAM 3132, Australia
Telephone: +61 3 9210 7777 • Fax: +61 3 9210 7788
Email: service@dadirect.com.au • Web site: <http://www.dadirect.com.au>

SLOVENIA

Cankarjeva Založba d.d., Kopitarjeva 2, SI-1512 Ljubljana
Telephone: +386 1 432 31 44 • Fax: +386 1 230 14 35
Email: import.books@cankarjeva-z.si • Web site: <http://www.cankarjeva-z.si/uvoz>

SPAIN

Díaz de Santos, S.A., c/ Juan Bravo, 3A, E-28006 Madrid
Telephone: +34 91 781 94 80 • Fax: +34 91 575 55 63
Email: compras@diazdesantos.es, carmela@diazdesantos.es, barcelona@diazdesantos.es, julio@diazdesantos.es
Web site: <http://www.diazdesantos.es>

UNITED KINGDOM

The Stationery Office Ltd, International Sales Agency, PO Box 29, Norwich, NR3 1 GN
Telephone (orders): +44 870 600 5552 • (enquiries): +44 207 873 8372 • Fax: +44 207 873 8203
Email (orders): book.orders@tso.co.uk • (enquiries): book.enquiries@tso.co.uk • Web site: <http://www.tso.co.uk>

On-line orders

DELTA Int. Book Wholesalers Ltd., 39 Alexandra Road, Addlestone, Surrey, KT15 2PQ
Email: info@profbooks.com • Web site: <http://www.profbooks.com>

Books on the Environment

Earthprint Ltd., P.O. Box 119, Stevenage SG1 4TP
Telephone: +44 1438748111 • Fax: +44 1438748844
Email: orders@earthprint.com • Web site: <http://www.earthprint.com>

UNITED NATIONS

Dept. I004, Room DC2-0853, First Avenue at 46th Street, New York, N.Y. 10017, USA
(UN) Telephone: +800 253-9646 or +212 963-8302 • Fax: +212 963-3489
Email: publications@un.org • Web site: <http://www.un.org>

UNITED STATES OF AMERICA

Bernan Associates, 4501 Forbes Blvd., Suite 200, Lanham, MD 20706-4346
Telephone: 1-800-865-3457 • Fax: 1-800-865-3450
Email: customercare@bernan.com • Web site: <http://www.bernan.com>

Renouf Publishing Company Ltd., 812 Proctor Ave., Ogdensburg, NY, 13669
Telephone: +888 551 7470 (toll-free) • Fax: +888 568 8546 (toll-free)
Email: order.dept@renoufbooks.com • Web site: <http://www.renoufbooks.com>

Orders and requests for information may also be addressed directly to:

Marketing and Sales Unit, International Atomic Energy Agency

Vienna International Centre, PO Box 100, 1400 Vienna, Austria
Telephone: +43 1 2600 22529 (or 22530) • Fax: +43 1 2600 29302
Email: sales.publications@iaea.org • Web site: <http://www.iaea.org/books>

INTERNATIONAL ATOMIC ENERGY AGENCY
VIENNA
ISBN 978-92-0-126810-5
ISSN 1011-4289